Characterization of pathway engineered strains of filamentous fungi in submerged cultures

Promotor:

> Prof. dr. ir. J Tramper
>
> Hoogleraar in de Bioprocestechnologie

Co-promotoren:

> M.Vetr.Sc., PhD JJL Iversen
>
> Associate professor, Department of Biochemistry and Molecular Biology, University of Southern Denmark
>
> Dr. GJG Ruijter
>
> Klinisch biochemisch geneticus io, Laboratorium Metabole Ziekten, Leids Universitair Medisch Centrum
>
> Dr. ir. J Visser
>
> Gastmedewerker Instituut voor Biologie, Universiteit Leiden

Promotiecommissie:

> Cand. Ing. K Hansen (Novozymes A/S, Bagsvaerd, Denmark)
>
> Prof. dr. CAMJJ van den Hondel (Universiteit Leiden)
>
> Prof. dr. JT Pronk (Technische Universiteit Delft)
>
> Prof. dr. WM de Vos (Wageningen Universiteit)

Bjarne Rask Poulsen

Characterization of pathway engineered strains of filamentous fungi in submerged cultures

Proefschrift

ter verkrijging van de graad van doctor
op gezag van de rector magnificus
van Wageningen Universiteit,
Prof. dr. ir. L. Speelman,
in het openbaar te verdedigen
op vrijdag 1 april 2005
des namiddags te half twee in de Aula

Welcome

Something totally beyond your control brought you here, into these pages:
THE PRIMAL PULL OF WATER
It resides in us all. Most fight against it's tug only to live dry, predictable existences. Others, like you, concede the water's power and accept its embrace, asking only for a chance to explore its mysteries and feed a desire to understand how we fit into all of this. You've come to the right place. You are among friends.

Wilderness Systems, North Carolina

Contents

Chapter 1

General Introduction

Filamentous fungi are widely used in the industry for synthesis of antibiotics, biomass, enzymes and organic acids. Examples of products are penicillin, high-protein food (Quorn^{TM}), esterases as an additive in washing powder and citric acid in soft drinks. The domestication of filamentous fungi has a long history probably starting hundreds of years ago with production of sake with *Aspergillus oryzae*. Another important step was the start of production of citric acid with *Aspergillus niger* in the early 20th century, which at the beginning of the 21st century has reached a size of around a million tons per year [Ruijter *et al.* 2002]. The extensive use for food products has given *A. niger* its GRAS status (Generally Recognized As Safe, U.S. Food and Drug Administration), which is one of the reasons that this fungus was chosen for this study. Other reasons are the extensive knowledge that already exist about *A. niger* and that filamentous fungi efficiently produce and secrete homologous as well as heterologous proteins and execute post-translational modifications similar to higher eukaryotes.

Strain improvement has so far been obtained mainly via classical methods, e.g. screening of mutants after radiation with UV. However, modern molecular techniques have made more direct approaches possible. The work described in this thesis presents such approaches and solutions to some of the problems encountered in growing and characterizing submerged cultures of filamentous fungi strains.

Synthesis of most of the products mentioned above requires reducing equivalents in the form of NADPH. The pentose phosphate pathway (PPP) is a central pathway in primary metabolism (Fig. 1). The oxidative part of this pathway is believed to be the major source of NADPH required for many biosynthetic and detoxification reactions. In the non-oxidative part erythrose 4-phosphate and ribose 5-phosphate are generated for subsequent biosynthesis of aromatic amino acids and nucleotides, respectively. In addition, the polyols arabitol, erythritol and xylitol and several pentose sugars are metabolised via the PPP in fungi.

There is an increasing interest to apply microorganisms in biotransformation processes for the synthesis of organic compounds. Microbial transformations have the advantage of proceeding under mild conditions preventing degradation of labile substrates or products. In addition, biotransformations are highly regio- and stereoselective conversions of complex organic molecules. A final advantage is that whole cell catalysts are inexpensive [Lehman and Stewart 2001]. Many processes are hydroxylations, oxidations or reductions done by fungal oxidoreductases probably in many cases involving cytochrome P450, which mostly require reducing power in the form of NADPH. For efficient biotransformation the supply of reducing equivalents should be sufficient and this might be accomplished by an elevated flux through the PPP.
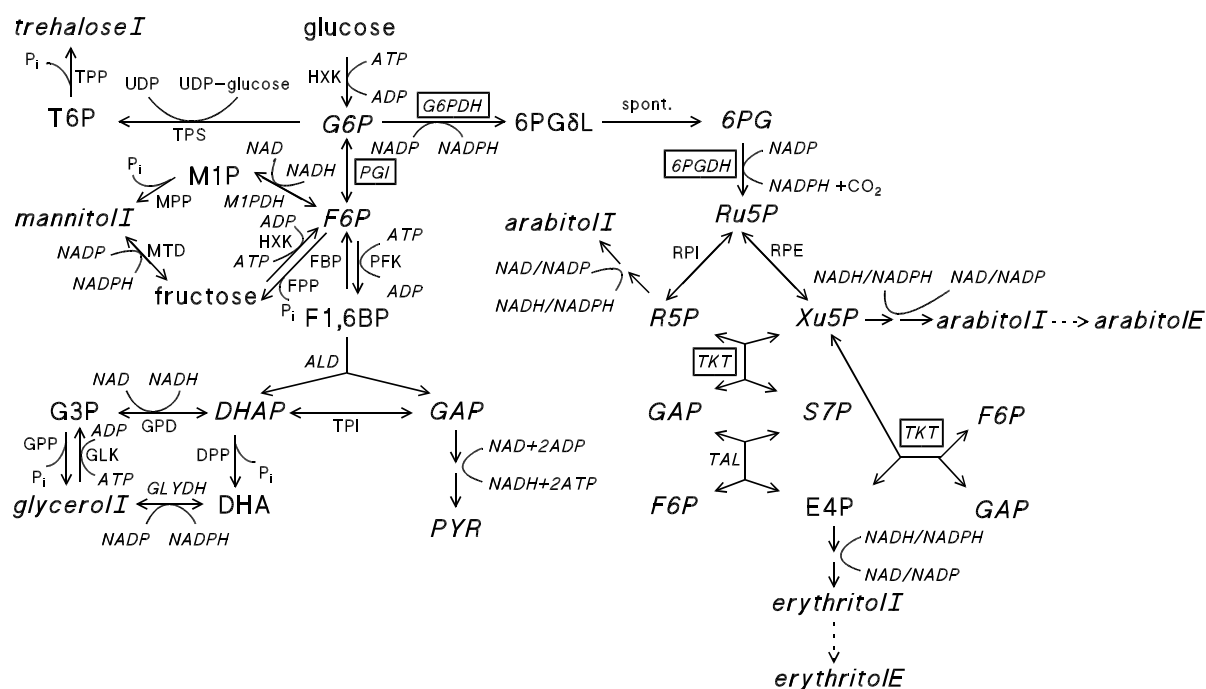
Figure 1. Glycolysis, pentose phosphate pathway and polyol formation in *Aspergilli*. Partly after [Witteveen 1993] and [Ruijter *et al.* 2003]. Two arrows in series mean two or more reactions. Enzymes in boxes were subjected to metabolic engineering in this study. E and I indicate extra- and intracellular polyols, respectively. Metabolites and enzymes in italics were measured in wild type and engineered strains. See Chapter 8 for abbreviations.

The aim of the work presented in this thesis is to increase the availability of NADPH and/or the flux through the PPP by metabolic engineering of *A. niger* wild-type and genetically modified strains. It might be possible to increase the flux through the PPP by overexpression of enzymes in the pathway or by disruption of genes in glycolysis. The objective is not merely to construct strains, but to do a thorough physiological investigation of wild type and transformant strains under various growth conditions by measurement of enzyme activities and concentrations of intracellular and extracellular metabolites at well-defined physiological states and during biotransformation. Such a comparison of wild type and modified strains requires reproducible culturing. This is particular challenging with filamentous fungi, since they have a strong tendency to adhere to surfaces and to form pellets and the interplay between these tendencies and physiology is very complicated.

OUTLINE OF THE THESIS

In **Chapter 2** a method for analysis of exponential data is described. The natural logarithm of the slope (LOS) plot enables identification of (1) data intervals that develop exponentially, (2) the rate constant (e.g. the growth rate) and (3) small and/or sudden changes in the rate constant.

A bioreactor specially designed for growth of filamentous fungi is described in **Chapter**

3. In this "Variomixing" bioreactor, wall growth is kept to a minimum by computer-controlled rotation of the baffles at a similar speed and direction as the impeller for 5 sec every 5 min, which results in a temporary cancellation of the effect of the baffles giving a deep vortex and high peripheral liquid flow rates at the reactor wall.

The "Macro-morphology Profiling System" (MPS) described in **Chapter 4** is a quantitative description of the amount of biomass in free hyphae and in pellets with core diameters smaller or larger than the critical core diameter, defined as the largest pellet core diameter without diffusion limitation of substrate in centre. In addition, MPS describes the amount of biomass limited by substrate diffusion into pellet cores larger than the critical core diameter. It was used to study the relationship between macro-morphology and physiology in batch, washout and chemostat cultures.

Invention and test of a filtrate sampling unit with a fast response time is given in **Chapter 5**. A response time of around 1 min for sampling of 1 mL·min^{-1} was obtained, enabling automatic sampling sufficiently accurate to monitor even glucose pulse experiments.

Biotransformation of nerolidol to hydroxy-nerolidol by *A. niger* is described in **Chapter 6**. The influence of physiological state and growth conditions on biotransformation and yield was determined.

In **Chapter 7** optimization of morphological stability in the chemostat cultures (Chapter 4) is described. An apparently stable aconidial (fluffy) mutant was characterized and conidiospores were produced in a cell containing the nucleus of the aconidial mutant together with the nucleus of a strain able to sporulate.

In **Chapter 8**, overexpression of glucose 6-phosphate dehydrogenase, 6-phosphogluconate dehydrogenase and transketolase is described. The modified strains were characterized in detail by measurement of a large number of variables: enzyme concentrations, intermediary metabolites, polyol pools (intra- and extracellular), organic acids, growth rates and rate constant of induction of acid production in the post-exponential phase. A partial least square regression was done to predict the NADPH concentration and to show the correlation between these variables and NADPH.

The reproducibility of submerged cultures of filamentous fungi is discussed in **Chapter 9**.

REFERENCES

Lehman LR, Stewart JD (2001) Filamentous fungi: potentially useful catalysts for the biohydroxylations of non-activated carbon centers. Curr Org Chem 5: 439-470.

Ruijter GJG, Kubicek CP, Visser J (2002) Production of organic acids by fungi. In: The Mycota, Industrial Applications, Osiewacz HD (Ed.), Chapter 10, pp 213-230. Springer-Verlag, Berlin.

Ruijter, GJG, Bax M, Patel H, Flitter SJ, van de Vondervoort PJI, de Vries RP, vanKuyk PA, Visser J (2003) Mannitol is required for stress tolerance in *Aspergillus niger* conidiospores. *Eukaryot. Cell* **2**, 690-698.

Witteveen CFB (1993) Gluconate formation and polyol metabolism in *Aspergillus niger*. PhD

thesis, Wageningen Agricultural University, The Netherlands.

Determination of first order rate constants by natural logarithm of the slope plot exemplified by analysis of *Aspergillus niger* in batch culture

ABSTRACT

Finding rate constants from experimental data is often difficult because of offset and noise. A computer program was developed to average experimental data points, reducing the influence of noise, and to produce a $\log_e$ of slope plot - a plot of the natural logarithm of the slope of a curve - eliminating the effect of any offset. Only if y-values depend exponentially on x-values the $\log_e$ of slope plot is rectilinear and the slope is equal to the first order rate constant. Therefore the $\log_e$ of slope plot provides easy identification of exponential sections of any experimental or calculated data, corresponding rate constants, and small changes in the rate constant as exemplified by analysis of titrant added to a batch culture of *Aspergillus niger*. The $\log_e$ of slope plot was easily applicable and superior to conventional methods of analysis of exponential decreasing or increasing data.

INTRODUCTION

Determination of the first order rate constant from experimental data is often hampered by an offset and disturbed by noise. Therefore, a plot of experimental data on semi-log paper or the natural logarithm of experimental data is often without meaning. Furthermore, it is mostly difficult to determine the offset or even identify the exponential part of experimental data.

A Guggenheim Plot [Guggenheim 1926], in which the natural logarithm of the difference between values measured with a constant time interval is plotted against time, can be a solution to the problem. However, it requires equidistant data points. In addition, the Guggenheim plot is rather laborious to explain, which also may have limited its use.

In this paper, we make use of a simple differential equation to derive a theory that explains how a 'log$_e$ of slope' (LOS) plot is used to find the rate constant from data containing an offset and sampled irregularly, without knowing which part of the data is exponential.

This method can be used to analyse exponential data from any source e.g. decay of a radioactive compound or increase of atmospheric CO_2 in industrial age measured in trapped air in ice cores of Antarctica (data from Friedli *et al.* [1986] and Neftel *et al.* [1985]). However, the main purpose of our research is to improve strains of filamentous fungi for industrial purposes, which requires tools for characterisation of strains. Therefore the example given here is analysis of an *Aspergillus niger* batch culture by LOS plot.

MATERIALS AND METHODS

Strain and media

A. niger NW131 (*csp*A1 *gox*C17) is a glucose-oxidase negative strain with short conidiophores and is derived from strain N400 (CBS 120.49).

Complete medium (CM, modified from Pontecorvo *et al.* [1953]) plates to prepare conidiospores contained per litre: 0.5 g KCl, 1.5 g KH_2PO_4, 0.5 g $MgSO_4 \cdot 7H_2O$, 6.0 g $NaNO_3$, 1.0 g casamino acids, 10 g glucose, 2.0 g peptone, 1 mL trace metal solution, 2.0 mL vitamin solution, 1.0 g yeast extract, 0.5 g yeast ribonucleic acids and 15 g agar, pH was adjusted to 6.0. Glucose was autoclaved separately.

The trace metal solution (essentially as described by Vishniac and Santer [1957]) contained per litre: 1.47 g $CaCl_2 \cdot 2H_2O$, 0.32 g $CoCl_2 \cdot 6H_2O$, 0.32 g $CuSO_4 \cdot 5H_2O$, 1.0 g $FeSO_4 \cdot 7H_2O$, 1.23 g $MnCl_2 \cdot 6H_2O$, 0.22 g $(NH_4)_6Mo_7O_{24} \cdot 4H_2O$, 4.4 g $ZnSO_4 \cdot 7H_2O$ and 10.0 g EDTA. EDTA and $ZnSO_4$ were brought in solution together and pH adjusted to 6 with concentrated NaOH, each of the other components were added one at a time and pH adjusted to 6 after each addition. Finally pH was lowered to 4 with HCl.

The vitamin solution contained per litre: 20 mg biotin, 1.0 g nicotinamide, 100 mg p-aminobenzoic acid, 100 mg pantothenic acid, 500 mg pyridoxine-HCl, 1.0 g riboflavin 5′-phosphate and 100 mg thiamine-HCl. The vitamin solution was filter sterilised on a 0.2 μm NC20 membrane filter (Schleicher & Schuell).

Minimal medium (MM) contained per litre: 0.5 g KCl, 1.5 g KH_2PO_4, 0.5 g $MgSO_4·7H_2O$, 1.12 g NH_4Cl (final cell density limiting substrate), 50 g glucose and 1 mL trace metal solution. Glucose was autoclaved separately.

As antifoam 0.15 mL polypropylene glycol (P 2000, Fluka Chemicals) per litre was added to the medium after germination. Approximately 12 hours after exhaustion of the final cell density limiting substrate, NH_4^+, 1 mL 0.25 g nerolidol·mL^{-1} ethanol was added.

Bioreactor

Submerged cultures were grown in a 3 L jacketed BTS06 bioreactor (Applikon BV) equipped with O_2 (Mettler Toledo, 12/420 T-Type) and pH (Mettler Toledo, InPro 3030/325) electrodes. Data acquisition and control were obtained with Bioexpert (Applikon BV) program via Biocontroller ADI 1030 (Applikon BV) interface. A Rushton turbine impeller, 4.5 cm diameter, placed 2-3 cm above the bottom of the bioreactor and a marine impeller, 5 cm diameter, 5 cm above the Rushton turbine impeller resulted in a suitable combination of axial and vertical liquid movement. Temperature was controlled at 30°C ± 0.1 and pH was controlled at 3.0 ± 0.05 by addition of 5 M NaOH.

Inoculation

Spores were prepared by growth at 30°C for 5 days on CM plates, kept at least 1 day (for maturation) and maximally 6 months at 4°C, and harvested with 10 mL of a solution containing 0.05% (w/v) Tween 80 and 0.9% (w/v) NaCl by scraping the agar surface using a Drigalski spatula. This treatment was repeated once. The spore suspension was filtered through sterile glass fibre, centrifuged for 2 min at 1620 g and resuspended in 5 mL sterile distilled water.

Spores were inoculated directly into the bioreactor to a density of 10^6 spores mL^{-1} in 2.5 L MM supplemented with 0.003% (m/v) yeast extract for germination. During the initial germination period of 5-8 hours stirrer rate was 750 rpm and aeration was through headspace at 2.5 L·min^{-1} to prevent blowing out the spores. When more than 50% of the spores were germinated, aeration was performed through the sparger at 1 L·min^{-1}, stirrer rate was increased to 1200 rpm, antifoam was added and pH control was activated. 1-2 hours after exhaustion of ammonium, the final cell density limiting substrate, 50 mL of the culture was sampled, the bioreactor was emptied, flushed once with medium and reinoculated in 2.5 L MM containing antifoam by addition of the 50 mL culture just sampled.

Determination of organic acids

Organic acids were determined in culture filtrates on a Dionex HPLC system (Sunnyvale) equipped with an HPX87H column (Biorad), thermostated at 50°C with detection by UV at 210 nm and refractive index. Isocratic elution with 25 mM HCl and a flow of 0.5 mL·min^{-1} was used.

RESULTS AND DISCUSSION

The theory of the LOS plot was derived and implemented for experimental (discrete) data in a specially-written program, exemplified by analysis of an artificial data set and by analysis of titrant added in a culture of *A. niger*.

Theory of $\log_e$ of slope plot

The inherent advantage of the LOS plot is that the first derivative (equal to the slope) of an exponential function is another exponential function with the same rate constant, but always without offset. Experimental data described by an exponential function often contain an offset (*C*):

$$y = y_0 \cdot \exp\left(k \cdot [x - x_0]\right) + C \tag{1}$$

This is the general exponential equation, which is exemplified in Figure 1 by an artificial data set describing a culture of exponentially growing cells. In Equation 1 x is time (*t*), y is total cell number (*n*), y_0 is number of viable cells at culture start, k is specific growth rate (μ), x_0 is time at culture start and C is number of non-viable cells. Other examples of offset are e.g. the background radiation when measuring the decay of a radioactive compound or the saturation concentration when measuring mass transfer. By differentiation of Equation 1 the offset is removed and the slope is obtained:

$$dy/dx = y_0 \cdot k \cdot \exp\left(k \cdot [x - x_0]\right) \tag{2}$$

and by taking the natural logarithm, $\log_e$, to the slope:

$$\log_e\left(\mathrm{abs}[dy/dx]\right) = \log_e\left(y_o \cdot k\right) + k[x - x_0] \tag{3}$$

it is seen that in a plot of the natural logarithm of the slope, $\log_e(dy/dx)$, against x, defined as a '$\log_e$ of slope (LOS) plot', the first order rate constant k is found as the slope of any rectilinear section of the LOS plot. This is possible without knowing the offset or which part of the data is exponential and any section of an exponential curve can be used to find k. Equally important, any exponential section and small changes in the rate constant (e.g. the specific growth rate of a culture) are easily visualised, since *only* an exponential dependency of y on x gives a straight line in a LOS plot.

Implementation of LOS plot to an artificial exponential data set

To compare analysis by LOS plot, exponential fit and $\log_e$, an artificial data set of total cell number was calculated as a function of time in an (*in silico*) exponentially growing batch culture, where the specific growth rate decreased momentarily from 0.28 h^{-1} to 0.22 h^{-1}, e.g. because of a

temperature decrease (Fig. 1). Increase of cell number in the artificial data set was analysed by the different analysis methods.
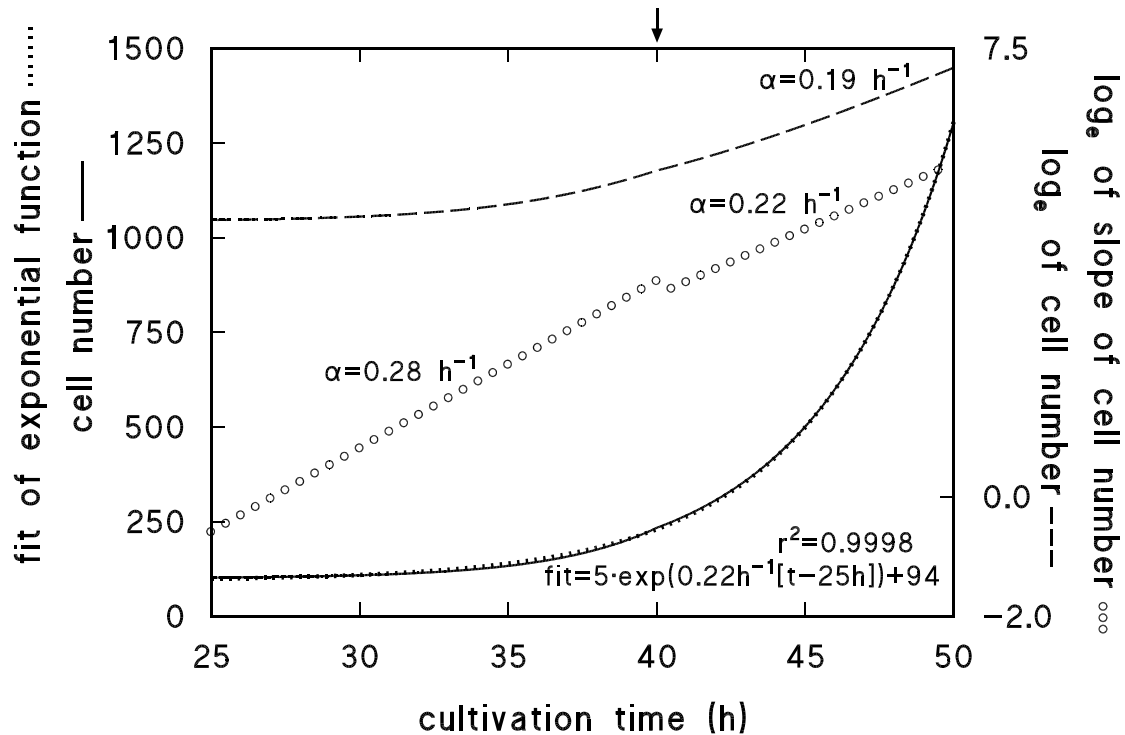

Figure 1. Analysis by $\log_e$ of slope (LOS) plot (ooo), $\log_e$ (----) and fit (····) of exponential function (Eq. 1) of (calculated) exponential data (—) with change in first order rate constant at 40 h. At 25 hours culture contained 2 viable and 100 non-viable cells. 25-40 h: $n(t) = 2 \exp(0.28$ h$^{-1}[t$-25 h$])$+100, resulting in 133 viable cells. At 40 hours (arrow) specific growth rate decreased from 0.28 h^{-1} to 0.22 h^{-1}. 40-50 h: $n(t) =$ 133·exp(0.22 h$^{-1}[t$-40 h$])$+100.

Only by LOS analysis the decrease ('shift down') in rate constant (specific growth rate) was identified in spite of the fact that all the analysis methods were performed on an artificial data set without noise. The decrease in rate constant we chose is easily seen in Figure 1 as a decrease of slope of the LOS plot. With a smaller decrease in rate constants the moment of change would be less clear, but then the discontinuation between the two rectilinear sections of the curve becomes a valuable tool for exact identification of the moment of change. The LOS plot resulted in a correct determination of rate constants before (0.28 h^{-1}) and after (0.22 h^{-1}) the change.

This is not the case for the fit of the exponential function (Eq. 1) to the entire artificial data set, giving a very good correlation ($r^2 = 0.9998$), which probably would assure any analyst that the data set was described by one rate constant (0.22 h^{-1}). However, this is a spurious result equal to the rate constant after the change because high numbers are weighted higher in calculation of the best fit.

Analysis by taking the natural logarithm, $\log_e$, also gave a wrong result with non-linearity in the beginning because of the offset of non-viable cells, but even the apparent linearity at the end resulted in a low slope (rate constant) of 0.19 h^{-1} compared to the real value of 0.22 h^{-1}. The non-linearity in the beginning could easily be misinterpreted as a lag-phase.

Prior knowledge of the nature of experimental results is unnecessary in LOS analysis contrary to conventional methods, for which the analyst must assume that certain sections of the

experimental data are exponential and extract them before analysis. This comprises at least three serious obstacles for use of conventional methods: 1) the chosen sections might not be exponential, which is very difficult to determine from the non-rectilinear data 2) exponential sections might not be detected 3) the rate constants determined might be erroneous, since a) non-exponential sections are included in the analysis and b) an offset might be included in the analysis. If e.g. the offset (C) in Equation 1 varies, y does not depend exponentially on x, is easily overlooked and results in erroneous determined rate constants in conventional analysis. However, in the LOS plot this is easily observed since *only* a non-exponential dependency of y on x will give a non-rectilinear LOS plot.

LOS plot compared to Guggenheim plot

Since the Guggenheim plot was published [Guggenheim 1926] it has been used mostly in chemical kinetics. However, the LOS plot is more general than the Guggenheim plot, in which the natural logarithm of the difference between values measured with a constant time interval is plotted against time, and therefore constitutes a special case of the LOS plot. A major obstacle of the Guggenheim plot is that the time between data-points must be constant. The user of the LOS plot is not restricted to equidistant data. The method is functional on data sampled irregularly and is therefore always applicable to experimental data in contrast to the Guggenheim plot.

LOS plot program

A specially-written program for an IBM compatible PC was used to average experimental data points, calculate $\log_e$ of the slope between averages and show the plot. Calculation of averages is done after the user has chosen the number of experimental data points from which the average is calculated (if 1 is chosen no averaging is performed) and the number of experimental data points between the first experimental data point in each average. The natural logarithm of the slope between two average values results in one data point in the LOS plot, in which the user can align a straight line (rectilinear cursor) to any rectilinear section of the LOS plot. The slope of the aligned rectilinear cursor, equal to the rate constant, is displayed simultaneously. In addition, the user can read values on both axes by positioning vertical and horizontal cursors in the plot to e.g. identify lengths of exponential intervals. The LOS data is also saved in a text file. The program is available at http://www.sdu.dk/nat/bmb/groups/tm/downloads/LOS.ZIP containing an executable file (LOS.EXE) and test data (TEST.TXT).

Implementation of LOS plot to base titrant added to maintain constant pH

Since experimental data are discrete it is impossible to determine the slope directly by differentiation. Instead, a point in the LOS plot is calculated as the natural logarithm of the slope between two data points or between two averages of data points. Iversen *et al*. [1994] showed that titrant added to maintain constant pH in microbial cultures is an indirect measure of growth. Implementation of Equation 3 for base titrant added to maintain constant pH in a culture growing

exponentially gives:

$$\log_e\left(\text{abs}\left[\varDelta OH_{add}/\varDelta t\right]\right) = \log_e\left(OH_{add,0}\cdot\mu\right) + \mu\cdot\left[t - t_0\right] \tag{4}$$

where OH_{add} (mmol) is accumulated base titrant added, $OH_{add,0}$ (mmol) is base titrant added at time t_0 (s) without offset, t (s) is time and μ (kg DW·kg DW^{-1}·s^{-1}) is specific growth rate.

Analysis of growth and metabolism by LOS plot

Two sequential batch cultures of *A. niger*, including biotransformation of nerolidol added in post-exponential phase, were analysed by LOS plot of titrant added to maintain constant pH (Fig. 2).
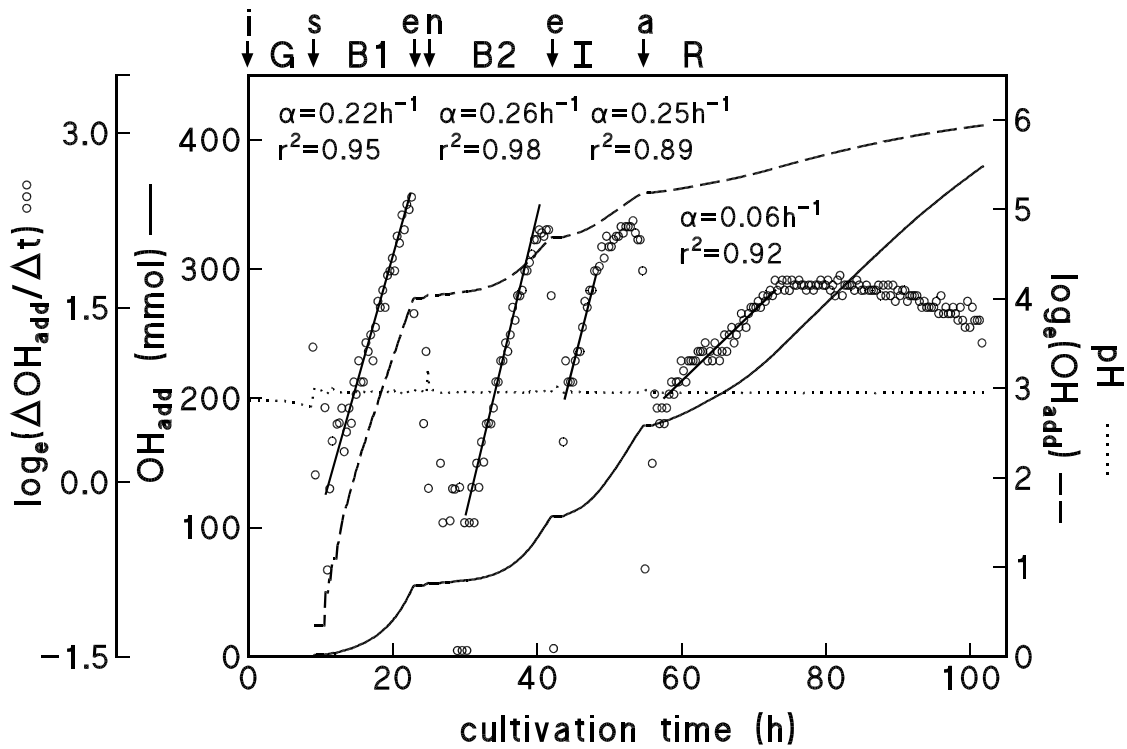
Figure 2. Base titrant added (—), pH (····), $\log_e$ of slope (LOS) of base titrant added shown in Equation 4 (ooo) and $\log_e$ of base titrant added (----) in *A. niger* repeated batch culture using minimal medium containing NH_4^+ as final cell density limiting substrate. Nerolidol is added in post-exponential phase. i: inoculation with spores, s: sparger aeration and pH control activated, e: NH_4^+ exhaustion, n: new medium, a: nerolidol addition. G: germination, B1: batch 1, B2: batch 2, I: induction of acid production, R: recovery after nerolidol addition. LOS plot was obtained by averaging 4 data points with 4 data points between first data point in each average. Straight lines are fitted to LOS plot of base titrant added.

Repeated batch cultures were used to minimize effects of nutrients in the spore inoculum, increase reproducibility and mimic the procedure of industrial scale cultures. During the growth phases of batches 1 and 2, base titration was mainly (95%) caused by protons released upon uptake of NH_4^+ [Iversen *et al*. 1994]. This was confirmed by HPLC analysis of organic acids. After batch 2 production of organic acids (90% oxalic acid and 10% citric acid) increased and when at an almost constant rate (slope of LOS plot approaching zero), a biotransformation

substrate, nerolidol, was added. This was done after the growth phase, because nerolidol is known to have antimicrobial effects [Kubo *et al.* 1992; Roussis *et al.* 2001]. An immediate inhibition, by nerolidol, of organic acid production was observed, since titration temporarily stopped.

The LOS plot shows four exponential phases, i.e. four straight lines: exponential growth phases in batches 1 and 2 (B1 and B2), respectively, exponential induction of acid production (I) and exponential recovery after nerolidol addition (R).

The first two exponential phases were expected, since all nutrients were in surplus. The specific ammonium uptake rate, which results in base titration [Iversen *et al.* 1994], was constant and the exponential increase in base titrant added was caused by exponential increase of cell number, i.e. growth was balanced. The maximal specific growth rate in batches 1 and 2 of 0.22 h^{-1} and 0.26 h^{-1}, respectively, were similar to literature values for *A. niger*: 0.24 h^{-1} [Trinci 1983] and 0.2 h^{-1} [Pedersen *et al.* 2000].

During induction of acid production and recovery after nerolidol addition the number of cells was constant because the final cell density limiting substrate, NH_4^+, was exhausted. To our knowledge exponential induction of specific acid production and exponential recovery after addition of biotransformation substrate have not been published before. This phenomenon is most likely caused by exponential induction of necessary enzymes. The duration of the exponential increase in acid production (4.4 h) is typical for induction in the sense of sequence of events: signalling a change in conditions, initiation of transcription and translation [Fell 1997]. However, to support this hypothesis and to determine which of these processes is rate limiting further investigation is necessary for which LOS plot is a potential tool, since it is independent of offset of variable measured (e.g. transcription levels or enzyme activities).

The similar rate constants (0.22 h^{-1}, 0.26 h^{-1} and 0.25 h^{-1}) of growth and of induction of acid production are probably accidental. There is only little chance that the same process is rate limiting, which is exemplified by the very different rate constant (0.06 h^{-1}) of the increase of acid production after nerolidol addition. In this period the cells recovered from addition of nerolidol. This may include synthesis of membrane lipids to compensate for a changed membrane fluidity caused by the highly hydrophobic nerolidol and/or replenishment of lost cell components as a result of leakage.

Part of the virtue of the LOS plot is illustrated here, since the analysis was performed without any prior knowledge of the nature of the experimental data. Each point in the LOS plot is calculated independently by using the slope between averages only - eliminating influence of the preceding development including any offset. Only few LOS plots are necessary to find the (minimal) number of experimental data points to average and the (minimal) number of experimental data points between first data point in each average. These depend on experimental data, but in all our applications these numbers varied between 1 (no averaging) and 20, corresponding to about a minimum of 5 times the detection limit. It was also our experience that these numbers can be chosen several times higher than the minima without influencing the value of the rate constant, but high numbers impair accurate identification of exponential sections. Taking averages can introduce artefacts. However, averaging is only necessary with frequent sampling, where the ratio of difference between measurements and noise is small. With infrequent sampling this ratio is large and averaging unnecessary. In practice, frequent (on-line) data require averaging and infrequent (off-line) data do not require averaging. For the same

reason the time interval for averaging on-line data is usually relatively small, and a high degree of detail is still obtained - much higher than for infrequent (off-line) measurements.

Comparison of different applications of the LOS plot

Table 1 shows rate constants determined from Figure 2 by different applications of the LOS plot: 1) manual alignment of a rectilinear cursor to the LOS plot, 2) linear fit to rectilinear sections of the LOS plot, and 3) fit of an exponential equation (Eq. 1) to exponential sections of titrant added identified by LOS plot. There is as expected agreement between methods 1, 2 and 3.

Method 3 depends on identification of the exponential sections by the LOS plot. This identification from experimental data is often difficult and without extraction of the exponential sections before a fit of the exponential equation a different, false rate constant is obtained as already shown in Figure 1.

Method 1 is the most direct: pretreatment e.g. subtraction of an offset or extraction of the exponential section of the experimental data or the LOS plot is unnecessary.

Only for batch 1 a representative result (0.25 h^{-1}) could be obtained by fit of a straight line to the $\log_e$ of titrant added because of the offset.

Table 1. Rate constants (h^{-1}) determined by different applications of the $\log_e$ of slope (LOS) plot.

Period[a]	1	2	3[b]
	Align rectilinear cursor to LOS plot	Linear fit to LOS plot	Exponential fit (Eq. 1)
B1	0.22	0.22	0.22
B2	0.25	0.26	0.24
I	0.26	0.25	0.25
R	0.06	0.06	0.06

[a] B1: batch 1, B2: batch 2, I: induction of acid production, R: recovery after nerolidol addition, all periods are shown in Figure 2.
[b] It was necessary to identify exponential sections by LOS plot as explained in text.

CONCLUSIONS

The most obvious advantage of the LOS plot is that rate constants (e.g. specific growth rates) are easily determined as the slope of rectilinear sections in the LOS plot.

In principle, the method has two disadvantages: 1) noise has a large influence on the slope between two experimental data points and 2) calculation of averages and $\log_e$ of slope from experimental data are less established than e.g. a fit of an exponential equation to experimental data. However, we have compensated for both of these disadvantages since 1) if necessary, the effect of noise is reduced by averaging the data points and 2) calculation of both averages and $\log_e$ of slope from experimental data is uncomplicated in conventional spreadsheet programs or in

specially-written computer programs (e.g. http://www.sdu.dk/nat/bmb/groups/tm/downloads/ LOS.ZIP).

As shown in Figures 1 and 2 prior knowledge of the nature of the experimental data is unnecessary in a LOS plot since 1) exponential sections of experimental data are easily identified by the naked eye, because they result in straight lines, 2) small changes - otherwise neglected - of the rate constant are easily identified as an abrupt change, 3) all sections of experimental data are weighted equally and are analysed independently contrary to a fit to experimental data, where high values are weighted too high and all data are assumed exponential with one rate constant, and 4) determination of rate constant - slope of the LOS plot - is independent of offset, which is often difficult or impossible to identify accurately.

Therefore, the LOS plot is superior to conventional methods of exponential analysis as an easily applicable, accurate method for determination of first order rate constants directly from any experimental data.

ACKNOWLEDGEMENTS

REFERENCES

Fell D (1997) Understanding the Control of Metabolism. London: Portland Press.

Friedli H, Lötscher H, Oeschger H, Siegenthaler U, Stauffer B (1986) Ice core record of 13C/12C ratio of atmospheric CO_2 in the past two centuries. Nature 324: 237-38.

Guggenheim EA (1926) On the determination of the velocity constant of a unimolecular reaction. Phil Mag 2: 538-543.

Iversen JJL, Thomsen JK, Cox RP (1994) On-line growth measurements in bioreactors by titrating metabolic proton exchange. Appl Microbiol Biotechnol 42: 256-262.

Kubo I, Muroi H, Himejima M (1992) Antimicrobial activity of green flavor components and their combination effects. J Agric Food Chem 40: 245-248.

Neftel A, Moor E, Oeschger H, Stauffer B. (1985) Evidence from polar ice cores for the increase in atmospheric CO_2 in the past two centuries. Nature 315: 45-47.

Pedersen H, Beyer M, Nielsen J (2000) Glucoamylase production in batch, chemostat and fed-batch cultivations by an industrial strain of *Aspergillus niger*. Appl Microbiol Biotechnol 53: 272-277.

Pontecorvo G (1953) The genetics of *Aspergillus nidulans*. p 141-238. In M. Demerec (ed.), Advances in genetics, vol. 5. Academic Press, New York.

Roussis V, Chinou IB, Tsitsimpikou C, Vagias C, Petrakis PV (2001) Antibacterial activity of volatile secondary metabolites from caribbean soft corals of the genus *Gorgonia*. Flavour

Fragr J 16: 364-366.

Trinci APJ (1983) Effect of junlon on morphology of *Aspergillus niger* and its use in making turbidity measurements of fungal growth. Trans Br Mycol Soc 81: 408-412.

Vishniac W, Santer M (1957). The Thiobacilli. Bacteriol Rev 21: 195-213.

Homogeneous batch cultures of *Aspergillus oryzae* by elimination of wall growth in the Variomixing bioreactor

ABSTRACT

A novel principle for mixing and aeration in stirred bioreactors, named Variomixing, was developed. Four baffles are rotated intermittently at a rotational speed slower or similar to the speed of a centrally placed axial flow impeller. Rotational speeds of the baffles and impeller of 5–10 and 500–600 rpm, respectively, results in the highly turbulent flow regime characteristic of conventional bioreactors with high mixing and mass transfer capacities. Stagnant zones around crevices and crannies in which wall growth may commence are avoided since the baffles are never completely at rest. Increasing the rotational speed of the baffles (5 s every 5 min), so that it follows the speed of the impeller (500–600 rpm), cancels the effect of the baffles and a deep vortex and high peripheral liquid flow rates at the reactor wall develop. The vortex ensures that also the head-space of the reactor wall is flushed and any deposits removed. The filamentous fungus *Aspergillus oryzae* has been grown in batch cultures in the Variomixing bioreactor. Compared to conventional laboratory-scale bioreactors, in which more than 30% of all biomass was found attached to walls, less than 2% of the total *A. oryzae* biomass was found on the walls in the Variomixing bioreactor.

INTRODUCTION

Filamentous fungi have a preference for growth on solid surfaces. Therefore, for successful submerged cultivation of these organisms it is important to minimize the surface area available for microbial attachment. This so-called wall growth consists of immobilized cells and may cause considerable changes in the apparent growth kinetics of submerged cultures. Indeed, even small quantities of wall growth, including non-visible films of biomass, may influence determination of growth parameters, with the most pronounced effect being spuriously high values of maximal specific growth rates [Topiwala and Hamer 1971]. In bioreactors, wall growth normally consists of several layers of microorganisms at certain locations. Attached colonies typically arise above the liquid surface, where splashed droplets hit the vessel walls, or in crevices and crannies in relatively stagnant zones below the surface. Since wall growth hampers the interpretation of growth experiments [Prosser 1994], attempts to minimize or remove biomass that has accumulated on reactor walls during fungal cultures have included maintaining a low head-space volume [Linton *et al*. 1984; Wiebe and Trinci 1991], temporarily increasing stirrer rate [Withers *et al*. 1994; Swift *et al*. 1998], and even physically dislodging attached biomass with sterile metal rods after removing the top plate [Withers *et al*. 1994] or by moving a magnet over the wall by an external horse-shoe magnet [Schrickx *et al*. 1993]. One way to avoid stagnant zones is to use a tank without baffles and other insertions, in which case the stirrer produces a simple circular flow with a high rate of liquid movement at the tank wall and the development of a vortex. If circular flow is left uninterrupted, liquid mixing and gas transfer become limiting in most processes.

In the present study, we introduce a novel mixing system in which the action of the baffles on liquid movements in the bioreactor is periodically eliminated, allowing the development of a circular flow pattern with a vortex by connecting the baffles to a motor via a central shaft. By intermittently changing the rotation speed of the baffles in the bioreactor, a simple circular flow spanning the entire reactor diameter alternates with a flow pattern consisting of smaller eddies similar to what is seen in conventional stirred tank reactors. As a result, the operational advantages of both simple circular (limitation of wall growth, one of the major obstacles to well-defined fungal cultures) and more turbulent (efficient mixing and aeration) flow patterns are maintained. The performance of this novel mixing/aeration regime, which we call Variomixing, is described here.

MATERIALS AND METHODS

Impeller design

The impeller is shown in Figure 1. In principle, this impeller is an axial-flow impeller similar to a pitched-blade turbine [Doran 1995]. Recommended impeller diameters for laboratory-scale bioreactors are 0.4 [Pirt 1975] and 0.5 [Solomons 1980] times the vessel diameter for growth of bacteria and filamentous fungi, respectively. We increased this ratio to 0.7 in order

to maximize the tip speed and thereby also the liquid velocities at the reactor wall. The impeller consisted of six circular segment blades (chord 95 mm and height 40 mm) angled 45° to the plane of rotation, resulting in a total diameter of 99 mm and a height of 67 mm. The material (AISI grade 304 stainless steel) thickness of the impeller blades was 2 mm.
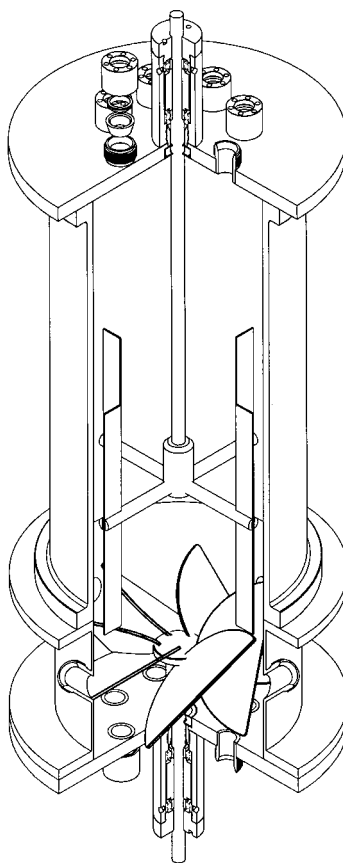
Figure 1. Isometric drawing of Variomixing bioreactor. Height of reactor = 410 mm, inner diameter = 142 mm.

Variomixing by rotating baffles

The eddies created by the stirrer were disrupted by means of four equally spaced baffles of width 0.1 times the vessel diameter (142 mm) and a thickness of 2 mm. The baffles were positioned perpendicular to the wall with a clearance of 0.06 times the vessel diameter, as recommended by Walker and Holdsworth [1958]. This gap of 8 mm resulted in a scouring action around and behind the baffles thus minimizing microbial growth on the baffles and on the bioreactor wall. When the width of the baffles was increased to 0.2 times the vessel diameter, the gas-liquid mass transfer coefficient, k_La decreased by 15% at all impeller speeds. Therefore, the dimension (width 0.1 times vessel diameter) generally recommended in the literature [Pirt 1975] was maintained throughout all growth experiments.

The baffles in the bioreactor (Fig. 1) were placed on a shaft. This enables the bioreactor to be operated in two alternating mixing/aeration modes — defined as Variomixing:

1. Baffles were controlled to rotate slowly, 5–10 rpm for 5 min, giving a flow regime with many smaller eddies and with efficient mixing and sparger aeration. There was

no difference in mixing/aeration between this mode and totally stagnant baffles, but the slow rotation gave an even distribution in time of regions with rapid fluid velocities, thus eliminating any low mixing pockets in which wall growth could become established.

2. Every 5 min, the baffles rotated for 5 s in the same direction and with the same speed (500–600 rpm) as the impeller, canceling out the hydrodynamic effect of the baffles and giving a vortex with circular flow as well as high peripheral liquid velocities, but with less efficient bulk mixing and aeration. By selecting a suitable liquid volume (3.5 L), the cylindrical part of the headspace was also flushed by the circular liquid movement during the vortex period, preventing any deposition of detritus or cells on this surface.

Bioreactor

The wall of the bioreactor consisted of a glass cylinder and a steel cylinder with four modified 12-mm Swagelok (Niagara Falls, Ontario) tube fittings with PTFE ferrules (Fig. 1). The inner diameter of both cylinders was 142 mm. The fittings were angled 45° to enable insertion of electrodes below the liquid surface. Bottom and top plates were equipped with nine insertion ports (modified Swagelok as above); the centre ports were installed with a FDA-approved Viton VR lipseal (OBC 008.022.07–93, NMF Techniek, Groningen, The Netherlands) for insertion of the stirring shafts, which were further supported by two stainless-steel ball bearings (608 2RS).

Two motors were necessary for the Variomixing configuration: a 700-W servomotor at the bottom for mixing and a 160-W servomotor at the top for baffle control (both from Robbins and Myers/Electro-Craft, Minn., USA). Excessive heating of the upper motor when the baffles were stagnant was prevented by connecting it to the baffle shaft via a 1:5 gearbox.

The bioreactor was equipped with a galvanometric O_2 electrode [Mackereth 1964] constructed in our workshop, an autoclavable glass pH electrode (Ingold, Urdorf, Switzerland) connected to a pH-meter (PHM 82, Radiometer, Copenhagen, Denmark) and a Pt-100 temperature sensor. Pulse addition of NaOH and HCl was used for pH control (band width 0.1 pH) and for on-line quantification of growth [Iversen *et al.* 1994]. Temperature was controlled at 30±0.1°C by hot air from a heating element (1,600 W) blown through a perspex jacket surrounding the middle glass part of the reactor (not shown in Fig. 1) and by constant cooling of the bottom, steel part of the reactor and above the liquid surface through coils of D-shaped tubing (not shown in Fig. 1). Computer control and data acquisition were obtained via a serial interface [Degn and Nielsen 1987] using a specially written program.

The Variomixing configuration was compared with that of a conventional 3-l BTS 0.5 bioreactor (Applikon, Schiedam, The Netherlands) with a working volume of 2.2 L and all insertions through the top plate. Accessory equipment, control, and experimental conditions were as described for the Variomixing bioreactor.

Strain and culture conditions

A. oryzae IFO 4177, Japan, was kindly provided by Novo Nordisk A/S. Slant cultures were carried out in 30 mL YPSS [Emerson 1941], which contained (per litre) 4.0 g yeast extract, 1.0 g K_2HPO_4, 0.5 g $MgSO_4·7H_2O$, 15 g soluble starch, and 20 g agar, pH 7, and grown for 5–6 days at 30°C. Subsequently, 20 mL 0.1% (v/v) Tween 80 was added and the cultures were shaken to harvest spores. The spore suspension was added to a 250-mL Erlenmeyer flask with 50 mL medium, which contained (per litre) 9.0 g $(NH_4)2SO_4$, 4.0 g KH_2PO_4, 7.2 g $Na_2HPO_4·2H_2O$, 0.3 g $MgSO_4·7H_2O$, 0.1 g $CaCl_2·2H_2O$, 0.6 g EDTA, 5.0 g glucose, and 0.5 mL trace metal solution (per litre: 14.3 g $ZnSO_4·7H_2O$, 2.5 g $CuSO_4·5H_2O$, 0.5 g $NiCl_2·6H_2O$, 13.8 g $FeSO_4·7H_2O$, 8.5 g $MnSO_4·H_2O$ and 10.0 g EDTA), pH 7. After incubation on a rotary shaker for 24 hours at 120 rpm and 30°C, the content of the Erlenmeyer flask was inoculated into the Variomixing bioreactor, containing 3.5 L minimal medium (per litre: 9.0 g $(NH_4)_2SO_4$, 1.5 g KH_2PO_4, 1.9 g K_2HPO_4, 0.3 g $MgSO_4·7H_2O$, 0.1 g $CaCl_2·H_2O$, 0.6 g EDTA, 30 g glucose, 0.5 mL trace metal solution, and 1.0 mL antifoam agent Pluronic L-61). The pH was adjusted to 5, 6, 7 or 8 with NaOH or HCl before inoculation.

Analysis

Dry weight (DW) samples were transferred directly into a graduated cylinder to determine volume, filtered on pre-dried and pre-weighed Whatman glass micropore filter (type GF/A), dried at 105°C for 24 hours, and weighed again. Culture filtrates were stored at −20°C for glucose and ammonium determination.

Glucose was determined enzymatically with hexokinase and glucose 6-phosphate dehydrogenase, according to the method of Bergmeyer *et al.* [1974], by measuring the absorbance change at 340 nm.

Cell carbon was determined on a Carlo Erba (Rodano, Italy) EA 1108 Elemental Analyzer after drying at 105°C for 48 hours and grinding in a mortar. Acetanilide was used as standard.

Ammonium was determined according to the colorimetric method of Mackereth *et al.* [1978] using ammonium chloride as standard.

Growth models

Growth kinetics were investigated using four different growth models:

1. Exponential:

$$x = x_0 \cdot \exp(\mu \cdot t) \tag{1}$$

2. Logistic [Bull and Trinci 1977]:

$$x = \frac{x_o \cdot \exp(\mu \cdot t)}{1 - \beta \cdot x_0 \cdot [1 - \exp(\mu - t)]}$$

(2)

3. Cubic [Pirt 1966]:

$$x = (x_o^{1/3} + k_c \cdot t)^3$$

(3)

4. Monod:

$$\frac{dx}{dt} = \frac{\mu_{max} \cdot s}{K_s + s} \cdot x \ \text{ and } \ \frac{ds}{dt} = Y_{x/s}^{-1} \cdot \frac{dx}{dt}$$

(4)

where x and x_0 are biomass concentrations at time t and time zero, respectively, s is glucose concentration, μ and μ_{max} are specific growth rate and maximum specific growth rate, respectively; k_c, $Y_{x/s}$, and K_s are constants. Models 2 and 4 take into account the decrease in specific growth rate as the limiting substrate becomes exhausted. Model 3 takes into account limitation by nutrient diffusion into pellets. Models 1–3 were fitted to experimental data of titrant addition or dry weight of samples from the bioreactor. Model 4, consisting of two coupled differential equations, was solved numerically and the solution was fitted to experimentally determined concentrations of dry weight and glucose.

In addition, titrant addition and dry weight data were analysed by log of slope (LOS) plots [Poulsen *et al*. 2003] to estimate μ. Experimental data often contain an offset (e.g. a lag phase, dead cells, insoluble medium components, or a signal offset) and therefore Model 1 becomes:

$$A = A_0 \cdot \exp(\mu \cdot t) + C$$

(5)

where A is a variable described by exponential growth, A_0 is the value of A at time 0 without offset and C is a constant offset. The offset is usually unknown and therefore a problem in data analysis. By differentiation of Equation 5, the offset is removed and the slope is obtained:

$$\frac{dA}{dt} = A_0 \cdot \mu \cdot \exp(\mu \cdot t)$$

(6)

and by taking the natural logarithm to the slope:

$$\ln\left(\frac{dA}{dt}\right) = \ln(A_0 \cdot \mu) + \mu \cdot t$$

(7)

Equation 7 shows that, in a plot of the natural logarithm of the slope, ln (dA/dt), against time, t, defined as a LOS plot, the specific growth rate, μ, is found as the slope of rectilinear sections of the LOS plot independently of unknown offsets. Equally important, any exponential sections of a growth curve and small changes in μ are easily identified, since only an exponential dependency of A on t gives a straight line (with a slope equal to μ) in a LOS plot. Implementation of Equation 3 for base titrant added to maintain constant pH in a culture growing exponentially gives:

$$\ln\left(\frac{\Delta OH_{add}}{\Delta t}\right) = \ln\left(OH_{add,0} \cdot \mu\right) + \mu \cdot t \qquad (8)$$

where OH_{add} (mM) is accumulated base titrant added and $OH_{add,0}$ (mM) is base titrant added at time 0 without offset.

RESULTS AND DISCUSSION

Growth in conventional bioreactor

Figure 2 shows massive accretions of wall growth of *A. oryzae* grown in a conventional bioreactor at pH 7, 30°C, and in medium with a composition identical to that used in batch cultures in the Variomixing bioreactor. The photograph of the top plate from below was taken after autoclaving the bioreactor and removing a peripheral layer of biomass in order to allow inspection of wall growth on all surfaces. In two experiments, the dry weight of the immobilized biomass was greater than 30% of total biomass. No meaningful kinetic or stoichiometric information — quantitative or qualitative — on submerged cultures can be obtained when immobilized biomass comprises such a substantial part of the total biomass. By contrast, the dry weight of immobilized biomass of the batch cultures in the Variomixing bioreactor (Table 1) never exceeded 2% of total biomass.

Figure 2. Massive accretion of *A. oryzae* biomass on headspace surfaces in a conventional Applikon BTS 0.5 bioreactor. *A. oryzae* was grown in batch culture on minimal medium with glucose as final cell density limiting substrate. After glucose exhaustion, the bioreactor was autoclaved and the head-plate removed.

Table 1. Specific growth rates of *A. oryzae* calculated from dry weights of samples taken throughout the growth phase or from base titrant added under pH control for five batch cultures grown in a Variomixing bioreactor. For comparison, the specific growth rate determined in a conventional bioreactor is shown. LOS Log of slope, n.d. not determined

pH	rpm	Exponential		LOS	
		μ_{DW} (h^{-1})	$\mu_{titrant}$ (h^{-1})	μ_{DW} (h^{-1})	$\mu_{titrant}$ (h^{-1})
5.0	600	0.079	0.071	0.083	0.075
6.0	600	0.070	n.d.	0.064	n.d.
7.0	500	0.12	0.15	0.17	0.17
7.0	600	0.15	0.16	0.14	0.17
8.0	600	0.050	0.043	0.059	0.065
7.0	600[a]	n.d.	0.040	n.d.	0.040

[a]Carried out in a conventional bioreactor.

Growth in the Variomixing bioreactor

Figure 3 shows two superimposed batch cultures of *A. oryzae* grown in the Variomixing bioreactor on a minimal medium with ammonium as nitrogen source. The final cell density limiting substrate, glucose, was exhausted when the dissolved oxygen tension, T_L, was at its lowest values. After glucose exhaustion, the pH increased to the upper limit of the bandwidth of the pH control and was kept constant thereafter by addition of acidic titrant.
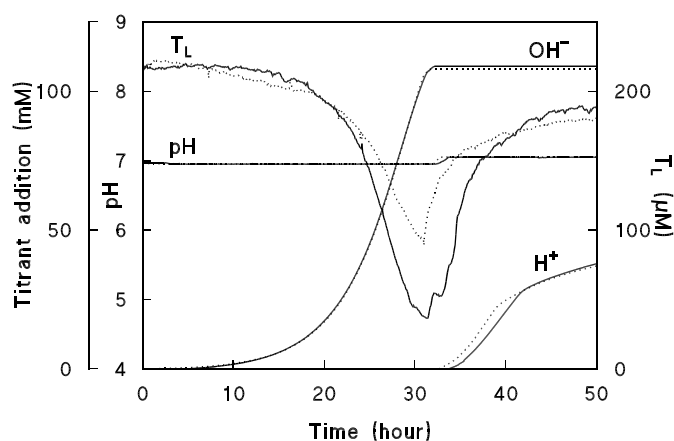
Figure 3. Titrant consumption and changes in dissolved oxygen tension, T_L, of two batch cultures of *A. oryzae* grown on minimal medium at pH 7, with glucose as final cell density limiting substrate and with identical control variables except impeller speed, 500 RPM (solid line) and 600 rpm (dotted line). T_L was at its minimum when glucose was exhausted from the growth medium.

The acidification observed during exponential growth resulted mainly (95%) from release of protons when ammonium was incorporated (Fig. 4). The remaining 5% was probably caused by production of organic acids. The pH increase in the post-exponential phase was caused by uptake of organic acids and excretion of ammonium, probably from deamination of intracellular protein (Fig. 4).

T_L reached lower values at 500 rpm than at 600 rpm as a result of the lower mass transfer of oxygen. After exhaustion of glucose, there was a plateau on the T_L curve of the

culture grown at 500 rpm. This suggests that an additional product was formed before glucose exhaustion at the lower impeller speed, and re-assimilated after glucose exhaustion. This interpretation is supported by the later onset of acid titrant addition in the culture grown at 500 rpm. In the last part (from 25 to 30 h) of the growth period, pellet formation took place in addition to filamentous growth, which had been characteristic for most of the growth period. Oxygen limitation, which is likely to occur inside pellets [Metz and Kossen 1977; Solomons 1980], may explain the differences in metabolism between batch cultures grown at 500 and 600 rpm (Fig. 3).
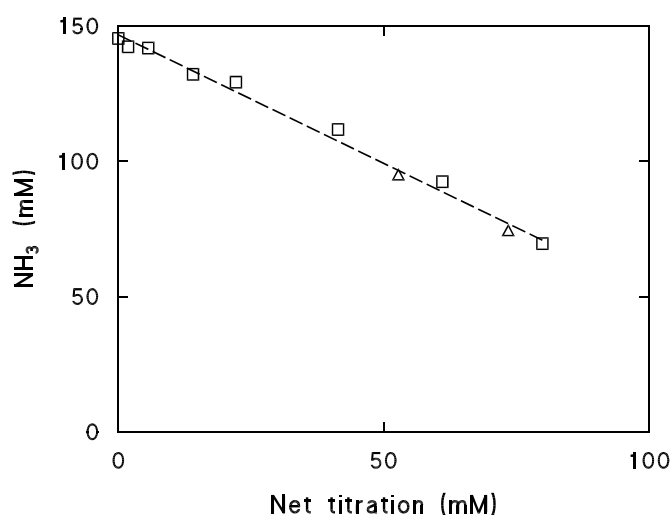

Figure 4. Concordance plot of NH_4^+ concentration versus net titration (base titration minus acid titration) before (□) and after (Δ) glucose exhaustion. Slope is -0.95 mM·mM^{-1}. Data from batch culture grown at pH 5.

Growth models

The most striking feature of Figure 3 is that the two curves describing addition of alkali are identical. In cultures of various unicellular microorganisms, including the bacteria *Escherichia coli*, and *Thiosphaera pantotropha* [Iversen *et al*. 1994], and the yeast *Candida utilis* [Castrillo *et al*. 1995], titrant additions to maintain constant pH have been used to accurately estimate biomass concentrations, specific growth rate, μ, and, growth yield, *Y*. Also in *A. oryzae* cultures, there was a constant relationship between titrant addition and biomass formation when the fungus was grown in homogeneous culture (Fig. 5).

In Figure 6 three different growth models describing growth of cultures without wall growth, exponential, logistic and cubic (Eqs. 1, 2 and 3, respectively), are fitted to dry weight and to titrant addition in the growth phase. In spite of the observed pellet formation and deviation from exponential growth in the last part of the growth period, the logistic and cubic models were unable to describe the experimental data (residuals between measured and modelled data points were large and non-randomly distributed). Only the experimental growth model was congruent with the experimental data; specific growth rates of five batch cultures estimated from this model are listed in Table 1. The discrepancy between the experimental data and the exponential model increases at the end of the growth phase at all pH values. This phenomenon is clearly seen in the LOS plot in Figure 7A. The exponential part of the curve is

easily identified, and the specific growth rate is determined from a linear regression to the rectilinear part of the LOS plot (Table 1). The LOS plot generally gives higher values of μ than the fit of the exponential model (Eq. 1), since data points from the last part of the growth period are disregarded in the linear regression of the LOS plot.
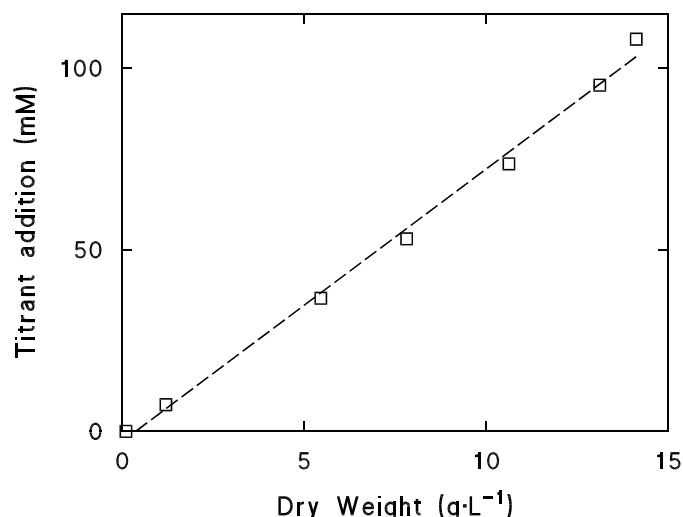

Figure 5. Concordance plot of biomass concentration (dry weight, DW) versus titrant addition (OH⁻) for batch culture of *A. oryzae* grown on minimal medium with glucose as final cell density limiting substrate. Biomass was measured as DW in samples removed from bioreactor and OH⁻ amount added at time of sampling. Linear regression (dashed line), slope = 7.50 mM·L·g⁻¹. Data from batch culture grown at pH 7 and 600 rpm.

Irrespectively of the calculation method, there is a good agreement between values of μ determined by the direct (dry weight) and indirect (titrant addition) methods. Also, carbon conversion efficiency (cell carbon produced per glucose carbon consumed) values were identical (0.42 ±0.01) throughout the exponential growth phase at all pH values despite differences in specific growth rates. All these results indicate that homogeneous submerged cultures of filamentous fungi are produced in the Variomixing bioreactor and, as a result of this, growth characteristics can be obtained by simple analytical methods.

Titrant addition and the LOS plot of titrant addition of a batch experiment with *A. oryzae* in an Applikon BTS 0.5 bioreactor are shown in Figure 7B. The data confirm that no meaningful information can be obtained from batch experiments using this fungus when significant amounts of biomass grow on the surfaces (more than 30% in this example) of the reactor. The low specific growth rate was caused by strong adhesion of biomass to surfaces and strong pelletation, in contrast to the filamentous morphology of the fungus in the Variomixing bioreactor.
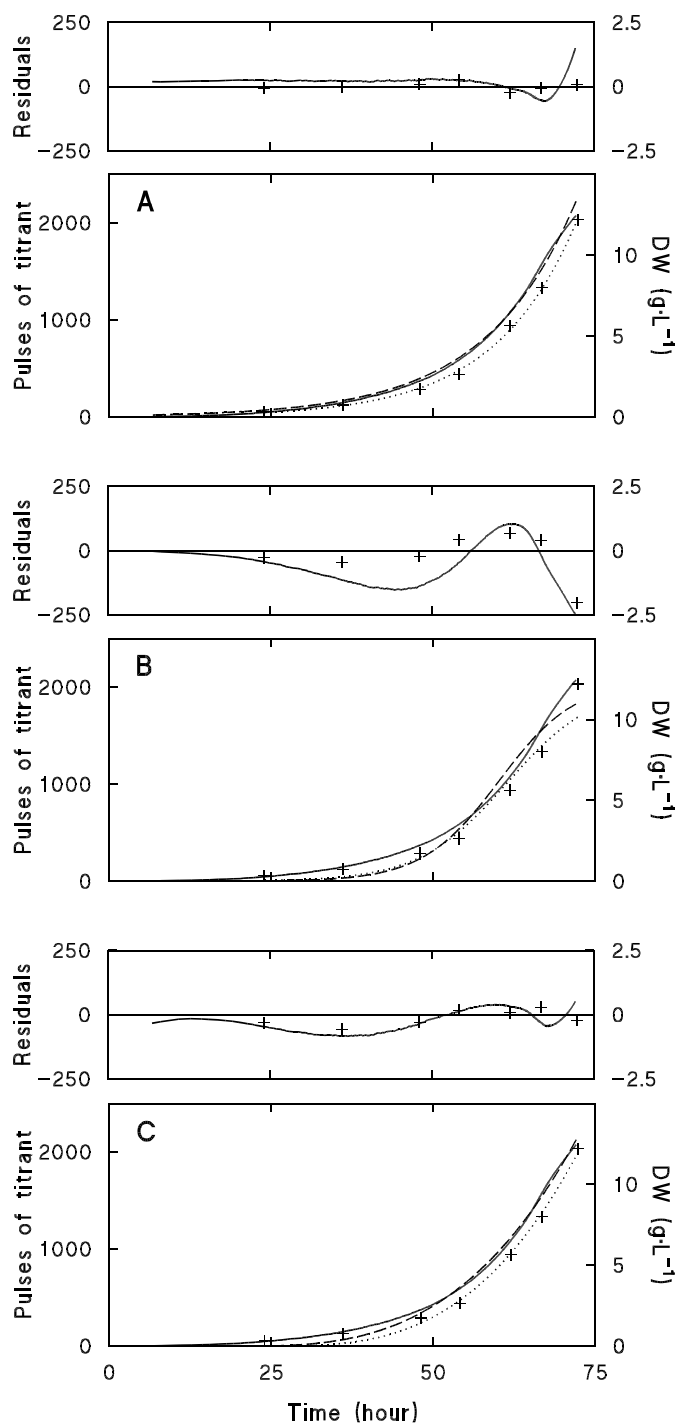
Figure 6A–C. Three growth models fitted to dry weight of samples from bioreactor, data (+), fit (dotted line), or pulses of titrant, data (solid line), fit (dashed line). **A** Exponential, **B** logistic, and **C** cubic models (Model 1, 2 and 3, respectively). Data from batch culture grown at pH 5.
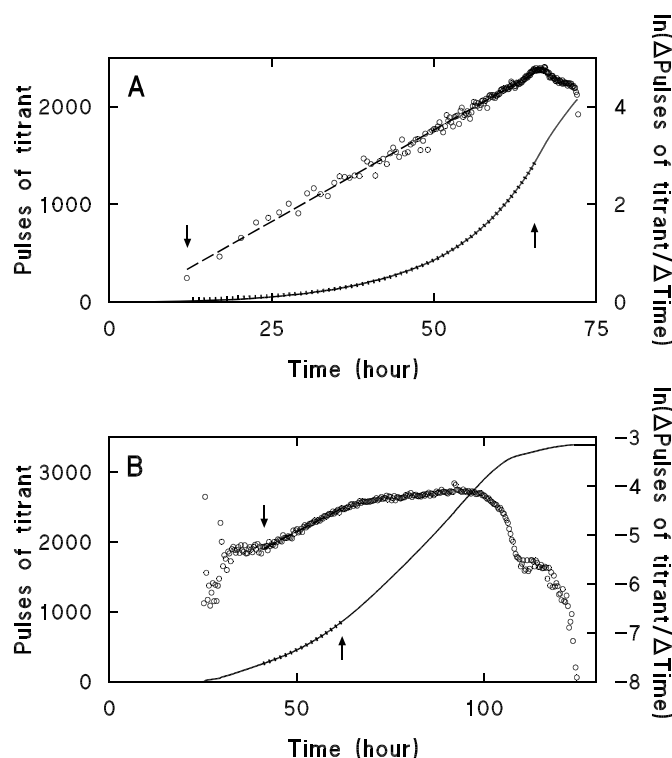
Figure 7. A Log of slope (LOS) plot (○) of pulses of titrant addition (solid line). Linear regression (dashed line) to rectilinear part of LOS plot indicated as interval between arrows, $\mu = 0.075$ h^{-1} (Table 1). The exponential equation (Model 1) fitted to the exponential part of the pulses of titrant addition, which was identified by LOS plot and is indicated as the interval between arrows (dotted line), $\mu = 0.076$ h^{-1}. Data from batch culture grown at pH 5. **B** Culture grown in a conventional bioreactor at pH 7. Legends as in A. LOS plot: $\mu = 0.040$ h^{-1} (Table 1). Fit of exponential equation (Model 1): $\mu = 0.040$ h^{-1}.

The decrease in the specific growth rate at the end of the growth experiment in the Variomixing bioreactor was a consequence of glucose limitation. In this period, glucose concentrations decreased to levels close to the K_s value of the low-affinity glucose uptake system of filamentous fungi. Typical K_s values range from 0.66 to 4.5 g·L^{-1} [Scarborough 1970; Schneider and Wiley 1971; Torres *et al*. 1996]. During the growth experiment at pH 6, samples for dry weight and glucose determinations were taken repeatedly throughout the growth phase, and the Monod model (Eq. 4) was fitted to these data (Fig. 8). An almost perfect description of these data was obtained by using $K_s = 3.45$ g·L^{-1} (19 mM) and $\mu_{max} = 0.097$ h^{-1}. Compared to the exponential model, residuals were more evenly distributed and their average size was reduced by 60%. Earlier observations [Bull and Trinci 1977] indicated that the growth of filamentous fungi is more accurately described by the logistic model than by the Monod model, but the results in Figure 8 show that when filamentous fungi are grown in homogeneous cultures their growth kinetics are similar to those of submerged cultures of unicellular microorganisms.
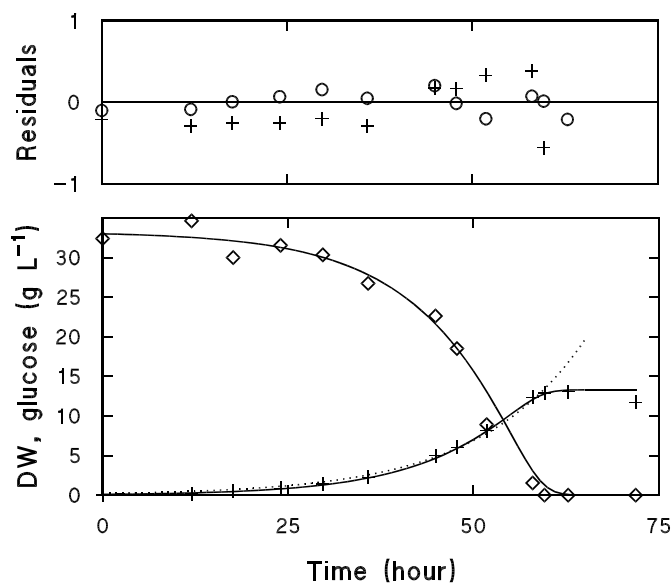
Figure 8. Exponential (dotted line) growth model (Model 1) fitted to dry weight (+), and Monod (solid line) growth model (Model 4) fitted to dry weight (+) and glucose concentration (◊) of samples from bioreactor. Residuals between dry weight and exponential model indicated by (+), and between dry weight and Monod model indicated by (○). Data from batch culture grown at pH 6.

CONCLUSION

We have designed a novel bioreactor, the Variomixing bioreactor, in which wall growth was virtually eliminated even with filamentous fungi. This was achieved by:

1) Minimizing the surface area in the headspace. All probes, sensors, cooling fingers, and ports for additions and sampling were removed from the top plate and inserted below the liquid surface, aligned with the inner surfaces to avoid regions with low liquid velocities.

2) Preventing growth on surfaces. A novel impeller type was constructed that gave axial flow with high peripheral liquid velocities and a deep vortex when baffles rotated in the same direction and with the same speed as the impeller. Wall growth in the head-space was additionally prevented by cooling the surface.

3) Maintaining high aeration capacity. The construction described above almost prevented wall growth, but the aeration capacity was low (vortex aeration). By introducing a submerged baffle system on a shaft it was possible to change the mixing regime from a simple, circular flow (baffles rotate with impeller) to a flow regime characterized by many smaller eddies (baffles are stationary) at predetermined computer controlled intervals, i.e. Variomixing.

Thus, Variomixing combines the advantages of circular (limitation of wall growth) and more turbulent (high mixing intensity, high k_La) flow regimes, and it was possible to obtain biomass densities of 10 g·L^{-1} in homogeneous batch cultures of a filamentous fungi that

otherwise has a high tendency to adhere to surfaces and form pellets. As a result, kinetic and stoichiometric parameters could be determined with an accuracy comparable to that achieved with batch cultures of unicellular microorganisms.

AKNOWLEGDEMENTS

REFERENCES

Bergmeyer HU, Bernt E, Schmidt F, Stork H (1974) D-glucose, determination with hexokinase and glucose-6-phosphate dehydrogenase. In: Bergmeyer HU (editor) Methods of enzymatic analysis, vol 3, 2nd edn. Academic, New York, pp 1196–1201.

Bull AT, Trinci APJ (1977) The physiology and metabolic control of fungal growth. In: Rose AH and Temptest DW (eds) Advances in Microbial Physiology, Vol. 15. Academic, London, pp 1–84.

Castrillo JI, de Miguel I, Ugalde UO (1995) Proton production and consumption pathways in yeast metabolism. A chemostat culture analysis. Yeast 11:1353–1365.

Degn H, Nielsen JB (1987) A general purpose serial interphase for the laboratory computer. Binary 10:25–28.

Doran PM (1995) Bioprocess engineering principles. Academic, London.

Emerson R (1941) An experimental study of the life cycles and taxonomy of allomyces. Lloydia 4:77–144.

Iversen JJL, Thomsen JK, Cox RP (1994) On-line growth measurements in bioreactors by titrating metabolic proton exchange. Appl Microbiol Biotechnol 42:256–262.

Linton JD, Austin RM and Haugh DE (1984) The kinetics and physiology of stipitatic acid and gluconate production by carbon sufficient cultures of *Penicillium stipitatum* growing in continuous culture. Biotechnol Bioeng 26:1455–1464.

Mackereth FJH (1964) An improved galvanic cell for determination of oxygen concentrations in fluids. J Sci Instrum 41:38–41.

Mackereth FJH, Heron J, Talling JF (1978) Water analysis: some revised methods for limnologists. Freshwater biological association, Ambleside.

Metz B, Kossen NWF (1977) The growth of molds in the form of pellets — a literature review. Biotechnol Bioeng 19:781–799.

Pirt SJ (1966) A theory of the mode of growth of fungi in the form of pellets in submerged culture. Proc R Soc B-Bio 166:369–373.

Pirt SJ (1975) Principles of microbe and cell cultivation. Blackwell Scientific, Oxford

Poulsen BR, Ruijter GJG, Visser J, Iversen JJL (2003) Determination of first order rate constants by Log of Slope plot applied to *Aspergillus niger* batch cultures. Biotechnol Lett 25:565–571.

Prosser JI (1994) Kinetics of filamentous growth and branching. In: Gow AR, Gadd GM (eds) The growing fungus. Chapman and Hall, pp 301–335.

Scarborough GA (1970) Sugar transport in *Neurospora crassa*. J Biol Chem 245:1694–1698.

Schneider RP, Wiley WR (1971) Kinetic characteristics of the two glucose transport systems in *Neurospora crassa*. J Bacteriol 106:479–486.

Schrickx JM, Krave AS, Verdoes JC, Hondel CAMJJ van den, Stouthamer AH, Verseveld HW van (1993) Growth and product formation in chemostat and recycling cultures by *Aspergillus niger* N402 and a glycoamylase overproducing transformant, provided with multiple copies of the glaA gene. J Gen Microbiol 139:2801–2810.

Solomons GL (1980) Fermenter design and fungal growth. In: Smith JE, Berry DR, Kristiansen B (eds) Fungal biotechnology. Academic, London, pp 55–79.

Swift RJ, Wiebe MG, Robson GD, Trinci APJ (1998) Recombinant glucoamylase production by *Aspergillus niger* B1 in chemostat and pH auxostat cultures. Fungal Genet Biol 25:100–109.

Topiwala HH, Hamer G (1971) Effect of wall growth in steady-state continuous culture. Biotechnol Bioeng 13:919–922.

Torres NV, Riol-Cimas JM, Wolschek M, Kubicek CP (1996) Glucose transport by *Aspergillus niger*: the low-affinity carrier is only formed during growth on high glucose concentrations. Appl Microbiol Biotechnol 44:790–794.

Walker JAH, Holdsworth H (1958) Equipment design. In: Steel R (ed) Biochemical engineering. Heywood, London, pp 223–273.

Wiebe MG and Trinci APJ (1991) Dilution rate as a determinant of mycelial morphology in continuous culture. Biotechnol Bioeng 38:75–81.

Withers JM, Wiebe MG, Robson GD, Trinci APJ (1994) Development of morphological heterogeneity in glucose-limited chemostat cultures of *Aspergillus oryzae*. Mycol Res 98:95–100.

Quantitative description of biomass distribution in free hyphae, pellets and diffusion-limited pellet cores in submerged cultures of filamentous fungi

ABSTRACT

In both laboratory and industrial scale cultures of filamentous fungi the ascription of biomass to different morphology classes is crucial for interpretation of results and optimization of processes. To quantify the macro-morphology of submerged cultures of filamentous microorganisms we developed a 'Macro-morphology Profiling System' (MPS) by using manual image analysis and determination of pellet core biomass density. Apparent core biomass density was determined by image analysis (volume determination) followed by sonication and measurement of optical density and by using a correlation between optical density and biomass (mass determination). By fitting a segregated model of the pellet, comprising a hairy region and a core, to the dependency of apparent core biomass density on core diameter, the core biomass density ($25 \ \mathrm{kg \cdot m^{-3}}$ in pH 6-batch cultures) was found independent of diameter. The critical core diameter, defined as the largest pellet core diameter without diffusion-limitation of substrate, was determined by direct and several indirect measurements of biomass activity and was 0.19 mm in pH 6-batch cultures of *Aspergillus niger*. MPS is a quantitative description of biomass in free hyphae, in pellets with core diameters smaller or larger than the critical core diameter, and in diffusion-limited biomass inside pellet cores larger than the critical core diameter. MPS was implemented at pH 3 in batch culture and in chemostat culture at steady state and wash-out. Pellet formation caused significant amounts of diffusion-limited biomass and explained why the apparent critical dilution rate ($0.23 \ \mathrm{h^{-1}}$) was lower than the maximum specific growth rate ($0.29 \ \mathrm{h^{-1}}$) observed in batch cultures with free hyphae only. We suggest that MPS can be an important tool when describing the complex interplay between morphology and cellular activity, which is of equal importance for the researcher and the process engineer.

INTRODUCTION

In submerged cultures of filamentous fungi there is a strong interplay between physiology and morphology, influencing expression, stoichiometry and kinetics. The most prominent example is formation of pellet cores larger than the critical core diameter – the largest core diameter without diffusion-limitation of substrate – resulting in at least two different populations of cells: those at the surface and those in the interior of the core [Cronenberg *et al.* 1994; Philips 1966, Pirt 1966, Wittler *et al.* 1986]. Pellets are in one way attractive in industrial scale cultures, since free filamentous mycelia give a viscous culture broth resulting in low mixing intensity, low gas-liquid mass transfer and high energy consumption. However, diffusion-limitation inside pellets results in less- or inactive biomass and metabolic inhomogeneity. This also makes interpretation of results from such cultures difficult or even impossible. For instance Carlsen *et al.* [1996] found ethanol production in an *Aspergillus oryzae* culture, but was able to correlate this observation to the theoretical diffusion-limited biomass inside large pellets. Also, when analysing e.g. transcription it is important not to have part of the culture under different conditions giving a mixed transcriptome.

Philips [1966] described how oxygen enters the interior of pellets by molecular diffusion and Pirt [1966] showed by calculation that oxygen is the diffusion-limited substrate in pellets in submerged batch cultures. Wittler *et al.* [1986] confirmed this by measuring the oxygen concentration profile inside pellets with a microprobe and found that the local turbulent diffusion coefficient decreased to a constant value at a depth of 40-80 μm. This distance most likely represented the transition zone between the hairy region (outer region of pellet with visible void volume) and the core – defining the core as the part of the pellet image without visible void volume between the hyphae [Cox and Thomas 1992], i.e. where there is no transport between the hyphae by convection, but only by molecular diffusion. The molecular diffusion can be described using an effective diffusion coefficient D_{eff} (m^2·h^{-1}):

$$D_{eff} = f_{eff} \cdot D_{medium} \tag{1}$$

where f_{eff} (-) is the effective diffusion factor, which depends on turbulent diffusion (moving eddies transport matter from one location to another [Yoshida *et al.* 1967], tortuosity (material restricts diffusion to certain directions) and pellet porosity (volume fraction of medium [Bailey and Ollis, 1986]) and D_{medium} (m^2·h^{-1}) is the diffusion coefficient in medium.

The "zero" critical core diameter $d_{crit,0}$ (m) is the largest core diameter without a concentration of zero of the diffusion-limiting substrate at the center and when assuming spherical symmetry it can be calculated from [Metz and Kossen 1977]:

$$d_{crit,0} = 2\sqrt{\frac{6 D_{eff} c_s Y}{\rho \mu}} \tag{2}$$

where c_s (mol·L^{-1}) is concentration of diffusion-limiting substrate at surface, Y (kg dry weight·mol^{-1}) is yield coefficient of biomass of diffusion-limiting substrate, ρ (kg dry weight·m^{-3}) is pellet core biomass density defined as biomass concentration in core, μ (kg dry weight·kg dry weight^{-1}·h^{-1}) is specific growth rate.

Simultaneous occurrence of free hyphae and pellets is often observed and mostly inevitable. A prerequisite for investigations of the relationship between an often very complex morphology and other variables is quantification of the morphology structures, including diffusion-limited biomass inside cores larger than the critical core diameter. A number of methods have already been developed partly based on more or less automatic image analysis [Pazouki and Panda 2000] with focus on branching, hyphal diameter, main or total length of free hyphae and on shape, structure and size of pellets. However, most of the current methods of image analysis rely only on projected area or numbers of structures for quantification. Exceptions are described by Treskatis *et al.* [1997], who developed a method by image analysis using grey values to represent the density and obtained a biomass distribution in different structures and Cui *et al.* [1998], who separated a large number of pellets from the free hyphae by means of a sieve for subsequent dry weight measurement.

In this study we describe a combination of relatively fast, manual image analysis, measurement of a critical core diameter, defined as the largest diameter without a significant change in physiology caused by diffusion-limitation in the centre, and determination of core biomass density to obtain a macro-morphology profile - a quantitative distribution of biomass in free hyphae, pellets with core diameters smaller and larger than the critical core diameter, and diffusion-limited biomass inside pellets larger than the critical core diameter.

MATERIALS AND METHODS

Definitions for Macro-morphology Profiling System (MPS)

Free hyphae:	Filament or agglomerate of filaments without a core
Pellet:	Filament or agglomerate of filaments with a core (Fig. 1)
Pellet core (core):	Part of pellet-image without visible void volume; Substrate transport presumably only by diffusion [Cox and Thomas 1992; Wittler *et al.* 1986]
Core diameter (d, m):	Diameter of core, arithmetic mean of longest and shortest core dimension
Critical core diameter (d_{crit}, m):	Largest core diameter without diffusion-limitation of substrate in centre
Core volume (V_{core}, m^3):	Volume of core calculated from core diameter
Total core volume (V_{total}, m^3):	Total volume of cores calculated from core diameters
Hairy region:	Part of pellet-image with visible void volume (Fig. 1); substrate transport presumably both by convection and diffusion [Cox and Thomas 1992; Wittler *et al.* 1986]

Width of hairy region:

($w_{hairy\ region}$, m)

Half of the difference between the convex diameter and the core diameter; the convex diameter is the arithmetic mean of longest and shortest dimension of the object obtained by joining the outer points of the pellet [Paul and Thomas 1998]

Volume of hairy region:

($V_{hairy\ region}$, m^2)

Volume of spherical shell of hairy region with inner diameter d and outer diameter

$d+2 \cdot w_{hairy\ region}$

Biomass (kg dry weight):

Freeze dried mass of microorganisms

Diffusion-limited biomass: (kg dry weight)

Part of core biomass limited by diffusion of a substrate

Core biomass density: (ρ_{core}, kg dry weight·m^{-3})

Biomass concentration in core, Core biomass/V_{core}

Apparent core biomass density: (ρ_{app}, kg dry weight·m^{-3})

Total pellet biomass/V_{total}

Hairy region biomass density: ($\rho_{hairy\ region}$, kg dry weight·m^{-3})

Biomass concentration in spherical shell of hairy region, hairy region biomass/$V_{hairy\ region}$
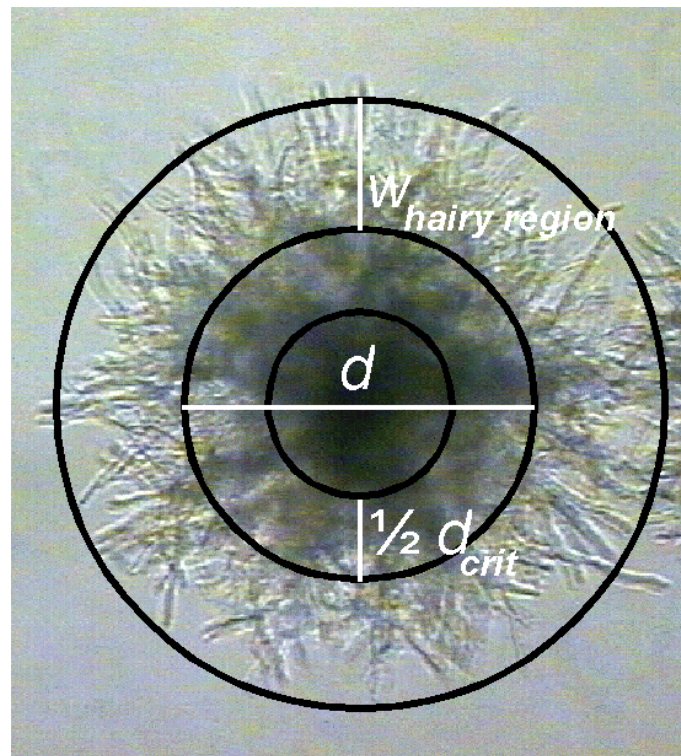

Figure 1. Representative pellet from pH 6-batch culture of *A. niger* 29 hours after inoculation. $d = 0.36$ mm (pellet core defined as part of pellet-image without visible void volume). Culture conditions: 30°C, 750 rpm, 0.40 vvm.

Strain and media

A. niger NW131 (cspA1 goxC17) is a glucose oxidase negative strain with short conidiophores and is derived from strain N400 (CBS 120.49).

Complete medium (CM, modified from Pontecorvo [1953]) plates to prepare conidiospores contained per litre: 0.5 g KCl, 1.5 g KH_2PO_4, 0.5 g $MgSO_4 \cdot 7H_2O$, 6.0 g $NaNO_3$, 1.0 g cas-amino acids, 10 g glucose, 2.0 g peptone, 1 mL trace metal solution, 2.0 mL vitamin solution, 1.0 g yeast extract, 0.5 g yeast ribonucleic acids and 15 g agar. pH was adjusted to 6.0 and glucose was autoclaved separately.

The trace metal solution (modified from Vishniac and Santer [1957]) contained per litre: 1.5 g $CaCl_2 \cdot 2H_2O$, 0.3 g $CoCl_2 \cdot 6H_2O$, 0.3 g $CuSO_4 \cdot 5H_2O$, 1.0 g $FeSO_4 \cdot 7H_2O$, 1.2 g $MnCl_2 \cdot 6H_2O$, 0.2 g $(NH_4)_6Mo_7O_{24} \cdot 4H_2O$, 4.4 g $ZnSO_4 \cdot 7H_2O$ and 10.0 g EDTA. EDTA and $ZnSO_4$ were brought in solution together and pH adjusted to 6 with concentrated NaOH. Each of the other components was added sequentially and pH adjusted to 6 after each addition. Finally pH was lowered to 4.0 with HCl.

The vitamin solution contained per litre: 20 mg biotin, 1.0 g nicotinamide, 100 mg p-amino benzoic acid, 100 mg pantothenic acid, 500 mg pyridoxine-HCl, 1.0 g riboflavin 5'-phosphate, and 100 mg thiamine-HCl. The vitamin solution was filter sterilized on a 0.2 μm NC20 membrane filter (Schleicher & Schuell, Dassel, Germany).

Minimal medium (MM) contained per litre: 0.5 g KCl, 1.5 g KH_2PO_4, 0.5 g $MgSO_4 \cdot 7H_2O$, 4.48 g NH_4Cl (final cell density limiting substrate in pH 6-batch cultures), 50 g glucose in pH 6-batch cultures or 7.43 g glucose as final cell density limiting substrate in pH 3-batch, chemostat and wash-out cultures and 1 mL trace metal solution. Glucose was autoclaved separately. Unless stated otherwise 0.15 mL polypropylene glycol (P 2000, Fluka Chemicals, Buchs, Switzerland) per litre was added as antifoam.

Reactor design

Cultures of pellets of uniform size were grown in a 3 L BTS05 bioreactor (Applikon, Schiedam, The Netherlands) modified to decrease wall growth by removing the baffles. Oxygen [Makereth 1964] and pH (Mettler Toledo GmbH, Urdorf, Switzerland) electrodes, temperature pocket, sparger and a 12 mm sampling tube gave sufficient turbulence to ensure sufficient aeration and mixing. A Rushton turbine impeller, 4.5 cm in diameter, placed 2-3 cm above the bottom of the bioreactor and a marine impeller, 5 cm in diameter, 5 cm above the Rushton turbine impeller resulted in a suitable combination of axial and vertical liquid movement. The liquid volume was 2.5 L. Stirrer rate was 750 rpm, temperature controlled at $30^{o}C \pm 0.1$, pH controlled at 6.0 ± 0.05 and aeration rate was 0.40 vvm (volume air·volume culture liquid^{-1}·min^{-1})

Chemostat cultures were performed in a 5 L "Variomixing" bioreactor specially designed for growth of filamentous fungi with minimal wall growth [Larsen *et al.* 2003]. This was achieved by computer controlled rotation of the baffles at a similar speed and direction as the impeller for 5 s every 5 min, which resulted in a temporary cancellation of the effect of the baffles; a deep vortex and high peripheral liquid flow rates at the reactor wall then developed.

When baffles were rotating slowly (5-10 rpm for 5 min) the highly turbulent flow regime characteristic of conventional bioreactors with high mixing and mass transfer capacities was developed. The following modifications were made to the Variomixing bioreactor: three impellers were placed with 5.5 cm distance: a marine impeller (6.0 cm diameter, 5 cm height, 3 blades angled 45° to the plane of rotation) 1.5 cm above the bottom plate and above this two Rushton impellers (5.5 cm diameter, 1.5 cm height, 6 blades). The four baffles had an outer diameter of 10.7 cm and were 1.5 cm wide and 26 cm long. The liquid volume was 4.3 L. The bioreactor was equipped with pH and oxygen electrodes inserted below the surface of the liquid. Temperature was controlled at 30°C $\pm$ 0.1 and pH was controlled at 3.0 $\pm$ 0.05. Unless stated otherwise the stirrer rate was 750 rpm and the aeration rate was 0.23 vvm.

Exhaust gases from both bioreactors were analyzed for CO_2 and O_2 by gas analysers (Binos 100M, Rosemount, Germany). Data acquisition and control were obtained via a serial interphase [Degn and Nielsen 1987] and an IBM-compatible PC running specially-written computer programs.

Inoculation

Spores were prepared by growth at 30°C for 5 days on CM plates, kept minimum 1 day and maximum 6 month at 4°C, and harvested with 10 mL of a solution containing 0.05% (vol/vol) Tween 80 and 0.9% (wt/vol) NaCl by scraping the agar surface with a Drigalski spatula. This treatment was repeated once. The spore suspension was filtered through sterile glass fiber, centrifuged for 2 minutes at 1600 g and resuspended in 5 mL sterile distilled water.

To obtain pellets of uniform size, 2.5×10^9 spores were germinated at pH 6 in a 1.0 L Erlenmeyer flask, in 300 mL MM (50 g glucose$\cdot$L^{-1}) without antifoam and supplemented with 0.025% (wt/vol) yeast extract to promote germination. The preculture was incubated for 5-7 hours at 30°C and 250 rpm in a rotary shaker before being added to the Applikon bioreactor containing 2.2 L MM (50 g glucose$\cdot$L^{-1}).

In the pH 3-chemostat culture, where growth with free hyphae was desired, spores were inoculated directly [Poulsen *et al.* 2003] into the Variomixing bioreactor to a density of 10^6 spores$\cdot$mL^{-1} in 4.3 L MM (7.43 g glucose$\cdot$L^{-1}) without antifoam and supplemented with 0.003% (wt/vol) yeast extract to promote germination. During the initial germination period of 5-7 hours a certain shear rate is necessary to keep spores separated, but the stirrer rate was kept low (450 rpm) and aeration was through the headspace at 0.23 vvm to prevent blowing out the spores. When germination exceeded 50%, aeration was changed from headspace aeration to sparger aeration at 0.23 vvm, stirrer rate was increased to 750 rpm, antifoam was added and computer controlled intervals of turbulent (5 min) and laminar (5 sec) flow, characteristic of the Variomixing bioreactor, were activated. Before the final cell density limiting substrate, glucose, was exhausted from the batch culture, i.e. late in the exponential phase, 100 mL of the culture was sampled, the bioreactor was emptied, flushed once with medium and reinoculated in 4.2 L MM (7.43 g glucose$\cdot$L^{-1}) by addition of the 100 mL of culture just sampled. Late in the exponential phase of this second batch the continuous flow was started with MM (7.43 g glucose$\cdot$L^{-1}) at a dilution rate of 0.16 h^{-1}.

Analysis

Dry weight

Dry weight concentration (DW, g dry weight·L^{-1}) was measured on samples containing at least 20 mg dry cell material. The culture was sampled directly into a measuring cylinder and suction filtered on a glass sintered funnel or through pre-dried and pre-weighed paper filters; the mycelium was washed twice by resuspension in distilled water, frozen in liquid nitrogen, and stored at -20^oC. The sample was freeze dried and weighed.

Enzymatic ammonium and glucose determinations

A P1000 adjustable Gilson pipet, for which the opening diameter of the disposable tip was increased by removal of 1 cm of the cone, was used to take a culture sample and transfer it to another disposable tip containing a piece of cotton wool. With this tip placed on the pipet the culture sample was filtered by pushing the filtrate through the cotton. Filtrates were frozen in liquid nitrogen and stored at -20^oC.

Ammonium was determined enzymatically essentially as described previously [Bergmeyer and Beutler 1985]. Quantofix®Ammonium sticks (Macherey-Nagel GmbH & Co. KG, Düren, Germany) were used to determine approximate concentrations in batch cultures. Glucose was determined enzymatically as described previously [Bergmeyer *et al.* 1974].

Image analysis and determination of biomass from optical density

Culture samples (10-20 µL, if necessary diluted) were photographed using a light microscope (Leica DMR, Wetzlar, Germany) with a digital camera (Kappa CF 15/4 MC) at 100 times magnification or using a stereo microscope (Leica MZ8, Wetzlar, Germany) with a digital camera (SONY Power HAD 3CCD Color Videocamera Model DXC-950P) at 16 times magnification. In the light microscope the sample was placed in a circular hole (diameter 0.5 cm) of a steel plate (thickness 1 mm) placed on a microscope slide. The sample just photographed was then collected from the microscope in a known volume of water. Samples containing pellets were sonicated on ice at 9-10 watts in 2 x 1 min with pulses of 1 sec at 1 sec intervals resulting in dispersed, but not disrupted, mycelium, followed by determination of optical density at 600 nm (OD_{600}, Abs). DW was calculated from the linear correlation between OD_{600} of sonicated samples and DW determined in separate experiments. A linear correlation between OD_{600} and DW of mycelium growing as free hyphae was previously found by Trinci [1983].

Determination of apparent biomass density in pellets

Typically a sample containing 40-60 pellets was analysed. In samples from pH 6 batch cultures the morphology was pellets only; in samples from pH 3 cultures pellets were separated from free hyphae by washing through 125 or 300 µm mesh polypropylene sieves and/or sorting with an adjustable Gilson pipet, for which the opening diameter of the disposable tip was increased by removal of part of the cone. Pellet core was defined as the part of the pellet-image without visible void volume (Fig. 1), i.e. where there is no transport by convection, but only by diffusion [Cox and Thomas 1992; Wittler *et al.* 1986]. For each

pellet the longest and shortest core dimension were measured. We define the arithmetic mean hereof as the core diameter (d, m) used to calculate total core volume (V_{total}, m^3) of n number of pellets:

$$V_{total} = \frac{\pi}{6} \sum_{i=1}^{n} d_i^3 \qquad (3)$$

From V_{total} and dry weight of pellets, determined by sonication and the OD_{600}-DW relation as described above, the apparent core biomass density (ρ_{app}, kg dry weight·m^{-3}) of pellets was calculated. When calculating ρ_{app} it is therefore assumed that all biomass is part of the core and that the pellet core is not hollow.

Determination of critical core diameter
The critical core diameter was determined by "Log of Slope" (LOS) plots [Poulsen *et al.* 2003] of different variables: accumulated base titrant added (OH_{add}, mol·L culture^{-1}), DW, OD_{600}, ammonium concentration ($[NH_4^+]$, mol·L culture^{-1}) in addition to CO_2 (r_{co2}, mol·L culture^{-1}·h^{-1}) and O_2 (r_{o2}, mol·L culture^{-1}·h^{-1}) in exhaust gas. Experimental data often contain an unknown offset, which disturbs and/or gives misleading results in analysis of exponential data by conventional methods [Poulsen *et al.* 2003]. In the LOS plot the offset is removed by only using the slope of the data. This means that at any data point the previous data points have no influence on the LOS plot of the rest of the data points, because the previous data points are considered as offset. Thereby, any exponential (or non-exponential) sections of a curve and small changes in the rate constant are easily identified and quantified. Implementation of the LOS plot for e.g. base titrant added to maintain constant pH in a culture growing exponentially gives:

$$\ln(\Delta OH_{add}/\Delta t) = \ln(OH_{add,0}\mu) + \mu t \qquad (4)$$

where $OH_{add,0}$ (mol·L^{-1}) is base titrant added at time 0 and t (s) is time. It is seen that in a plot of the natural logarithm of the slope, $\ln(\Delta OH_{add}/\Delta t)$, against time, t, defined as a "Log of Slope" (LOS) plot, the specific growth rate, μ, is found as the slope of rectilinear sections of the LOS plot without knowledge of the offset or which part of the data is exponential.

The onset of non-exponential growth was identified by a decrease in μ, i.e. slope in the LOS plot, when pellets had reached a critical core diameter d_{crit} (m) with an oxygen diffusion-limited centre [Pirt 1966], since preliminary experiments showed that increasing the concentration of all other nutrients failed to extend the exponential period whereas it was extended in a culture with free hyphae on the same medium.

Determination of biomass distribution in pH 3-batch, chemostat and wash-out cultures
Culture samples from pH 3-cultures, containing both free hyphae and pellets of different diameters, were analysed by image analysis to determine the biomass distribution in macro-morphology structures including diffusion-limited biomass in the culture. The different biomass fractions were calculated from the core diameter distribution found in image analysis

of culture samples (as described above) using measurements of pellet biomass densities, the critical core diameter and culture conditions as described below.

If necessary for the image analysis of the culture sample, pellets were separated from free hyphae by washing through a 125 μm mesh polypropylene sieve. To ease the separation the sieve was repeatedly submerged in water. Pellets were photographed, core diameter distribution was determined from the image and biomass of the photographed sample determined by OD_{600} after sonication as described above.

In batch and wash-out [Jannasch 1969] cultures the diffusion-limiting substrate in pellets is dissolved oxygen [Pirt 1986], whereas it is likely to be the final cell density limiting substrate in chemostat cultures. The specific growth rate in the former is equal to μ_{max} and in the latter to the dilution rate D (h^{-1}).

Since it is very difficult to obtain a culture exclusively of pellets of uniform size in a pH 3-culture, and d_{crit} depends on conditions (Eq. 2), we calculated the critical core diameter in the pH 3-chemostat culture, $d_{crit, pH3-chem}$ (m), from the critical core diameter found in the pH 6-batch culture, $d_{crit, pH6-batch}$ (m), using Equation 2. This equation is derived for $d_{crit,0}$. When the oxygen concentration was controlled at 10% of air saturation in a batch culture containing only free hyphae the maximum specific growth rate (μ_{max}, h^{-1}) remained unchanged as expected in view of the very low saturation constant [Wimpenny 1969] for oxygen uptake in fungi. Also the saturation constant for glucose uptake is low in glucose-limited chemostat cultures [Carlsen *et al.* 1996a]. Therefore, we assume that the oxygen concentration in batch and wash-out cultures and glucose concentration in chemostat cultures, respectively, in the centre of a pellet with diameter d_{crit} is close to zero and that the relations shown in Equation 2 for $d_{crit,0}$ are also valid for d_{crit}.

Assuming that the effective diffusion factor f_{eff} is the same in the pH 3- and pH 6-cultures we obtain from Equation 2:

$$d_{crit,pH3-chem} = d_{crit,pH6-batch} \sqrt{\frac{D_{glc}c_{glc,pH3-chem}Y_{glc}\mu_{max,pH6}\rho_{core,pH6}}{D_{O2}c_{O2,pH6-batch}Y_{O2}D_{chem}\rho_{core,pH3}}} \tag{5}$$

where D_{glc} and D_{O2} ($m^2 \cdot h^{-1}$) are diffusion coefficients for glucose and oxygen respectively, $c_{glc, pH3-chem}$ ($mol \cdot L^{-1}$) is glucose concentration in pH 3-chemostat and $c_{O2, pH6-batch}$ ($mol \cdot L^{-1}$) is oxygen concentration in pH 6-batch culture at onset of limitation, Y_{glc} and Y_{O2} (kg dry weight$\cdot mol^{-1}$) are yield coefficients for glucose and oxygen, respectively, $\rho_{core,pH6}$ and $\rho_{core,pH3}$ are core biomass densities (kg dry weight$\cdot m^{-3}$) at pH 6 and pH 3, respectively.

Similarly, in the pH 3-batch and wash-out experiments the critical core diameter was calculated from:

$$d_{crit,pH3-batch/washout} = d_{crit,pH6-batch} \sqrt{\frac{\mu_{max,pH6}\rho_{core,pH6}c_{O2,pH3}}{\mu_{max,pH3}\rho_{core,pH3}c_{O2,pH6-batch}}} \tag{6}$$

where $c_{O2,pH3}$ is oxygen concentration in pH 3-culture at sampling.

From the core diameter distribution determined in image analysis of the culture sample the fractions of small ($d < d_{crit}$) and large ($d > d_{crit}$) pellets were determined as volume fractions. The volume fraction of the diffusion-limited biomass ($V_{limited}$, m^3) was found as:

$$V_{limited} = \frac{\pi}{6} \sum_{i=1}^{n_L} (d_{large,\,i} - d_{crit})^3 \qquad (7)$$

where n_L is number of large pellets in sample, d_{large} is core diameter of large pellets and it is assumed that the effect of curvature can be neglected.

The biomass fractions of small ($d < d_{crit}$) and large ($d > d_{crit}$) pellets were calculated from the volume fractions by multiplication with the apparent core biomass density. The biomass fraction of free hyphae was calculated by subtracting the total pellet biomass concentration from the total biomass concentration determined by OD$_{600}$ after sonication of the photographed sample. The biomass fraction of diffusion-limited pellet cores was found from $V_{limited}$ by multiplication with the core biomass density.

RESULTS

To obtain a Macro-morphology Profiling System (MPS) we determined 1) the core biomass density and 2) the critical core diameter. Firstly, we investigated the correlation between biomass and optical density after sonication of pellets. Secondly, the physiologically significant critical core diameter was determined in cultures of growing, uniformly sized pellets by monitoring decreases in specific metabolic activity using several direct and indirect measurements.

Apparent core biomass density and core biomass density

Germination of spores in shake flask cultures at pH 6 caused the spores to agglomerate, because of the relatively low shear rate in a shake flask culture. When the pH 6-batch cultures were inoculated with the germinated and agglomerated spores the morphology comprised entirely pellets (Fig. 1) of uniform size, which were used to determine the relationship between optical density and biomass in a pelletous culture in addition to the relationship between apparent core biomass density and core diameter.

Figure 2 shows a linear relationship between optical density and biomass in samples from a pelletous culture when they were sonicated to dispersed mycelium. The variation is caused by a low sample volume despite vigorous shaking before taking two aliquots of 0.5 mL for sonication followed by OD$_{600}$ measurement. Furthermore, the correlation coefficient changes as a function of DW (or culture age).
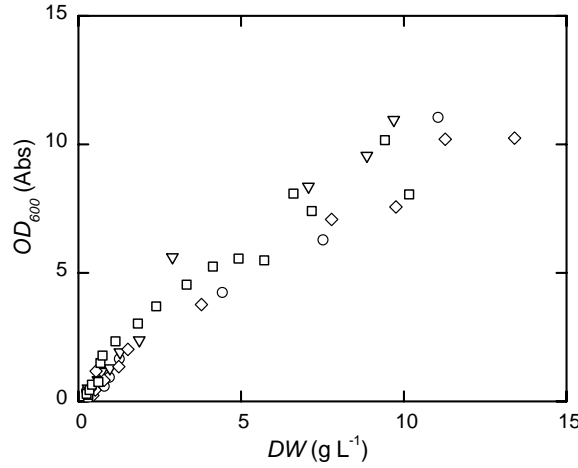
Figure 2. Correlation between optical density (OD_{600}) and dry weight (DW) of *A. niger* in four different pH 6-batch cultures of pellets only. Samples were sonicated, resulting in dispersed mycelium before measurement of OD_{600}. The different symbols correspond to different batch cultures at same culture conditions (as in Figure 1).

From the first part of the curve (until approximately 2 g dry weight·L^{-1}) the rectilinear relationship between optical density and DW (Fig. 2) was used to determine the biomass content in pellets after measurement of total core volume by image analysis. From the biomass content and total core volume we calculated the apparent core biomass density ρ_{app} of the pellets. This is an *apparent* core biomass density because the biomass in the hairy region (Fig. 1) is included in the optical density measurement of the biomass. ρ_{app} is therefore an overestimation of the density in the core and can be expressed as:

apparent core biomass density = [core biomass+hairy region biomass]/core volume (8)

Assuming that the biomass in the hairy region can be described as a concentric spherical shell around the pellet with an average density $\rho_{hairy\ region}$ (kg dry weight·m^{-3}) and a volume $V_{hairy\ region}$ (m^3) Equation 8 can be written as:

$$\rho_{app} = \frac{\rho_{core}V_{core} + \rho_{hairy\ region}V_{hairy\ region}}{V_{core}}$$ (9)

where ρ_{core} (kg dry weight·m^{-3}) is biomass density of core and V_{core} (m^3) is core volume. The inner diameter of the hairy region shell is d and the outer diameter is d plus two times the width of the hairy region $w_{hairy\ region}$ (m) as shown in Figure 1. Therefore $V_{hairy\ region}$ can be written as:

$$V_{hairy\ region} = \pi[(d + 2w_{hairy\ region})^3 - d^3]/6$$ (10)

Inserting this and V_{core} into Equation 9 we get:

$$\rho_{app} = \rho_{core} + \rho_{hairy\ region}(6w_{hairy\ region}d^{-1} + 12w_{hairy\ region}^2 d^{-2} + 8w_{hairy\ region}^3 d^{-3}) \qquad (11)$$

In the pH 6-batch culture we measured a width of the hairy region, which was independent of the core diameter: $w_{hairy\ region}$ = 0.13 mm ± 0.03 (SD) and Equation 11 becomes:

$$\rho_{app} = \rho_{core} + \rho_{hairy\ region}(0.804 mmd^{-1} + 0.216 mm^2 d^{-2} + 0.0192 mm^3 d^{-3}) \qquad (12)$$

The fit of Equation 12 to experimental data in Figure 3 shows that this segregated model is consistent with experimental results and gives $\rho_{core,pH6}$ = 25 kg·m^{-3} and $\rho_{hairy\ region,pH6}$ = 11 kg·m^{-3}. Since ρ_{core} is a constant in Equation 12 the core biomass density is independent of diameter. At small core diameters the hairy region biomass constituted a large part of the total biomass of the pellet (84% at d = 0.2 mm), but even at a diameter of 0.55 mm the hairy region comprised 50% of the pellet biomass.
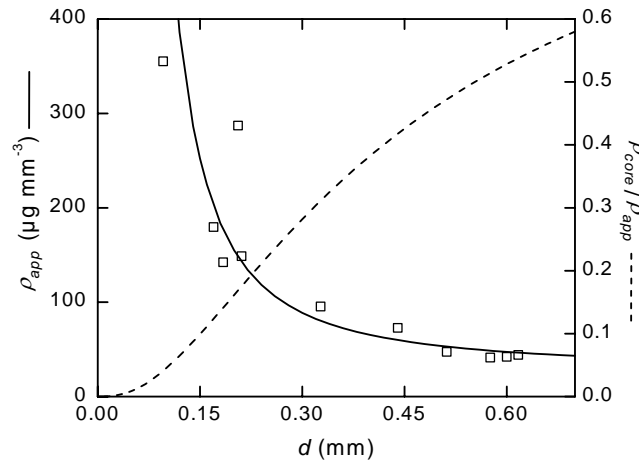
Figure 3. Correlation between apparent core biomass density (ρ_{app}) and mean diameter of pellet core (d) measured in pH 6-batch culture of *A. niger*. Solid line (——) shows Equation 12, with $\rho_{core,pH6}$ = 25 kg·m^{-3} and $\rho_{hairy\ region,pH6}$ = 11 kg·m^{-3}. Dashed line (----) shows ratio of core and apparent core biomass density. Culture conditions as in Figure 1.

Critical pellet diameter

As shown in Figure 4 the LOS plot of accumulated base, added to keep pH constant in a pH 6-batch culture, was rectilinear during the first 15-16 hours. This shows that the rate of base addition was exponential in this period. If growth and base addition are coupled base addition can be used as an indirect measurement of growth [Iversen *et al.* 1994]. Balanced growth is expected in a batch culture after a certain lag phase of 1-3 generation times (here 4-12 h). LOS plots, exemplified in Figure 4 for base addition, were performed with several other direct and several indirect measurements of growth from up to 5 different pH 6-batch experiments as shown in Figure 5. Since LOS plots of all variables gave rectilinear curves with the same slope (maximum specific growth rate) the correlation factors between the different variables

were constant and consequently they were coupled. Averages of $\mu_{max,pH6} = 0.25$ h^{-1} $\pm$ 0.04 (SD) and $d_{crit,pH6} = 0.19$ mm $\pm$ 0.08 (SD) were found. There is no significant difference (Student's t-test, 95% confidence interval) between μ_{max}-values or between d_{crit}-values determined from the different direct (OD$_{600}$ after sonication and DW) and indirect ([NH$_4^+$], OH_{add}, r_{O2} and r_{CO2}) measurements of growth except for μ_{max} determined from oxygen tension in exhaust gas. Large errors in measurements of O$_2$ consumption are inevitable because it is calculated from a small difference between two high values.
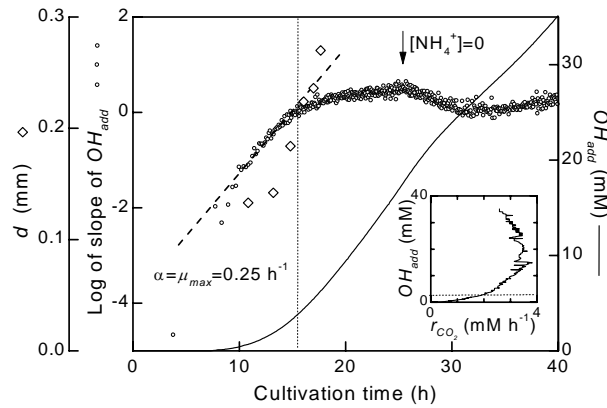
Figure 4. Pellet core diameter (d) and Log of Slope (LOS) plot of accumulated NaOH addition (OH_{add}) during pH 6-batch culture of *A. niger*. Vertical dotted line (····) indicates onset of limitation determined from LOS plot. Dashed line (----) represents linear regression to LOS plot before onset of limitation. Arrow indicates exhaustion of final cell density limiting substrate, NH$_4^+$. Inset shows concordance plot of CO$_2$ in exhaust gas (r_{CO2}) and accumulated NaOH addition. Horizontal dotted line in inset indicates onset of limitation identified from LOS plot. Culture conditions as in Figure 1.
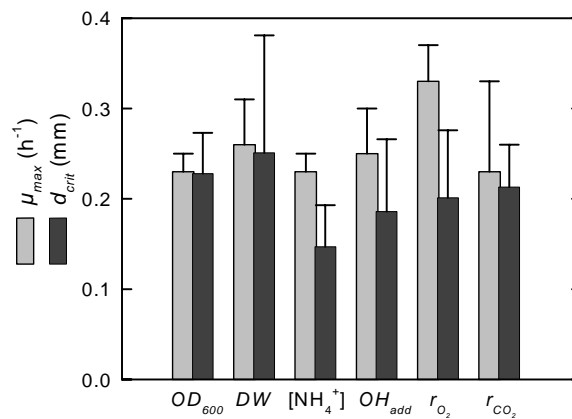
Figure 5. Critical pellet core diameters (d_{crit}) at onset of diffusion-limitation and maximum specific growth rates (μ_{max}) before onset of diffusion-limitation determined from LOS plots of different variables in pH 6-batch cultures of *A. niger* as shown in Figure 4. Error bars represent standard deviations of 5 (OD$_{600}$), 3 (DW), 3 ([NH$_4^+$]), 5 (OH_{add}), 4 (r_{O2}) and 3 (r_{CO2}) batch cultures. Average of all data: $d_{crit,pH6} = 0.19$ mm $\pm$ 0.08 (SD) and $\mu_{max,pH6} = 0.25$ h^{-1} $\pm$ 0.04 (SD). Culture conditions as in Figure 1.

After 15-16 hours the slope decreased (indicated by vertical dotted line in Figure 4), because pellets grew larger than the critical core diameter and became limited in oxygen in the centre [Cronenberg *et al.* 1994; Philips 1966; Pirt 1966; Wittler *et al.* 1986], since the final cell density limiting substrate NH$_4^+$ was exhausted much later (arrow). Also a change of

stoichiometry (or coupling) between NaOH added and CO_2 produced at the onset of limitation is seen in the concordance plot inserted in Figure 4, representing a change in physiological state for at least part of the mycelium.

Implementation of Macro-morphology Profiling System (MPS)

Figure 6 shows the macro-morphology profile of a pH 3-chemostat culture based on biomass of macro-morphology structures. The pH 3-chemostat culture comprised several morphologies. To create the macro-morphology profile we isolated pellets of approximately the same size and determined apparent core biomass density as described above: $\rho_{app,\ pH3}$ = 27.1 kg·m^{-3} ± 1.7 (SD) at d = 0.35 mm ± 0.13 (SD). The OD_{600}-DW correlation was also determined for the pH 3-cultures (results not shown), because the correlation depends on the physiological state. Since we observed the same width of hairy region (0.13 mm ± 0.05 SD) as for the pellets from the pH 6-batch culture we assumed the same distribution of biomass between the core and the hairy region as in the pH 6 culture. From the results of Figure 3 we calculate that at d = 0.35 mm the core contains 34% of the biomass, giving $\rho_{core,\ pH3}$ = 9.2 kg·m^{-3} and $\rho_{hairy\ region,\ pH3}$ = 4.0 kg·m^{-3}.
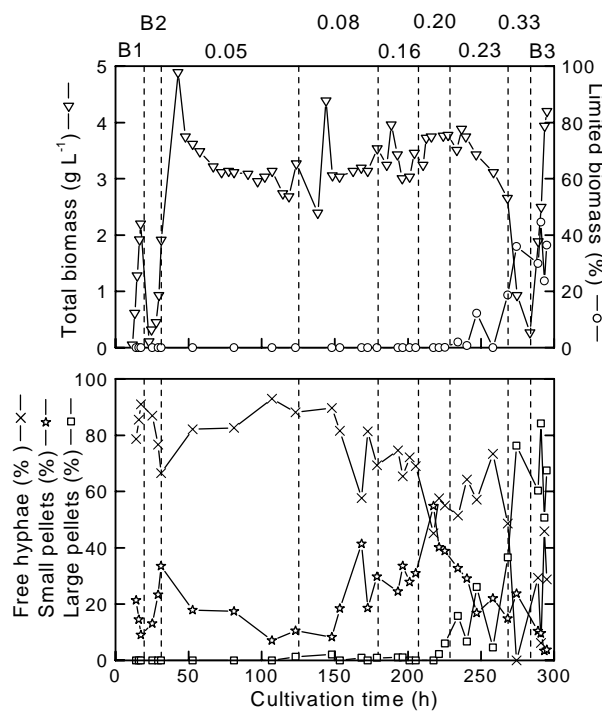
Figure 6. Dry weight (DW) of total biomass (∇) and biomass distribution in macro-morphology structures, free hyphae ($\times$), small pellets ($\star$), large pellets ($\square$), and fraction of diffusion-limited biomass (O) in batch, chemostat and wash-out cultures of *A. niger* at pH 3. Vertical dotted lines indicate change in dilution rate of medium with glucose (7.43 g·L^{-1}) as final cell density limiting substrate. Biomass distributions were calculated from pellet core diameter distribution found by image analysis combined with measurement of OD_{600} after sonication to find total biomass of photographed samples and using d_{crit} calculated in Table 1 and 2, $\rho_{core,pH3}$ = 9.2 kg·m^{-3}, $\rho_{hairy\ region,\ pH3}$ = 4.0 kg·m^{-3} and Equations 7 and 12 as explained in Materials and Methods. Culture conditions as in Table 1.

Table 1 shows critical core diameters at different dilution rates in the pH 3-chemostat culture calculated using Equation 5, whereas Table 2 shows selected critical core diameters in the pH 3-batch ($D = 0$; B1, B2 and B3) and wash-out experiments ($D = 0.23$ h^{-1} and $D = 0.33$ h^{-1}) calculated using Equation 6. The $\mu_{max,\ pH3}$ of 0.25 h^{-1} is the average between μ_{max} determined in batch (0.29 h^{-1} ± 0.01) and wash-out experiments (0.23 h^{-1} ± 0.04).

Table 1. Steady state glucose concentrations and growth yield in *A. niger* pH 3-chemostat culture[a] and critical core diam calculated using Equation 5[b]. Numbers in brackets are SD (3 determinations).

D	c_{glc}	Y_{glc}	d_{crit}
h^{-1}	μM	g·mol^{-1}	mm
0.05	8 (5)	72 (5)	0.11
0.08	8 (1)	76 (3)	0.09
0.16	15 (3)	76 (6)	0.09
0.20	41 (3)	90 (1)	0.14

[a] 30°C, 750 rpm, 0.23 vvm.
[b] $d_{crit,pH6\ ,batch} = 0.19$ mm, $D_{glc} = 2.5 \cdot 10^{-6}$ m^2·h^{-1}, $D_{O2} = 9.0 \cdot 10^{-6}$ m^2·h^{-1}, $c_{O2,\ pH6\ batch} = 0.16$ mM, $\mu_{max,pH6} = 0.25$ h^{-1}, $\rho_{core,pH6} = 25$ kg·m^{-3}, $\rho_{core,pH3} = 9.2$ kg·m^{-3}, $Y_{O2} = 43$ g dry weight·mol^{-1}.

Table 2. Oxygen concentration in *A. niger* pH 3-batch and wash-out cultures[a] and critical core diameter calculated using Equation 6[b]

Time	D	$c_{O2,pH3}$	d_{crit}
h	h^{-1}	mM	mm
16.0	0	0.16	0.31
31.1	0	0.13	0.28
237.9	0.23	0.11	0.26
268.2	0.23	0.14	0.29
274.3	0.33	0.17	0.33
282.9	0.33	0.19	0.34
288.9	0	0.15	0.31
295.0	0	0.10	0.25

[a] Culture conditions as in Table 1
[b] $d_{crit,\ pH6\ batch} = 0.19$ mm, $\mu_{max,\ pH6} = 0.25$ h^{-1}, $\rho_{core,pH6} = 25$ kg·m^{-3}, $c_{O2,\ pH6\ batch} = 0.16$ mM $\mu_{max,\ pH3} = 0.25$ h^{-1}, $\rho_{core,pH3} = 9.2$ kg·m^{-3}.

Equation 12 was used to calculate the apparent core biomass density since it depends on the core diameter (Fig. 3). Therefore, the contribution to the biomass fractions of small ($d < d_{crit}$) and large ($d > d_{crit}$) pellets in Figure 6 were calculated for each individual core diameter found in the core diameter distributions by multiplying the core volume with the corresponding apparent core biomass density.

We also observed a few large pellets with a high density ($\rho_{app,high\ density} = 89$ kg·m^{-3} ± 9 at $d = 0.54$ mm ± 0.08) and consequently low d_{crit} (approximately a factor 3 lower than the rest of the pellets, calculated from Equation 2). They were always large (>400 μm) and easily

identified on dark field images. These high density pellets comprised up to 60% of the biomass fraction of large pellets and diffusion-limited biomass.

DISCUSSION

Pellet biomass density estimated by image analysis in combination with optical density measurements

Our results showed that sonication of samples containing pellets made measurement of biomass by optical density possible (Fig. 2). Trinci [1983] also found a rectilinear relationship between optical density and biomass, but only in cultures of free hyphae. The change in correlation coefficient between OD_{600} and DW as a function of culture age was probably caused by a change in physiological state. A change in the correlation coefficient was also observed with mycelium growing as free hyphae, but was explained by increased shadowing from larger hyphal units [Trinci 1983]. The reduction in specific growth rate shown in Figure 4 occurs at a DW of 1.8 g dry weight·L^{-1}, where a change in the correlation coefficient was observed (Fig. 2). The data in Figure 2 were all obtained from culture broth sampled before the final cell density limiting substrate (NH_4^+) was exhausted. After exhaustion (data not shown) samples showed even larger changes in the correlation coefficient confirming that it was dependent on the physiological state of the fungi. Absorbance due to light scattering may have changed because of increased vacuolization and/or accumulation of storage compounds. Transects of pellets showed that pellets in this study were without a hollow core.

Biomass measurement by optical density is three orders of magnitude more sensitive than drying followed by weighing. Therefore biomass could be measured in samples sufficiently small for detailed image analysis of the entire sample. This enabled us to determine the apparent core biomass density (Fig. 3).

Segregated pellet model

A segregated model of the pellet was developed, describing the pellet as a core surrounded by a concentric spherical shell. The pellet core is defined as the central part without any visible void volume on the image [Cox and Thomas 1992; Wittler *et al.* 1986]. The concentric spherical shell is the hairy region. We have to use the apparent core biomass density as a "temporary" variable because the biomass in the hairy region is impossible to exclude in measurement of the pellet biomass. The segregated model enabled us to find the biomass density of the pellet core and of the hairy region. The latter was surprisingly high, which could easily lead to overestimation of the core biomass density and to the (perhaps erroneous) conclusion that core biomass density decreases with increasing pellet diameter. Although Figure 3 contains too little information to completely reject such a possibility, the results support that core biomass density is independent of diameter. In addition it suggests a large

contribution from the hairy region even at relatively large pellet diameters. The apparent core biomass densities found in this study were in the range of others for filamentous fungi [Cui *et al.* 1997; Trinci 1970; Yano *et al.* 196].

Critical pellet core diameter

The critical pellet core diameter (0.19 mm) was determined in pH 6-batch cultures, where the only morphology present was pellets of uniform size. Also Carlsen *et al.* [1996b] found pellets as the (predominant) morphology at pH>5. In this study we identified the onset of limitation as a deviation from exponential growth by LOS plots of several different direct and indirect measurements of growth (Figs. 4 and 5) giving identical critical core diameters. The LOS plot as exponential analysis method was crucial for these findings because it makes detection of small, sudden changes in the rate constant possible. Since all different methods for measurements of growth gave the same μ_{max} (slope in the LOS plot) before the onset of limitation the variables were coupled and we therefore define the growth in the exponential phase as balanced. The coupling of the direct and indirect measurements of growth until the onset of limitation validates the use of the indirect measurements for determination of d_{crit} and μ_{max}, and also indicated that d_{crit} was a *physiologically significant* critical diameter. Therefore above this diameter the mycelium, or part of it, was at a different physiological state. The critical diameters found in this study were comparable to values previously reported in literature [Cronenberg *et al.* 1994; Pirt 1966; Wittler *et al.* 1986] although our definition is different. Both calculations [Pirt 1966] and measurements [Cronenberg *et al.* 1994; Pirt 1966; Wittler *et al.* 1986] have shown that the diffusion-limiting substrate is oxygen at the conditions in the pH 3-batch and wash-out cultures. However, in the chemostat culture at the low steady state glucose concentrations observed here glucose is the diffusion-limited substrate resulting in 2-3 times lower estimated critical diameters as it is seen from Tables 1 and 2.

For calculation of the critical diameter in the pH 3-chemostat culture we assumed that the effective diffusion factor f_{eff} is the same as in the pH 6-batch culture. As described in Materials and Methods f_{eff} may depend on physical properties turbulent diffusion, tortuosity and pellet porosity. A prerequisite for turbulent diffusion is free liquid movement, which was excluded in the core by Wittler *et al.* [1986]. Molecular diffusion depends on porosity because the space occupied by the hyphae is unavailable for diffusion. We have measured different core densities in the pH 6-batch cultures and pH 3-chemostat culture, but this corresponds to only minor differences in porosity, since only a small volume fraction is occupied by hyphae in the pellet. By image analysis in combination with OD_{600} measurement we measured the biomass per hyphal length at pH 3 to 4.4 µg dry weight·m^{-1} ± 1.1 (SD). The hyphal diameter was 4 µm. If the hypha is described as a cylinder, the hyphal volume per biomass is 2.9 mL·g dry weight^{-1}. Assuming a similar value at pH 6 and using the core biomass densities determined here the hyphae occupy only 7 and 3% of the volume, resulting in a porosity of 0.93 and 0.97 in the pH 6-batch cultures and pH 3-chemostat culture, respectively. Most of the pellet core volume is therefore occupied by medium in both cases and the difference is

unlikely to have a significant effect on molecular diffusion. Tortuosity depends on the hyphal structure in the pellet restricting diffusion to occur only in allowed directions [Bailey and Ollis 1986]. Also the effect of tortuosity is most likely low because of a low hyphal volume fraction. In addition, no obvious difference in hyphal branching in the hairy region was observed between the pH 6-batch and pH 3-chemostat cultures. Therefore, it is likely that the structure and the effect of tortuosity in the pellets are similar in both cultures.

Therefore, in the calculation of the critical core diameter we used only the core biomass density and omitted indirect effects of the core biomass density on molecular diffusion. However we included the direct effect of the core biomass density on the volumetric consumption rate ($\rho \cdot \mu / Y$) of the diffusion-limited substrate as seen from Equations 5 and 6.

Formation of pellets and diffusion limited biomass

If the fraction of diffusion-limited biomass inside large pellets is significantly large, the culture becomes inhomogeneous making any interpretation of results difficult or impossible. The fraction of diffusion-limited biomass was insignificant at all dilution rates lower than the apparent critical dilution rate between 0.22 h^{-1} and 0.23 h^{-1} above which wash-out occurs (Fig. 6). The apparent critical dilution rate was lower than expected from measurements of μ_{max} in batch cultures, where the only morphology was free hyphae (0.29 h^{-1} ± 0.01), but was of the same value as determined from wash-out experiments, where μ_{max} (0.23 h^{-1} ± 0.04) was measured from subtraction of the biomass wash-out rate from the dilution rate [Jannasch 1969]. The reason was most likely formation of large pellets resulting in diffusion limited biomass as shown in Figure 6. Diffusion limited biomass is not growing exponentially and therefore wash-out occurs.

Pellets are formed by aggregation of spores or hyphae or by growth of filaments [Metz and Kossen 1977]. We assume that the high density pellets were older than the rest of the pellet population, since they have probably been formed either by longer exposure to shear stress (stirring) or by growth. A longer residence time of some pellets is inevitable in a chemostat. Sampling at the outlet and at different locations in the bioreactor showed that no tendency to retain pellets. It is unlikely that the high density pellets originate from wall growth, since this was virtually absent in the Variomixing bioreactor [Larsen *et al.* 2003]. Also high dilution rates at the beginning of a continuous culture resulted in pellet formation and wash-out (results not shown). The increase of the specific growth rate/shear stress ratio might explain the increase of the pellet fraction with increasing dilution rate shown in Figure 6. Righelato *et al.* [1986] and Wiebe and Trinci [1991] also observed this phenomenon.

In conclusion, by combination of image analysis, measurement of core biomass densities and the critical diameter determined in the pH 6-batch cultures we have developed a novel quantitative characterisation, the macro-morphology profile of a pH 3-chemostat culture comprising several morphologies. The Macro-morphology Profile System (MPS) is a quantitative description of biomass distribution in free hyphae, in pellets with core diameters

smaller and larger than the critical core diameter and in diffusion-limited biomass inside pellets larger than the critical core diameter.

Pellet formation as explanation for decreased maximum specific growth rate in pelletous chemostat cultures is one example of the virtue of MPS in the interpretation of results from submerged fungal cultures. Another example is the identification and quantification of diffusion-limited biomass, which if neglected in physiological studies may lead to erroneous conclusions. Therefore MPS can be an important tool in applications where a more detailed understanding of the interplay between morphology and cellular activity is crucial for process optimization.

ACKNOWLEDGMENTS

REFERENCES

Bailey JE, Ollis DF (1986) Biochemical engineering fundamentals, 2nd ed. McGraw-Hill, Singapore.

Bergmeyer HU, Bernt E, Schmidt F, Stork H (1974) Determination with hexokinase and glucose-6-phosphate dehydrogenase. p. 1196-1201. In H. U. Bergmeyer (ed.) Methods of enzymatic analysis, vol. 3, 2nd ed. Weinheim: Verlag Chemie.

Bergmeyer HU, Beutler HO (1985) Ammonia, p 454-461. In H. U. Bergmeyer (ed.) Methods of enzymatic analysis, vol. 8, 3rd ed. Weinheim: VCH.

Carlsen M, Nielsen J, Villadsen J (1996a) Growth and alfa-amylase production by *Aspergillus oryzae* during continuous cultivations. J Biotechnol 45: 81-93.

Carlsen M, Spohr AB, Nielsen J, Villadsen J (1996b). Morphology and physiology of an alfa-amylase producing strain of *Aspergillus oryzae* during batch cultivations. Biotechnol Bioeng 49: 266-276.

Cox PW, Thomas CR (1992) Classification and measurement of fungal pellets by automated image analysis. Biotechnol Bioeng 39: 945-952.

Cronenberg CCH, Ottengraf SPP, van den Heuvel JC, Pottel F, Sziele D, Schügerl K, Bellgardt KH (1994) Influence of age and structure of *Penicillium chrysogenum* pellets on the internal concentration profiles. Bioproc Eng 10: 209-216.

Cui YQ, van der Lans RGJM, Luyben KCAM (1997) Effect of agitation intensities on fungal morphology of submerged fermentation. Biotechnol Bioeng 55: 715-726.

Cui YQ, van der Lans RGJM, Luyben KCAM (1998) Effects of dissolved oxygen tension and mechanical forces on fungal morphology in submerged fermentation. Biotechnol Bioeng 57: 409-419.

Degn H, Nielsen JB (1987) A general purpose serial interphase for the laboratory computer. Binary 10: 25-28.

Iversen JJL, Thomsen JK, Cox RP (1994) On-line growth measurements in bioreactors by titrating metabolic proton exchange. Appl Microbiol Biotechnol 42: 256-262.

Jannasch HW (1969) Estimations of bacterial growth rates in natural waters. J Bacteriol 99: 156-160.

Larsen B, Poulsen BR, Eriksen NT, Iversen JJL (2003) Homogeneous batch cultures of *Aspergillus oryzae* by elimination of wall growth in the Variomixing bioreactor. Appl Microbiol Biotechnol *In press*.

Mackereth FJH (1964) An improved galvanic cell for determination of oxygen concentration in fluids. J Sci Instrum 41: 38-41.

Metz B, Kossen NWF (1977) The growth of molds in the form of pellets a literature review. Biotechnol Bioeng 19: 781-799.

Paul G.C, Thomas CR (1998) Characterisation of mycelial morphology using image analysis. In T. Scheper (ed.), Advances in Biochemical Engineering/Biotechnology, vol. 60. Springer-Verlag, Berlin.

Pazouki M, Panda T (2000) Understanding the morphology of fungi. Bioproc Eng 22: 127-143.

Philips DH (1966) Oxygen transfer into mycelial pellets. Biotechnol Bioeng 8: 456-460.

Pirt SJ (1966) A theory of the mode of growth of fungi in the form of pellets in submerged culture. Proc Roy Soc B 166: 369-373.

Pontecorvo G (1953) The genetics of *Aspergillus nidulans*. p 141-238. In M. Demerec (ed.), Advances in genetics, vol. 5. Academic Press, New York.

Poulsen BR, Ruijter GJG, Visser J, Iversen JJL (2003) Determination of first order rate constants by natural logarithm of the slope plot exemplified by analysis of *Aspergillus niger* in batch culture. Biotechnol Lett 25: 565–571.

Righelato RC, Trinci APJ, Pirt SJ (1968) The influence of maintenance energy and growth rate on the metabolic activity, morphology and conidiation of *Penicillium chrysogenum*. J Gen Microbiol 50: 399-412.

Treskatis SK, Orgeldinger V, Wolf H, Gilles ED (1997) Morphological Characterisation of filamentous microorganisms in submerged cultures by on-line digital image analysis and pattern recognition. Biotechnol Bioeng 53: 191-201.

Trinci APJ (1970) Kinetics of the growth of mycelial pellets of *Aspergillus nidulans*. Arch Mikrobiol 73: 353-367.

Trinci APJ (1983) Effect of junlon on morphology of *Aspergillus niger* and its use in making turbidity measurements of fungal growth. Trans Br Mycol Soc 81: 408-412.

Vishniac W, Santer M (1957) The Thiobacilli. Bacteriol Rev 21: 195-213.

Wiebe MG, Trinci APJ (1991) Dilution rate as a determinant of mycelial morphology in continuous culture. Biotechnol Bioeng 38: 75-81.

Wimpenny JWT (1969) Oxygen and carbon dioxide as regulators of microbial growth and metabolism. p. 161-197. In Meadow P and Pirt SJ (ed.) Microbial Growth, Nineteenth Symposium of the Society for General Microbiology. London: Cambridge University Press.

Wittler R, Baumgartl H, Lübbers DW, Schügerl K (1986) Investigations of oxygen transfer into *Penicillium chrysogenum* pellets by microprobe measurements. Biotechnol Bioeng 28: 1024-1036.

Yano T, Kodama T, Yamada K (1961) Fundamental studies on the aerobic fermentation, Part VIII. Oxygen transfer within a mold pellet. Agr Biol Chem 25: 580-584.

Yoshida T, Shimizu T, Taguchi H, Teramoto S (1967) Studies on submerged culture of basidiomycetes (III) The oxygen transfer within the pellets of *Lentinus edodes*. J Ferment Technol 45: 1119-1129.

<div align="right"># Chapter 5</div>

Fast response filter module with plug flow of filtrate for on-line sampling from submerged cultures of filamentous fungi

ABSTRACT

Automatic and accurate sampling is both convenient and sometimes necessary to obtain detailed information about cell cultures. We developed an autoclavable sampling system in which culture broth was pumped through an ultrafiltration cross-flow module with a novel filtrate collecting principle and a novel regulation of filter back pressure. Filtrate was collected from equal membrane filter areas through holes connected to channels with an even length to the collecting point, resulting in a near plug flow of filtrate and a reduction in the response time to 1 min (98% of full signal of the tracer molecule glucose). Constant pressure difference (0.3 bar) across the membrane filter (30 kDa cutoff value) and prevention of leakage was obtained by squeezing the tubing with culture broth between two flexible spring steel plates fixed at one corner (filtrate flow 1 mL·min^{-1}). The large contact area allowed the tubing to open the passage more when pressure increased. Using this design of sampling system, the metabolite profiles of *Aspergillus niger* wild type and a phosphofructokinase overexpressing strain (three times wild type) were concluded to be indistinguishable by detailed monitoring of fast transients of substrates and products in batch culture and glucose pulse experiments. The combination of the fast response filter module and prevention of high pressure peaks with the flexible resistance to flow enables long-term (>5 days) and automatic monitoring of cultures of filamentous fungi or other microorganisms with fast changes in extracellular concentrations.

INTRODUCTION

On-line sampling systems

Characterization of cell cultures of different strains and conditions requires detailed information about time dependent concentrations of substrates and products. This calls for frequent sampling and therefore an automated sampling system. In addition, a feedback regulation requires an on-line sampling system in combination with analysis by, e.g., GC, HPLC, MS or flow-injection analysis (FIA). Also, by intelligent on-line analysis of data it is possible to obtain a high sampling frequency only when this is required.

In MIMS (membrane inlet MS [Kotiaho and Lauritsen 2002]), ROBIN (rotating ball inlet [Ørsnes et al. 1998]) and SLM (supported liquid membrane [Megerska et al. 2001]) culture and analysis system is separated by a membrane, a rotating ball and a porous membrane impregnated with a water immiscible solvent, respectively. However, an on-line sampling system where a sample volume of culture broth is withdrawn and saved, requires inactivation by addition of inhibitor [Håkanson et al. 1991] or more often by separation of cells from the broth. Separation can be performed by filtration [Schügerl et al. 1991], microdialysis [Marko-Varga et al. 1993] or centrifugation [Turner et al. 1993]. Removal of cells by microfiltration is sufficient for preparation of samples for FIA, but for on-line HPLC analysis, an ultrafiltration step for removal of macromolecules can be necessary to prevent clogging of the analytical column. Therefore, and because we expected less clogging from a small pore filter, ultrafiltration was chosen for the on-line sampling system in this study.

Filtration

It is obviously important to prevent clogging of the membrane filter when using it in an on-line sampling system. Two processes can cause the filtration flow to decline with time and limit the lifetime of a membrane filter (membrane clogging): fouling, which is blocking of membrane pores by material or collapse of pores, and concentration polarization, which is a build-up of retained species larger than the pore size at the suspension side of the filter. Concentration polarization can be minimised by low pressure difference across the membrane, cross-flow filtration and turbulent cross-flow. Cross-flow gives an additional advantage when the liquid to be filtrated contains suspended particles (e.g. cells) called the "Tubular Pinch Effect": the suspended particles have a tendency to pinch each other off the membrane. Membrane fouling can be diminished by using an anisotropic membrane, which consists of two layers. At the suspension side there is a thin skin with a small pore diameter. The rest of the filter is an open substructure of progressively larger voids, largely open to the filtrate side of the filter ensuring that most of the particles which pass through the pores of the thin skin also leave the membrane again.

For the purpose of sampling from bioreactors prevention of contamination is important and the filtrate unit is placed either directly inside the bioreactor or outside in an external loop (as in Fig.1). The cells may be harmed or inhibited irreversibly if the culture

broth is pumped through an external loop because of physical stress or because the growth conditions in the external loop differ from the growth conditions in the bioreactor (e.g. depletion of oxygen). However, with the filter unit inside the bioreactor it is impossible to ensure a turbulent flow at the filter surface, the filter easily clogs and it is difficult to replace.

Therefore, if residence time in the external loop is sufficiently reduced this configuration is preferred. Short residence times are achieved by a high liquid velocity and a low volume of the external loop, i.e. sampling system installed close to the bioreactor. A high liquid velocity might result in high physical stress and damage sensitive cells such as plant cells. However, since plant cells grow slowly, resulting in low consumption rates of nutrients, longer residence times in the external loop are allowed and in those cases the liquid velocity can be reduced. Fast growing cells such as bacteria require low residence times in the external loop. However, they are less sensitive to physical stress. Reduction of physical stress is also possible by choosing the right pump. This subject is relatively unexamined but peristaltic pumps have been used for shear-sensitive algae [Eriksen and Iversen 1997].
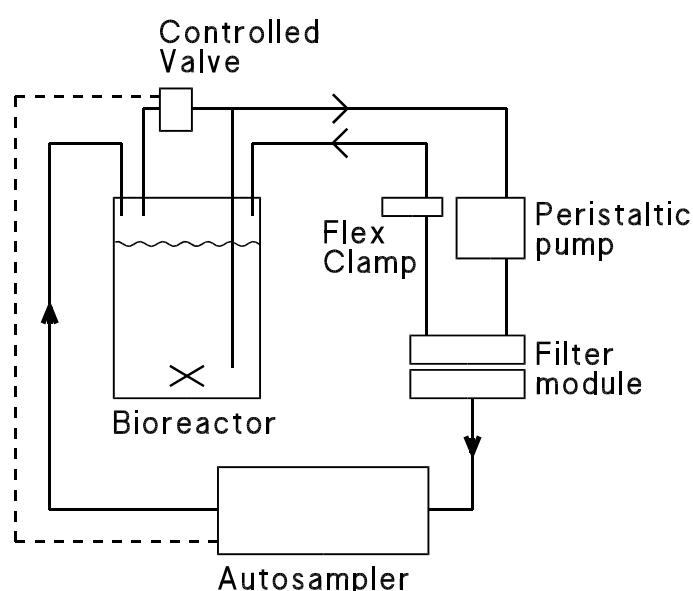
Figure 1. Schematic of sampling system with filtrate flow regulation via Flex Clamp and interval pumping via controlled valve (dashed line shows electrical connection). Flex Clamp is resistance against flow and creates filter back pressure. Filtrate side and suspension side stainless steel parts of autoclavable filter module is shown.

In this study we developed an autoclavable on-line sampling system for submerged cultures of microorganisms including filamentous fungi by pumping the broth through a fast response, cross-flow filter module designed according to a novel principle for filtrate collecting channels.

As an example, the sampling system was used for detailed comparison of batch cultures and glucose pulse experiments of *A. niger* wild type and a strain overexpressing phosphofructokinase [Ruijter *et al.* 1997] designed to have increased glycolytic flux presumably influencing secretion of polyols and organic acids.

EXPERIMENTAL

Strains and culture conditions

As the wild type strain we used A. *niger* NW 131 (*csp*A1 *gox*C17), which is a glucose oxidase negative strain with short conidiophores. The phosphofructokinase (PFK, EC 2.7.1.11) overexpressing strain 49-11 (*csp*A1 *gox*C17 *pyr*A$^+$ *pfk* 4-5 copies) has a PFK activity of about three-fold the wild type activity [Ruijter *et al.* 1997]. Both strains are derived from strain N400 (CBS 120.49)

All chemicals were of analytical grade and deionised water (>18 MΩ·cm^{-1}) was used. Spores were harvested with 2×10 mL 0.05% (w/v) Tween-80 and 5-10 sterile glass beads (ca. 2 mm diameter) from cultures grown at 30°C on complete medium (modified from [Pontecorvo 1953]), which contained per litre: 6.0 g NaNO$_3$, 1.5 g KH$_2$PO$_4$, 0.5 g KCl, 0.5 g MgSO$_4$·7H$_2$O, 2.0 g trypticase peptone, 1.0 g casamino acids, 1.0 g yeast extract, 0.5 g yeast ribonucleic acids, 10 g glucose, 15 g agar, 1.0 mL trace metal solution and 2.0 mL vitamin solution. pH was adjusted to 6. The trace metal solution (modified from Vishniac and Santer [1957]) contained per litre: 1.47 g CaCl$_2$·2H$_2$O, 0.32 g CoCl$_2$·6H$_2$O, 0.32 g CuSO$_4$·5H$_2$O, 1.0 g FeSO$_4$·7H$_2$O, 1.23 g MnCl$_2$·6H$_2$O, 0.22 g (NH$_4$)$_6$Mo$_7$O$_{24}$·4H$_2$O, 4.4 g ZnSO$_4$·7H$_2$O and 10.0 g EDTA. EDTA and ZnSO$_4$ were brought in solution together and pH adjusted to 6 with concentrated NaOH, each of the other components were added one at a time and pH adjusted to 6 after each addition. Finally, pH was lowered to 4.0 with HCl. The vitamin solution contained per litre: 0.10 g thiamine-HCl, 1 g riboflavin, 0.10 g *p*-aminobenzoic acid, 1 g nicotinamide, 0.50 g pyridoxine-HCl, 0.10 g pantothenic acid and 0.020 g biotin.

Submerged cultures were grown in a 3 L bioreactor, jacketed vessel BTS06 (Applikon) with a maximum working volume of 2.7 L and equipped with temperature, pH, dissolved oxygen tension and stirring control.

Phenotypic characterisation of the two strains was done in batch cultures at 30°C with 55 mM (1%) glucose and in 5 mM glucose pulse experiments added in stationary phase. Two hours after exhaustion of the initial 55 mM glucose the first pulse of 5 mM glucose was given. Two hours after exhaustion of the first glucose pulse a second one was given. In addition to glucose the medium contained per litre: 1.2 g NaNO$_3$, 0.5 g KH$_2$PO$_4$, 0.2 g MgSO4·7H$_2$O, 0.5 g yeast extract and 0.2 mL trace metal solution. pH was adjusted to, and in the bioreactor controlled at 6. The airflow was 0.2 vvm and the dissolved oxygen tension was kept above 30% of air saturation by addition of O$_2$. The stirrer speed was 750 rpm.

A 1 L Erlenmeyer flask containing 300 mL medium was inoculated with 2.5·10^9 spores corresponding to a final level of 10^6 spores per mL culture liquid in the bioreactor and incubated at 30°C in a rotary shaker at 200 rpm for 5-7 hours. To remove large agglomerates in the inoculum it was filtrated through a Nylon grid with a pore size of about 250 μm before being transferred to the bioreactor. The number of germinated spores removed by filtration was estimated around 20%.

An amount of 0.15 mL polypropyleneglycol (P 2000, Fluka) per litre was added as antifoam in the bioreactor. At the end of each batch culture a contamination check on plates of complete medium was performed.

Sampling

An automated on-line ultrafiltration sampling system was designed and used to obtain filtrate samples at a predetermined frequency (Fig. 1). The filter module was autoclavable and consisted of filtrate and suspension parts in stainless steel bolted together. The peristaltic pump was a Bio 2000 TC (Bio-Flo) with a 9 mm × 2 mm tubing. The rest of the tubing was a 5 mm × 1.5 mm silicone tubing on the suspension side and a capillary Teflon tubing with an internal diameter of 1 mm on the filtrate side. Filter membrane was an anisotropic YM30 Diaflo ultrafiltration membrane of inert regenerated cellulose (Amicon) with a molecular weight cutoff value of 30,000 Dalton and a diameter of 90 mm. It was cleaned after each batch culture with a 5% Decon-90 (Decon) solution and light scrubbing with a vinyl glove.

Suspension flow through the sampling system was 300 mL·min^{-1} with a residence time of 10 s and by applying a pressure difference across the membrane of approximately 0.3 bar a filtrate flow of approximately 1 mL·min^{-1} was obtained. A programmable autosampler (Gilson) was set at predetermined sampling frequency and sampling time. The sample vials were preloaded with sodium azide corresponding to 0.05% in the sampled volume (1 mL) to prevent microbial activity. Un-sampled filtrate was led back into the bioreactor through an inlet in the top plate. Both here and at the sample vial, it was possible to count the number of drops per time from which the filtrate flow was determined.

Filter module and tubing in the sampling system was filled with water and submerged while autoclaving. To prevent damage of the membrane, contact between suspension side of the membrane and steel part during autoclaving was prevented by inserting cone-shaped plastic tips between the two steel parts. After autoclaving, the tips were removed and bolts were tightened.

Response time was measured by abruptly increasing or decreasing the concentration of glucose in the suspension liquid. The response time was defined as the time required to achieve 98% of full signal.

Mycelium samples were collected by filtration in a funnel with a glass sintered filter. After washing, the mat of mycelium was frozen in liquid nitrogen. Dry weight (DW) samples were washed three times in distilled water. Samples for measurement of enzymes were washed once with 50 mM potassium phosphate buffer, pH 7. Samples for measurement of intracellular polyols were not washed since this can cause loss of up to 60% of the intracellular polyols [Witteveen *et al.* 1994]. Sampling for intermediary metabolites was done directly into a methanol solution at -40°C for inactivation [Ruijter and Visser 1996].

Analysis

Dry weight samples were lyophilised and weighed. Glucose was determined either by glucose test strips (Roche), by HPLC analysis or enzymatically essentially as described in [Bergmeyer *et al.* 1974]. Nitrate was detected by nitrate/nitrite test strips (Merck). Citric acid was either determined enzymatically according to [Möllering 1985] in 75 mM glycylglycine and 0.1 mM $ZnSO_4$, pH 7.8 or by HPLC analysis.

Glucose, polyols and organic acids were determined by HPLC analysis using a Dionex system. For glucose and polyols, an anion-exchange CarboPac MA1 column (Dionex) was used. Elution was isocratic at 0.4 mL·min^{-1} with 0.48 M NaOH and amperometric detection. For organic acids an Aminex ion exclusion HPX-87H column (Biorad), thermostated at 50°C was used. Elution was isocratic at 0.5 mL·min^{-1} with 25 mM HCl and detection by UV at 210 nm and refractive index.

Extraction of enzymes and enzyme assays were performed as described in Ruijter *et al.* [1997]. Protein concentration in extracts was determined after denaturation and precipitation of protein with sodium deoxycholate and trichloroacetic acid [Bensadoun and Weinstein 1976] using the BCA method as described by the manufacturer (Sigma). Intracellular polyols were extracted from mycelium according to Witteveen *et al.* [1994]. Extraction and determination of intermediary metabolites were performed as described in Ruijter and Visser [1996].

RESULTS AND DISCUSSION

Response time measured in a previously constructed filter module [van de Merbel *et al.* 1994] was too slow for monitoring of submerged microbial cultures. Therefore a principle for construction of filtrate collecting channels to reduce response time was developed and implemented in an on-line sampling system together with a flexible clamp for creation of filter back pressure. The sampling system was tested on *A. niger* cultures.

Construction of filtrate collecting channels

The idea for construction of filtrate collecting channels in the filter module originated from the venous system of biological tissue (Fig. 2), from which it appeared that an ideal membrane filter would be a half sphere with the filtrate collected in the centre. However, ultrafiltration membranes are produced as flat discs. Therefore, the system was transformed to two dimensions. A guideline for construction of filtrate collecting channels was derived using the following principle for collection of filtrate: "the flow time of filtrate to the collecting point should be independent of location on the filter". Therefore,

$$t_{flow} = constant \tag{1}$$

where t_{flow} (s) is the flow time of filtrate through a filtrate collecting channel; it is the length of the channel l (m) divided by the liquid velocity v_L (m·s^{-1}) through the channel:

$$t_{flow} = l/v_L \qquad (2)$$

The liquid velocity is the flow through the channel F (m^3·s^{-1}) divided by the cross sectional area of the channel A_{cross} (m^2):

$$v_L = F/A_{cross} \qquad (3)$$

The flow through the channel is the filtrate flux through the membrane filter J (kg·s^{-1}·m^{-2}) times the area of the filter $A_{collect}$ (m^2) from which the channel collects filtrate:

$$F = J \cdot A_{collect} \qquad (4)$$

Combining Equations 2, 3 and 4 gives:

$$t_{flow} = l \cdot A_{cross}/\ J \cdot A_{collect} \qquad (5)$$

Combining Equations 1 and 5 and assuming that the filtrate flux is constant over the entire membrane filter gives:

$$l \cdot A_{cross}/\ A_{collect} = constant \qquad (6)$$

This implies that if, e.g. the length of one filtrate collecting channel is double compared to another either the cross sectional area should be half or the area from which the channel collects filtrate should be double.
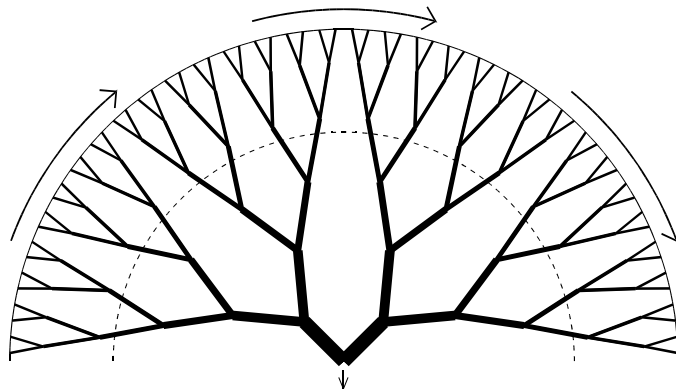
Figure 2. Cross section of ideal spherical filter system, which resembles venous system of biological tissue. Total cross sectional area of channels is equal at any radius (exemplified by dashed line). Large arrows show flow of suspension. Small arrow shows flow of filtrate.

In the construction of the channels we kept both l, A_{cross} and $A_{collect}$ constant, because this is the most convenient way to implement the above derived relation and because it is difficult to predict effects from e.g. resistance against flow in channels of different sizes, which will also

depend on fluidity of the filtrate. By keeping all three variables constant at each level of branching of the filtrate collecting channels, we ensured that the principle for collection of filtrate through the channels described above was approximately fulfilled. The approximation to the principle is better the more the channels are branched.
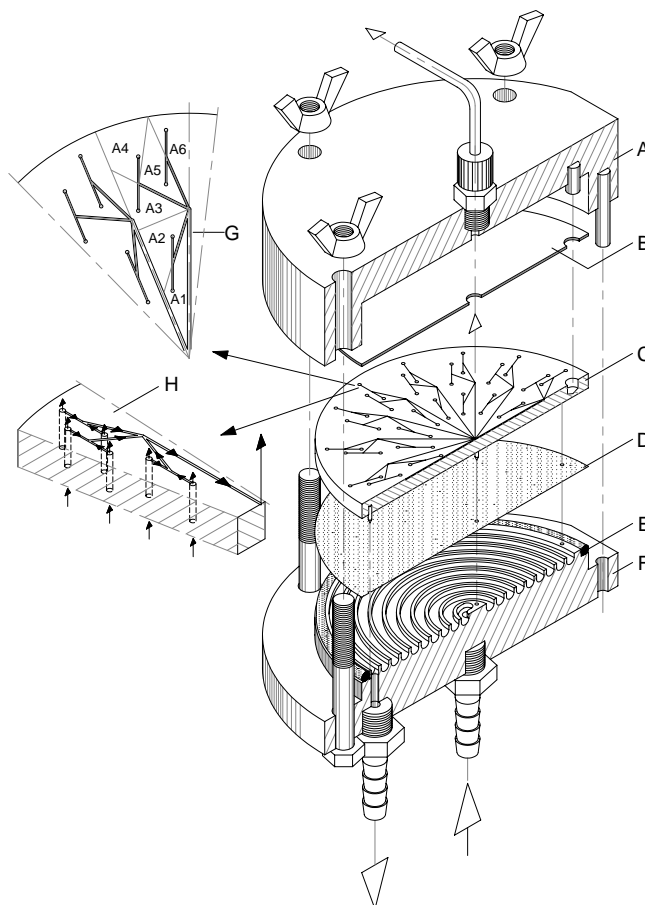
Figure 3. Cross section of fast response, autoclavable filter module. Outer diameter 120 mm. Large arrows and small arrows show suspension and filtrate flow, respectively. **A:** Stainless steel part on filtrate side. Short pin (4×8 mm) ensures correct alignment of rubber seal (**B**) and channel disc (**C**). Large pin (4×25 mm) ensures correct assembly with stainless steel part on suspension side (**F**). **B:** Rubber seal (Viton, 90×0.5 mm). **C:** Channel disc (PSU, 90.3×6 mm). Three pins (1×6 mm) ensure consistent positioning of membrane. **D:** Ultrafiltration membrane (YM30 Diaflo, Amicon). **E:** Rubber O-ring (Viton, 84.3×3 mm). **F:** Stainless steel part on suspension side, where suspension flows in a loop in a semicircular groove (3 mm diameter).**G:** Top view of enlargement of channel disc (**C**). Channels are engraved into channel disc. Channels begin at holes, which collect filtrate from approximately equal areas (**A1-A6**) and channel lengths from holes to centre are equal - ensuring approximately same flow time from each hole to centre. **H:** Enlargement of channel disc showing filtrate flow.

The module constructed in this study is shown in Figure 3. The result of a three level branching is shown in the enlargement of a section of the channel disc in Figure 3G. The channels were engraved into the channel disc and started at holes leading to the filtrate side of the membrane. The membrane areas (A1-A6 in Fig. 3G) from which the holes collect filtrate were approximately equal, giving the same filtrate flow in holes and channels. Furthermore, the holes were placed approximately in the centre of mass of the membrane area from which

they collect filtrate. The channel lengths from the holes to the collecting point were equal. This resulted in equal flow time from anywhere on the membrane filter to the collecting point or in other words resulted in plug flow of filtrate through the filter module.

The design of the filtrate collecting channels was based on the assumption of a constant filtrate flux over the entire membrane filter. This was confirmed by measuring the filtrate flux with only certain holes in the channel disc open. The filtrate flux was always proportional to the number of open holes.

Response times

As seen in Figure 4 the response time measured with the filter module used by van de Merbel *et al.* [1994] was too long (>15 min) to monitor rapid changes in concentrations of substrates and products at e.g. depletion of the limiting substrate in batch cultures. Therefore the principle described above was used to design filtrate collecting channels of new filter modules. A module with only one branching level with eight branches (details not shown) had a significantly decreased response time of 4 min, which was decreased further to 1 min when three branching levels with 16, 3 and 2 branches, respectively (Fig. 3), was used. A response time of 1 min is sufficiently low for monitoring of submerged microbial cultures.
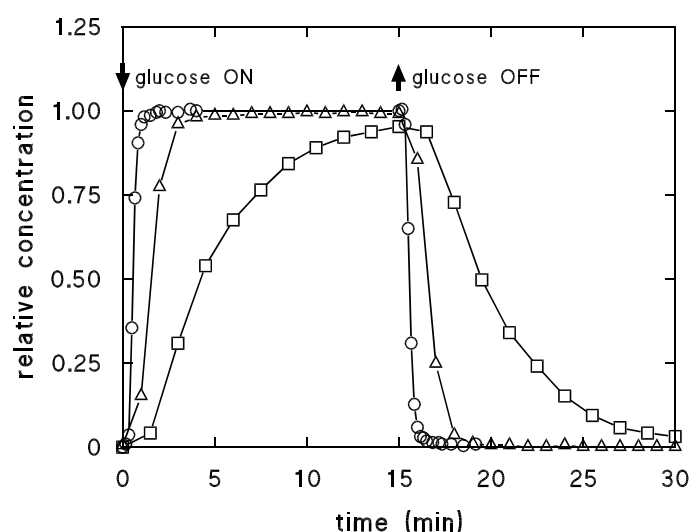
Figure 4. Response time measurements of filter modules. (□) Module used by van de Merbel *et al.* [1994] without branching of filtrate collecting channel and large dead volume of filter support; response time >15 min. (Δ) Module having 1 branching level of filtrate collecting channels with 8 branches; response time = 4 min. (O） Module shown in Fig. 3 having 3 branching levels with 16, 3 and 2 branches, respectively; response time = 1 min. Response times measured with 1 mL·min^{-1} filtrate flow. At time 0 and 15 min suspension liquid was changed instantaneously between water and a solution of glucose (0.40 g·L^{-1} = 2 mM).

The slow response time of the module used by van de Merbel *et al.* [1994] was partly caused by a large dead volume of the filtrate, which was 3 mL compared to 0.37 mL and 0.29 mL in the modules with 1 and 3 branching levels, respectively. However, since the latter two modules have approximately the same dead volume, their different response times are most likely only caused by their different degree of branching of the filtrate collecting channels.

It would also have been possible to decrease the response time by increasing the filtrate flow. However, this would increase the risk of membrane clogging. It should be noted that the response time measurements were done with the physiologically relevant molecule glucose, which has a tendency to adsorb to many different materials.

Response times of other cross-flow filter modules are around 10 min [Kroner and Kula 1984]. Garn *et al.* [1989] measured a response time of 10 s at 90% of full signal using a dye as tracer molecule in a Millipore designed module. The fast response time is caused by the small size, which unfortunately makes it unsuitable for filamentous microorganisms. We found approximately the same membrane area to response time ratio. If a lower sample volume than the 1 mL used here is sufficient, a reduction of the membrane area is beneficial, since this will decrease the response time. However, it will also decrease the filtration flow. Assuming a constant membrane area to response time ratio, we have used an optimal membrane area for a sample volume of 1 mL, since a filtrate flow of 1 mL·min^{-1} and a response time of 1 min was obtained and total sample time (2 min) is the added response time (1 min) and the time to filtrate the sample (1 min). Increasing or decreasing the membrane area would increase the total sample time: e.g. total sample time at a 50% increase of the membrane area = 1.5 × 1 min (response time) + 1 mL/1.5 mL·min^{-1} (filtrate time) = 2.2 min and total sample time at a 50% decrease of the membrane area = 0.5 × 1 min (response time) + 1 mL/0.5 mL·min^{-1} (filtrate time) = 2.5 min.

Flex Clamp

Indirect control of filtrate flow through control of filter back pressure, previously used by e.g. van de Merbel *et al.* [1994], is easily disturbed by variations in the characteristics of the culture broth and clogging of the membrane. The filtrate flow is an important variable because it determines the response time and the volume sampled. Therefore direct control of filtrate flow is preferred.

This can be obtained simply by inserting a rigid clamp as resistance against flow at the outlet of the filter module. However, suspended particles will inevitably block the tubing because a plug of e.g. mycelium will function as a strainer or a filter. Subsequently, the pressure will increase further and a considerable risk of leakage will arise.

Therefore a novel resistance against flow was designed as a flexible clamp by which the filtrate flow was regulated. The Flex Clamp was made of two plates of spring steel held together at one corner with a conventional clamp (Fig. 5). The silicone tubing connecting the filter module with the bioreactor (Fig. 1) was placed between the two plates. The filtrate flow was adjusted by moving the tubing sideways as indicated in Figure 5A. When the tubing is moved towards the clamp the resistance against flow and the filter back pressure increases. The Flex Clamp had the advantage of damping the pressure variations from the pump and preventing creation of large aggregates of mycelium, which would otherwise clog the tubing. The tubing and the spring steel plates had a large contact area where the tubing was compressed. Therefore a relative large force **F** (small arrows in Fig. 5B) was acting on the plates when the pressure in the tubing increased (force = pressure × area), and the plates

opened, e.g. allowing aggregates of material to pass through. In addition, the Flex Clamp was without dead volume and autoclavable contrary to most pressure regulation units.
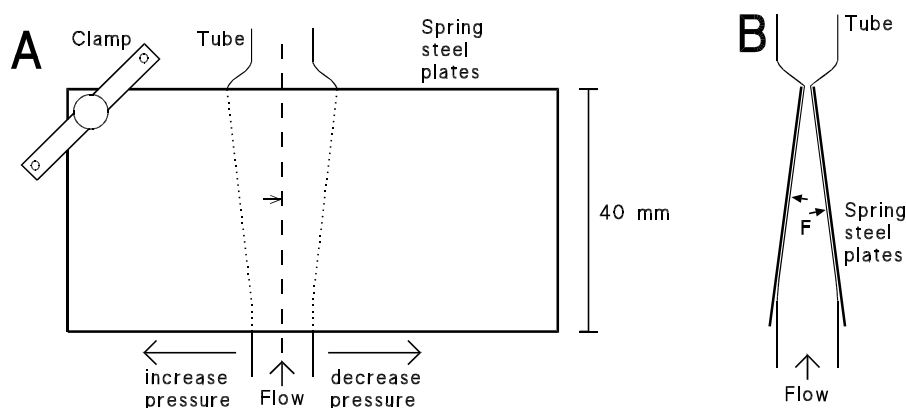
Figure 5. Flex Clamp. **A:** Top view. Two plates of spring steel (Standard No. 1.4300, DIN×12 Cr/Ni 18/8, hardness 130-180 HB, 0.6×40×80 mm) held together at one corner with a clamp. Tubing is 5 × 1.5 mm silicone. Two large arrows (increase and decrease pressure) show directions of movement of tubing for high and low resistance against flow in tubing. Dashed line and small arrow indicate cross section shown in **B**. **B:** Cross section of Flex Clamp. Small arrows show force **F** from flattened tubing area acting on spring steel plates.

Alternate pumping using controlled valve in external loop

The controlled valve in the external loop (Fig. 1) made it possible to pump the culture broth through the sampling system only when sampling was required. When the valve was open, headspace gas was pumped through the external loop. Headspace gas is saturated with water and prevented drying of the filter membrane, which would otherwise destroy it. When the valve was closed, culture broth was pumped through the sampling loop. Pumping of culture broth must begin at least one response time in advance of sample collection by the autosampler. Because of the risk of an increase in response time resulting from reduction of filtrate flow by membrane clogging, a safe period of 7 min was used here, which was found much longer than necessary as discussed below.

At a flow of 300 mL·min^{-1} for 7 min a volume corresponding to the total bioreactor volume of 2 L was pumped through the external loop once at every sampling with a residence time of 10 s. A sampling frequency around once per hour is sufficient to monitor most submerged microbial cultures. Therefore, the culture broth on average was pumped through the sampling loop once per hour and was in the loop only 1/10 of the time compared to continuous pumping. However, even with continuous pumping we observed no effect of using the on-line sampling unit neither on morphology nor on metabolite concentrations. One of the reasons for this is probably that oxygen transfer from the air bubbles to the liquid also occurred in the external loop, where mixing was vigorous because of the high liquid velocity of approximately 25 cm·s^{-1}.

The major advantage of using alternate pumping clearly was prevention of membrane clogging and consequently a constant filtrate flow. Alternate pumping of suspension and

headspace gas could also have been obtained by control of the pump direction. However, control of a valve is simpler. Stopping the pump would capture the cells in the external loop.

Membrane clogging (fouling and concentration polarisation)

In the continuous pumping mode a limited decrease in filtrate flow of about 20% was usually seen after 1.5 days. This decrease was probably caused by fouling of the membrane filter by a thin rim of cells that settled on the membrane at the inner wall of the spiral groove channel (Fig. 3F). The suspension pumped from the bioreactor into the spiral groove contained air bubbles and because of the centripetal force in the circular path the suspension was divided into air bubbles with a low density, which collected at the inner wall of the spiral groove, and liquid with a high density, which was forced away from the centre. Consequently, the inner wall of the spiral groove was not flushed continuously by turbulent liquid and cells and debris settled there.

When the decrease in filtrate flow was observed, the original flow was re-established by increasing the back pressure by re-adjusting the position of the tubing through the Flex Clamp (see Fig. 5). Since only a slow decrease in the filtration flow was observed after this, further membrane fouling or concentration polarisation apparently only occurred to a low extent. Culturing and sampling was performed for up to five days. Severe membrane fouling occurred if the filter back pressure was increased to more than 0.5 bar.

Membrane fouling was completely avoided when the controlled valve was used and filtration performed in intervals (sampling once per hour for up to five days). Therefore, using the controlled valve extended the lifetime of the membrane filter. But even in the continuous pumping mode, the membrane filter was reused up to five times.

The sampling system was validated by simultaneous manual sampling using filtration through cotton wool in a pipette tip. Both samples were analysed on HPLC and the results agreed within 5% as expected from this type of analysis.

Substrates and products in A. niger batch cultures and glucose pulse experiments

In bioreactor cultures of *A. niger* wild type (NW 131) and a transformant overexpressing phosphofructokinase (49-11) substrates and products were measured in samples obtained with the on-line sampling system facilitating detailed comparison of the two strains.

During glucose consumption polyols and organic acids were produced and excreted (Figs. 6 and 7). Except for oxalate, they were consumed simultaneously after glucose exhaustion. This is in agreement with previous results obtained with *A. niger* [van de Merbel *et al.* 1994; Witteveen and Visser 1995], but in contrast to what has been observed in bacteria [Degn *et al.* 1973], where substrates mostly are consumed successively.

An explanation for this difference is lack of catabolite repression or catabolite inactivation from any of the substrates present after glucose exhaustion. All the transport and enzyme systems necessary for uptake and consumption of the different substrates were either expressed simultaneously or present in the fungi after glucose exhaustion. Mannitol is believed to be a catabolite repressor [Arst *et al.* 1990; Ruijter *et al.* 1996], but it is not known

at which concentrations. In this case mannitol was present at relatively low concentrations; apparently too low to have an effect.
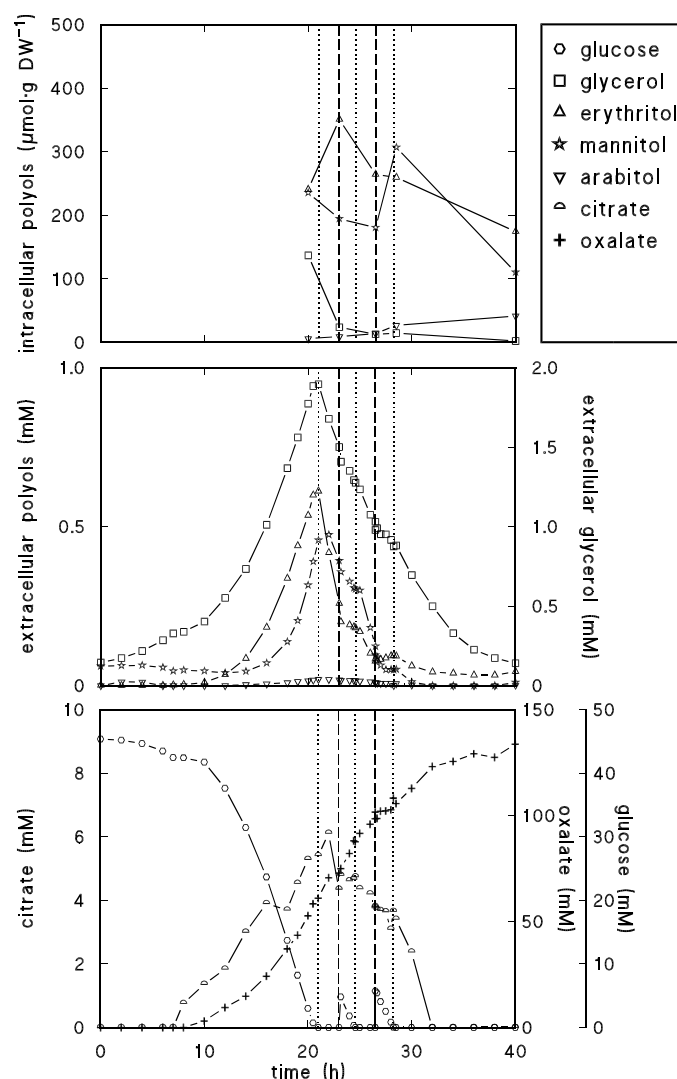
Figure 6. Concentration of extracellular glucose, polyols and organic acids measured in samples taken with on-line sampling system and intracellular polyols measured after extraction of mycelium in batch culture of *Aspergillus niger* NW131 (wild type) and at addition of two 5 mM glucose pulses. Legends are given in box. Vertical dotted lines (····) show times of glucose exhaustion and vertical dashed lines (----) show times of glucose addition.

However, consumption and uptake of metabolites other than glucose was subject to catabolite repression and/or catabolite inactivation by glucose during consumption of the initial 55 mM glucose and the glucose pulses. For arabitol, citrate, erythritol and mannitol the rate of uptake became close to zero when a glucose pulse was added, but for glycerol the reduction was rather low. In addition, the inactivation of uptake of mannitol was not immediate since it took about 30 min before full inactivation. During consumption of the glucose pulses the intracellular concentrations of polyols were maintained or increased and therefore, assuming the absence of production/consumption cycles, glucose prevents catabolism of the polyols present.

The increase in intracellular mannitol during consumption of the second glucose pulse must be caused by a (net) production since the increase in the intracellular pool of mannitol

(0.35-0.49 mmol·L^{-1} culture broth) was about four times higher than the decrease in the extracellular pool (0.09 mmol·L^{-1} culture broth) using the dry weight concentration of about 2.7 g DW·L^{-1}. Contrary to sampling for extracellular compounds with the on-line sampling system, which only subtract the (pre-programmed) volume needed for analysis, the frequency of sampling for intracellular polyols was limited by the contents of the bioreactor.

In addition to the metabolites mentioned above extracellular pyruvate was also detected, but was shown to be unstable in the filtrate by addition of internal standard and therefore not investigated further.
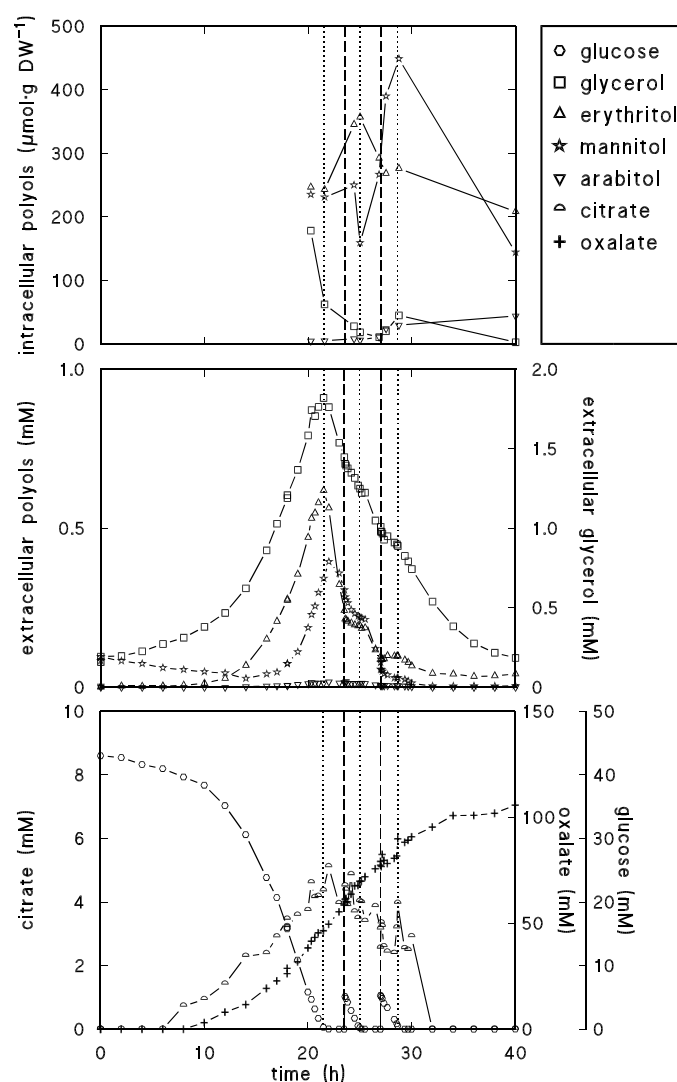
Figure 7. Concentration of extracellular glucose, polyols and organic acids measured in samples taken with on-line sampling system and intracellular polyols measured after extraction of mycelium in batch culture of *Aspergillus niger* phosphofructokinase overexpressing strain 49-11 and at addition of two 5 mM glucose pulses. Legends are given in box. Vertical dotted lines (····) show times of glucose exhaustion and vertical dashed lines (----) show times of glucose addition.

The specific glucose uptake rate q_{glc} following a glucose pulse was constant at 1.2 mmol·g DW^{-1}·h^{-1} throughout the consumption of the glucose pulses. q_{glc} was higher at the end of the batch culture during consumption of the initial 55 mM glucose (1.7 mmol·g DW^{-1}·h^{-1}). This seems reasonable since q_{glc} depends not only on the uptake system but also on the catabolism of glucose. The metabolic states during consumption of the initial glucose and during

consumption of the glucose pulses were different: cells were growing during consumption of the initial glucose, since the nitrogen source (NO_3^-) was exhausted almost simultaneously. The q_{glc} obtained here was lower but comparable to a value measured for glucose pulses added to a glucose limited chemostat culture of *A. oryzae* of about 2 mmol·g DW^{-1}·h^{-1} [Carlsen *et al.* 1996].

No significant difference between the strain 49-11 overexpressing PFK, and the reference strain NW131 was observed (Figs. 6 and 7). We assumed that if PFK overproduction changed flux through glycolysis, this would result in different polyol levels. Since no such difference was found between the wild type and the overexpressing strain apparently the *in vivo* activity of PFK in the overexpressing strain was decreased to wild type *in vivo* activity. Ruijter *et al.* [1997] found decreased levels of the PFK activator fructose 2,6-bisphosphate (F2,6BP) in the PFK overexpressing strain 49-11. They showed that the reduction could be sufficient to decrease the *in vivo* PFK activity to wild type level. Indeed, we also measured a reduction to 30% of wild type level of F2,6BP (16.3 nmol·g DW^{-1}) in the PFK overexpressing strain 49-11 (4.8 nmol·g DW^{-1}), which might explain the apparent similar *in vivo* PFK activity in overexpressing strain and wild type. In addition, we found only 60% of wild type level of ATP (5.8 µmol·g DW^{-1}) in 49-11 (3.5 µmol·g DW^{-1}). The reason for this is unknown. New attempts to increase the *in vivo* activity of PFK will be performed by metabolic engineering of the PFK2 (EC 2.7.1.105) and/or the F2,6BP-phosphatase (EC 3.1.3.46).

Other possible applications

On-line sampling from submerged cultures of filamentous fungi is one of the most challenging techniques due to the nature of the culture broth: inhomogeneous suspension of cells, variation in size of growth units, tendency to bridging (blocking) of tubings, fast settling of cells, viscous suspension and strong tendency to stick to and grow on surfaces. Therefore, we expect this sampling system to be applicable in most other submerged cell cultures from which a fast response sampling with minimal dispersion is required. An adaptation of the pumping system is possibly necessary with very sensitive cells as discussed in section 1. For suspensions with very different properties, e.g. viscosity, a modification of the suspension side of the filter module (**F** in Fig. 3) may be required, e.g. an increase of the diameter of the semicircular groove. However, the filtrate side of the module needs no modification unless an even shorter response time is required. This can be obtained by a higher degree of branching of channels in the channel disc (**C** in Fig. 3) using the principle of equal transport time of filtrate to the point of collection. For suspensions with smaller particles or when a smaller filtrate flow is required the module might be miniaturised, which also would ease mass production.

The principle for collection of liquid, here implemented in the channel disc (**C** in Fig. 3), is a method to decrease the diameter of a plug flow with minimal dispersion. If the flow is reversed the principle is a method to increase the diameter of a plug flow. Also, the flow may be of any fluid, e.g. gas or liquid. Therefore the collection principle could be implemented with opposite directions of flow at the in- and outlet of a plug flow reactor. At the inlet it

would function as an application system with minimal dispersion. Furthermore, the collection principle allows a minimal time between mixing of reactants and introduction into the column.

CONCLUSIONS

A filter module suited for sampling from submerged cultures of filamentous fungi and having a faster response time than reported before for measurement of rapid metabolite transients was designed. A novel filtrate collecting principle through a branched channel system was used with equal transport time of filtrate to the point of collection independent of location on the filter. The filtrate flow was regulated directly by means of a flexible clamp constructed from two plates of spring steel, which automatically opened if passage was hindered and pressure increased. Including both the filter module and the flexible clamp made the sampling system autoclavable.

The metabolite profiles of wild type strain NW 131 and the PFK overexpressing strain 49-11 showed apparent similarity between the two strains in batch cultures and in glucose pulse experiments.

AKNOWLEDGEMENTS

REFERENCES

Arst HNJr, Tollervey D, Dowzer CEA, Kelly JM (1990) An inversion truncating the *creA* gene of *Aspergillus nidulans* results in carbon catabolite derepression. Mol Microbiol 4: 851-854.

Bensadoun A, Weinstein D (1976) Assay of proteins in the presence of interfering materials. Anal Biochem 70: 241-250.

Bergmeyer HU, Bernt E, Schmidt F, Stork H (1974) Determination with hexokinase and glucose-6-phosphate dehydrogenase. p. 1196-1201. In H. U. Bergmeyer (ed.) Methods of enzymatic analysis, vol. 3, 2nd ed. Weinheim: Verlag Chemie.

Carlsen M, Nielsen J, Villadsen J (1996) Growth and alfa-amylase production by *Aspergillus oryzae* during continuous cultivations. J Biotechnol 45: 81-93.

Degn H, Lilleør M, Iversen JJL (1973) The occurence of a stepwise-decreasing respiration rate during oxidative assimilation of different substrates by resting *Klebsiella aerogenes* in a system open to oxygen. Biochem J 136: 1097-1104.

Eriksen NT, Iversen JJL (1997) On-line determination of respiration rates of aquatic organisms in a mono-phase oxystat at steady-state dissolved oxygen tensions. Mar Biol 128: 181-189.

Garn M, Gisin M, Thommen C (1989) A flow injection analysis system for fermentation monitoring and control. Biotechnol Bioeng 34: 423-428.

Håkanson H, Nilsson M, Mattiason B (1991) General sampling system for sterile monitoring of biological processes. Anal Chim Acta 249: 61-65.

Kotiaho T, Lauritsen FR (2002) Membrane inlet mass spectrometry. In: Sample preparation in field and laboratory. Pawliszyn JB (ed.), Comprehensive Analytical Chemistry, Elsevier, Amsterdam, Vol 37: 531-557.

Kroner KH, Kula MR (1984) On-line measurement of extracellular enzymes during fermentation by using membrane techniques. Anal Chim Acta 163: 3-15.

Marko-Varga G, Buttler T, Gorton L, Grönsterwall C (1993) A study of the use of microdialysis probes as a sampling unit in on-line bioprocess monitoring in conjunction with column liquid chromatography. Chromatographia 35: 285-289.

Megersa N, Chimuka L, Solomon T, Jönsson JÅ (2001) Automated liquid membrane extraction and trace enrichment of triazine herbicides and their metabolites in environmental and biological samples. J Sep Sci 24: 567-576.

Merbel NC van de, Ruijter GJG, Lingeman H, Brinkman UATh, Visser J (1994) An automated monitoring system using on-line ultrafiltration and column liquid chromatography for *Aspergillus niger* fermentations. Appl Microbiol Biotechnol 41: 658-663.

Möllering H (1985) in Bergmeyer HU (ed.) Methods of enzymatic analysis, 3rd edition, Vol. VII, VCH, Weinheim, p. 2.

Ørsnes H, Graf T, Bohatka S, Degn H (1998) Rapid Commun. Mass Spectrom. 12: 11-14.

Pontecorvo G (1953) The genetics of *Aspergillus nidulans*. p 141-238. In M. Demerec (ed.), Advances in genetics, Vol. 5. Academic Press, New York.

Ruijter GJG, Panneman H, van den Broeck HC, Bennett JM, Visser J (1996) Characterization of the *Aspergillus nidulans* frA1 mutant: hexose phosphorylation and apparent lack of involvement of hexokinase in glucose repression. FEMS Microbiol Lett 139: 223-228.

Ruijter GJG, Panneman H, Visser J (1997) Overexpression of phosphofructokinase and pyruvate kinase in citric acid-producing *Aspergillus niger.* Biochim Biophys Acta 1334: 317-326.

Ruijter GJG, Visser J (1996) Determination of intermediary metabolites in *Aspergillus niger.* J Microbiol Meth 25: 295-302.

Schügerl K (1991) On-line analysis of broth. In H.J. Rehm, G. Reed, A. Pühler, P. Stadler, (eds.), Biotechnology, 2nd edition, Vol. 4, VCH, Weinheim, 149-178.

Turner C, Thornhill NF, Fish NM (1992) A novel method for the on-line analysis of fermentation broth using a sampling device, microcentrifuge and HPLC. Biotechnol Tech 7: 19-24.

Vishniac W, Santer M (1957) The Thiobacilli. Bacteriol Rev 21: 195-213.

Witteveen CFB, Visser J (1995) Polyol pools in *Aspergillus niger*. FEMS Microbiol Lett 134: 57-62.

Witteveen CFB, Weber F, Busink R, Visser J (1994) Isolation and characterization of two xylitol dehydrogenases from *Aspergillus niger*. Microbiology 140: 1679–1685.

Characterization of nerolidol biotransformation based on indirect on-line estimation of biomass concentration and physiological state in batch cultures of *Aspergillus niger*

ABSTRACT

Biotransformation of the sesquiterpenoid *trans*-nerolidol by *Aspergillus niger* has previously been investigated as a method for the formation of 12-hydroxy-*trans*-nerolidol, a precursor in the synthesis of the industrially interesting flavour α-sinensal. We characterized biotransformations of *cis*-nerolidol, *trans*-nerolidol and a commercially available *cis/trans*-nerolidol mixture in repeated batch cultures of *A. niger* grown in computer-controlled bioreactors. On-line quantification of titrant addition in pH control allowed characterization of 1) maximum specific growth rate in exponential growth phases, 2) exponential induction of acid formation in postexponential phases, 3) inhibition of organic acid formation after nerolidol addition and 4) exponential recovery from this inhibition. Addition of a ($\pm$)-*cis/trans*-nerolidol mixture during exponential or postexponential phase to cultures grown in minimal medium at high dissolved oxygen tension (above 50 % air saturation), to cultures at low dissolved oxygen tension (5 % air saturation) or to cultures grown in rich medium demonstrated that the physiological state before nerolidol addition had a major influence on biotransformation. The maximal molar yield of 12-hydroxy-*trans*-nerolidol (9%) was obtained by addition of a ($\pm$)-*cis/trans*-nerolidol mixture to the culture in the postexponential phase at high dissolved oxygen tension in minimal medium. Similar yields were obtained in rich medium, where the rate of biotransformation was doubled.

INTRODUCTION

Functionalization of industrially important terpenes and terpenoids using oxidative biotransformation by microorganisms [e.g. Li *et al.* 2002; Lehman and Stewart 2001] including *A. niger* has been extensively studied [e.g. Agrawal and Joseph 2000; Lahlou *et al.* 2000; Demyttenaere *et al.* 2000; Demyttenaere *et al.* 2001; Aranda *et al.* 2001; Chen and Reese 2002] as a cheap and environmentally friendly alternative to chemical oxidations. Nonstereoselective [Bertele and Schudel 1967; Baumann *et al.* 1976] and stereoselective conventional chemical syntheses [Buchi and Wuest 1974; Desai *et al.* 1990] of the industrially interesting flavor α-sinensal **1** (Scheme 1) are known. However, because of side reactions resulting in low yields and the use of toxic reagents, Arfmann and coworkers [1988] have suggested biotransformation of the sesquiterpenoid *trans*-nerolidol **2** by *A. niger* as an alternative approach for obtaining suitably functionalized intermediates for the synthesis of α-sinensal. They and others [Madyastha and Gururaja 1993] have shown that shake flask cultures of *A. niger* growing in rich media without control of pH and dissolved oxygen tension convert *trans*-nerolidol **2** stereoselectively in 5-20 % yield to the potential α-sinensal precursor **4**. The vicinal diol **5** and the 2Z-isomer, carboxylic acid, acetate ester and 11,12-dihydroxy derivatives of **4** were formed in low yield. The isomeric *cis*-nerolidol **3** was converted to the vicinal diol **6** and allylic alcohol **7** [Arfmann *et al.* 1988].
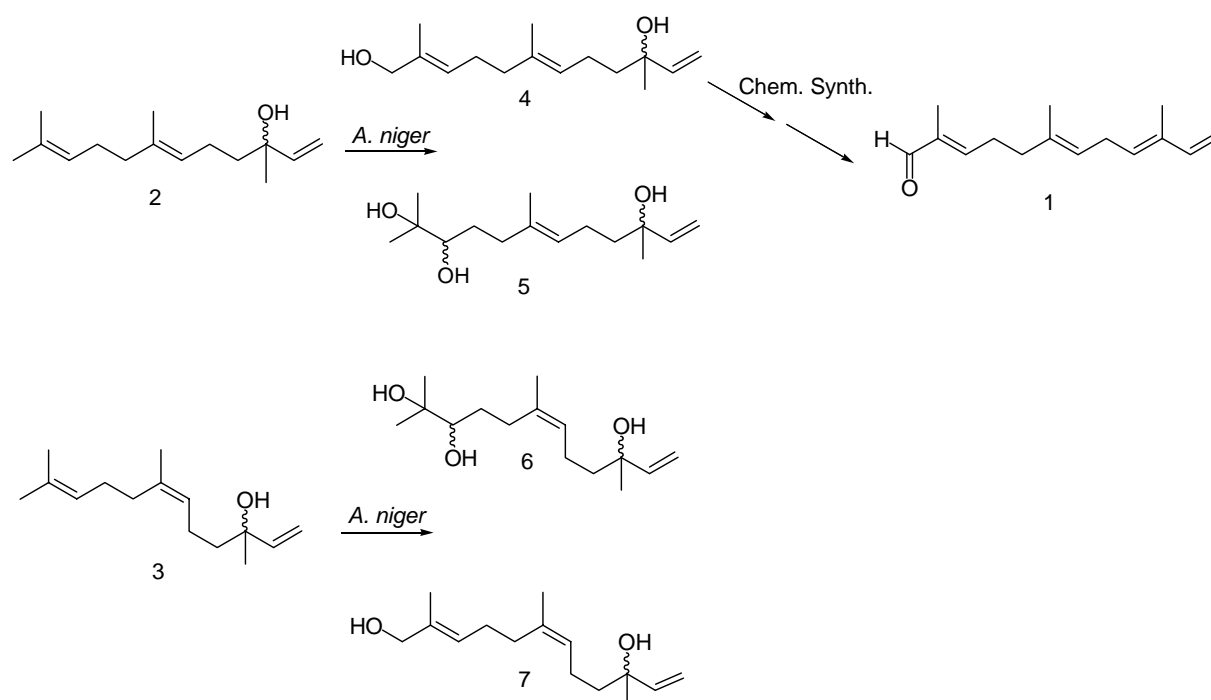
Scheme 1. Products from biotransformation of cis- and trans-nerolidol by *A. niger,* and chemical synthesis of α-sinensal from 12-hydroxy-trans-nerolidol 4 (Further details in Introduction section).

Although antimicrobial activities [Kubo 1992] of nerolidol are known, including antifungal activities against *Cladosporium cucumerinum* [Terreaux *et al.* 1994], the effects of biotransformation of *cis*-nerolidol and *trans*-nerolidol on the metabolism of *A. niger* have not yet been studied.

Accurate measurements of titrant addition, required to maintain constant pH in bioreactors where cell metabolism causes pH changes, have been used to monitor growth and physiological states of microbial cultures [Iversen *et al.* 1994; Vicente *et al.* 1998; Eriksen *et al.* 2001; Christensen and Eriksen 2002; Larsen *et al. in press*; Poulsen *et al.* 2003; Poulsen *et al. submitted*]. Despite its simplicity and general applicability, this inherent information in pH control has not been used to obtain detailed information about the kinetics of growth and metabolism in microbial cultures during biotransformation.

In this paper, we describe how on-line quantification of titrant addition in computer-controlled bioreactors is used to

- Define the physiological state of *A. niger* NW131 before and after addition of biotransformation substrates.
- Characterize biotransformations of (±)-*cis*-nerolidol, (±)-*trans*-nerolidol and a commercially available (±)-*cis/trans*-nerolidol mixture by *A. niger* NW131, with emphasis on the inhibition of oxalic and citric acid formation during biotransformations.

MATERIALS AND METHODS

Chemicals

Cis-nerolidol (98 %, Fluka), *trans*-nerolidol (95 %, Aldrich) and a *cis/trans*-nerolidol mixture (98%, Aldrich) were used. GC measurements showed that the *cis/trans*-nerolidol mixture contained 61 % *trans*- and 39 % *cis*-nerolidol. All other chemicals and solvents were of analytical grade and obtained from various commercial suppliers. Solvents of highest available purity were used for HPLC experiments.

Reactor design

To obtain a uniform culture a 3 L BTS 05 bioreactor (Applikon, B.V., Schiedam, The Netherlands) was modified to decrease wall growth by removing the baffles. Oxygen and pH electrodes, temperature pocket, sparger and a 10 mm sampling tube gave sufficient turbulence to ensure sufficient aeration and mixing. The sampling tube was connected to the air inlet via a pinch valve to enable flushing of the sampling system. A Rushton turbine impeller, 4.5 cm in diameter, placed 2-3 cm above the bottom of the bioreactor and a marine impeller, 5 cm in diameter, 5 cm above the Rushton turbine impeller, gave a suitable combination of axial and vertical liquid movement. The bioreactor was equipped with a galvanometric O_2 electrode [Makereth 1964] constructed in our workshop, a Pt 100 temperature sensor and an autoclavable glass pH electrode (Mettler Toledo, Ingold, Urdorf, Switzerland) connected to a pH-meter (PHM 82, Radiometer, Copenhagen, Denmark). Accurate on-line quantification of titrant addition was obtained by pulse addition of 1, 2 or 5 M NaOH and 1 M HCl as previously described by Iversen and co-workers [1994], with the modification that a positive

pressure in the silicone tubing was achieved by placing titrants above the bioreactor and pump. The total number of pulse additions varied from 2000 to 6000. The temperature was controlled by airflow from a heating element (1600 W) blown through a Perspex jacket surrounding the lower part of the bioreactor and by constant cooling of the upper part through a coil of tubing, which prevented wall growth in the headspace. Computer control of temperature, pH, dissolved oxygen tension and stirring was obtained via a serial interface [Degn and Nielsen 1987] running a specially written program.

Strain and culture conditions

A. niger NW 131 (*csp*A1 *gox*C17) is a glucose oxidase negative strain (*gox*C17) with short conidiophores (*csp*A1) minimizing undesired spore spreading. It is derived from the strain N400 (CBS 120.49).

Complete medium [Pontecorvo 1953] contained per litre: 0.5 g KCl, 1.5 g KH_2PO_4, 0.5 g $MgSO_4 \cdot 7H_2O$, 6.0 g $NaNO_3$, 1.0 g casamino acids, 1.0 g yeast extract, 0.5 g yeast ribonucleic acids, 2.0 g peptone, 10.0 g glucose, 1.0 mL trace metal solution, 2.0 mL vitamin solution and 15 g agar. The pH was adjusted to 6.0. Glucose was autoclaved separately. Rich medium contained per litre: 0.5 g KCl, 1.5 g KH_2PO_4, 0.5 g $MgSO_4 \cdot 7H_2O$, 1.0 g casamino acids, 1.0 g yeast extract, 0.5 g yeast ribonucleic acids, 2.0 g peptone, 50.0 g glucose, 1.0 mL trace metal solution and 2.0 mL vitamin solution. The pH was adjusted to 3.0. Glucose was autoclaved separately. The vitamin solution contained per litre: 20 mg biotin, 1.0 g nicotinamide, 100 mg *para*-aminobenzoic acid, 100 mg pantothenic acid, 500 mg pyridoxine-HCl, 1.0 g riboflavin 5'-phosphate and 100 mg thiamine-HCl and was filtered through a 0.2 μm NC20 membrane filter (Schleicher & Schuell, Dassel, Germany). Minimal medium contained per litre: 1.13 g NH_4Cl (21 mM in the medium, the final cell density limiting substrate), 1.5 g KH_2PO_4, 0.5 g $MgSO_4 \cdot 7H_2O$, 0.5 g KCl, 50.0 g glucose and 1.0 mL trace metal solution. The pH was adjusted to 3.0. Glucose was autoclaved separately. Trace metal solution [Vishniac and Santer 1957] contained per litre: 1.5 g $CaCl_2 \cdot 2H_2O$, 0.32 g $CoCl_2 \cdot 6H_2O$, 0.32 g $CuSO_4 \cdot 5H_2O$, 1.0 g $FeSO_4 \cdot 7H_2O$, 1.2 g $MnCl_2 \cdot 6H_2O$, 0.22 g $(NH_4)_6Mo_7O_{24} \cdot 4H_2O$, 4.4 g $ZnSO_4 \cdot 7H_2O$ and 10.0 g ethylenediamine tetraacetic acid (EDTA). EDTA and $ZnSO_4$ were brought in solution and the pH adjusted to 6.0 with NaOH. The remaining components were added sequentially and the pH adjusted to 6.0 after each addition. Finally, the pH was lowered to 4.0 with HCl.

Spores were grown on complete medium agar plates [Pontecorvo 1953] for 4-6 days at 30°C, kept minimum 1 day (for maturation) and maximal 6 months at 4°C, and harvested with 10 mL of a solution containing 0.05% Tween 80 and 0.9% NaCl by scraping the agar surface with a Drigalski spatula. The spore suspension was filtered through sterile glass fibre, centrifuged for 2 min at 1620 *g* and resuspended in 5 mL of sterile distilled water. The bioreactor containing 2.5 L of minimal medium with 0.003% yeast extract (for germination) was inoculated with 10^6 spores per mL. Throughout cultivation, the pH was 3.00 ± 0.05 and the temperature 30 ± 0.1°C. Initially, agitation was at 500 rpm with aeration through headspace to prevent spores from entering headspace via bursting bubbles. When the

dissolved oxygen tension decreased below 50 % air saturation, the agitation was increased to 750 rpm. Aeration through a sparger at 1 vvm and pulses of oxygen ensured a dissolved oxygen tension above 50 % air saturation during growth. After germination, 0.15 ml·L^{-1} medium of polypropylene glycol (antifoam) was added. When cultures grown on minimal medium were exhausted of the final cell density limiting substrate, ammonium, as estimated from on-line base titration and dissolved oxygen tension kinetics, a 100 mL sample was taken, the bioreactor emptied, flushed once with medium, reinoculated in 2.4 L minimal medium by addition of the 100 mL of culture broth just sampled (kept under axenic conditions) and 0.15 ml·L^{-1} medium of polypropylene glycol was added. Essentially the same procedure was used for cultures grown on rich medium, but then exhaustion of limiting substrate was estimated by wet weight. One-half millilitre of *cis-*, *trans*-nerolidol or (±)-*cis/trans*-nerolidol mixture per litre culture broth (1.97 mM) was dissolved in EtOH (1:1 v/v) and added either 0.5 h before or 2-9 hours after exhaustion of ammonium (minimal medium) or in the post-exponential phase as estimated by wet weight (rich medium). The dissolved oxygen tension was kept at either 5 % or above 50 % air saturation during biotransformation (low and high dissolved oxygen tension, respectively). Low dissolved oxygen tension was controlled by adjusting the airflow through the sparger. High dissolved oxygen tension was maintained as described above. Biotransformation was monitored by withdrawal of samples (approx. 10 ml) with 6-10 hours intervals for 96 hours. Samples were taken after flushing the sampling tube three times with culture broth. The experiment with addition of (±)-*cis/trans*-nerolidol to heat-inactivated culture was performed after raising the temperature to 70°C for 30 min, 5 hours after exhaustion of ammonium.

Analysis

Dry weight was measured on samples containing at least 20 mg of dry cell material. The culture was sampled directly into a measuring cylinder and filtered through a glass sintered funnel or pre-dried and pre-weighed paper filters; the mycelium was washed twice by resuspension in distilled water, frozen in liquid nitrogen, and stored at -20°C. The sample was lyophilized and weighed.

An adjustable Gilson pipette (P1000), with the opening diameter of the disposable tip increased by partial removal of the cone, was used to take a culture sample and transfer it to another disposable tip containing a piece of cotton. Placed on the pipette, the culture sample was filtered by pushing the filtrate through the cotton. The culture filtrates were frozen in liquid nitrogen and stored at -20°C.

The extracellular concentration of organic acids was determined after centrifuging the culture filtrate samples to remove precipitate after freezing. The supernatant was analysed on a HPLC system (Dionex Corp., Sunnyvale, CA, USA) equipped with an HPX87H column (BioRad, Richmond, CA, USA), thermostated at 50°C with detection by UV at 210 nm and refractive index. Isocratic elution with 25 mM HCl and a flow of 0.5 mL·min^{-1} was used. The standard mixture contained oxalate, citrate, glucose, mannitol, pyruvate, erythritol, glycerol and acetate.

The previously reported method for carbohydrate determination [Dubois *et al.* 1956] was modified: 10-15 mg of lyophilized and grinded (Micro-Dismembrator S, B. Braun Biotech Int. GmBH, Melsungen, Germany) biomass was homogenised in 2.5 mL of distilled water by sonication. 1 mL of aqueous 5% phenol (w/v) was added to 1 mL of a 25-fold diluted sample. After mixing, 5 mL of concentrated H_2SO_4 was added. The absorbance at 488 nm was measured after 30 min and compared to standards (25, 50, 100, 125 and 200 g·L^{-1}) of glucose.

The previously reported method for determination of lipids [Folch *et al.* 1957] was modified: to 15-20 mg of lyophilised and grinded biomass was added 200 µL of distilled water and 3.75 mL of a 1:2 $CHCl_3/CH_3OH$ solution (v/v). The suspension was homogenised for 20 min by sonication. The homogenate was filtered through glass wool, and was subsequently washed with 1 mL of $CHCl_3$. Next, 1.25 mL of a 0.9% NaCl solution was added and the suspension was mixed and then centrifuged for 20 min at 18,000 *g*. To the isolated aqueous phase was added 1 mL of $CHCl_3$, and the suspension mixed and centrifuged. Combined organic phases were collected in a pre-weighed glass tube, and dried to constant weight at 105°C from which the mass of lipids was determined.

The glucose concentration was determined enzymatically as described previously [Bergmeyer *et al.* 1974].

The ammonium concentration was determined enzymatically in 150 mM triethanolamine (pH 8.6) in the presence of 12 mM 2-ketoglutarate, 0.3 mM NADH and 1.5 mM ADP, by addition of 5 units·mL^{-1} glutamate dehydrogenase (beef liver, Roche Diagnostics) at 30°C and measuring the absorbance change at 340 nm.

To find exponential parts of complex trajectories and determine rate constants, the accumulated titrant was analyzed by a "Log of Slope (LOS) plot" [Poulsen *et al.* 2003] given as:

$$\ln(dA/dt) = \ln(A_0 \cdot k) + k \cdot t \tag{1}$$

where the natural logarithm of the slope, $\ln(dA/dt)$, plotted against time, *t*, gives the rate constants (e.g. specific growth rate, μ) as the slope, *k*, of any rectilinear sections of the LOS plot without knowing the offset or which part of the data is exponential. Equally important, any exponential sections of a curve and small changes in the rate constant are easily identified, since *only* an exponential dependency of *A* on *t* gives a straight line with a slope equal to the rate constant, *k*, in a LOS plot. Implementation of Equation 1 to the base titrant added to maintain constant pH in a culture growing exponentially gives:

$$\ln(\Delta OH_{add}/\Delta t) = \ln(OH_{add,0} \cdot \mu) + \mu \cdot t \tag{2}$$

where OH_{add} (mM) is the accumulated base titrant added, $OH_{add,0}$ (mM) is base titrant added at time 0 and μ (kg DW·kg DW^{-1}·s^{-1}) is the specific growth rate.

The concentration of protons released from a mixture of polyprotic acids in a bioreactor with constant pH was calculated to analyse the medium titration during post-

exponential phases. For a general polyprotic acid H_xA, the stepwise dissociation constants K_{A_i} and formal concentration C (mol·l^{-1}) are given as:

$$K_{A_i} = \frac{[H^+][H_{(x-i)}A^{-i}]}{H_{(x-i+1)}A^{1-i}} \; ; \; 1 \leq i \leq x \tag{3}$$

$$C = [H_xA] + \sum_{i=1}^{x} [H_{(x-i)}A^{-i}] \tag{4}$$

where $[H^+]$ (mol·L^{-1}) is the controlled and constant proton concentration in the bioreactor. If the formal concentration of acid is known, rearrangement of Equations 3 and 4 yield the concentration of undissociated acid $[H_xA]$ (mol·L^{-1}) as:

$$[H_xA] = \frac{C}{1 + \sum_{i=1}^{x} \frac{\prod_{j=1}^{i} K_{A_1}}{[H^+]^i}} \tag{5}$$

The concentrations of dissociated species $[H_{(x-i)}A^{-i}]$ (mol·L^{-1}), are then calculated from Equation 3:

$$[H_{(x-i)}A^{-i}] = \frac{[H_xA]\prod_{j=1}^{i} K_{A_i}}{[H^+]^i} \; ; \; 1 \leq i \leq x \tag{6}$$

Hence, in a mixture of two polyprotic acids H_xA and H_yB of known formal concentrations, the concentration of protons titrated to maintain constant pH in a bioreactor $[H^+]_{titrated}$ (mol·L^{-1}) is calculated as:

$$[H^+]_{titrated} = \sum_{i=1}^{x} i[H_{(x-i)}A^{-i}] + \sum_{i=1}^{y} i[H_{(y-i)}B^{-i}] \tag{7}$$

In calculations for oxalic and citric acid pK$_a$-values of 1.23, 4.19, and 3.13, 4.76 and 6.39, respectively were used [CRC Handbook of Chemistry and Physics 1999].

Quantification of metabolites by GC analysis

A modified Bligh and Dyer extraction procedure [Bligh and Dyer 1959] had to be used, since a significant proportion of *cis/trans*-nerolidol remained in the mycelium when using the procedure for development of GC standards described in the Supporting Information section. The culture broth was extracted for 20 min without preliminary filtration with a mono-phase solution of culture broth/CHCl$_3$/CH$_3$OH (0.8:1:2 v/v/v), followed by addition of cetyl alcohol (internal standard). Addition of CHCl$_3$ and water gave a two-phase system (aqueous

phase/$CHCl_3$/CH_3OH 1:1:1 v/v/v). The chloroform phase was isolated, the aqueous phase was extracted ($CHCl_3$/aq. phase 1:3 v/v), the combined chloroform phases were concentrated under reduced pressure, and the crude extract was collected.

The crude extract was dissolved in 2.00 mL of ethyl acetate and analysed on a Chrompack CP 9001 gas chromatograph with a 25 m 0.32 mm fused silica WCOT CP-SIL 8CB column with 0.25 μm film thickness. The column pressure was set at 70 kPa and the temperature at 150°C. Helium was used as carrier gas. The products were detected by flame ionization. Quantification of compounds was accomplished by measuring the peak area relative to internal standard (cetyl alcohol) for quantification of extraction efficiency, and external standard (*trans*-nerolidol) for calibration of chromatograms.

RESULTS AND DISCUSSION

Experimental design

Growth conditions were chosen to ensure well-defined and reproducible cultures of *A. niger* NW131 for characterisation of biotransformation. Using spores as inoculum impedes reproducibility of batch cultures and therefore cells from vegetative cells formed from spores in an initial batch culture were used to generate inoculum for the final (second) batch culture. Inoculum size and medium composition were designed to support exponential growth for four to five generations. Preliminary experiments showed that addition of biotransformation substrate in the beginning of exponential phase severely inhibited growth in accordance with the previously reported antimicrobial properties of nerolidol [Kubo 1992; Terreaux *et al.* 1994]. Hence, the biotransformation substrate was added to the culture either in late exponential phase or during post-exponential phase shortly after exhaustion of the final cell density limiting substrate, ammonium. High concentrations of glucose (35-45 g·L^{-1}) were present before addition of biotransformation substrate to provide the cells with ample energy for biotransformation. Experiments were terminated when the cultures were (or very close to be) exhausted of glucose.

On-line estimation of growth and metabolism by quantification of titrant addition

A minimal medium was used (with one exception as described later) in order to simplify the on-line indirect measurements of growth by titration of excreted protons upon ammonium uptake or organic acid formation as previously described for batch cultures of *E. coli* [Iversen *et al.* 1994]. Figure 1 shows the correlation between the growth and NH_4^+ uptake with a molar growth yield of 190 g·mol^{-1}, which corresponds to a cellular N-content of 7.4 % compared to a literature value of 8.8 % [Nielsen and Villadsen 1994]. The inset of Figure 1 is a concordance plot of added NaOH to balance the acidification from proton release on NH_4^+ uptake, vs NH_4^+ concentration in samples taken from the batch culture. The excellent concordance with a slope close to unity between the variables shows that the principle of on-line indirect measurement of growth is valid for batch cultures of *A. niger* as well. In the

exponential growth phase each titrant pulse corresponded to only 10 mg dry weight showing the high resolving power of titrant registration.
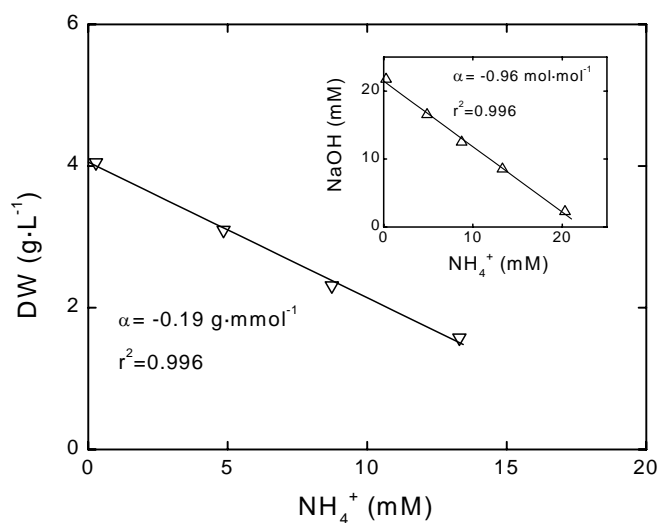
Figure 1. On-line estimation of growth by quantification of titrant addition. Concordance plot of dry weight vs [NH_4^+]. Inset shows concordance plot of accumulated NaOH addition vs [NH_4^+]. (Data from first batch culture in experiment shown in Fig. 6)

In addition to growth it is also possible to measure metabolism by registration of NaOH addition. After exhaustion of ammonium, formation of oxalic and citric acid was strongly induced (Fig. 2). Precipitation of oxalate was observed above a concentration of approximately 140 mM, seen as a constant level of dissolved oxalic acid despite a continued formation observed as a further titration with base (as shown below) and formation of visible crystals. The inset of Figure 2 shows accumulated NaOH addition in post-exponential phase vs calculated proton concentration from dissociated acids (Eq. 7). The correlation with a slope close to unity shows that acidification after exhaustion of NH_4^+ almost exclusively resulted from organic acid formation.
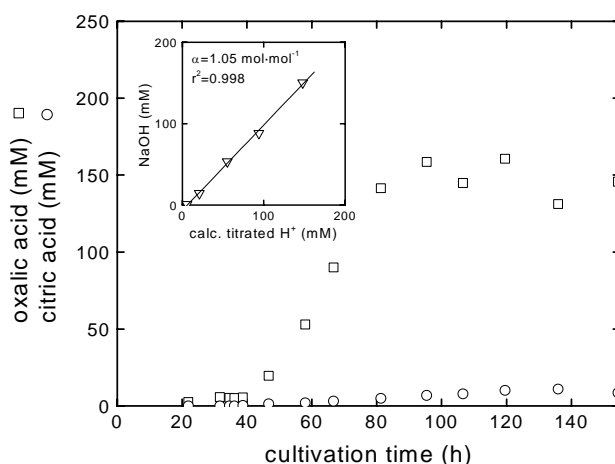
Figure 2. On-line estimation of organic acid formation by quantification of titrant addition. Concentrations of oxalic acid (□) and citric acid (○) (Data from experiment shown in Fig. 4 upper panel). Inset shows a concordance plot of accumulated NaOH addition in post-exponential phase from 39 h to 81 h vs. calculated concentrations of protons from dissociated oxalic and citric acids at pH 3 (Eq. 7).

Figure 3 shows the glucose uptake during growth and acid production. Measurements of dry weight showed that only 40 % of the total biomass formation occurred in the growth phase. The formation of the remaining 60 % of the total biomass occurred in the post-exponential phase, constituting storage material, including carbohydrates (79 %; inset of Figure 3) and lipids (10 %), both of which accumulated in the absence of cell division. A modified anthrone method was used for estimation of carbohydrate [Dubois *et al.* 1956]. The anthrone method often underestimates carbohydrates [Martens and Loeffelman 2002], which could account for the missing 11 % of energy storage material. However, most importantly the inset shows a distinct separation of growth and production phases in terms of specific carbohydrate concentration.
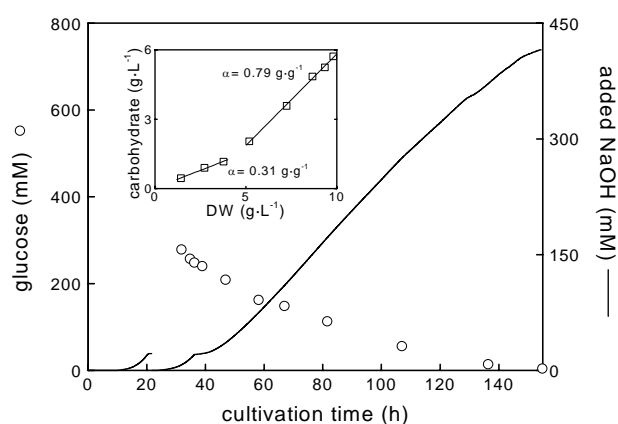
Figure 3. Accumulated NaOH addition and glucose concentration (○) during exponential growth phase and post-exponential acid production phase (Data from experiment shown in Fig. 4, upper panel). Inset shows intracellular carbohydrate in growth phase ($\alpha = 0.31$ g·g^{-1} DW) and acid production phase ($\alpha = 0.79$ g·g^{-1} DW).

Abiotic changes of (±)-*cis*/*trans*-nerolidol under cultivating conditions

The stability of the used (±)-*cis*/*trans*-nerolidol mixture was studied in experiments where *A. niger* was cultivated at conditions described in the legend of Figure 4, but killed in post-exponential phase by heat treatment (70° C for 30 min.) followed by cooling to pre-shock levels (30°C) prior to addition of biotransformation substrate. The (±)-*cis*/*trans*-nerolidol mixture was stable under the acidic cultivation conditions as biotransformation products were not detected even 90 hours after the heat treatment. It was observed that (±)-*cis*/*trans*-nerolidol accumulated on surfaces in the headspace and condenser throughout the experiment (up to 45% of added substrate), presumably due to the hydrophobicity of nerolidol. Thorough rinsing of the headspace and condenser with 96 % EtOH and extraction of mycelia and supernatant, recovered 93 % of the initially added substrate, indicating limited substrate loss due to gas stripping.

In experiments with living cells, rinsing of the headspace and condenser after termination of biotransformation experiments recovered 40 % of initially added (±)-*cis*/*trans*-nerolidol without detection of the more polar biotransformation products **4-7**. Since similar quantities of substrate accumulated on the surfaces irrespective of the presence of active biomass, this indicated that once substrate was trapped in the headspace and condenser of the

bioreactor, it remained inaccessible for biotransformation. This resulted in a lower bioavailability of substrate for which no corrections were made during calculation of biotransformation yields, which consequently are underestimated.

Effect on metabolism of a (±)-*cis/trans*-nerolidol mixture added at high dissolved oxygen tension.

Figure 4 shows dissolved oxygen tension (pO_2), dry weight, pH and titrant addition to maintain pH at 3.0 during repeated batch cultures of *A. niger* NW131 without (upper panel) and with (lower panel) addition of a commercially available (±)-*cis/trans*-nerolidol mixture (61 % *trans*-, 39 % *cis*-nerolidol) after 44 hours.
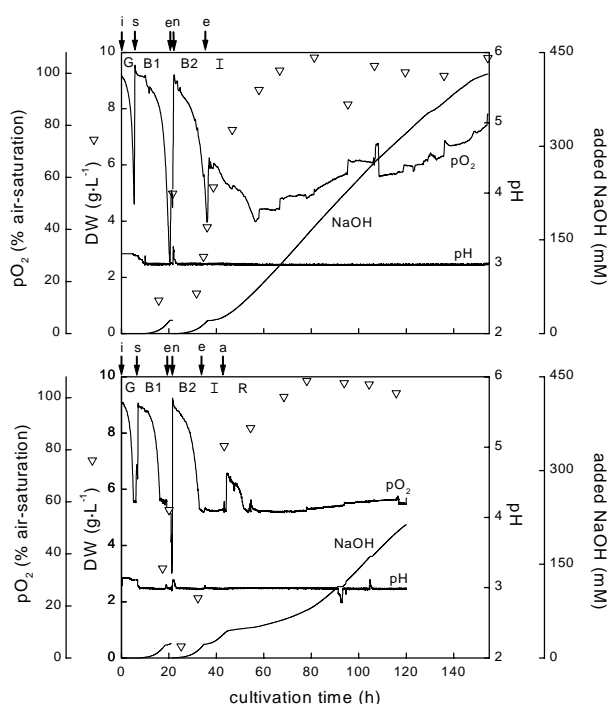
Figure 4. Repeated batch experiments with *A.niger* NW131 with (lower panel) and without (upper panel) addition of a (±)-*cis/trans*-nerolidol mixture in post-exponential phase of second batch culture. *A. niger* NW131 was grown on minimal medium with NH_4Cl (21 mM) as final cell density limiting substrate, 5 % glucose and with dissolved oxygen tension >50 % air saturation. Dissolved oxygen tension (pO_2), dry weight (DW), pH and accumulated NaOH added to maintain pH at 3.0 are shown. i: inoculation with spores, s: sparger aeration started, e: NH_4^+ exhaustion, n: new medium, a: cis/trans-nerolidol addition. G: germination, B1: batch 1, B2: batch 2, I: induction of acid formation, R: recovery from cis/trans-nerolidol. Pulses of added base titrant: 3090 (upper panel), 7810 (lower panel).

The rectilinear part of the LOS plots of accumulated base (22) shows that the exponential growth lasted for approximately 14 hours with similar maximum specific growth rates viz. µ of 0.28/0.30 h^{-1} and 0.24/0.27 h^{-1} for first and second batch cultures, respectively (Fig. 5). After exhaustion of ammonium, instantaneous decreases in the respiration rate (e in Fig. 4) and base addition rate (e in Fig. 5) identified a transition into the post-exponential phase. Subsequently the organic acid formation expressed as the base addition rate increased exponentially for approximately 5-6 hours, with rate constants of induction k_I between 0.32-

$0.37 \ h^{-1}$, followed by non-exponential base addition seen as a decrease in the slope of the LOS plots (Fig. 5). In the control experiment maximal base addition rate ($4.3 \ mM·h^{-1}$), found as the exponential to the maximal value (1.46) of the y-axis in the LOS plot ($\exp [1.46] = 4.3 \ mM·h^{-1}$) of upper panel of Figure 5, was reached after 30 h in the post-exponential phase.
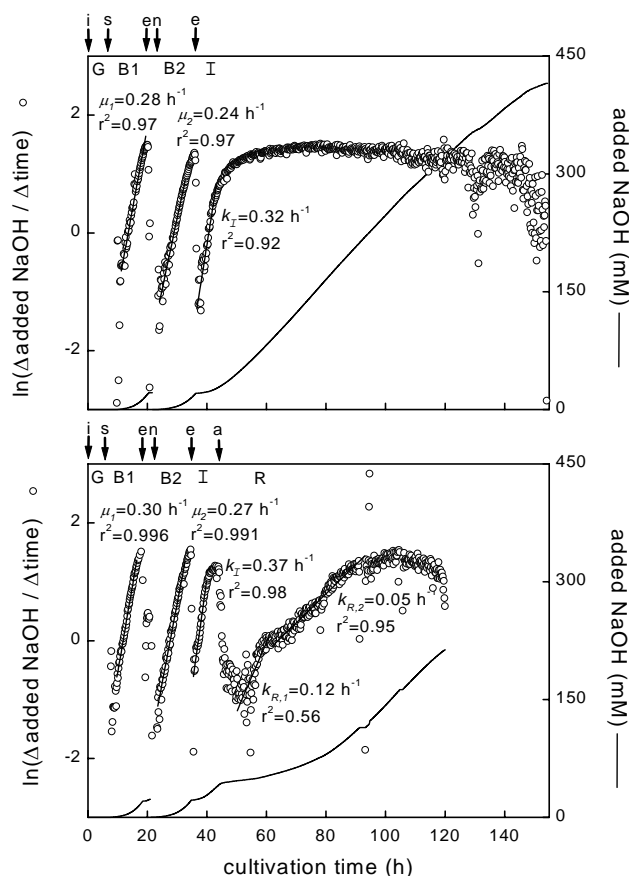
Figure 5. Accumulated NaOH addition and Log of Slope plot of accumulated NaOH during batch culture with (lower panel) and without (upper panel) addition of a (±)-*cis/trans*-nerolidol mixture in post-exponential phase of second batch culture. (Data from experiments shown in Figure 4.)

Inhibition of metabolism following addition of an ethanolic (±)-*cis/trans*-nerolidol mixture in the post-exponential phase was seen as an abrupt increase in the dissolved oxygen tension, i.e. decrease in respiration rate (a in Fig. 4, lower panel) and decreased base addition rate, i.e. decreased organic acid formation rate (a in Fig. 5, lower panel). This was not observed in control experiments (Fig. 4, upper panel and Fig. 5, upper panel) or experiments where only the co-solvent (EtOH) was added (results not shown). Both rates of respiration and organic acid formation recovered exponentially. Initially the rate constant of recovery of acid formation $k_{R,1}$, determined from the LOS plot of accumulated base, was $0.12 \ h^{-1}$ but decreased to $0.05 \ h^{-1}$ (Fig. 5, lower panel). When a (±)-*cis/trans*-nerolidol mixture was added to a culture late in the exponential phase (1.9 mM [NH_4^+], representing 9% of the initial concentration) at high dissolved oxygen tension (Fig. 6) a higher rate constant of recovery of acid formation $k_{R,1}$ ($0.20 \ h^{-1}$) was observed compared to addition during the post-exponential phase (0.05-$0.12 \ h^{-1}$). The maximal rate of organic acid formation was not affected by the time of substrate addition (compare lower panel Fig. 5 and Fig. 6).
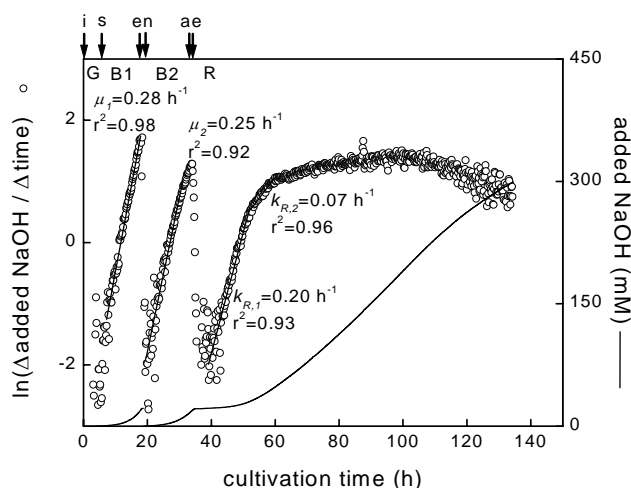
Figure 6. Accumulated NaOH addition and Log of Slope plot of accumulated NaOH during batch culture with addition of a (±)-cis/trans-nerolidol mixture late in exponential phase. Pulses of added base titrant: 5960. (Other experimental conditions as described in legend of Fig. 4.)

Electron Spin Resonance (ESR) studies indicated that a (±)-*cis/trans*-nerolidol mixture increased membrane fluidity in the fungal membrane [JZ Pedersen, personal communication]. This is in agreement with the description of antimicrobial activities of terpenoids [Cantwell *et al.* 1978; Cowan 1999] and the use of nerolidol as a chemical penetration enhancer in transdermal drug delivery [Yamane *et al.* 1995]. Therefore, the inhibition of organic acid formation was most likely part of a general inhibition of cellular activities. Inhibition of organic acid formation was not accompanied by any detectable cell lysis, which was confirmed by similar maximal rate of organic acid formation with and without addition of nerolidol (Fig. 5). Furthermore, biotransformation of a (±)-*cis/trans*-nerolidol mixture did not affect dry weight (Fig. 4) or carbohydrate content. However, measurements of extracellular organic acid and glucose concentrations showed that more carbon was converted from glucose into organic acids in control experiments than in biotransformation experiments, since glucose consumption remained unchanged. This indicated that recovery from the inhibition of organic acid formation required energy and carbon sources for de novo synthesis of cell material.

Product formation

Figure 7 shows conversion of a (±)-*cis/trans*-nerolidol mixture after addition during post-exponential phase. Only products **4-7** (Scheme 1) from stereoselective hydroxylation of 2E-methyls and dihydroxylation of the remote double bonds were observed. The maximal molar yield of 12-hydroxy-*trans*-nerolidol **4** (9%) was reached 25 hours after addition of the biotransformation substrate which was significantly faster and in higher yield compared to previously reported bioreactor cultures (5%) [Arfmann *et al.* 1988]. However, the maximum yield was lower than in previously reported shake flask cultures (13-20 %) of *A. niger* after addition of pure trans-nerolidol **2** [Arfmann *et al.* 1988; Madyastha and Gururaja 1993]. Nonetheless, it is an attractive option to use a *cis/trans*-nerolidol mixture instead of the more

expensive trans-nerolidol for biocatalysed bioreactor scale production of 12-hydroxy-*trans*-nerolidol **4**, especially as **4** constituted 80 % of the total products after 25 hours.
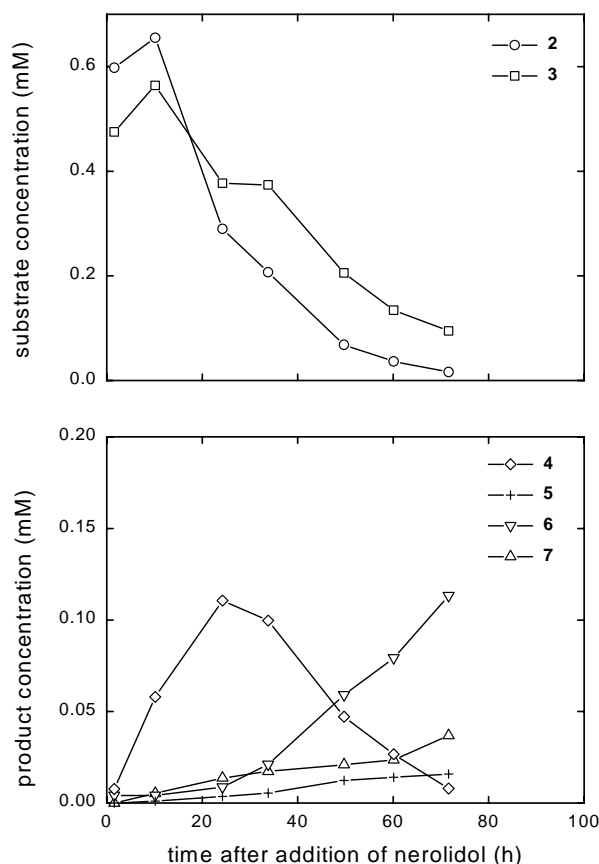
Figure 7. Concentration of *trans*-nerolidol **2**, *cis*-nerolidol **3**, 12-hydroxy-*trans*-nerolidol **4**, 10,11-dihydroxy-*trans*-nerolidol **5**, 10,11-dihydroxy-*cis*-nerolidol **6** and 12-hydroxy-*cis*-nerolidol **7** during biotransformation of a (±)-*cis/trans*-nerolidol mixture added in post-exponential phase. (Data from experiment shown in Figure 4 lower panel.)

The concentration of the main *cis*-product, 10,11-dihydroxy-*cis*-nerolidol **6** increased throughout biotransformation and reached a yield of 15 %, which was considerably lower than the previously reported 41 % yield [Arfmann *et al.* 1988]. 10,11-Dihydroxy-*trans*-nerolidol **5** and 12-hydroxy-*cis*-nerolidol **7** were only observed in small quantities, 1% and 5% respectively, confirming previous literature data [Arfmann *et al.* 1988]. However, we did not observe the 2Z-isomer, carboxylic acid and acetate ester of 12-hydroxy-*trans*-nerolidol **4**, found in that study as minor products from biotransformation of *trans*-nerolidol. Only a small proportion of the converted (±)-*cis/trans*-nerolidol (< 40 % *cis*-nerolidol, < 20 % *trans*-nerolidol) resulted in formation of *cis/trans*-products, while the remaining of converted (±)-*cis/trans*-nerolidol most likely was metabolised to CO_2 and/or cell components, which partly explained the modest biotransformation yields. Most likely this is a detoxification process since high glucose concentrations (approximately 36 g·L^{-1}) were present before addition of biotransformation substrate (Fig. 3) and glucose is a strong catabolite repressor.

As described above, significantly lower inhibition of organic acid formation was observed when a (±)-*cis/trans*-nerolidol mixture was added to the culture late in the exponential phase (Fig. 6) compared to addition in the post-exponential phase (lower panel Fig. 5), but this did not result in increased yields of 12-hydroxy-*trans*-nerolidol **4** (5%) and

10,11-dihydroxy-*cis*-nerolidol **6** (4%). However, the significantly lower maximal yields emphasizes the importance knowing the physiological state of *A. niger* before addition of biotransformation substrate in order to maximise biotransformation yields, which is easily monitored by measurements of titrant addition.

Biotransformation of (±)-*cis*-nerolidol and (±)-*trans*-nerolidol added in post-exponential phase at high dissolved oxygen tension

To further explore the inhibitory properties of nerolidol, separate biotransformations of (±)-*cis*-nerolidol and (±)-*trans*-nerolidol were carried out. Both isomers inhibited the respiration rate (data not shown) and organic acid formation. The rate constant of initial recovery in acid formation $k_{R,1}$ was smaller in biotransformation of (±)-*trans*-nerolidol (0.09 h^{-1}) than of (±)-*cis*-nerolidol (0.15 h^{-1}) indicating greater inhibition after addition of *trans*-nerolidol than of *cis*-nerolidol. Interestingly, the rate constant of initial recovery in acid formation $k_{R,1}$ observed in biotransformation of the (±)-*cis/trans*-nerolidol mixture, was lying between these values (0.12 h^{-1}, Fig. 5, lower panel). However, although *cis*- and *trans*-nerolidol apparently inhibited the organic acid formation differently, kinetics of product formation from the biotransformations of (±)-*cis*-nerolidol and (±)-*trans*-nerolidol were similar (data not shown) to the biotransformation of the (±)-*cis/trans*-nerolidol mixture (Fig. 7) and the yields of the main products 12-hydroxy-*trans*-nerolidol **4** and 10,11-dihydroxy-*cis*-nerolidol **6** were 6% and 5%, respectively.

Biotransformation of a (±)-*cis/trans*-nerolidol mixture added in post-exponential phase at low dissolved oxygen tension

To examine the influence of dissolved oxygen tension on biotransformations and to mimic conditions during oxygen limited shake flask biotransformations, a (±)-*cis/trans*-nerolidol mixture was added to a culture during the post-exponential phase at low dissolved oxygen tension (5%). In agreement with preliminary biotransformations in shake flasks, yields of the main products 12-hydroxy-*trans*-nerolidol **4** and 10,11-dihydroxy-*cis*-nerolidol **6** (7% and 6% respectively) were lower than in biotransformations at high dissolved oxygen tension. Interestingly, the kinetics of 12-hydroxy-*trans*-nerolidol **4** formation (data not shown) differed noticeably from biotransformations at high levels of dissolved oxygen tension (Fig. 7), since the concentration of 12-hydroxy-*trans*-nerolidol **4** increased rectilinearly throughout the biotransformation. Since 12-hydroxy-*trans*-nerolidol **4** apparently was metabolized only at high dissolved oxygen tension, biotransformations may be optimized by separating formation of cell mass (high dissolved oxygen tension) and products (low dissolved oxygen tension) by computer controlled ramp decrease of dissolved oxygen tension.

Biotransformation of a (±)-*cis/trans*-nerolidol mixture added to cells grown in rich medium in post-exponential phase at high dissolved oxygen tension

Effects of medium composition on biotransformation were examined in experiments where biotransformation of a (±)-*cis/trans*-nerolidol mixture was carried out in rich medium at dissolved oxygen tension above 50 % air saturation (data not shown). The monitoring of growth kinetics by titrant addition was, as expected, more complex in this medium, because of polyphasic growth on several medium components. However, it was still possible to follow growth rate, induction and inhibition of organic acid formation by the titration data. It is noteworthy that addition of the (±)-*cis/trans*-nerolidol mixture only caused a slight decrease in the base addition rate in contrast to cells grown in minimal medium, which indicates a smaller inhibition of organic acid formation arising from an increased metabolic capacity for recovery. However, the maximal yield of 12-hydroxy-*trans*-nerolidol **4** (8%) was almost unchanged but was reached approximately 14 h (50 %) faster than in minimal medium. This is similar to observations obtained from hydroxylation of benzoate by *A. niger* [J Visser, personal communication].

CONCLUSIONS

The computer-aided registration of titrant addition is experimentally uncomplicated but despite its simplicity the resolving power of the method is to our knowledge superior to other off- or on-line measurement of growth and metabolism and a prerequisite for the full exploration of the virtue of the log of slope plots in kinetic analysis, i.e., identification and quantification of different physiological states: growth, organic acid formation, inhibition of metabolism after addition of nerolidol and recovery from this inhibition. Acidification during exponential growth and in post-exponential phase was caused by excretion of protons during ammonium uptake and formation of oxalic and citric acid, respectively. Addition of *cis*-, *trans*-nerolidol or a *cis/trans*-nerolidol mixture to *A. niger* grown in minimal medium instantaneously inhibited respiration and formation of organic acids, but was followed by exponential recovery of cellular activities. Analysis of titrant addition by LOS plots easily identified specific growth rate (μ), a rate constant for induction of organic acid formation (k_I) and rate constants of recovery of organic acid formation ($k_{R,1}$) and ($k_{R,2}$) after biotransformation substrate addition. The physiological state of the culture before addition of biotransformation substrate had significant influence on the yield of α-sinensal precursor 12-hydroxy-*trans*-nerolidol 4, although the yield of biotransformation did not correlate with inhibition of organic acid formation. Higher yields (9%) and rates of 12-hydroxy-*trans*-nerolidol 4 formation were observed in biotransformation of *cis/trans*-nerolidol mixtures than in previous literature reports of bioreactor scale biotransformations of the more expensive *trans*-nerolidol.

It is difficult to envisage microbial activity without proton exchange, and therefore the analysis of the biotransformation reported here is only one example of application of a method with potential for characterization of any biotransformation.

ACKNOWLEDGEMENTS

SUPPORTING INFORMATION AVAILABLE

Procedure for isolation of biotransformation products used as standards in GC analysis. GC chromatogram of an extraction sample taken after 60 h of biotransformation. Characterisation of biotransformation products. This material is available free of charge via the Internet at http://pubs.acs.org.

REFERENCES AND NOTES

Agrawal R, Joseph R (2000) Bioconversion of alpha pinene to verbenone by resting cells of *Aspergillus niger*. Appl Microbiol Biotechnol 53: 335–337.

Aranda G, Moreno L, Cortes M, Prange T, Maurs M, Azerad RA (2001) New example of 1α-hydroxylation of drimanic terpenes through combined microbial and chemical processes. Tetrahedron 57: 6051–6056.

Arfmann HA, Abraham WR, Kieslich K (1988) Microbial ω-hydroxylations of *trans*-nerolidol and structurally related sesquiterpenoids. Biocatalysis 2: 59–67.

Baumann M, Hoffmann W, Pommer H (1976) Synthesis of sinensal. Liebigs Ann Chem 9: 1626–1633.

Bergmeyer HU, Bernt E, Schmidt F, Stork H (1974) D-glucose, Determination with hexokinase and glucose-6-phosphate dehydrogenase. In *Methods of enzymatic analysis*; Bergmeyer, H. U., Ed.; Vol. 3, 2nd edition, Verlag Chemie, Weinheim, 1196–1201.

Bertele E, Schudel P (1967) Synthesis of alpha- and beta-sinensal. Helv Chim Acta 50: 2445–2456.

Bligh EG, Dyer WJ (1959) A rapid method of total lipid extraction and purification. Can J Biochem Phys 37: 911–917.

Buchi G, Wuest H (1974) Stereoselective synthesis of alpha-sinensal. J Am Chem Soc 96: 7573–7574.

Cantwell SG, Lau EP, Watt DS, Fall RR (1978) Biodegradation of acyclic isoprenoids by *Pseudomonas* species. J Bacteriol 135: 324–333.

Chen ARM, Reese PB (2002) Biotransformation of terpenes from *Stemodia maritime* by *Aspergillus niger* ATCC 9142. Phytochemistry 59: 57–62.

Christensen ML, Eriksen NT (2002) Growth and proton exchange in recombinant *Escherichia coli* BL21. Enzyme Microb Technol 31: 566–574.

Cowan MM (1999) Plant products as antimicrobial agents. Clin Microbiol Rev 12: 564–582.

CRC Handbook of Chemistry and Physics (1999) 80th edition Lide, D. R., Ed.; CRC Press, Boca Raton, U.S.A. 8-46–8-56.

Degn H, Nielsen JB (1987) A general purpose serial interphase for the laboratory computer. Binary 10: 25–28.

Demyttenaere JCR, Adams A, Vanoverschelde J, de Kimpe N (2001) Biotransformation of (*S*)-(+)-Linalool by *Aspergillus niger*: An investigation of the culture conditions. J Agric Food Chem 49: 5895–5901.

Demyttenaere JCR, del Carmen Herrera M, de Kimpe N (2000) Biotransformation of geraniol, nerol, citral by sporulated surface cultures of *Aspergillus niger* and *Penicillium* sp. Phytochemistry 55: 363–373.

Desai SR, Gore VK, Bhat SV (1990) Highly stereoselective synthesis of α-sinensal and trans-β-ocimenal. Synthetic Commun 20: 523–533.

Dubois M, Gilles KA, Hamilton JK, Rebers PA, Smith F (1956) Colorimetric method for determination of sugars and related substances. Anal Chem 28: 350–356.

Eriksen NT, Kratchmarova I, Neve S, Kristiansen K, Iversen JJL (2001) Automatic inducer addition and harvesting of recombinant *Escherichia coli* cultures based on indirect on-line estimation of biomass concentration and specific growth rate. Biotechnol Bioeng 75: 355–361.

Folch J, Lees M, Stanley GHS (1957) A simple method for the isolation and purification of total lipids from animal tissues. J Biol Chem 226: 497–509.

Iversen JJL, Thomsen JK, Cox RP (1994) On-line growth measurements in bioreactors by titrating metabolic proton exchange. Appl Microbiol Biotechnol 42: 256–262.

Kubo I (1992) Antimicrobial activity of green tea flavor components and their combination effects. J Agric Food Chem 40: 245–248.

Lahlou EH, Noma Y, Hashimoto T, Asakawa Y (2000) Microbial transformation of dehydropinguisenol by *Aspergillus* sp. Phytochemistry 54: 455–460.

Larsen B, Poulsen BR, Eriksen NT, Iversen JJL. (In press) Homogeneous batch cultures of *Aspergillus oryzae* by elimination of wall growth in the Variomixing bioreactor. Appl Microbiol Biotechnol.

Lehman LR, Stewart JD (2001) Filamentous fungi: Potentially useful catalysts for the biohydroxylations of non-activated carbon centers. Curr Org Chem 5: 439–470.

Li Z, van Beilen JB, Duetz WA, Schmid A, de Raadt A, Griengl H, Witholt B (2002) Oxidative biotransformations using oxygenases. Curr Opin Chem Biol 6: 136–144.

Mackereth FJH (1964) An improved galvanic cell for determination of oxygen concentration in fluids. J Sci Instrum 41: 38–41.

Madyastha KM, Gururaja TL (1993) Utility of microbes in organic synthesis: Selective transformations of allylic isoprenoids by *Aspergillus niger*. Indian J Chem B 32: 609–614.

Martens DA, Loeffelmann KL (2002) Improved accounting of carbohydrate carbon from plants and soils. Soil Biol Biochem 34: 1393–1399.

Nielsen J, Villadsen J (1994) In Bioreaction engineering principles; Plenum Press, New York.

Pontecorvo G (1953) The Genetics of *Aspergillus nidulans*. In Advances in genetics; Demerec, M., Ed.; Vol 5, Academic Press, New York, 141–238.

Poulsen BR, Ruijter GJG, Visser J, Iversen JJL (2003) Determination of first order rate constants by natural logarithm of the slope plot exemplified by analysis of *Aspergillus niger* in batch culture. Biotechnol Lett 25: 565-571.

Poulsen BR, Sørensen AB, Schuleit T, Ruijter GJG, Visser J, Iversen JJL. Quantitative description of biomass distribution in filaments, pellets and diffusion-limited pellet cores in submerged cultures of filamentous fungi. Appl Environ Microb, submitted.

Terreaux C, Maillard M, Hostettmann K, Lodi G, Hakizamungu E (1994) Analysis of the fungicidal constituents from the bark of *Ocotea-usambarensis* Engl. (Lauraceae). Phytochem Analysis 5: 233–238.

Vicente A, Castrillo JI, Teixeira JA, Ugalde U (1998) On-line estimation of biomass through pH control analysis in aerobic yeast fermentation systems. Biotechnol Bioeng 58: 445–450.

Vishniac W, Santer M (1957) The thiobacilli. Bacteriol Rev 21: 195–213.

Yamane MA, Williams AC, Barry BW (1995) Terpene penetration enhancers in propylene glycol/water co-solvent systems: effectiveness and mechanism of action. J Pharm Pharmacol 47: 978–989.

Isolation of a fluffy mutant of *Aspergillus niger* from chemostat culture and its potential use as a morphologically stable host for protein production

ABSTRACT

Chemostat cultivation of *Aspergillus niger* and other filamentous fungi is often hindered by the spontaneous appearance of morphologic mutants. Using the Variomixing bioreactor and applying different chemostat conditions we tried to optimize morphologic stability in both ammonium- and glucose-limited cultures. In most cultivations, mutants with fluffy (aconidial) morphology became dominant. From an ammonium-limited culture, a fluffy mutant was isolated and genetically characterized using the parasexual cycle. The mutant contained a single morphological mutation, causing an increased colony radial growth rate. The fluffy mutant was subjected to transformation and finally conidiospores from a forced heterokaryon were shown to be a proper inoculum for fluffy strain cultivation.

INTRODUCTION

Aspergillus niger is an industrially important fungus, often used for the production of organic acids and proteins. Production processes using filamentous fungi are often designed as batch or fed-batch cultivations, but some of them seem to be suitable for continuous culturing [Swift *et al.* 1998; Wiebe *et al.* 2000]. Chemostat cultivation is mainly used for determining process variables and for characterizing strains at different specific growth rates. A major problem in the use of continuous cultures is the rapid appearance of morphological mutants, often leading to a reduction in protein production and altered growth characteristics [Christensen *et al.* 1995; Mainwaring *et al.* 1999; Wiebe *et al.* 1994; Withers *et al.* 1998]. The mutants were affected in sporulation, branching or both [Swift *et al.* 1998; Wiebe *et al.* 1993; Withers *et al.* 1995] and were often demonstrated to have a selective advantage over the parental strain. Also non-morphological mutations with altered production characteristics may occur [Mainwaring *et al.* 1999; Pederson *et al.* 2000; Wiebe *et al.* 1996]. The high frequency of mutants appearing is a symptom of genetic instability, which is even more problematic when genetically engineered strains are used. Usually these strains carry multiple copies of the gene of interest. Losing some of these copies is advantageous for the organism, but reduces the desired protein production [Christensen *et al.* 1995; Mainwaring *et al.* 1999; Swift *et al.* 1998].

Wiebe *et al.* [1994] have isolated stable "variants" of *Fusarium graminearum* from a chemostat culture. These variants had a selective advantage over their parent and were morphologically more stable in chemostat cultures. Similarly, from a glucoamylase overproducing *A. niger* strain, mutants with increased selective advantage were isolated, but unfortunately, in most cases their productivity appeared to be reduced [Swift *et al.* 2000; Withers *et al.* 1998]. However, Withers *et al.* [1998] isolated a mutant with less densely, brown spores, which sustained production for 735 hours, and Swift *et al.* [1998] isolated a white aconidial strain with higher glucoamylase production than the parent strain. However, an aconidial strain is difficult to maintain and use as an inoculum. In *A. niger* chemostat cultures, lowering pH from pH 5.4 to 4.0 increased morphological and genetic stability [Swift *et al.* 1998], but in other cases mutations still occurred [Mainwaring *et al.* 1999; Withers *et al.* 1998]. Another method to increase morphologic stability was used in *Fusarium graminearum*. There, Wiebe *et al.* [1996] frequently changed growth conditions, limiting the selective advantage of a mutant to a short period of the cultivation. Although these approaches increased morphologic and genetic stability in individual cases, they have not led to the development of a morphologically stable generally applicable host, suitable for the production of different proteins in *A. niger*.

According to the theory of Monod [1942] spontaneous mutants with increased maximum specific growth rate will always dominate a continuous culture at high dilution rates and spontaneous mutants with increased affinity for the limiting substrate will always dominate a continuous culture at low dilution rates [Tempest, 1970]. However, Swift *et al.* [1998] found that a mutant without a significant higher maximum specific growth rate than that of the original strain (0.27 ± 0.03 h^{-1}) constituted around 90% of a continuous culture at a dilution rate of 0.26 h^{-1} within 100 hours after appearance of the first mutant. This shows that

the mutation rate and/or other factors also are of importance. If such a fast exchange would originate from a single mutant and be caused by growth competition the mutant should have a very high maximum specific growth rate of around 0.35 h^{-1}. Theoretically, a combination of genetic instability and selection pressure in the culture seems to define the problem of morphologic instability in using continuous cultures. In order to increase genetic stability in *A. niger* chemostats, one could try to manipulate genetic factors controlling it. We focussed initially on the selection pressure, which we tried to reduce by optimising growth conditions. We used a bioreactor specially designed to avoid wall growth with filamentous fungi, the Variomixing [Larsen *et al.* 2003], and monitored the appearance of morphological mutants. Finally, the isolation of a fluffy mutant proved to be a further solution to the problem of morphologic instability. We show that such an aconidial strain is well accessible for modern genetic techniques. Using classical methods, conidiospores of an aconidial strain can be produced in a forced heterokaryon, which can serve as a proper inoculum for a liquid culture.

MATERIALS AND METHODS

Strains and media

Strain NW131 is derived from N400 (CBS 120.49) and carries the *cspA1* mutation affecting conidiophore height and density [Bos *et al.* 1988] and the *goxC17* mutation, which is a glucose oxidase loss-of-function mutation [Swart *et al.* 1990]. Fluffy mutant 982.1 was isolated from NW131 in this study and its mutation was designated *fluA1*. Masterstrain 982.2 was constructed as described by Bos *et al.* [1988] using mutations *cspA1, leuA1, nicA1* [Bos *et al.* 1988], *pyrA6* [Goosen *et al.* 1987], *goxC17* and *ΔargB* [Lenouvel *et al.* 2002] and by adding an UV induced colour mutation *fwnA22*. Strains 982.7 (*goxC17; cspA1 fluA1; niaD22*) and 982.11 (*ΔargB fwnA27; goxC17; cspA1 fluA1; leuA1*) were constructed in this study as described in Genetic manipulations (below). Strains 1012.9 (*ΔargB; goxC17; cspA1*, [Lenouvel *et al.* 2002]) and N402 (*cspA1* [Bos *et al.* 1988]) were used as control strains in the colony radial growth rate measurement. In plates, synthetic minimal medium containing 1 % (w/v) glucose (MM) or complete medium (CM) was used, both described by Pontecorvo *et al.* [1953]. To CM, 5 mM uridine and 2 mM arginine was added. The MM of the ammonium-limited continuous cultures contained 50 g glucose per litre and 1.13 g·L^{-1} NH$_4$Cl, while the glucose-limited continuous cultures contained 7.5 g glucose per litre and 4.5 g·L^{-1} NH$_4$Cl. After germination 0.15 mL polypropylene glycol (P 2000, Fluka chemicals) per litre was added as antifoam.

Chemostat conditions

Chemostat cultures were performed in a 5 L Variomixing bioreactor especially designed for growth of filamentous fungi with minimal wall growth [Larsen *et al.* 2003]. This was achieved by computer controlled rotation of the baffles at a similar speed and direction as the

impeller for 5 s every 5 min, which resulted in a temporary cancellation of the effect of the baffles; a deep vortex and high peripheral liquid flow rates at the reactor wall then developed. When baffles were rotating slowly (5-10 rpm for 5 min) the highly turbulent flow regime characteristic of conventional bioreactors with high mixing and mass transfer capacities was developed. Temperature was controlled at 30°C ± 0.1 and pH was controlled at 3.0 ± 0.05. Spores were harvested with saline water containing 9 g·L^{-1} NaCl and 0.5 g·L^{-1} Tween 80. After filtering through glass wool and washing in distilled water, the spores were inoculated directly into the Variomixing bioreactor to a density of 10^6 spores mL^{-1}, in a working volume of 4.3 L. For proper germination 0.03 g·L^{-1} yeast extract was added. During the initial germination period of 5-7 hours, aeration was through the headspace at 1 L·min^{-1} and stirrer rate was 450 rpm. After germination the aeration was performed through spargers at 1 L·min^{-1}, stirrer speed was increased to 750 rpm, computer controlled intervals of turbulent (5 min) and laminar (5 sec) flow, characteristic of the Variomixing bioreactor, was activated, and antifoam added. Before the final cell density-limiting substrate, ammonium or glucose, was exhausted from the germination batch culture, i.e., late in the exponential phase, the bioreactor was emptied, flushed once with medium and re-inoculated in 4.2 L medium by addition of 100 mL of the culture broth just sampled and kept under axenic conditions. Late in the exponential phase of this second batch the continuous medium flow was started at dilution rates between 0.05 and 0.27 h^{-1}. Ammonium and glucose were determined enzymatically essentially as described by Bergmeyer and Beutler [1985] and Bergmeyer et al. [1974], respectively.

Colony radial growth rate measurements

Colony radial growth rate measurements were performed essentially as described by Withers et al. [1995]. Per strain six Petri dishes with a 9 cm diameter, containing 20 mL MM + 50 mM glucose supplemented with 20 mg·L^{-1} leucine and 20 mg·L^{-1} arginine were used. Fluffy strain 982.11 was inoculated using a round 2 mm diameter mycelial plug from a plate with the same medium. The fluA+ control strains 1012.9 and N402 were stab inoculated.

Genetic manipulations

Selection of chlorate-resistant mutants was done as described by Debets et al. [1990]. UV irradiated spores of 982.1 were plated on medium containing 0.2 M chlorate and 10 mM urea, resulting in the selection of nitrate non-utilizing mutant 982.7. Heterokaryosis of this mutant with masterstrain 982.2 was induced using protoplast fusion as described by van Diepeningen et al. [1998] with the modification that the enzymatic treatment of mycelium was done in 1.3 M L-sorbitol, 50 mM CaCl$_2$, 10 mM TrisHCl pH7.5 (STC, [Kusters-van Someren et al. 1991]). For the selection of heterokaryons on MM with nitrate, we used p.a. chemicals and no. 1 agar from Oxoid, to avoid contamination of a nitrogen source other than nitrate. This was important because the chlorate resistant mutant was dependent on the other strain only for supply of nitrate reductase. The masterstrain was dependent on the chlorate resistant mutant

for the biosynthesis of leucine, nicotinamide, uridine and L-arginine, and was therefore much less likely to disturb the balance between the two different types of nuclei in the heterokaryon. Heterozygous diploids were isolated as intense black sectors of heterokaryotic colonies and haploidised by plating 100 cfu of the diploid spores on CM plates containing 66 ppm L, D-benomyl. Sporulating and fluffy colonies were transferred to masterplates using tweezers and replica plated on MM-based test medium using thick needles. The procedure to transform protoplasts was essentially as described before [Kusters-van Someren *et al.* 1991], using 5 * 10^6 protoplasts and 1 µg of the *argB* gene of *A. niger* [Buxton *et al.* 1985].

Heterokaryon inoculation

Heterokaryons were grown on MM plates, using p.a. chemicals and no. 1 agar from Oxoid. After 5 days incubation at 30°C spores were harvested, filtered and washed as described above. A 250 mL Erlenmeyer flask containing 100 mL MM with 1.13 g·L^{-1} NH$_4$Cl instead of NaNO$_3$, 50 g·L^{-1} glucose and 0.5 g·L^{-1} yeast extract was inoculated with 10^8 spores. The proportion of both parents and of the diploid in the culture was estimated after 19 and 26 hours, using two different approaches: 1) by plating dilutions of culture samples on supplemented medium (SM), and 2) by generating protoplasts by Novozyme 234 (Novo Nordisk A/S, Copenhagen Denmark) treatment of mycelium samples in STC, filtering out the protoplasts on a glass wool plug, and plating out dilutions on sucrose-stabilised SM plates. After incubation for 3 days at 30°C the colonies appearing were identified by their spore colour.

RESULTS AND DISCUSSION

Optimising growth conditions to increase morphologic stability

Genetic instability is a problem in studies using continuous cultures, disturbing the steady state [Swift *et al.* 1998]. Also morphologic heterogeneity of the culture caused by wall growth can disturb this steady state [Topiwala and Hamer 1971]. The Variomixing bioreactor design reduces the problem of wall growth, therefore, we used this bioreactor to study the problem of genetic instability in NW131 using different growth regimes. We monitored morphologic stability by taking samples at regular intervals and plating them directly on CM. After incubation the plates were checked for morphological mutants (see Table I). The cultures were performed at pH 3 because low pH increases strain stability in *A. niger* [Mainwaring *et al.* 1999; Wallis *et al.* 1999]. We used both ammonium-limited and glucose-limited cultures.

      The ammonium-limited culture Ammonium-One-Dilution-rate was grown at one steady-state at a dilution rate of 0.16 h^{-1}, which resulted in a very fast appearance of the first morphological (aconidial) mutant after 110 hours. This aconidial mutant resembles *A. nidulans* fluffy mutations [Dorn 1970]. Ammonium-Wash-out/Batch was performed as an alternating wash-out and batch culture. During the wash-out [Jannasch 1969] the dilution rate

exceeds the specific growth rate, avoiding nutritional limitation. The batch growth periods allow the restoration of biomass, after which we switched back to wash-out conditions, exposing the fungus to ammonium limitation for only very short periods.

Table I. Culture time and number of generations[a] before the appearance of the first morphological (fluffy) mutant in cultures limited in nitrogen (ammonium) or carbon source (glucose).

Culture[b]	Time (h)	Generation[a]
Ammonium-One-Dilution-rate[c]	110	27
Ammonium-Wash-out/Batch[d]	130	37
Glucose-Low-Medium-Low[e]	210	44
Glucose-Low-to-High[f]	240	40
Glucose-Chemostat-Batch-Chemostat[g]	>240	>60

[a]Total number of generations since spore germination. Duration of batch periods before start of medium flow was 8 to 12 generations (28 to 39 h, including 6 hour germination) in all cultures.
[c]Ammonium-limited chemostat culture with a dilution rate of 0.16 h^{-1}.
[b]30°C, pH 3.0, 750 rpm, 1 L air min^{-1}
[d]Alternating wash-out and batch culture with ammonium as final cell density-limiting substrate. The duration of the batch and wash-out phases were 14 and 25 h, respectively, and the dilution rate during wash-out was 0.27 h^{-1}.
[e]Glucose-limited chemostat culture with increase followed by decrease in dilution rates: 0.08, 0.12, 0.16 and 0.08 h^{-1} with a duration of 61, 33, 26 and 54 h, respectively.
[f]Glucose-limited chemostat culture with increase in dilution rates: 0.05, 0.08, 0.16, 0.20 and 0.23 h^{-1}, with a duration of 94, 55, 27, 22 and 11 h, respectively
[g]Glucose-limited chemostat culture interrupted by a batch and with the following dilution rates: 0.16, 0.05, 0, 0.08, 0.18 and 0.21 h^{-1} with a duration of 36, 70, 17, 8, 48, and 25 h, respectively.

The glucose-limited cultures were grown at different dilution rates. In Glucose-Chemostat-Batch-Chemostat an intermediate batch experiment was performed after 140 hours. The rationale behind both alternating growth regimes is to counteract selection of mutations only advantageous during a part of the cultivation. Both the wash-out and batch growth conditions result in selection pressure for increased maximum specific growth rate, whereas steady-state growth conditions result in selection pressure for increased maximum specific growth rate and/or increased affinity for the limiting substrate [Tempest 1970].

Morphologic mutations appeared earlier in the ammonium-limited cultures than in the glucose-limited ones, although the number of generations was almost the same in cultivation Ammonium-Wash-out/Batch compared to Glucose-Low-Medium-Low and Glucose-Low-to-High. The use of alternating growth regimes in cultivation Ammonium-Wash-out/Batch and Glucose-Chemostat-Batch-Chemostat delayed the appearance of the first morphologic mutant, especially when considering the number of generations. The condition of the chemostat phase of Ammonium-One-Dilution-Rate was a constant ammonium limitation, whereas the Ammonium-Wash-out/Batch cultivation was alternating between ammonium-limiting and non-limiting conditions. The conditions for cultivation Glucose-Chemostat-Batch-Chemostat were more alternating than for the other two glucose-limiting cultures because the interruption by a batch phase resulted in non-limiting conditions, whereas during all phases of the other two glucose-limiting cultures the limitation remained.

In all cultures, the fluffy mutants were the main morphological mutant type found. No densely sporulating mutants or yellow pigment producing mutants were found and only a few brown mutants were observed.

Isolation of a stable fluffy mutant

A rapid appearance of a fluffy mutant was observed in cultivation Ammonium-One-Dilution-rate (Table I). Ten generations (43 h) after the appearance of the first fluffy mutant, it constituted ~99% of the culture, at which time it was isolated and purified by repeated cultivation on CM plates. This fluffy morphology appeared to be stable for the rest of the culture (600 h). A similar aconidial "white" *A. niger* mutant was isolated by Swift *et al.* ([1998], see figure 3 of their report) and was reported to have an increased colony radial growth rate. Also our fluffy or "white" mutant had a higher colony radial growth rate compared to wild type (202 ± 17 µm h^{-1} vs. 152 ± 15 µm h^{-1}). Assuming the increase of the fluffy morphology from first appearance (~0.1%) to ~99% in 43 hours is caused by an increased maximum specific growth rate only, the maximum specific growth rate of the mutant should be almost four times that of the parent. This is very unlikely. Another explanation for the rapid increase of the fluffy morphology could be an increased affinity for the limiting substrate, ammonium. However, the fluffy strains would have to have a 100-fold lower Ks, which is also very unlikely. Therefore we suggest that mutations resulting in fluffy phenotype have occurred in several cells independently during the 43 hours. The fluffy mutation in the different fluffy mutants might not be the same. We have isolated only one of these mutants and denoted its fluffy mutation as *fluA1*.

The fluffy mutant did not sporulate at 30°C, but slight sporulation was observed at the centre of a colony after a rather long incubation of 7 days at 37°C on CM. In a colony with a diameter of 8 cm, the sporulating centre had a diameter of 2.5 cm, carrying $2.5 \ 10^{7}$ spores, which is only 1/100 of the amount required to inoculate a 2.5 L bioreactor.

In previous studies with *A. niger* chemostats grown at pH 5.4, the morphologic mutants that appeared were mainly brown conidia bearing mutants, and those were scarcely observed in cultures grown at pH 4.0 [Mainwaring *et al.* 1999; Swift *et al.* 1998 and 2000; Wallis *et al.* 2001; Withers *et al.* 1998]. In these studies, Swift *et al.* [1998] and Withers *et al.* [1998] reported the appearance of white, non-sporulating mutants, but only as a small proportion of the total population and only at pH 5.4 or 5.5. It is therefore striking that we found mainly non-sporulating mutants, at pH 3.0. The difference in the morphologic mutants appearing could be caused by several factors. We used different culture conditions with a different pH, we used a different reactor design and we used an *A. niger* strain with different genetic markers. The *A. niger* strains used in above mentioned studies as well as our strain are all descendants of N402 carrying the *cspA1* mutation conferring low conidiospores. The strain used by Mainwaring *et al.* [1999] was constructed from N402 via AB4.1 [van Hartingsveldt *et al.* 1987], a *pyrG* mutant transformed with a fusion gene of *glaA* and a cDNA encoding the mature hen egg white lysozyme. The strains used by Swift *et al.* [1998 and 2000], Wallis *et al.* [2001] and Withers *et al.* [1998] were constructed directly from N402 using acetamidase selection with four copies of *glaA* on the same cosmid vector. Our strain, NW131, is not

transgenic and carries only one additional mutation, a glucose oxidase null mutation *goxC17* selected at a low UV dose [Swart *et al.* 1990].

For understanding the selective advantage of fluffy mutations, it is useful to look at the situation in *A. nidulans* where sporulation has been studied quite well [Adams *et al.* 1998]. Mutants in all stages of sporulation have been isolated, ranging from the total aconidial *fluffy* mutations [Dorn 1970], to mutants having aberrant conidial structures such as the *bristle*, *wet* and *abacus* mutants [Timberlake 1980]. In liquid cultures, asexual sporulation is induced by nitrogen or carbon limitation [Lee and Adams 1995; Skromne *et al.* 1995]. The regulatory cascade leading to sporulation in *A. nidulans* starts with *fluG*, and is directed via a number of *flb* genes, towards modulation of genes at the end of the central regulatory pathway, *brlA*, *abaA* and *wetA* [Adams *et al.* 1998]. By modulation of *fluG* Yu *et al.* [1996] showed that the onset of sporulation directly antagonises filamentous growth itself, which explains why most of the *A. nidulans* fluffy mutants have an increased maximum specific growth rate. Similarly, an *A. niger* fluffy mutant might also have an increased maximum specific growth rate, giving it a selective advantage at high dilution rates.

Schrickx *et al.* [1993] have shown that at dilution rates lower than 0.12 h^{-1} N402 starts to differentiate. In *A. nidulans*, sporulation was shown to involve the expression of many genes [Sanchez *et al.* 1998; Timberlake 1980], and it is likely that this differentiation uses a considerable part of the fungal resources. Therefore, a fluffy mutant disabled in an early part of the sporulation signalling pathway is also expected to have a selective advantage at lower dilution rates. With the fluffy mutation located in an early part of the sporulation pathway, no other mutations in this pathway can arise, which probably makes the fluffy phenotype morphologically more stable than its parent.

Genetic analysis and manipulation of the *fluA1* mutant

The *fluA1* containing mutant isolated from cultivation Ammonium-One-Dilution-rate was designated 982.1. Genetic analysis of *A. niger* strains can only be done by mitotic recombination, which requires at least one auxotrophic mutation to force a heterokaryon with a complementary auxotrophic master strain [Pontecorvo *et al.* 1953]. For this purpose a *niaD* mutant of 982.1 was isolated, using 10^7 spores on a selection plate containing chlorate. Of the resulting mutants 21 were rescreened by inoculating pieces of mycelium on plates with different nitrogen sources. A strain fitting the phenotype of a *niaD* mutant [Debets *et al.* 1990] was designated 982.7 (*goxC17; cspA1 fluA1; niaD22*). Protoplast fusion of 982.7 with master strain 982.2 (*ΔargB fwnA27; goxC17; cspA1 pyrA6; leuA1; nicA1*) resulted in heterokaryotic colonies, bearing both black and fawn coloured spores. The black conidiospores originated from 982.7 cells. Therefore, the *fluA1* mutation appeared to be recessive and was complemented in a heterokaryon.

Although *A. niger* heterokaryons rarely form spontaneous diploid sectors, the heterokaryon of 982.7//982.2 produced them at high frequency. The diploids sporulated normally, indicating that the *fluA1* mutation is completely recessive in a diploid. We inoculated one representative diploid on plates with CM + benomyl and analysed 66 of the resulting haploids, with approximately an equal number of fluffy recombinants and normal

ones. The *fluA1* mutation had a recombination frequency of 17% with *pyrA6*, locating *fluA1* on linkage group III. As expected, a linkage between *ΔargB* and *fwnA27* was found, and no linkage between any of the other markers.

For a fluffy mutant to serve as a suitable host for protein production, it should be easily transformable. In order to see if the fluffy mutant indeed could be transformed using a common procedure, an arginine requiring recombinant, 982.11 (*ΔargB fwnA27; goxC17; cspA1 fluA1; leuA1*), was used in a standard transformation protocol [Kusters-van Someren *et al.* 1991]. From 10^7 protoplasts and 1 μg pIM2101, containing *argB$_{niger}$* [Lenouvel *et al.* 2002] 91 transformants were obtained, which is at least 10-fold lower than usual. However, this transformation frequency is quite acceptable for routine transformations.

The use of conidiospores from a heterokaryon as an inoculum for a fluffy strain

Conidiospores are the preferred inoculum to obtain a proper morphology in submerged cultures. As shown above, a sufficient number of spores of the fluffy mutant is difficult to obtain because of the reduced sporulation. As described in the previous section, spores of the recessive aconidial mutant (982.7) are fairly easily obtained from a heterokaryon. Because conidiospores from *Aspergillus* are mononucleate, the spore suspension from heterokaryon 982.2//982.7 contains spores from both 982.2 and 982.7, as well as spores from the heterozygous diploid.

We wanted to investigate if such a mixture of spores could be used as an inoculum for the fluffy strain 982.7. Spores from the heterokaryon were harvested as described. To determine the proportion of the three different strains present in the inoculum and in the culture samples, samples were spread on plates. The different strains could easily be distinguished phenotypically, 982.7 as non-sporulating, 982.2 having fawn coloured spores and the diploid carrying black spores.

In the inoculum the proportion of the three different strains could be determined accurately, from the mycelium samples that was more difficult. Plating dilutions of the mycelium samples could give an overestimation of the sporulating strains because a pellet containing at least one of the sporulating strains was scored as black (diploid) or fawn (982.2). Assuming Novozyme 234 is equally active on the cell wall of all three strains, an estimation of the proportion based on plating out protoplasts would be more accurate. Surprisingly, using both methods we did not find much difference in the estimation of proportions of the different strains in the culture (data not shown). Strain 982.2 was hardly able to proliferate, which is not surprising as it lacks a proper amount of its auxotrophic growth requirements, L-arginine, uridine, L-leucine and nicotinamide (Fig 1). The diploid as prototroph had no obvious disadvantage compared to 982.7, but still decreased in proportion, indicating a lower maximum specific growth rate. This could be due to the auxotrophic mutations present in the heterozygous diploid, which, although assumed to be recessive, could also have a slightly intermediate effect. It is more likely, however, that the diploid has a lower maximum specific growth rate compared to the fluffy mutation because the beneficial effect of the recessive fluffy mutation is complemented, and therefore absent in the heterozygous

diploid. The fluffy mutation appeared to be beneficial in this culture, allowing the heterokaryon to be a proper source for 982.7 inoculum.

Despite the difficulty to manipulate fluffy mutants, their morphologic stability in continuous cultures may be a great advantage. A fluffy mutant would be a suitable strain to test if increased morphological stability results in more stable production and thus would be an improved host for protein production.
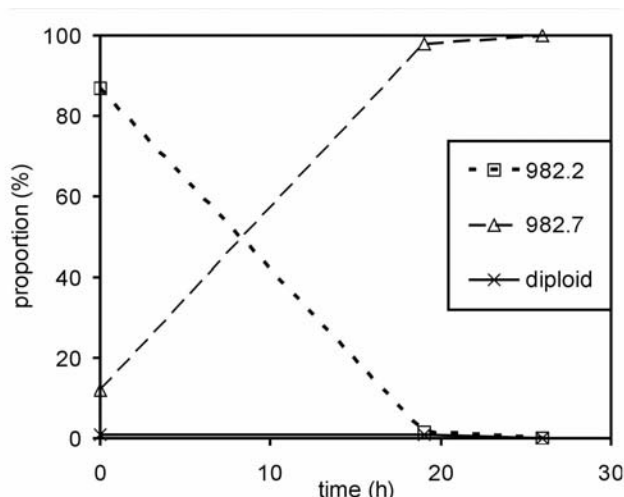
Figure 1. Proportion of 982.2 (*fluA+*), 982.7 (*fluA1*) and diploid 982.2//982.7 in a batch culture on minimal medium containing ammonium as a nitrogen source. Estimation of proportion was done using spores at 0 hours and protoplasts at 19 and 26 hours.

CONCLUSIONS

We showed a fluffy mutant to be manageable in commonly used laboratory procedures. Using the very few conidiospores it produces, we were able to select additional chlorate resistance markers and use the resulting nitrate auxotroph in a mitotic recombination. Thus adding selectable transformation markers to its genotype, we successfully transformed a fluffy strain using a regular transformation protocol. Although we expect the presence of multiple copy integrations of a gene of interest to be at least as stable as in the wild type, this still has to be investigated. Also the enzyme production and secretion properties may be different in a fluffy mutant, although Swift *et al.* [1998] showed a similar "white" mutant to produce even more glucoamylase compared to its parent in a batch culture, despite it contained a lower number of glucoamylase genes. For large-scale inoculations an inoculum obtained from a forced heterokaryon was shown to be appropriate.

REFERENCES

Adams TH, Wieser JK, Yu JH (1998) Asexual sporulation in *Aspergillus nidulans*. Microbiol Mol Biol Rev 62: 35-54.

Bergmeyer HU, Bernt E, Schmidt F, Stork H (1974) D-glucose, Determination with hexokinase and glucose-6-phosphate dehydrogenase. In: Bergmeyer HU, editor. Methods of enzymatic analysis, Vol. 3, 2nd edition. Weinheim: Verlag Chemie, p 1196–1201.

Bergmeyer HU, Beutler HO (1985) Ammonia. In: Begmeyer HU, editor. Methods of enzymatic analysis, Vol. 8, 3rd edition. Weinheim: VCH, p 454-461.

Bos CJ, Debets AJ, Swart K, Huybers A, Kobus G, Slakhorst SM (1988) Genetic analysis and the construction of master strains for assignment of genes to six linkage groups in *Aspergillus niger*. Curr Genet 14: 437-443.

Buxton FP, Gwynne DI, Davies RW (1985) Transformation of *Aspergillus niger* using the *argB* gene of *Aspergillus nidulans*. Gene 37: 207-214.

Christensen LH, Henriksen CM, Nielsen J, Villadsen J, Egel Mitani M (1995) Continuous cultivation of *Penicillium chrysogenum*. Growth on glucose and penicillin production. J Biotechnol 42: 95-107.

Debets AJ, Swart K, Bos CJ (1990) Genetic analysis of *Aspergillus niger*: isolation of chlorate resistance mutants, their use in mitotic mapping and evidence for an eighth linkage group. Mol Gen Genet 221: 453-458.

Diepeningen AD van, Debets AJ, Hoekstra RF (1998) Intra- and interspecies virus transfer in *Aspergilli* via protoplast fusion. Fungal Genet Biol 25: 171-180.

Dorn GL (1970) Genetic and morphological properties of undifferentiated and invasive variants of *Aspergillus nidulans*. Genetics 66: 267-279.

Goosen T, Bloemheuvel G, Gysler C, de Bie DA, van den Broek HW, Swart K (1987) Transformation of *Aspergillus niger* using the homologous orotidine-5'-phosphate-decarboxylase gene. Curr Genet 11: 499-503.

Hartingsveldt W van, Mattern IE, van Zeijl CM, Pouwels PH, van den Hondel CA (1987) Development of a homologous transformation system for *Aspergillus niger* based on the *pyrG* gene. Mol Gen Genet 206: 71-75.

Jannasch HW (1969). Estimations of bacterial growth rates in natural waters. J Bact 99: 156-60.

Kusters-van Someren MA, Harmsen JAM, Kester H, Visser J (1991) Structure of the *Aspergillus niger pelA* gene and its expression in *Aspergillus niger* and *Aspergillus nidulans*. Curr Genet 20: 293-299.

Larsen B, Poulsen BR, Eriksen NT, Iversen JJL (2003) Homogeneous batch cultures of *Aspergillus oryzae* by elimination of wall growth in the Variomixing bioreactor. Appl Microbiol Biotechol *in press*.

Lee BN, Adams TH (1995) FluG and flbA function interdependently to initiate conidiophore development in *Aspergillus nidulans* through *brlA* beta activation. EMBO J 15: 299-309.

Lenouvel F, van de Vondervoort PJI, Visser J (2002) Disruption of the *Aspergillus niger argB* gene: a tool for transformation. Curr Genet 41: 425-431.

Mainwaring DO, Wiebe MG, Robson GD, Goldrick M, Jeenes DJ, Archer DB, Trinci AP (1999) Effect of pH on hen egg white lysozyme production and evolution of a recombinant strain of *Aspergillus nige*r. J Biotechnol 75: 1-10.

Monod J (1942) Recherches sur la croissance des cultures bacteriennes. Paris: Hermann.

Pedersen H, Beyer M, Nielsen J (2000) Glucoamylase production in batch, chemostat and fed-batch cultivations by an industrial strain of Aspergillus niger. Appl Microbiol Biotechnol 53:272-277

Pontecorvo G, Roper JA, Hemmons LJ, Macdonals KJ, Bufton AWJ (1953) The genetics of *Aspergillus nidulans.* Adv Genet 5: 141-238.

Sanchez O, Navarro RE, Aguirre J (1998) Increased transformation frequency and tagging of developmental genes in *Aspergillus nidulans* by restriction enzyme-mediated integration (REMI). Mol Gen Genet 258: 89-94.

Schrickx JM, Krave AS, Verdoes JC, van den Hondel CA, Stouthamer AH, van Verseveld HW (1993) Growth and product formation in chemostat and recycling cultures by *Aspergillus niger* N402 and a glucoamylase overproducing transformant, provided with multiple copies of *glaA* gene. J Gen Microbiol 139: 2801-2810.

Skromne I, Sanchez O, Aguirre J (1995) Starvation stress modulates the expression of the *Aspergillus nidulans brlA* regulatory gene. Microbiology 141: 21-28.

Swart K, van de Vondervoort PJI, Witteveen CF, Visser J (1990) Genetic localization of a series of genes affecting glucose oxidase levels in *Aspergillus niger.* Curr Genet 18: 435-439.

Swift RJ, Wiebe MG, Robson GD, Trinci AP (1998) Recombinant glucoamylase production by *Aspergillus niger* B1 in chemostat and pH auxostat cultures. Fungal Genet Biol 25: 100-109.

Swift RJ, Karandikar A, Griffen AM, Punt PJ, van den Hondel CA, Robson GD, Trinci AP, Wiebe MG (2000) The Effect of organic nitrogen sources on recombinant glucoamylase production by *Aspergillus niger* in chemostat culture. Fungal Genet Biol 31: 125-133.

Tempest DW (1970) Theory of the chemostat. In: Norris JR. Ribbons DW. editors. Methods in Microbiology. London and New York: Academic Press. p 259-276.

Timberlake WE (1980) Developmental gene regulation in *Aspergillus nidulans*. Dev Biol 78: 497-510.

Topiwala HH, Hamer G (1971) Effect of wall growth in steady-state continuous culture. Biotechnol Bioeng 13: 919-922.

Wallis GL, Swift RJ, Hemming FW, Trinci AP, Peberdy JF (1999) Glucoamylase overexpression and secretion in *Aspergillus niger*: analysis of glycosylation. Biochim Biophys Acta 1472: 576-586.

Wiebe MG, Robson GD, Cunliffe B, Oliver SG, Trinci AP (1993) Periodic selection in longterm continuous-flow cultures of the filamentous fungus *Fusarium graminearum*. J Gen Microbiol 139: 2811-2817.

Wiebe MG, Robson GD, Oliver SG, Trinci AP (1994) Use of a series of chemostat cultures to isolate 'improved' variants of the Quorn mycoprotein fungus, *Fusarium graminearum* A3/5. Microbiology 140: 3015-3021.

Wiebe MG, Robson GD, Oliver SG, Trinci AP (1996) pH oscillations and constant low pH delay the appearance of highly branched (colonial) mutants in chemostat cultures of the Quorn(R)Myco-Protein fungus, *Fusarium graminearum* A3/5. Biotechnol Bioeng 51: 61-68.

Wiebe MG, Robson GD, Shuster J, Trinci AP (2000) Growth-rate-independent production of recombinant glucoamylase by *Fusarium venenatum* JeRS 325. Biotechnol Bioeng 68: 245-251.

Withers JM, Wiebe MG, Robson GD, Osborne D, Turner G, Trinci AP (1995) Stability of recombinant protein production by *Penicillium chrysogenum* in prolonged chemostat culture. FEMS Microb Lett 133: 245-251.

Withers JM, Swift RJ, Wiebe MG, Robson GD, Punt PJ, van den Hondel CA, Trinci AP (1998) Optimization and stability of glucoamylase production by recombinant strains of *Aspergillus niger* in chemostat culture. Biotechnol Bioeng 59: 407-418.

Yu JH, Wiezer J, Adams TH (1996) The *Aspergillus* FlbA RGS domain protein antagonizes G protein signalling to block proliferation and allow development. EMBO J 15: 5184-5190.

Increased NADPH concentration obtained by metabolic engineering of the pentose phosphate pathway in *Aspergillus niger*

ABSTRACT

Many biosynthetic reactions and bioconversions are limited by low availability of NADPH. With the purpose of increasing the NADPH concentration and/or the flux through the pentose phosphate pathway in *Aspergillus niger*, the genes encoding glucose 6-phosphate dehydrogenase (*gsdA*), 6-phosphogluconate dehydrogenase (*gndA*) and transketolase (*tktA*) were cloned and overexpressed in separate strains. Intracellular NADPH concentration was increased 2 to 9-fold as a result of 13-fold overproduction of 6-phosphogluconate dehydrogenase. Although overproduction of glucose 6-phosphate dehydrogenase and transketolase changed the concentration of several metabolites it did not result in increased NADPH concentration. To establish the effects of overexpression of the three genes, wild type and overexpressing strains were characterized in detail in exponential and stationary phase of bioreactor cultures containing minimal media with glucose as carbon source and ammonium or nitrate as nitrogen source and final cell density limiting substrate. Enzymes, intermediary metabolites, polyol pools (intra- and extracellular), organic acids, growth rates and rate constant of induction of acid production in post-exponential phase were measured. None of the modified strains had a changed growth rate. Partial least square regressions showed the correlations between NADPH and up to 40 other variables (concentration of enzymes and metabolites) and it was possible to predict the intracellular NADPH concentration from relatively easily obtainable data (concentration of enzymes, polyols and oxalate). This prediction might be used in screening for high NADPH levels in engineered strains or mutants of other organisms.

Abbreviations: 6PG, 6-phosphogluconate; a, ammonium; ARC, anabolic reduction charge; CRC, catabolic reduction charge; DHAP, dihydroxyacetone phosphate; e, exponential growth phase; E, extracellular; F6P, fructose 6-phosphate; G6P, glucose 6-phosphate; GAP, glyceraldehyde 3-phosphate; I, intracellular; IAP: induction of acid production; n, nitrate; R5P, ribose 5-phosphate; Ru5P, ribulose 5-phosphate; s, stationary phase; S7P, sedoheptulose 7-phosphate, wt, wild type; Xu5P, xylulose 5-phosphate; μ_{max}, maximum specific growth rate.

Enzymes: ALD, Aldolase (EC 4.1.2.13); 6PGDH, 6-phosphogluconate dehydrogenase (EC 1.1.1.44); G6PDH, glucose 6-phosphate dehydrogenase (EC 1.1.1.49); GLYDH, glycerol dehydrogenase (EC 1.1.1.156); M1PDH, mannitol 1-phosphate dehydrogenase (EC 1.1.1.17); PGI, phosphoglucose isomerase (EC 5.3.1.9); TAL, transaldolase (EC 2.2.1.2); TKT, transketolase (EC 2.2.1.1).

Note: The nucleotide sequences reported are in the GenBank database under the accession numbers AJ551178, AJ551177 and AJ550995.

INTRODUCTION

The pentose phosphate pathway (PPP) and glycolysis comprise the most central pathways in primary metabolism (Fig. 1). The PPP is believed to be the major source of NADPH required for many biosynthetic and detoxification reactions. The flux through this pathway has been reported to increase at high NADPH requirements for e.g. penicillin formation [Henriksen *et al.* 1996; Jørgensen *et al.* 1995], methylenomycin synthesis [Obanye *et al.* 1996] and reduction of (growth on) nitrate [Pedersen *et al.* 1999; Schmidt *et al.* 1998] and to decrease when the need for NADPH production is decreased [Marx *et al.* 1999; dos Santos *et al.* 2003]. In cell-free enzyme systems the NADPH is regenerated enzymatically or electrochemically [Li *et al.* 2002], but whole-cell systems are often the only available, more stable and inexpensive enzyme source [Lehman and Stewart 2001].

The availability of NADPH in whole-cell systems might be increased by metabolic pathway engineering e.g. overproduction of enzymes in the PPP or deletion of genes in glycolysis. NADPH is produced in two of the steps in the PPP: conversion of glucose 6-phosphate (G6P) to 6-phosphoglucono-δ-lactone (6PGδL), catalysed by G6PDH and conversion of 6-phosphogluconate (6PG) to ribulose 5-phosphate (Ru5P) catalysed by 6PGDH (Fig. 1). In the non-oxidative part of the PPP two out of three reactions are catalysed by transketolase. Overproduction of these enzymes might lead to increased flux through the PPP. The level of NADPH has previously been increased in *Escherichia coli* by overproduction of G6PDH or 6PGDH [Lim *et al.* 2002] and in *Ralstonia eutropha* by overproduction of G6PDH [Choi *et al.* 2003] or by overproduction of 6PGDH or TKT [Lee *et al.* 2003].
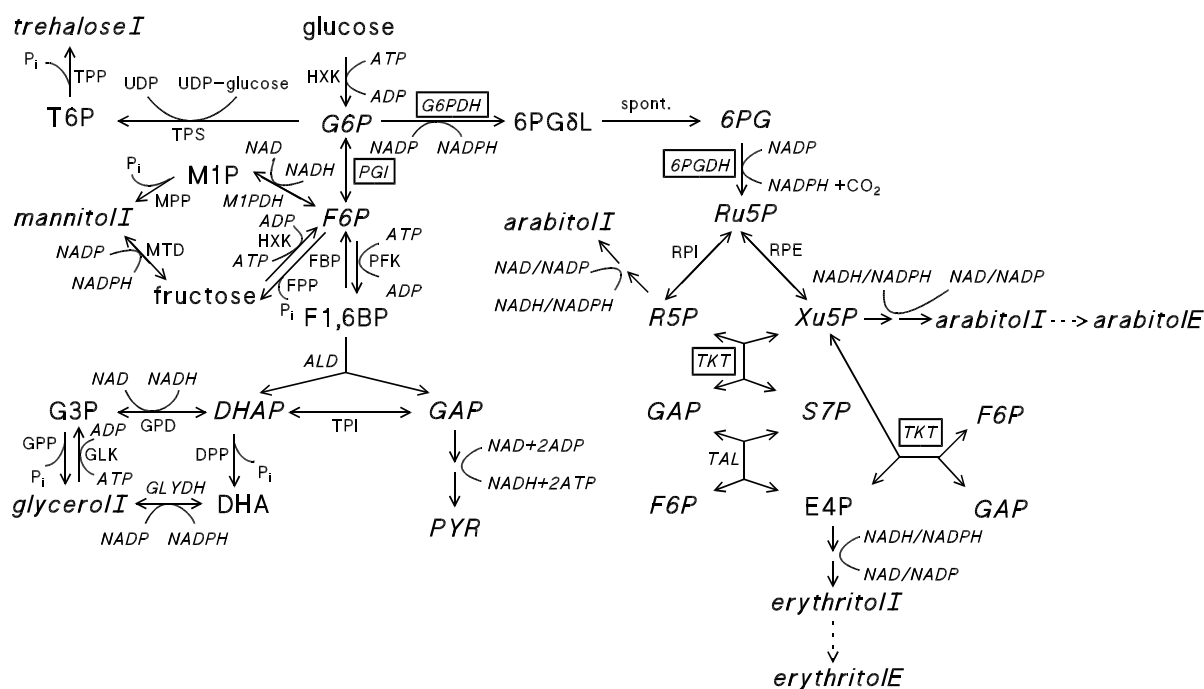
116

Figure 1. Glycolysis, pentose phosphate pathway and polyol formation in *Aspergilli*. Partly after [Witteveen 1993] and [Ruijter *et al.* 2003]. Two arrows in series mean two or more reactions. Enzymes in boxes were subjected to metabolic engineering in this study. E and I indicate extra- and intracellular polyols, respectively. Metabolites and enzymes in italics were measured in wild type and engineered strains (see Enzymes and Abbreviations lists for abbreviations). Other metabolite abbreviations: 6PGδL, 6-phosphoglucono-δ-lactone; DHA, dihydroxyacetone; E4P, erythrose 4-phosphate; F1,6BP, fructose 1,6-bisphosphate; G3P, glycerol 3-phosphate; M1P, mannitol 1-phosphate; T6P, trehalose 6-phosphate. Other enzyme abbreviations: DPP, dihydroxyacetone phosphate phosphatase; FPB, fructose1,6-bisphosphatase; FPP, fructose 6-phosphate phosphatase; GPD, glycerol 3-phosphate dehydrogenase; GPP, glycerol 3-phosphate phosphatase; GLK, glycerol kinase; HXK, hexokinase; MPP, mannitol 1-phosphate phosphatase; MTD, mannitol dehydrogenase; PFK, phosphofructokinase; RPI, ribosephosphate isomerase; RPE, ribulosephosphate 3-epimerase; TPP, trehalose 6-phosphate phosphatase; TPS, trehalose 6-phosphate synthase; TPI, triosephosphate isomerase.

The most likely means to increase the pentose phosphate pathway flux, however, is to increase the activity of G6PDH, since it is a committing step in the distribution of carbon [Beutler and Kuhl 1986]. Glucose 6-phosphate is a branching point to several pathways. It is distributed to the pentose phosphate pathway, glycolysis, and the pathways leading to biosynthesis of cell wall components. The *A. niger* gene encoding G6PDH (*gsd*A) has been cloned, but transformation of the fungus with this gene resulted in only low levels of overproduction of G6PDH [van den Broek *et al.* 1995]. It is possible that a reason for this is that the higher levels of G6PDH result in a low NADP/NADPH ratio. This explanation would be in line with the observation that *A. niger* strains overproducing G6PDH grow poorly on media containing glucose and ammonium compared to growth on L-arabinose and nitrate [van den Broek *et al.* 1995], since L-arabinose and nitrate catabolism requires NADPH. Therefore, in this study isolation of transformants with a higher overproduction of G6PDH was attempted by a rescue on media giving a high oxidation rate of NADPH to NADP.

In glycolysis the conversion of G6P to fructose 6-phosphate (F6P) is accomplished by phosphoglucose isomerase (PGI). A disruption of the gene encoding for PGI (*pgiA*) is likely to

increase the flux through the PPP, since this would force all conversion of G6P to intermediates in glycolysis through the PPP (Fig. 1). Canonaco and co-workers [2001] had strong indications that using this strategy in *E. coli* increases the NADPH concentration. We have tried a similar approach and cloned the pgi gene (AJ551177) but we failed to obtain a disruptant, although we analysed more than 120 transformants.

The aim of the present study is to increase the availability of NADPH for synthesis or bioconversions by overproduction of three enzymes in the PPP, G6PDH, 6PGDH and TKT. Wild type and engineered strains were characterized in detail in bioreactor cultures using multivariate data analysis showing that overproduction of 6PGDH resulted in increased NADPH levels.

MATERIALS AND METHODS

Strains and culture conditions

As the wild type strain (wt) we used *Aspergillus niger* NW 131 (*cspA1 goxC17*), which is a glucose oxidase negative strain [Swart *et al.* 1990] with short conidiophores [Bos *et al.* 1988]. All strains used were derived from N400 (CBS 120.49) and are listed in Table 1.

Unless stated otherwise medium composition, plate cultures and bioreactor cultures were as described previously [Poulsen *et al.* 2003]. Shake flask cultures for preliminary characterization (Southern analysis, transcript analysis and enzyme activity) and screening of isolated transformants contained minimal medium (MM) with 70 mM $NaNO_3$ as nitrogen source and 1% (mass/vol) glucose as carbon source. Bioreactor cultures for detailed characterization of strains contained MM with 21 mM NH_4Cl or $NaNO_3$ as nitrogen source (final cell density limiting substrate) and 5% (mass/vol) glucose as carbon source. Titrants for maintaining pH at 3 were 2 M NaOH and 2 M HCl.

Table 1. *A. niger* strains used in this study

Strain	Trivial name	Genotype	Reference for characterized mutation or strain
NW131	wt	cspA1 goxC17	[Bos *et al.* 1988], [Swart *et al.* 1990]
NW129		cspA1 goxC17 pyrA6	[Goosen *et al.* 1987]
NW342	Gnd5	cspA1 goxC17[gndA]$_5$	This work
NW341	Gnd8	cspA1 goxC17[gndA]$_8$	This work
NW340	Gnd20	cspA1 goxC17[gndA]$_{20}$	This work
NW323	Gsd11	cspA1 goxC17[gsdA]$_{11}$	This work
NW329	Tkt15	cspA1 goxC17 [tktA]$_{15}$	This work

[a]Subscript is copy number estimated by Southern analysis.

Molecular biology techniques

DNA manipulations were essentially as described by [Sambrook *et al.* 1989]. *E. coli* DH5α was used for propagation of plasmid DNA. Unless stated otherwise the plasmid used was pBluescript (SK+). Preliminary and control DNA sequencing were carried out using a Ready Reaction Dye Deoxy Terminater Cycle Sequencing kit (Perkin Elmer) in an Applied Biosystems automatic DNA sequencer model 310 (ABI Prism 310 Genetic Analyser, Perkin Elmer). *tktA* was sequenced by sub-cloning into pUC19 and using ^{33}P ddNTPs (Amersham-Pharmacia) by standard methods [Sambrook *et al.* 1989; Sanger *et al.* 1977] covering all parts of the sequence at least twice in each direction. *gndA* and *pgiA* were sequenced using the BigDye sequencing kit and an ABI Prism 310 capillary sequencer (Perkin-Elmer). *A. niger* DNA was isolated as described in de Graaff *et al.* [1988] and RNA was isolated using TRIZOL (Life Technologies).

Transformations of *A. niger* were performed essentially as described by Kusters-van Someren *et al.* [1991] using $2 \cdot 10^7$ protoplasts. Overexpressing strains were obtained by co-transformation of the uridine requiring strain [Goosen *et al.* 1987] NW129 (*cspA1 goxC17 pyrA6*) with 1 µg of the plasmid pGW635 containing the *pyrA* gene and 20 µg of a plasmid containing the gene encoding for the enzyme to be overproduced. After transformation the protoplasts were plated on minimal medium, which unless otherwise stated contained 0.95 M sucrose as osmotic stabilizer and carbon source in addition to 70 mM nitrate as nitrogen source. The protoplasts transformed with pIM440 (*gsdA*, descibed below) were plated on minimal media osmotically stabilized with sorbitol and with different carbon and nitrogen sources to obtain different rates of intracellular NADPH oxidation: 1% glucose and 70 mM ammonium, 1% glucose and 70 mM nitrate, 1% dihydroxyacetone and 70 mM nitrate, and 1% L-arabinose and 70 mM nitrate, since NADPH is needed for growth on nitrate, dihydroxyacetone and L-arabinose.

Sampling and analysis

Culture filtrate samples were obtained as described before [Hrdlicka *et al.* 2004]. Mycelium samples were collected by filtration in a funnel with a sintered glass filter. After washing, the mat of mycelium was frozen in liquid nitrogen. Dry weight (DW) samples were sampled directly into a measuring cylinder and mycelium was washed twice on the sintered glass filter by resuspension in distilled water, frozen in liquid nitrogen, and stored at -20°C. Samples for measurement of enzymes were washed twice with 50 mM potassium phosphate buffer (pH 7), frozen in liquid nitrogen, and stored at -70°C. Samples for measurement of intracellular polyols were not washed since this can cause loss of up to 60% of the intracellular (I) polyols [Witteveen *et al.* 1994]; mycelium was frozen in liquid nitrogen, and stored at -70°C. Sampling for intermediary metabolites was done directly into a methanol buffer at -40°C to inactivate metabolism [Ruijter and Visser 1996], and samples were frozen in liquid nitrogen, and stored at -70°C.

Biochemicals were from Boehringer Mannheim, Roche or Sigma. Glucose was determined either by glucose test strips (Roche), by HPLC analysis or enzymatically essentially as described by Bergmeyer [1974]. Nitrate was detected by nitrate/nitrite test strips (Merck). Glucose, polyols and organic acids were determined by HPLC analysis using a Dionex system

(Dionex Corp., Sunnyvale, CA, USA). Extracellular (E) concentrations were determined after centrifuging culture filtrate samples to remove any precipitate after freezing. Intracellular (I) polyols were extracted from mycelium according to Witteveen *et al.* [1994]. For glucose and polyols, an anion-exchange CarboPac MA1 column (Dionex) was used. Elution was isocratic at 0.4 mL·min^{-1} with 0.48 M NaOH and amperometric detection. For organic acids an Aminex ion exclusion HPX-87H column (Biorad), thermostated at 50°C was used. Elution was isocratic at 0.5 mL·min^{-1} with 25 mM HCl and detection by refractive index and UV at 210 nm. Extracellular polyols and acids were calculated as concentration measured extracellularly (mol·L^{-1}) divided by dry weight concentration (g DW·L^{-1}) to compensate for slightly different times of sampling.

Dry weight samples were lyophilized and weighed. Frozen mycelium sampled for measurement of enzymes and for isolation of DNA and RNA was precooled in liquid nitrogen and powdered in a precooled Teflon container with a stainless steel ball using a Micro-Dismembrator II (B. Braun, Melsungen, Germany). For measurement of enzymes 0.1-0.4 g powder·mL^{-1} was suspended in extraction buffer containing 50 mM potassium phosphate (pH 7.0), 0.5 mM EDTA, 5 mM MgCl$_2$ and 5 mM 2-mercaptoethanol at 0°C. The suspension was mixed by pipetting and the enzyme extract was obtained as the supernatant after centrifugation at $40000 \times g$ for 10 min. Enzyme assays were based on measurement of NAD(P)H and performed at 30°C using a Cobas Bio autoanalyzer (Roche, Basel, Switzerland, absorbance at 340 nm, $\varepsilon = 6.22$ mM^{-1}·cm^{-1}). ALD, G6PDH, PGI and M1PDH activities were determined as described by Ruijter *et al.* [1997]. GLYDH activity was determined as described by de Vries *et al.* [2003]. 6PGDH was determined as described by Rippa and Signorini [1975] with the modification that EDTA was omitted. TAL activity was determined as described in [Bruinenberg 1983] with the modifications that the buffer was 100 mM Pipes pH 7.6, the concentration of F6P was increased to 3 mM and EDTA was omitted. The specific TAL activity was found by subtraction of the M1PDH activity. TKT activity was determined as described by Bruinenberg [1983] with the modifications that the buffer was 50 mM Pipes pH 7.6, the concentration of R5P was doubled to 4 mM and the reaction was started with Xu5P. Protein concentration in enzyme extracts was determined after denaturation and precipitation of protein with sodium deoxycholate and trichloroacetic acid [Bensadoun and Weinstein 1976] using the BCA method as described by the manufacturer (Sigma).

Extraction and determination of intermediary metabolites were performed as described by Ruijter and Visser [1996]. The assays for G6P, F6P, PYR, ADP, AMP, NAD and ATP were also as described by Ruijter and Visser [1996]. The assay for 6PG was the same as for G6P except that G6PDH was exchanged with 6PGDH. The assay for NADP was as described by Klingenberg [1985] with the modification that 50 mM triethanolamine (pH 7.6) was used, G6P was 0.5 mM, G6PDH was 1.4 U·mL^{-1} and 2.5 mM MgCl$_2$ was added instead of MgSO$_4$. The assay for NADH and NADPH was as described by Klingenberg [1985] with the modifications that 50 mM triethanolamine (pH 7.6) was used, 2-ketoglutarate was 1.25 mM and instead of absorbance the fluorescence was measured ($\lambda_{excitation}$ = 340 nm and $\lambda_{emission}$ = 460 nm, F4500 Fluorescence Spectrophotometer, Hitachi) to increase the sensitivity. G6P, F6P and S7P were determined in a modified version of the assay developed by Racker [1970] in the presence of 25 mM glycylglycine (pH 7.4), 0.5 mM NADP and 0.2 mM GAP by addition of 0.3 U·mL^{-1} 6PGDH, 0.3

U·mL^{-1} PGI and 0.3 U·mL^{-1} TAL, respectively. DHAP, GAP, R5P and Ru5P were determined in a modified version of the assay from [Racker 1984]. Our assay is carried out in the presence of 25 mM glycylglycine (pH 7.4), 6 mM MgCl$_2$, 2.4 mM thiamine pyrophosphate, 1 mM NADH and 0.5 mM Xu5P by addition of 0.7 U·mL^{-1} glycerol 3-phosphate dehydrogenase, 40 U·mL^{-1} triosephosphate isomerase, 0.33 U·mL^{-1} TKT and 1 U·mL^{-1} ribosephosphate isomerase, respectively. DHAP, GAP and Xu5P were determined in a similar assay by exchanging 0.5 mM Xu5P with 0.5 mM R5P, whereby Xu5P is measured by the addition of 0.33 U·mL^{-1} TKT and the addition of ribosephosphate isomerase is omitted.

Accumulated titrant added to maintain constant pH was analyzed with natural logarithm of slope (LOS) plots [Poulsen *et al.* 2003] to ensure correct sampling time points (exponential growth phase, e, and stationary phase, s) and to measure the maximum specific growth rate (μ_{max}, h^{-1}) and the rate constant of induction of acid production (IAP, h^{-1}) in the post-exponential phase. Samples from exponential growth phase (e) were taken 13-20 hours after inoculation with spores, which corresponds to 1-8 hours before exhaustion of the final cell density limiting substrate (ammonium or nitrate). Samples from stationary phase (s) were taken 11-14 hours after exhaustion of the final cell density limiting substrate.

Partial least square (PLS) regressions (see Martens and Næs [1989], Höskuldsson [1996] and Esbensen [2002] for a general introduction to PLS regression) were made with the statistical software package for multivariate data analysis Unscrambler v. 7.8 (CAMO Process AS, Norway). Since the number of samples (16) was relatively small full cross validation was applied. Skewed (asymmetric) variables with a skewness higher than 1 or lower than -1 were pre-processed by a simple log-transformation (a = log[a]), which reduced the absolute value of the skewness to lower than 1. Variables were centralized (subtraction of mean) and weighted (division with standard deviation) to obtain a mean of zero and a standard deviation of 1 for all variables. Variables with little correlation to the Y-variable (low absolute values of X-loading weights) were excluded from the PLS regression, because they contribute little to the prediction but significantly to the error. Several PLS regressions were performed with different X-variables with low X-loading weights excluded to optimize the correlation and minimize the error.

RESULTS AND DISCUSSION

Cloning of the genes *gndA*, *gsdA* and *tktA*

To be able to manipulate the genes *gndA*, *gsdA* and *tktA* encoding for 6PGDH, G6PDH and TKT, respectively, these genes were cloned by screening of an *A. niger* N400 genomic library in λEMBL4 [Harmsen *et al.* 1990] with PCR products obtained by using the PCR-oligos in Table 2. Fragments obtained for these three genes were a 5.3 kb *EcoRI-SalI* fragment (AJ551178, *gndA* including 1.1 kb upstream and 2.1 kb downstream of the gene), a 5.0 kb *SalI-NsiI* fragment (part of S78375, [van den Broek *et al.* 1995], *gsdA* including 1.1 kb upstream and 1.5 kb downstream of the gene) and a 3.8 kb *EcoRI-ClaI* fragment (AJ550995, *tktA* including 0.7 kb upstream and 0.5

kb downstream of the gene), which were cloned into pBluescript resulting in the pIM445, pIM440, pIM446 and pIM448 plasmids, respectively.

Table 2. PCR-oligos for probes and site-directed mutagenesis

Oligo	Position[a]	Sequence	Comments
Gnd1	1617-1633 (Z46631)	AAR ATG GTN CAY AAY GG	Degenerate PCR on *A. niger* cDNA
Gnd2	1867-1851 (Z46631)	GTC CAY TTN CCN GTN CC	
Gsd-1	733-752 (S78375[b])	GCA GCT GGA CAG CTT CTG CC	Specific PCR on *A. niger* DNA
Gsd-2	1603-1584 (S78375[b])	CGT TCT TGG GCT CAA TGG CG	
nctkt1	600-584 (NC4B12-T7[c])	GCC ATT GAT GCC GTC AA	Specific PCR on *N. crassa* DNA
nctkt4	256-272 (NC4B12-T7[c])	CTG GAA AGC CCT GTT GA	

[a]Position in the accession number given.
[b][van den Broek *et al.* 1995].
[c]Putative *Neurospora crassa* transketolase EST sequence from http://biology.unm.edu/

The encoded 6PGDH and TKT proteins are highly similar to previously published proteins from other organisms. The highest similarities were with the 6PGDH from *Aspergillus oryzae* (BAC06328, 94% identity) and the TKT from *Neurospora crassa* (CAC18218, 74% identity), respectively.

Both *gndA* and *tktA* contain an exceptionally long first intron of 407 and 267 bp, respectively, which is much longer than generally observed in filamentous fungal genes [Gurr *et al.* 1987]. Strikingly, this is also the case for the other PPP enzyme encoding gene *gsdA* [van den Broek *et al.* 1995] cloned so far, but whether this is a general feature of all the PPP genes of *A. niger* still remains to be shown.

Transformations of *A. niger* to obtain overexpression of *gndA*, *gsdA*, and *tktA*

With the purpose of overproducing the enzymes 6PGDH, G6PDH and TKT in separate strains, the plasmids pIM445 (*gndA*), pIM440 (*gsdA*) and pIM448 (*tktA*) were used in co-transformations, which resulted among others in the multi-copy strains given in Table 1.

After transformation with pIM445 (*gndA*) we isolated 20 transformants of which approximately half overproduced 6PGDH in the range from 2- to 13-fold. This is a higher level of overproduction than previously obtained in both *E. coli* [Lim *et al.* 2002] and *R. eutropha* [Lee *et al.* 2003], which was 1.7 and 3.8 times wild type activity, respectively. As shown in Figure 2, the activity did correlate to both the number of copies of the *gndA* gene introduced (up to 20) and to the transcription level. We chose the *gndA* multicopy strain Gnd20 (NW340, Table 1) with 20 introduced copies and a 6PGDH activity of 13 times wt activity for detailed characterization.
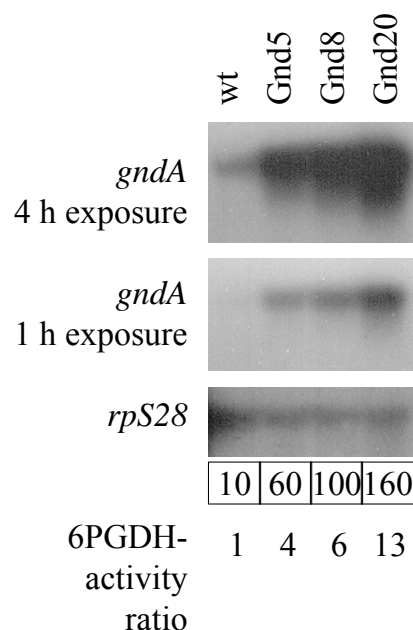
Figure 2. Transcript analysis of *gndA* expression in multicopy transformants. Probe: 0.25 kb PCR product of oligos gnd1 and -2 (Table 2). Both 1 and 4 h exposure to film are shown because of large differences in transcription level. Probe for loading control: 0.7 kb EcoRI-XhoI fragment of ribosomal protein gene *rpS28* [Melchers *et al.* 1994]; high intensity on left side of wt band is an artefact: exposure from strong neighbouring band. Numbers in boxes indicate the relative levels of *gndA* transcripts corrected for loading differences on basis of the *rpS28* signal. Signals for wt were set at 10. Bottom: 6PGDH-activity relative to wild type (wt 6PGDH activity = 0.4 U·mg protein^{-1}).

High, lethal levels of NADPH upon high overproduction of G6PDH was believed to be the reason why *gsdA* could not be overexpressed to high levels in *A. niger* [van den Broek *et al.* 1995]. Therefore, the protoplasts transformed with pIM440 (*gsdA*) were plated on minimal media with different carbon and nitrogen sources to obtain different rates of intracellular NADPH oxidation. Approximately half of 30 transformants isolated from each medium (120 in total) overproduced G6PDH. However, the overproduction did not differ significantly between the media and was only up to 3 times wt activity. This result is in agreement with previous attempts to overproduce G6PDH in *A. niger* [van den Broek *et al.* 1995], *E. coli* [Lim *et al.* 2002] and *R. eutropha* [Choi *et al.* 2003]. The rescue of transformants on media which lead to increased oxidation of NADPH therefore had no influence on the G6PDH overproduction levels obtained. However, whereas van den Broek and co-workers [1995] found only up to 4 introduced copies of the *gsdA* gene, we found up to 40 introduced copies and no correlation with enzyme activity. This was confirmed by transcript analysis (Fig. 3), which showed very high transcription levels compared to wild type even for strains with a few introduced copies. We therefore concluded that the *gsdA* gene product(s) must be subject to post-transcriptional regulation, either at the mRNA or at the enzyme level. We chose *gsdA* multicopy strain Gsd11 (NW323, Table 1) with 11 introduced copies and a G6PDH activity of 3 times wt activity for detailed characterization.
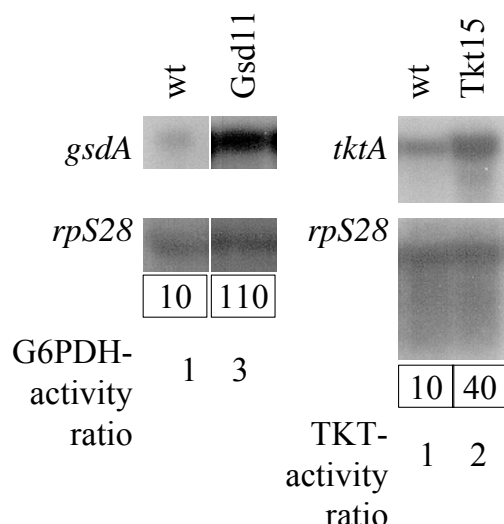
Figure 3. Transcript analysis of *gsdA* and *tktA* expression in multicopy transformants. Probes: 1.4 kb XhoI-NcoI fragment of *gdsA* (S78375) and 2.1 kb *SmaI-SphI* of *tktA* (AJ550995), respectively. Probe for loading control: 0.7 kb *EcoRI-XhoI* fragment of ribosomal protein gene *rpS28* [Melchers *et al.* 1994]. The numbers in boxes indicate the relative levels of *gsdA* and *tktA* transcripts corrected for loading differences on basis of the *rpS28* signals. Signals for wt were set at 10. Bottom: G6PDH- and TKT-activities relative to wild type (wt G6PDH activity = 1.0 U·mg protein^{-1}, wt TKT activity = 0.3 U·mg protein^{-1}).

After transformation of *A. niger* with pIM448 (*tktA*) we isolated 20 transformants of which approximately one third overproduced TKT, but only up to 2×wt activity. This level of overproduction is comparable to that previously obtained in *R. eutropha* [Lee *et al.* 2003], but in *Saccharomyces cerevisiae* [Schaaff-Gerstenschläger *et al.* 1994] and *Corynebacterium glutamicum* [Ikeda 1999] overproduction of up to 15 and 30×wt activity, respectively, was obtained. Southern analysis showed up to 15 introduced copies and no apparent correlation to enzyme activity, but the differences and the accuracies in enzyme activity were too low to exclude this. In contrast to the high transcription level of the *gndA* and *gsdA* multi-copy strains, the transcription level of the *tktA* multicopy strains was only slightly higher than wild type level (Fig. 3), which confirmed the low level of overproduction of only two-fold. One reason for this could be that the 0.7 kb promotor of pIM448 is too short to obtain high level transcription. The *tktA* multicopy strain Tkt15 (NW339, Table 1) with 15 extra (introduced) copies and a TKT activity of 2 times wt activity was chosen for detailed characterization.

Detailed characterization of wild type and overproducing strains

To determine physiological changes caused by overproduction of G6PDH, TKT or 6PGDH repeated batch cultures were performed in computer controlled bioreactors with the wild type, Gsd11, Tkt15 and Gnd20 strains. Macro-morphology profiling [Poulsen BR, Sørensen AB, Schuleit T, Ruijter GJG, Visser J, unpublished results] showed that the cultures were without large pellets containing a substrate diffusion-limited centre and contained about 30% (DW/DW) pellets smaller than 0.3 mm diameter and 70% (DW/DW) free hyphae. This mainly filamentous morphology was obtained only at low pH (here: 3). If pH was increased above 4.5 pellet fraction and size increased resulting in diffusion-limited biomass in the centre of large pellets (> 0.3 mm

diameter).

The added titrants in the exponential growth phase were NaOH and HCl in ammonium and nitrate cultures, respectively, and they were added in quantities equivalent to the amount of these nitrogen sources. This can be explained by the observation that only minor quantities of organic acid were produced during the exponential phase and the release of a proton upon uptake of an ammonium ion [Iversen *et al.* 1994] and the uptake of a proton upon uptake of a nitrate molecule. The added titrant in the stationary phase of both ammonium and nitrate cultures was NaOH, which was caused by equivalent quantities of organic acid produced [Hrdlicka *et al.* 2004].

A number of obvious tendencies from the characterization of wild type under the different conditions were found. In the exponential phase of the ammonium cultures all the PPP enzyme activities were lower and the NADPH concentration was higher than during other conditions. It is difficult to explain the higher PPP enzyme activities in stationary phase, since in this phase most of the carbon taken up is converted to carbohydrates as storage compounds [Hrdlicka *et al.* 2004] (about 35%) and to oxalate (about 20%) and only about 6% to polyols. Of the products formed only polyol formation requires NADPH and similar quantities of polyols were formed in the exponential and stationary phases.

In the exponential phase of the nitrate cultures high PPP enzyme activities and a low NADPH level were probably caused by a higher demand for NADPH for the reduction of nitrate. It is possible that the control mechanism for the high and low PPP enzyme activities in the exponential phase of the nitrate and ammonium cultures, respectively, is the NADPH level. During growth on ammonium NADPH consumption is low compared to growth on nitrate and therefore the concentration of NADPH is high. This leads to the downregulation of PPP genes. Conversely, during growth on nitrate NADPH consumption is high and therefore the concentration of NADPH is low which makes the upregulation of PPP genes necessary. Concentration of intermediary metabolites had a general tendency to be higher in exponential phases than in stationary phases. One could speculate that growth requires these high levels and/or that they are part of the regulation of growth.

A number of obvious tendencies from the characterization of the overproducing strains were also found. The 6PG level was generally increased in the Gsd11 strain and generally decreased in the Gnd20 strain. This is expected since 6PG is the product and the substrate for the enzyme overproduced in Gsd11 and Gnd20, respectively. Although NADPH is a product of both enzymes it was only increased in the latter strain and under all conditions. Also the concentration of NADP and NAD had a tendency to be increased in Gnd20, which might counterbalance the regulatory effect of the high NADPH concentration. The lack of a significant increase in NADH parallel to the increase in NADPH indicates that there is no significant transhydrogenase activity in *A. niger* under the conditions used here, whereas this has been suggested for citric acid-producing mycelium [Führer *et al.* 1980]. Overproduction of 6PGDH resulted in an increase of synthesis of pyridine nucleotide cofactors since the total pool of these increased. It might be that the synthesis is regulated by the NADPH concentration. Since we have shown that it is possible to increase the NADPH concentration in *A. niger* by overproduction of 6PGDH and since rescue of transformants on media with fast oxidation of NADPH had no influence on the G6PDH overproduction obtained, high and lethal concentrations of NADPH is probably not the reason for

the relatively low overproduction of G6PDH (2-3 times wild type level) obtained in this study and previously by van den Broek *et al.* [1995]. The G6PDH overproducing strain has wild type levels of NADPH under the conditions applied for detailed characterization which contradicts the arguments previously used [van den Broek *et al.* 1995] that high and lethal concentrations of NADPH are the reason for only low overproduction of G6PDH found in *A.niger*. However, the reason might be too low NADP concentration, since the concentration of this metabolite had a tendency to be decreased in the G6PDH overproducing strain.

Furthermore, it was found that the Tkt15 strain had a tendency to a higher level of acid production. The reason for this is unknown, but one suggestion could be that in this strain with increased transketolase activity carbon is more efficiently converted from the oxidative PPP via Ru5P to glycolysis in the form of GAP and F6P and thereby made available for acid production.

Partial Least Square (PLS) regressions

For future metabolic engineering of strains with the purpose of obtaining increased NADPH levels and for the understanding of the regulation of the NADPH level it is important to know which variables are correlated with NADPH concentration. Because of the relative high number of variables obtained in this study from analysis of samples from exponential (e) and stationary (s) phases not all correlations are obvious. One statistic tool, which is suitable to find correlations between multiple variables and at the same time to make a regression in order to predict one or more variables, is a Partial Least Square (PLS) regression. In a PLS regression the most important part of the variation in the X-variables for description of the Y-variables is found as one or more principal components (PCs). Details of algorithms used in PLS regressions are given in Martens and Næs [1989], Höskuldsson [1996] and Esbensen [2002].

We performed PLS regressions to predict the NADPH concentration (Y) from, and find correlations with, the other measured variables (X). The variables G6PDH, 6PGDH, TKT, M1PDH, S7P, DHAP, Xu5P, F6P, PYR, R5P, GAP, 6PG, NADP, NADPH, NADH, erythritolI, arabitolI, mannitolI, arabitolE, trehaloseE, oxalate and NADH (E, extracellular; I, intracellular) were skewed and therefore pre-processed by log-transformation. The rest of the variables (ALD, TAL, PGI, GLYDH, G6P, ADP, AMP, NAD, CRC, glycerolI, trehaloseI, glycerolE, erythritolE and mannitolE) had a skewness between -1 and 1 and were not pre-processed. Citrate, DW and μ_{max}/IAP, were excluded from the regression, because they are very different in the exponential and stationary phases. ATP and energy charge were excluded because for some of the samples from the cultures of overproducing strains the determination of ATP was not reproducible. We found no explanation for this other than that the turnover of ATP is very high. Ru5P was excluded, because of an incomplete dataset for this variable. ARC was excluded because it is calculated partly from the Y-variable (NADPH).

Figure 4 shows a PLS regression with both exponential phase (e) and stationary phase (s) samples from ammonium (a) and nitrate (n) grown cultures after excluding variables with only minor correlation with NADPH (TAL, M1PDH, S7P, R5P, GAP, 6PG, ADP, AMP, CRC, glycerolE, arabitolE, mannitolE and citrate) from the prediction. Two PCs were chosen since this gave a minimum in the Y-variance. Figure 4A shows the scores on the two PCs of the samples (from different strains and different conditions). Figure 4B shows the X-loading weights of the X-

variables (measured variables other than NADPH) and the Y-loading of NADPH on the two PCs. Since NADPH is in the 1st quadrant of Figure 4B (the four quadrants in a system of co-ordinates are counted from upper right and clockwise) all the variables in this quadrant are positively correlated to NADPH in the two PCs. The variables in the 3rd quadrant are all negatively correlated to NADPH in the two PCs. The variables in the 2nd quadrant are mainly positively correlated to NADPH, because they are positively correlated in PC1 and negatively correlated in PC2, and much more of the NADPH is explained on PC1 (73%) than on PC2 (12%). For the same reason the variables in the 4th quadrant are mainly negatively correlated to NADPH. Similarly, the samples (Gnd) in the 1st quadrant of Figure 4A have a tendency to have a high NADPH level. However, the position of the samples in Figure 4A is influenced by the level of all variables in these samples. For instance the samples of the strains in the 3rd quadrant of Figure 4A have a tendency to a high erythritolI level, since this variable is in the 3rd quadrant of Figure 4B. A total of 85% of NADPH is explained on the basis of two principal components. The coefficient of determination (r^2) is 0.72, which confirms the correlation, although it is not very precise. RMSEP (root mean square error of prediction or average relative error in prediction) is 0.046 µmol·g DW^{-1} (Fig. 4C), which corresponds to about 20% of the NADPH concentration in Gnd20 in the exponential phase and is satisfactory considering that the coefficient of variation (CV = standard deviation/average x 100%) of the NADPH determination is about 30%.

Samples from exponential (e) and stationary (s) phase form two separate groups in Figure 4A. This is expected, since identical conditions such as growth in exponential phase have a tendency to result in the same concentrations of variables. Similarly, the conditions ammonium (a) and nitrate (n) have a tendency to form separate groups. In addition, the strain Gnd20 forms a group, although it is relatively disseminated, which indicates that this strain differs clearly from the other strains; the main differences being high 6PGDH activity and NADPH concentration.

From Figure 4B it is possible to deduce a number of correlations with NADPH concentration. The correlations with enzyme concentrations are interesting, because it is possible to change these by genetic engineering. First of all, the 6PGDH correlates with NADPH. Similarly, the little success we had with increasing NADPH by overproduction of G6PDH and TKT is confirmed by a negative correlation between these enzymes and NADPH. Also ALD, PGI and GLYDH are negatively correlated to NADPH. However, this does not necessarily imply that a high expression of these enzymes is irrelevant for a high NADPH production. For example, it is known that the flux through the PPP is increased during growth on nitrate compared to growth on ammonium [Pedersen *et al.* 1999; Schmidt *et al.* 1998] and we observed a two- to four-fold increase in PPP enzyme levels, but a five-fold decrease in NADPH concentration; most probably because NADPH is used for the reduction of nitrate. These data apparently have a stronger influence on calibration of the PLS regression than the data from the Gnd20 strain in which the G6PDH activity and NADPH concentration was generally increased. Therefore the correlations shown in Figure 4B should be interpreted with caution taking into account the knowledge of e.g. the pathways shown in Figure 1. A PLS regression gives correlations but not the cause of the correlations.

Figure 4. Prediction of NADPH using a partial least square (PLS) regression with samples from exponential and stationary phase. Variables with less correlation to NADPH were excluded (TAL, M1PDH, S7P, R5P, GAP, 6PG, ADP, AMP, CRC, glycerolE, arabitolE and mannitolE). Gsd11, Tkt15 and Gnd20 are strains overproducing G6PDH, TKT and 6PGDH, respectively. a and n are cultures with ammonium and nitrate, respectively, as final cell density limiting substrate. e and s are exponential and stationary phase, respectively. RMSEP is root mean square of error of prediction. Two PCs were used. X explained: 40% on PC1 and 17% on PC2. Y (NADPH) explained: 73% on PC1 and 12% on PC2. **A:** Scores. **B:** X-loading Weights and Y-loadings. **C:** Predicted versus measured NADPH.

Surprisingly 6PG has no strong (negative) correlation with NADPH although the concentration is decreased 3-7 fold under most conditions in the Gnd20 strain. This may be caused by a 3-7 fold increase in 6PG and a slight tendency to an increase in NADPH in the Gsd11 strain.

It is possible that PPP flux is increased in the Gnd20 strain and that a higher G6PDH

activity is required for this. Concentrations of polyols and intermediary metabolites had a tendency to be increased in this strain which could be caused by a higher NADPH concentration and precursor production originating from an increased flux through the PPP. It seems likely that the increased NADPH and intermediary metabolite levels caused an increased polyol formation. This is probably the reason for the correlation between NADPH, most intracellular polyols and intermediary metabolites. Despite this, the total pool of polyols was only increased significantly (doubled) in the stationary phase of the nitrate cultures of the TKT and the 6PGDH overproducing strains.

Of the polyols only erythritol is negatively correlated with NADPH and has a tendency to be low in the 6PGDH overproducing strain and under conditions with high NADPH concentrations. Low E4P concentration might be the cause, but this can not be established since even in the wild type it is too low to be measured in *A. niger* [Ruijter and Visser 1999]. Alternatively, the formation of erythritol might use NADH as a cofactor instead of NADPH. However, the cofactor is most likely NADPH in *A. oryzae* [Ruijter *et al.* 2004], but this has not been investigated in *A. niger*.

The consumption of NADPH upon formation of glycerol by GLYDH (Fig. 1) confirms the negative correlation with this enzyme. This is a very interesting observation since it indicates that a disruption or a down-regulation of the gene encoding for GLYDH might result in higher NADPH concentrations.

The PLS regression in Figure 4 shows quite well how variables are correlated to NADPH. However, this prediction of NADPH concentration requires measurement of concentrations of intermediary metabolites G6P, F6P, DHAP, NAD, NADP, PYR and Xu5P. Since sampling for and extraction of intermediary metabolites is quite tedious it would be of great advantage if these could be left out of the prediction. Also, since NADPH is an intermediary metabolite itself one could argue that if an extraction is necessary for the prediction it has little value since measurement of NADPH concentration in the extract is little work compared to performing the extraction.

Without the intermediary metabolites a good correlation is obtained when the samples from the stationary phase are also excluded (Fig. 5). A total of 96% of NADPH is explained by two PCs, the coefficient of determination (r^2) is 0.76 and RMSEP is 0.067 μmol·g DW^{-1}, corresponding to about 30% of the NADPH concentration in Gnd20 in exponential phase and therefore in the range of the CV of the NADPH determination.
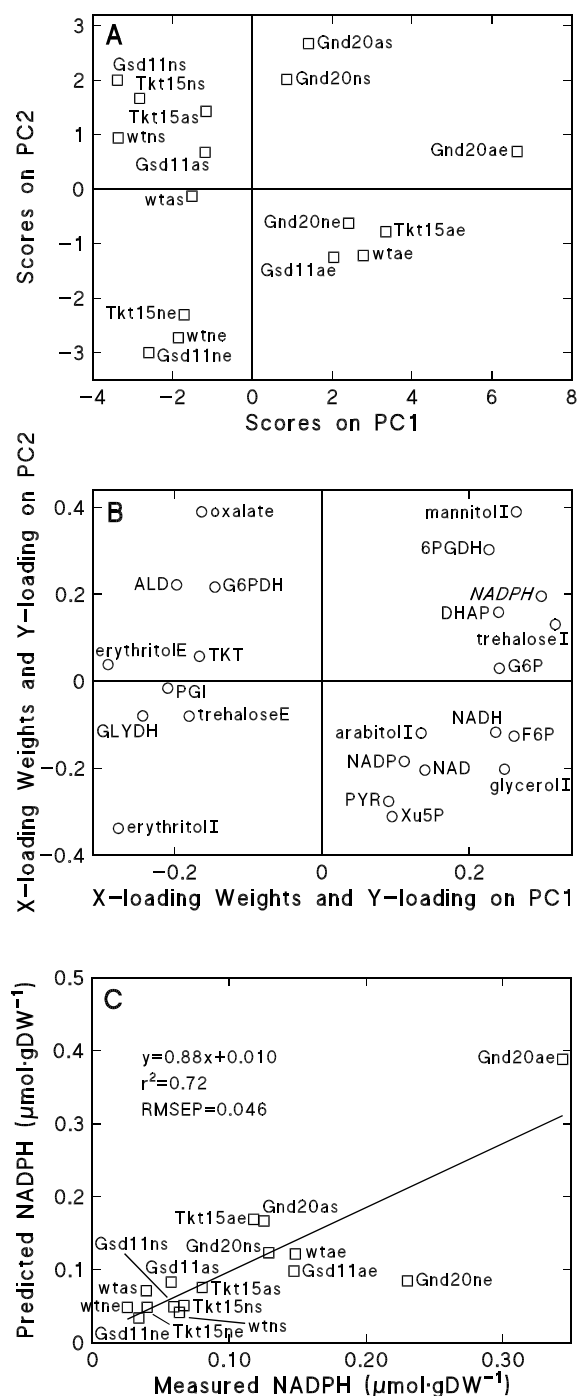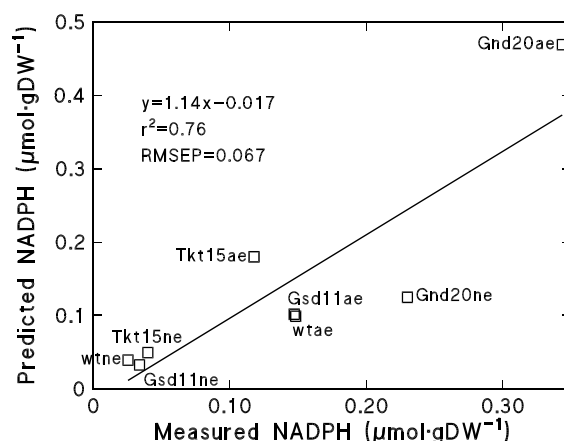
Figure 5. Prediction of NADPH using a partial least square (PLS) regression with samples from exponential phase only and without values of intermediary metabolites. Variables with less correlation to NADPH were excluded (TAL, M1PDH, arabitolI, glycerolE and arabitolE). Legends as in Figure 4. Two PCs were used. X explained: 62% on PC1 and 19% on PC2. Y (NADPH) explained: 89% on PC1 and 7% on PC2.

Applicability of PLS regression to other metabolic engineered strains or mutants

The prediction of NADPH in Fig. 5 is sufficiently precise to be used for screening for a strain with elevated NADPH content. Extractions of enzymes and intracellular polyols are relatively simple and they are stable compounds compared to intermediary metabolites. These extractions could therefore be automatized to screen a large number of strains. In addition, all the polyols can be measured by one injection on HPLC.

The PLS regression in Figure 5 was calibrated with samples from four strains having different PPP enzyme concentrations and cultivated under two different conditions (exponential phase in ammonium or nitrate containing media), which should make it relatively robust. In addition, the variables in these eight samples were in most cases determined as averages of several independent measurements. However, eight samples is an insufficient number to avoid cross validation of the regression, which means that the same samples are used for calibration and validation of the regression. Therefore, whether this calibration is generally applicable to a wide range of different genetically modified strains still remains to be shown.

In our case, samples from the exponential phase were shown to be the most important; a regression using only the samples from the exponential phase was successful, but a regression using only samples from the stationary phase was not. The LOS plot [Poulsen *et al.* 2003] was therefore an important tool, since it shows exactly when a culture grows exponentially. The extra- and intracellular polyol concentrations are important for the regression and it might be applicable to other filamentous fungi since they generally produce polyols. Enzyme concentrations are also important for the prediction of the NADPH concentration and other compounds than polyols which require reduction of NADPH to NADP upon formation may also be useful.

The main conclusion from this work is that NADPH concentration was successfully increased by overproducing 6PGDH (Figs. 4C and 5). This is in contrast with previous studies of *A. niger* where overproduction of citrate synthase [Ruijter *et al.* 2000], phosphofructokinase and pyruvate kinase [Ruijter et al 1997] showed no effect on metabolism other than decreased levels

of the activator fructose 2,6-biphosphate and of ATP in the phosphofructokinase overproducing strain [Poulsen *et al.* 2004]. Although many significant differences in enzyme and metabolite levels were observed in the 6PGDH overproducing strain compared to wild type, overproduction had no significant influence on overall physiology. For example, specific growth rate and spore formation remained unchanged, which is of great advantage when propagating the engineered fungal strains. This indicates that *A. niger* has a relatively robust primary metabolism which is in contrast to results obtained in *E. coli* [Canonaco *et al.* 2001; Lim *et al.* 2002] and *R. eutropha* [Choi *et al.* 2003; Lee *et al.* 2003], where increased NADPH levels as a result of metabolic engineering had a negative effect on growth rate. The increased NADPH concentration might result in increased biotransformation rates of substrates that require reducing equivalents. However, this still remains to be shown by application of strains overproducing 6PGDH in NADPH dependent processes. Since overproduction of both G6PDH and TKT results in significant changes in concentrations of intracellular metabolites it would be interesting to overproduce all three enzymes or combinations hereof in the same strain.

AKNOWLEDGEMENTS

REFERENCES

Bensadoun A, Weinstein D (1976) Assay of proteins in the presence of interfering materials. Anal. Biochem 70: 241-250.

Bergmeyer HU, Bernt E, Schmidt F, Stork H (1974) Determination with hexokinase and glucose-6-phosphate dehydrogenase. In *Methods of enzymatic analysis* (Bergmeyer H.U. ed.), 2nd edition, Vol. 3, pp. 1196-1201. Verlag Chemie, Weinheim.

Beutler E, Kuhl,W (1986) Characteristics and significance of the reverse glucose-6-phosphate dehydrogenase reaction. J Lab Clin Med 107: 502-507.

Bos CJ, Debets AJM, Swart K, Huybers A, Kobus G, Slakhorst SM (1988) Genetic analysis and the construction of master strains for assignment of genes to six linkage groups in *Aspergillus niger*. Curr Genet 14: 437-443.

Broek P van den, Goosen T, Wennekes B, van den Broek H (1995) Isolation and characterization of the glucose-6-phosphate dehydrogenase encoding gene (*gsdA*) from *Aspergillus niger*. Mol Gen Genet 247: 229-239.

Bruinenberg PM, van Dijken JP, Scheffers WA (1983) An enzymic analysis of NADPH

production and consumption in *Candida utilis*. J Gen Microbiol 129: 965-971.

Canonaco F, Hess TA, Heri S, Wang T, Szyperski T, Sauer U (2001) Metabolic flux response to phosphoglucose isomerase knock-out in *Escherichia coli* and impact of overexpression of the soluble transhydrogenase UdhA. FEMS Microbiol Lett 204: 247-252.

Choi JC, Shin HD, Lee YH (2003) Modulation of 3-hydroxyvalerate molar fraction in poly(3-hydroxybutyrate-3-hydroxyvalerate) using *Ralstonia eutropha* transformant co-amplifying *phb*C and NADPH generation-related *zwf* genes. Enzyme Microbial Technol 32: 178-185.

Esbensen KH (2002) Multivariate data analysis - in practice. 5th edition. CAMO Process AS, Oslo.

Führer L, Kubicek CP, Röhr M (1980) Pyridine nucleotide levels and ratios in *Aspergillus niger*. Can J Microbiol 26: 405-408.

Goosen T, Bloemheuvel G, Gysler C, de Bie DA, van den Broek HWJ, Swart K (1987) Transformation of *Aspergillus niger* using the homologous orotidine-5'-phosphate-decarboxylase gene. Curr Genet 11: 499-503.

Graaff L de, van den Broek H, Visser J (1988) Isolation and expression of the *Aspergillus nidulans* pyruvate kinase gene. Curr Genet 13: 315-321.

Gurr SJ, Unkles SE, Kinghorn JR (1987) The structure and organization of nuclear genes of filamentous fungi. In: Gene structure in eukaryotic microbes. (Kinghorn J.R.). Chapter 5. pp 93-139.

Harmsen JAM, Kusters-van Someren MA, Visser J (1990) Cloning and expression of a second *Aspergillus niger* pectin lyase gene (*pel*A): indications of a pectin lyase gene family in *A. niger*. Curr Genet 18: 161-166.

Henriksen CM, Christensen LH, Nielsen J, Villadsen J (1996) Growth energetics and metabolic fluxes in continuous cultures of *Penicillium chrysogenum*. J Biotechnol 45: 149-164.

Hrdlicka PJ, Poulsen BR, Sørensen AB, Ruijter GJG, Visser J, Iversen JJL (2004) Characterization of Nerolidol Biotransformation Based on Indirect On-Line Estimation of Biomass Concentration and Physiological State in Batch Cultures of *Aspergillus niger*. Biotechnol Prog 20: 368 - 376.

Höskuldsson A (1996) Prediction methods in Science and Technology, Vol 1. Basic theory. Thor Publishing, Denmark.

Ikeda M, Okamoto K, Katsumata R (1999) Cloning of the transketolase gene and the effect of its dosage on aromatic amino acid production in *Corynebacterium glutamicum*. Appl Microbiol Biotechnol 51: 201-206.

Iversen JJL, Thomsen JK, Cox RP (1994) On-line growth measurements in bioreactors by titrating metabolic proton exchange. Appl Microbiol Biotechnol 42: 256-262.

Jørgensen H, Nielsen J, Villadsen J (1995) Metabolic flux distributions in *Penicillium chrysogenum* during fed-batch cultivations. Biotechnol Bioeng 46: 117-131.

Klingenberg M (1985) End-point UV-methods. In: Methods of enzymatic analysis (Bergmeyer H.U. ed.), 3rd edition, Vol. 7, pp. 251-271. VCH, Weinheim.

Kusters-van Someren MA, Harmsen JAM, Kester HCM, Visser J (1991) Structure of the *Aspergillus niger pel*A gene and its expression in *Aspergillus niger* and *Aspergillus nidulans*. Curr Genet 20: 293-299.

Lee JN, Shin HD, Lee YH (2003) Metabolic engineering of pentose phosphate pathway in

Ralstonia eutropha for enhanced biosynthesis of poly-ß-hydroxybutyrate. Biotechnol Prog 19: 1444-1449.

Lehman LR, Stewart JD (2001) Filamentous fungi: potentially useful catalysts for the biohydroxylations of non-activated carbon centers. Curr Org Chem 5: 439-470.

Li Z, van Beilen JB, Wouter AD, Schmid A, de Raadt A, Griengl H, Witholt B (2002) Oxidative biotransformations using oxygenases. Curr Opin Chem Biol 6: 136-144.

Lim SJ, Jung YM, Shin HY, Lee YH (2002) Amplification of the NADPH-related genes *zwf* and *gnd* for the oddball biosynthesis of PHB in an *E. coli* transformant harboring a cloned *phbCAB* operon. J Biosci Bioeng 93: 543-549.

Martens H, Næs T (1989) Multivariate Calibration. John Wiley and Sons Ltd., Chichester.

Marx A, Eikmanns BJ, Sahm H, de Graaf AA, Eggeling L (1999) Response of the central metabolism in *Corynebacterium glutamicum* to the use of an NADH-dependent glutamate dehydrogenase. Metab Eng 1: 35-48.

Melchers WJG, Verweij PE, van den Hurk P, van Belkum A, de Pauw BE, Hoogkamp-Korstanje JAA, Meis JFGM (1994) General primer-mediated PCR for detection of *Aspergillus* species. J Clin Microbiol 32: 1710-1717.

Obanye AIC, Hobbs G, Gardner DCJ, Oliver SG (1996) Correlation between carbon flux through the pentose phosphate pathway and production of the antibiotic methylenomycin in *Streptomyces coelicolor* A3(2). Microbiology 142: 133-137.

Pedersen H, Carlsen M, Nielsen J (1999) Identification of enzymes and quantification of metabolic fluxes in the wild type and in a recombinant *Aspergillus oryzae* strain. Appl Environ Microbiol 65: 11-19.

Poulsen BR, Ruijter GJG, Visser J, Iversen, JJL (2003) Determination of first order rate constants by natural logarithm of the slope plot exemplified by analysis of *Aspergillus niger* in batch culture. Biotechnol Lett 25: 565-571.

Poulsen BR, Ruijter GJG, Panneman H, Iversen JJL, Visser J (2004) Fast response filter module with plug flow of filtrate for on-line sampling from submerged cultures of filamentous fungi. Anal Chim Acta 510: 203-212.

Racker E (1970) D-sedoheptulose-7-phosphat. In: Methoden der enzymatischen analyse (Bergmeyer H.U. ed.), 2nd edition. Vol. 2, pp. 1156-1159. Verlag Chemie, Weinheim.

Racker E (1984) D-ribulose 5-phosphate. In: Methods of enzymatic analysis (Bergmeyer HU ed.) 3rd edition. Vol 6, pp. 437-441. VCH, Weinheim.

Rippa M, Signorini M (1975) 6-phosphogluconate dehydrogenase from *Candida utilis*. In: Methods in enzymology (Wood WA ed.), Vol. 41, pp 237-240.

Ruijter GJG, Panneman H, Visser J (1997) Overexpression of phosphofructokinase and pyruvate kinase in citric acid producing *Aspergillus niger*. Biochim Biophys Acta 1334: 317-326.

Ruijter GJG, Panneman H, Xu DB, Visser J (2000) Properties of *Aspergillus niger* citrate synthase and effects of citA overexpression on citric acid production. FEMS Microbiol Lett 184: 35-40.

Ruijter GJG, Visser J (1996) Determination of intermediary metabolites in *Aspergillus niger*. J Microbiol Meth 25: 295-302.

Ruijter GJG, Visser J (1999) Characterization of *Aspergillus niger* phosphoglucose isomerase. Use for quantitative determination of erythrose 4-phosphate. Biochimie 81: 267-272.

Ruijter GJG, Bax M, Patel H, Flitter SJ, Van de Vondervoort PJI, de Vries RP, vanKuyk PA, Visser J (2003) Mannitol is required for stress tolerance in *Aspergillus niger* conidiospores. Eukaryot Cell 2: 690-698.

Ruijter GJG, Visser J, Rinzema A (2004) Polyol accumulation by *Aspergillus oryzae* at low water activity in solid-state fermentation. Microbiology 150: 1095-1101.

Sambrook J, Fritsch EF, Maniatis T (1989) Molecular cloning: A laboratory Manual. 2nd Ed. Cold Spring Harbor Laboratory Press, Cold Spring Harbor, NY.

Sanger F, Nicklen S, Coulsen AR (1977) DNA squencing with chain-terminating inhibitors. Proc Natl Acad Sci USA 74: 5463-5467.

Santos M dos, Thygesen G, Kotter P, Olsson L, Nielsen J (2003) Aerobic physiology of redox-engineered *Saccharomyces cerevisiae* strains modified in the ammonium assimilation for increased NADPH availability. FEMS Yeast Res 4: 59-68.

Schaaff-Gerstenschläger I, Miosga T, Zimmermann FK (1994) Genetics of pentose-phosphate pathway enzymes in *Saccharomyces cerevisiae*. Biores Technol 50: 59-64.

Schmidt K, Marx A, de Graaf AA, Wiechert W, Sahm H, Nielsen J, Villadsen J (1998) ^{13}C tracer experiments and metabolite balancing for metabolic flux analysis: comparing two approaches. Biotechnol Bioeng 58: 254-257.

Swart K, Van der Vondervoort PJI, Witteveen CFB, Visser J (1990) Genetic localization of a series of genes affecting glucose oxidase levels in *Aspergillus niger*. Curr Genet 18: 435-539.

Vries RP de, Flitter SJ, Van de Vondervoort PJI, Chaveroche MK, Fontaine T, Fillinger S, Ruijter GJG, d'Enfert C, Visser J (2003) Glycerol dehydrogenase, encoded by gldB is essential for osmotolerance in *Aspergillus nidulans*. Mol Microbiol 49: 131-141.

Witteveen CFB (1993) Gluconate formation and polyol metabolism in *Aspergillus niger*. PhD thesis, Wageningen Agricultural University, The Netherlands.

Witteveen CFB, Weber F, Businsk R, Visser J (1994) Isolation and characterization of two xylitol dehydrogenases from *Aspergillus niger*. Microbiology 140: 1679-1685.

SUPPLEMENTARY MATERIAL

Table S1. Table of variables measured in cultures for detailed characterization of wild type and overexpressing strains.

wt: wild type (NW131)
Gsd11: NW323
Tkt15: NW339
Gnd20: NW340
a after strain name: NH_4^+ as nitrogen source and final cell density limiting substrate
n after strain name: NO_3^- as nitrogen source and final cell density limiting substrate
e after strain name: exponential phase
s after strain name: stationary phase
SD: standard deviation
n: number of individual samples analyzed
/: indicate a ratio between two conditions or between modified strain and wt
EC: energy charge
ARC: anabolic reduction charge
CRC: catabolic reduction charge
nd: not determined
μ_{max}: maximum specific growth rate in e samples (in exponential phase)
IAP: rate constant of induction of acid production in s samples (in post-exponential phase)
Gray fields are ratios with significant difference (Student's t-test 95% confidence) between numerator and denominator.
Extracellular polyols and acids were calculated as concentration measured extracellularly ($mol \cdot L^{-1}$) divided with dry weight concentration (g $DW \cdot L^{-1}$) to compensate for slightly different times of sampling.
The final dry weight concentration in exponential phase was about 4 g $DW \cdot L^{-1}$ and the dry weight increase in stationary phase (in wt to 5.1 and 6.4 g $DW \cdot L^{-1}$ in ammonium and nitrate cultures, respectively) was therefore caused by storage of mainly carbohydrates [Hrdlicka et al. 2004] and not caused by an increase in active biomass.
[a] For some of the samples of the overexpressing strains the ATP determinations were difficult to reproduce - very low values were obtained; therefore the ATP and EC values should be interpreted with carefullness.

		Enzymes ALD U/g protein	G6PDH U/g protein	6PGDH U/g protein	TKT U/g protein	TAL U/g protein	PGI U/g protein	M1PDH U/g protein	GLYDH U/g protein
wt	wtae	248	554	329	187	463	1601	24	61
	SD	85	128	118	46	227	185	9	4
	n	13	12	13	13	6	12	12	6
	wtas	326	1014	492	346	383	3050	73	103
	SD	166	444	248	244	232	1670	47	54
	n	10	7	10	10	5	9	10	5
	wta s/e	1.31	1.83	1.50	1.85	0.83	1.91	3.09	1.69
	wtne	542	1038	715	343	392	6182	28	137
	SD	116	56	185	145	19	1205	8	16
	n	8	4	8	8	4	8	8	4
	wte n/a	2.18	1.87	2.18	1.83	0.85	3.86	1.17	2.24
	wtns	690	1317	729	458	444	5159	64	159
	SD	133	53	110	191	100	806	7	5
	n	4	2	4	4	2	4	4	2
	wtn s/e	1.27	1.27	1.02	1.34	1.13	0.83	2.31	1.16
	wts n/a	2.12	1.30	1.48	1.32	1.16	1.69	0.87	1.54
Gsd11	Gsd11ae	242	1158	360	163	503	1557	22	67
	SD	40	216	75	38	337	282	6	5
	n	5	5	5	6	3	6	6	3
	Gsd11ae/wt	0.98	2.09	1.09	0.87	1.08	0.97	0.92	1.09
	Gsd11as	206	1385	290	182	244	1406	31	52
	SD	55	791	93	36	124	563	23	4
	n	4	3	4	3	2	4	3	2
	Gsd11as/wt	0.63	1.37	0.59	0.53	0.64	0.46	0.43	0.51
	Gsd11ne	550	1737	731	347	384	5936	39	156
	SD	150	116	133	150	18	1009	10	4
	n	4	2	4	4	2	4	4	2
	Gsd11ne/wt	1.01	1.67	1.02	1.01	0.98	0.96	1.42	1.14
	Gsd11ns	641	3347	637	423	413	4524	63	101
	SD	162	148	16	112		200	7	2
	n	3	2	3	3	1	3	3	2
	Gsd11ns/wt	0.93	2.54	0.87	0.92	0.93	0.00	0.99	0.63
Tkt15	Tkt15ae	313	540	376	452	277	1755	46	86
	SD	72	105	77	133	37	229	13	2
	n	6	5	5	5	3	6	6	3
	Tkt15ae/wt	1.26	0.97	1.14	2.42	0.60	0.00	1.94	1.41
	Tkt15as	505	1095	620	1606	382	3554	82	125
	SD	77	167	114	259	162	840	19	7
	n	5	5	6	5	2	6	6	4
	Tkt15as/wt	1.55	1.08	1.26	4.64	1.00	1.17	1.13	1.21
	Tkt15ne	498	915	588	1156	341	4981	31	157
	SD	85	104	150	747	18	1474	22	27
	n	4	2	4	4	2	4	4	2
	Tkt15ne/wt	0.92	0.88	0.82	3.37	0.87	0.81	1.13	1.15
	Tkt15ns	609	833	552	1058	394	3967	45	110
	SD	184	83	44	108		353	10	9
	n	3	2	3	2	1	3	3	2
	Tkt15ns/wt	0.88	0.63	0.76	2.31	0.89	0.77	0.71	0.69
Gnd20	Gnd20ae	214	726	6654	167	262	1735	29	58
	SD	58	171	2425	57	50	368	12	15
	n	5	5	4	6	3	5	6	3
	Gnd20ae/wt	0.86	1.31	20.24	0.89	0.57	1.08	1.24	0.95
	Gnd20as	501	1345	10079	416	506	3962	192	105
	SD	227	364	2041	141	207	744	32	19
	n	5	4	5	5	2	5	5	3
	Gnd20as/wt	1.54	1.33	20.49	1.20	1.32	1.30	2.63	1.02
	Gnd20ne	437	1276	17839	282	367	5495	50	115
	SD	146	140	3171	114	129	1315	29	8
	n	4	2	2	4	2	4	4	2
	Gnd20ne/wt	0.81	1.23	24.94	0.82	0.94	0.89	1.80	0.84
	Gnd20ns	423	730	9242	256	281	3588	34	100
	SD	138	88	1661	83		200	8	8
	n	3	2	3	3	1	3	3	2
	Gnd20ns/wt	0.61	0.55	12.68	0.56	0.63	0.70	0.54	0.63

Intermediary Metabolites (continued on next page)

	G6P	S7P	DHAP	Xu5P	F6P	PYR	R5P	GAP	6PG	Ru5P
	μmol/gDW	μmol/gDW	μmol/gDW	μmol/gDW	μmol/gDW	μmol/gDW	μmol/gDW	μmol/gDW	μmol/gDW	μmol/gDW
wtae	2.92	2.95	0.18	0.64	4.18	0.49	2.09	0.06	0.25	6.71
SD	0.46	1.38	0.01	0.10	1.52	0.18	0.47	0.02	0.08	1.56
n	7	10	7	9	8	10	10	8	8	7
wtas	2.54	0.61	0.15	0.17	0.50	0.13	1.01	0.09	0.19	9.09
SD	1.20	0.16	0.04	0.09	0.27	0.02	0.13	0.04	0.06	1.74
n	3	2	4	6	5	5	4	6	3	3
wta s/e	0.87	0.21	0.88	0.27	0.12	0.27	0.48	1.45	0.74	1.35
wtne	1.65	4.85	0.17	0.97	0.53	0.55	2.76	0.12	0.50	nd
SD	0.53	1.79	0.10	0.38	0.23	0.22	0.71	0.09	0.12	
n	8	5	8	8	8	8	6	8	6	
wte n/a	0.57	1.64	0.95	1.52	0.13	1.13	1.32	2.00	1.95	
wtns	2.23	0.60	0.15	0.10	0.41	0.16	1.10	0.08	0.27	nd
SD	0.54	0.28	0.03	0.03	0.10	0.06	0.18	0.04	0.16	
n	4	2	3	4	4	4	2	4	4	
wtn s/e	1.35	0.12	0.92	0.10	0.76	0.30	0.40	0.61	0.55	
wts n/a	0.88	0.99	0.99	0.55	0.81	1.24	1.08	0.84	1.45	
Gsd11ae	2.35	2.45	0.18	0.68	2.75	0.32	2.26	0.06	1.79	6.37
SD	0.40	0.50	0.03	0.12	0.38	0.09	0.25	0.01	0.35	1.55
n	4	4	4	4	4	4	4	4	3	4
Gsd11ae/wt	0.80	0.83	1.01	1.07	0.66	0.66	1.08	0.90	7.04	0.95
Gsd11as	0.55	0.39	0.07	0.09	0.31	0.07	0.54	0.04	0.64	2.18
SD	0.04		0.04	0.04	0.28	0.02	0.42	0.00	0.26	2.03
n	3	1	3	3	3	3	3	2	3	2
Gsd11as/wt	0.22	0.64	0.47	0.49	0.61	0.52	0.53	0.47	3.40	0.24
Gsd11ne	1.48	5.05	0.19	1.18	0.48	0.49	3.89	0.11	1.33	nd
SD	0.35	1.32	0.06	0.23	0.21	0.15	2.53	0.06	0.75	
n	4	3	4	4	4	4	3	4	3	
Gsd11ne/wt	0.89	1.04	59.84	1.21	0.90	0.89	1.41	0.90	2.68	
Gsd11ns	1.46	0.08	0.13	0.07	0.23	0.08	0.76	0.06	0.08	nd
SD	0.02	0.02	0.03	0.02	0.01	0.01	0.02	0.04	0.02	
n	2	2	2	2	2	2	2	2	2	
Gsd11ns/wt	0.65	0.13	0.84	0.74	0.56	0.49	0.69	0.83	0.30	
Tkt15ae	3.51	2.80	0.22	0.49	4.17	0.41	2.04	0.24	0.07	6.83
SD	0.38	0.84	0.05	0.10	0.49	0.14	0.36	0.02	0.01	0.97
n	3	3	3	3	3	3	3	3	3	3
Tkt15ae/wt	1.20	0.95	1.26	0.77	1.00	0.84	0.97	3.96	0.26	1.02
Tkt15as	3.34	0.86	0.14	0.06	1.25	0.09	0.74	0.06	0.10	8.38
SD	1.64	0.09	0.03	0.01	0.24	0.03	0.02	0.01	0.03	4.05
n	2	2	2	2	2	2	2	2	2	2
Tkt15as/wt	1.31	1.41	0.92	0.35	2.48	0.68	0.73	0.63	0.52	0.92
Tkt15ne	2.05	4.60	0.22	0.81	0.67	1.56	0.62	0.13	0.55	nd
SD	0.66	1.45	0.05	0.33	0.22	0.59		0.04	0.19	
n	4	4	4	4	4	4	1	4	4	
Tkt15ne/wt	1.24	0.95	1.31	0.83	1.25	2.83	0.22	1.07	1.11	
Tkt15ns	2.24	0.08	0.30	0.08	0.33	0.13	0.80	0.07	nd	nd
SD	1.08	0.03	0.23	0.03	0.14	0.11	0.48	0.07		
n	2	2	2	2	2	2	2	2		
Tkt15ns/wt	1.00	0.13	1.94	0.79	0.80	0.79	0.73	0.99		
Gnd20ae	4.25	3.16	0.49	1.12	5.58	1.12	0.08	2.79	0.08	12.58
SD	0.58	1.16	0.27	0.30	0.87	0.18	0.03	0.57	0.03	3.75
n	2	4	5	5	5	5	5	4	5	3
Gnd20ae/wt	1.46	1.07	2.79	1.76	1.34	2.30	0.04	45.34	0.30	1.87
Gnd20as	2.89	1.32	0.35	0.23	0.55	0.10	0.76	0.06	0.02	5.67
SD	0.84	0.15	0.13	0.09	0.01	0.03	0.12	0.01	0.03	1.71
n	3	2	3	3	2	3	2	3	2	2
Gnd20as/wt	1.14	2.17	2.28	1.34	1.09	0.76	0.75	0.65	0.13	0.62
Gnd20ne	1.95	8.20	0.41	2.92	0.60	1.03	4.86	0.21	0.16	nd
SD	0.19	0.93	0.16	0.29		0.32		0.04	0.04	
n	2	2	2	2	1	2	1	2	2	
Gnd20ne/wt	1.18	1.69	2.46	3.01	1.13	1.86	1.76	1.72	0.32	
Gnd20ns	2.15	0.12	0.21	0.08	0.45	0.16	1.24	0.06	0.93	nd
SD	0.30	0.00	0.05	0.02	0.08	0.05	0.15	0.01	1.07	
n	2	2	2	2	2	2	2	2	2	
Gnd20ns/wt	0.96	0.20	1.37	0.80	1.11	0.99	1.13	0.81	3.42	

Intermediary Metabolites (continued from previous page)

		ADP	AMP	NAD	NADP	NADH	NADPH	ATP[a]	EC	ARC	CRC
		μmol/gDW	μmol/gDW	μmol/gDW	μmol/gDW	μmol/gDW	μmol/gDW	μmol/gDW			
wt	wtae	1.21	0.47	1.79	0.240	0.084	0.148	4.12	0.841	0.386	0.047
	SD	0.37	0.25	0.30	0.042	0.038	0.023	0.84	0.032	0.054	0.020
	n	10	8	9	8	4	7	7	7	5	4
	wtas	0.31	0.24	0.50	0.052	0.037	0.039	1.31	0.781	0.426	0.056
	SD	0.01	0.06	0.14	0.020	0.018	0.008	0.38	0.048	0.111	0.031
	n	4	4	4	4	3	3	4	4	3	4
	wta s/e	0.26	0.51	0.28	0.21	0.44	0.27	0.32	0.93	1.10	1.21
	wtne	1.49	0.50	1.72	0.407	0.019	0.025	4.22	0.751	0.064	0.012
	SD	0.66	0.09	0.46	0.130	0.009	0.015	0.93	0.156	0.041	0.006
	n	8	6	8	8	4	6	5	6	8	4
	wte n/a	1.24	1.05	0.96	1.70	0.23	0.17	1.03	0.89	0.17	0.26
	wtns	0.34	0.20	0.72	0.096	0.005	0.063	1.81	0.845	0.417	0.006
	SD	0.02	0.07	0.17	0.040	0.002	0.010	0.06	0.043	0.104	0.002
	n	4	3	4	3	3	4	2	2	4	3
	wtn s/e	0.23	0.40	0.42	0.24	0.28	2.49	0.43	1.13	6.53	0.50
	wts n/a	1.11	0.81	1.45	1.86	0.15	1.61	1.38	1.08	0.98	0.11
Gsd11	Gsd11ae	1.19	0.38	1.68	0.194	0.068	0.147	4.32	0.833	0.428	0.040
	SD	0.37	0.13	0.07	0.041	0.008	0.049	0.62	0.057	0.111	0.003
	n	4	4	4	4	2	4	4	4	4	2
	Gsd11ae/wt	0.99	0.81	0.94	0.81	0.81	0.99	1.05	0.99	1.11	0.86
	Gsd11as	0.27	0.13	0.30	0.029	0.022	0.058	0.98	0.808	0.681	0.068
	SD	0.10	0.04	0.01	0.004	0.004	0.005	0.29	0.012	0.030	0.010
	n	3	3	3	3	2	2	3	3	2	2
	Gsd11as/wt	0.89	0.53	0.60	0.56	0.60	1.46	0.75	1.03	1.60	1.20
	Gsd11ne	1.27	0.38	1.91	0.356	0.008	0.034	4.59	0.842	0.102	0.007
	SD	0.44	0.00	0.55	0.075	0.001	0.018	1.00	0.028	0.010	0.004
	n	4	2	4	4	3	3	3	3	3	4
	Gsd11ne/wt	0.85	0.76	1.11	0.87	0.42	1.33	1.09	1.12	1.59	0.57
	Gsd11ns	0.38	0.06	0.46	0.060	0.013	0.059	0.11	0.528	0.499	0.027
	SD	0.03		0.00	0.007	0.001	0.004	0.02		0.043	0.002
	n	2	1	2	2	2	2	2	1	2	2
	Gsd11ns/wt	1.10	0.31	0.64	0.62	2.37	0.94	0.06	0.62	1.20	4.43
Tkt15	Tkt15ae	1.14	0.35	1.83	0.249	0.044	0.118	4.92	0.858	0.325	0.023
	SD	0.17	0.05	0.12	0.070	0.006	0.030	0.32	0.009	0.073	0.005
	n	3	3	3	3	2	3	3	3	3	2
	Tkt15ae/wt	0.94	0.73	1.03	1.04	0.52	0.79	1.19	1.02	0.84	192.80
	Tkt15as	0.32	0.21	0.59	0.059	0.022	0.080	1.61	0.819	0.569	0.035
	SD	0.09	0.11	0.29	0.008	0.014	0.029	0.53	0.074	0.055	0.005
	n	2	2	2	2	2	2	2	2	2	2
	Tkt15as/wt	1.02	0.86	1.19	1.14	0.61	2.03	1.23	1.05	1.34	0.62
	Tkt15ne	1.01	0.41	1.84	0.326	0.007	0.040	4.24	0.837	0.115	0.003
	SD	0.34	0.15	0.48	0.110	0.003	0.016	1.32	0.032	0.033	0.001
	n	4	4	4	4	2	3	4	4	3	2
	Tkt15ne/wt	0.68	0.83	1.07	0.80	0.38	1.57	1.00	1.11	1.80	0.28
	Tkt15ns	0.39	0.09	0.57	0.089	0.010	0.067	0.10	0.461	0.461	0.020
	SD	0.12		0.21	0.062	0.006	0.015	0.06		0.133	0.018
	n	2	1	2	2	2	2	2	1	2	2
	Tkt15ns/wt	1.13	0.44	0.79	0.93	1.85	1.05	0.05	0.55	1.11	3.32
Gnd20	Gnd20ae	1.12	0.35	1.96	0.517	0.087	0.343	5.58	0.870	0.396	0.043
	SD	0.18	0.08	0.36	0.108	0.036	0.129	0.87	0.018	0.134	0.025
	n	5	5	5	5	4	5	5	5	4	3
	Gnd20ae/wt	0.93	0.75	1.10	2.16	1.04	2.32	1.36	1.03	1.02	0.92
	Gnd20as	0.42	0.22	1.06	0.050	0.011	0.125	2.13	0.858	0.715	0.011
	SD	0.05		0.16	0.010	0.003	0.011	0.09		0.058	0.005
	n	3	1	3	2	2	2	2	1	2	2
	Gnd20as/wt	1.35	0.89	2.14	0.97	0.29	3.18	1.63	1.10	1.68	0.20
	Gnd20ne	0.96	0.41	2.64	0.749	0.034	0.230	4.80	0.853	0.235	0.012
	SD	0.07	0.10	0.32	0.077	0.030	0.077	0.89	0.040	0.079	0.010
	n	2	2	2	2	2	2	2	2	2	2
	Gnd20ne/wt	0.64	0.84	1.54	1.84	1.76	9.02	1.14	1.14	3.68	0.98
	Gnd20ns	0.49	0.16	0.59	0.132	0.011	0.129	0.21	0.512	0.494	0.018
	SD	0.03		0.00	0.012	0.009	0.002	0.05		0.027	0.014
	n	2	1	2	2	2	2	2	1	2	2
	Gnd20ns/wt	1.42	0.80	0.82	1.38	1.98	2.03	0.12	0.61	1.18	2.89

Intracellular polyols

	glycerolI μmol/gDW	erythritolI μmol/gDW	arabitolI μmol/gDW	trehaloseI μmol/gDW	mannitolI μmol/gDW
wtae	403	63	3.4	16.4	18.7
SD	86	11	1.2	5.5	4.2
n	6	6	5	5	5
wtas	219	58	4.0	7.4	8.3
SD	66	30	3.3	2.5	2.1
n	4	4	2	4	3
wta s/e	0.54	0.92	1.20	0.45	0.44
wtne	352	225	8.0	7.3	5.9
SD	86	94	2.7	4.8	2.0
n	4	4	4	3	4
wte n/a	0.87	3.55	2.38	0.44	0.31
wtns	147	85	1.9	8.1	19.5
SD	108	58		5.9	13.9
n	2	2	1	2	2
wtn s/e	0.42	0.38	0.24	1.11	3.32
wts n/a	0.67	1.46	0.48	1.10	2.34
Gsd11ae	456	60	3.1	14.8	10.8
SD	101	20	1.1	1.0	1.2
n	2	2	2	2	2
Gsd11ae/wt	1.13	0.95	0.93	0.90	0.58
Gsd11as	355	73	5.6	16.1	39.0
SD	344	74			52.2
n	2	2	1	1	2
Gsd11as/wt	1.62	1.26	1.38	2.18	4.68
Gsd11ne	421	323	11.7	0.0	6.9
SD	10	151	4.1	0.0	2.4
n	2	2	2	2	2
Gsd11ne/wt	1.20	1.44	1.46	0.00	0.85
Gsd11ns	113	54	0.0	6.3	16.7
SD					
n	1	1	1	1	1
Gsd11ns/wt	0.77	0.63	0.00	0.78	0.86
Tkt15ae	557	71	6.0	20.1	50.9
SD	128	35		13.0	19.1
n	3	3	1	3	2
Tkt15ae/wt	1.38	1.11	1.77	1.22	2.71
Tkt15as	234	96	3.7	11.5	55.2
SD	102	14	0.2	0.5	11.8
n	2	2	2	2	2
Tkt15as/wt	1.07	1.66	0.92	1.56	6.62
Tkt15ne	410	97	5.6	5.6	6.5
SD	280	74	4.6		2.7
n	2	2	2	1	2
Tkt15ne/wt	1.16	0.43	0.70	0.77	1.10
Tkt15ns	160	66	1.5	5.2	18.3
SD					
n	1	1	1	1	1
Tkt15ns/wt	1.09	0.78	0.80	0.64	0.94
Gnd20ae	687	22	15.4	31.8	46.3
SD	304	11	6.9	21.1	19.2
n	3	3	3	3	2
Gnd20ae/wt	1.70	0.35	4.57	1.94	2.47
Gnd20as	418	87	13.8	26.7	131.6
SD	366	41	5.9	13.9	46.4
n	2	2	2	2	2
Gnd20as/wt	1.91	1.50	3.42	3.62	15.79
Gnd20ne	561	66	32.0	13.6	34.5
SD	11	45	14.7	7.6	29.4
n	2	2	2	2	2
Gnd20ne/wt	1.59	0.29	3.99	1.87	5.89
Gnd20ns	399	106	10.0	26.8	79.9
SD					
n	1	1	1	1	1
Gnd20ns/wt	2.72	1.25	5.16	3.31	4.10

Extracellular polyols

	glycerolE μmol/gDW	erythritolE μmol/gDW	arabitolE μmol/gDW	trehaloseE μmol/gDW	mannitolE μmol/gDW
wtae	668	104	2.3	27.2	7.3
SD	162	20	0.5	8.9	2.9
n	7	7	4	7	4
wtas	1231	227	7.4	79.3	84.2
SD	401	94	3.9	55.7	47.1
n	3	5	5	5	5
wta s/e	1.84	2.18	3.29	2.91	11.47
wtne	567	276	4.3	32.8	3.1
SD	294	153	1.4	5.5	1.1
n	3	4	3	3	3
wte n/a	0.85	2.66	1.93	1.20	0.43
wtns	154	312	4.0	41.5	56.0
SD	28	77	0.7	1.9	11.8
n	2	2	2	2	2
wtn s/e	0.27	1.13	0.91	1.27	17.82
wts n/a	0.13	1.37	0.54	0.52	0.67
Gsd11ae	663	90	1.6	32.6	4.7
SD	39	26	0.1	7.2	1.8
n	2	2	2	2	2
Gsd11ae/wt	0.99	0.87	0.73	1.20	0.65
Gsd11as	899	181	6.9	71.1	64.1
SD	413	77	3.7	59.7	23.6
n	2	2	2	2	2
Gsd11as/wt	0.73	0.80	0.93	0.90	0.76
Gsd11ne	503	252	1.6	40.1	3.3
SD	148	74	1.2	4.3	
n	2	2	2	2	1
Gsd11ne/wt	0.89	0.91	0.37	1.22	1.06
Gsd11ns	152	342	4.9	36.3	67.7
SD					
n	1	1	1	1	1
Gsd11ns/wt	0.98	1.10	1.23	0.88	1.21
Tkt15ae	587	73	1.1	23.9	10.7
SD	36	28	0.4	9.0	1.4
n	2	2	2	2	2
Tkt15ae/wt	0.88	0.70	0.48	0.88	1.46
Tkt15as	117	132	4.0	43.8	58.1
SD	48	11	0.9	0.8	45.2
n	2	2	2	2	2
Tkt15as/wt	0.09	0.58	0.54	0.55	0.69
Tkt15ne	988	169	0.0	58.2	6.3
SD	198	45	0.0	6.8	1.2
n	2	2	2	2	2
Tkt15ne/wt	1.74	0.61	0.00	1.78	2.01
Tkt15ns	504	413	6.0	36.5	89.3
SD					
n	1	1	1	1	1
Tkt15ns/wt	3.27	1.32	1.52	0.88	1.59
Gnd20ae	535	21	5.9	30.4	11.4
SD	86	8	0.1	5.9	0.8
n	3	3	2	3	2
Gnd20ae/wt	0.80	0.20	2.64	1.12	1.56
Gnd20as	50	42	9.5	44.1	64.8
SD	2	2	1.4	8.7	42.1
n	2	2	2	2	2
Gnd20as/wt	0.04	0.19	1.29	0.56	0.77
Gnd20ne	840	55	15.5	43.1	16.0
SD	159	34	4.7	6.7	11.0
n	2	2	2	2	2
Gnd20ne/wt	1.48	0.20	3.57	1.32	5.09
Gnd20ns	533	132	17.0	36.2	57.5
SD					
n	1	1	1	1	1
Gnd20ns/wt	3.46	0.42	4.30	0.87	1.03

Row group labels (left margin): wt, Gsd11, Tkt15, Gnd20

Characterization of pathway engineered strains of filamentous fungi in submerged cultures

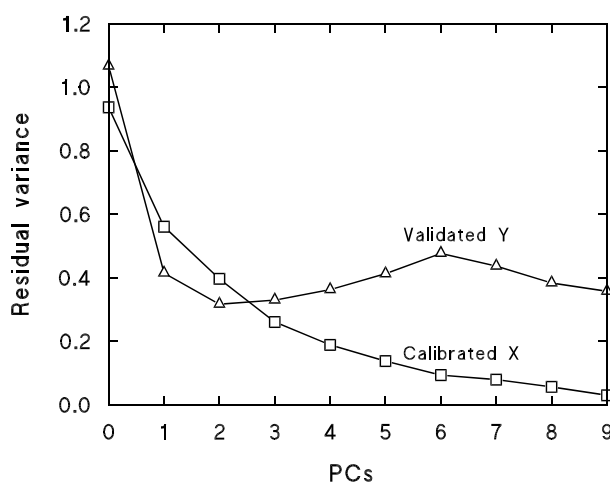| Group		Acids oxalate (mmol/gDW)	citrate (mmol/gDW)		Dry Weight DW (gDW/L)		μmax/IAP (per hour)
wt	wtae	1.19	0.00	wtae	2.45	wtae	0.24
	SD	0.15	0.00	SD	0.62	SD	0.02
	n	3	3	n	7	n	7
	wtas	5.06	0.60	wtas	5.12	wtas	0.26
	SD	1.40	0.13	SD	1.70	SD	0.04
	n	4	4	n	5	n	3
	wta s/e	4.26	>>1	wta s/e	2.09	wta s/e	
	wtne	1.78	0.00	wtne	1.51	wtne	0.23
	SD	0.09	0.00	SD	0.27	SD	0.05
	n	2	2	n	4	n	3
	wte n/a	1.50		wte n/a	0.62	wte n/a	0.96
	wtns	9.50	1.25	wtns	6.38	wtns	0.27
	SD	0.39	0.06	SD	0.17	SD	0.03
	n	2	2	n	2	n	2
	wtn s/e	5.33	>>1	wtn s/e	4.22	wtn s/e	1.19
	wts n/a	1.88	2.09	wts n/a	1.25	wts n/a	1.05
Gsd11	Gsd11ae	0.92	0.00	Gsd11ae	2.66	Gsd11ae	0.23
	SD	0.39	0.00	SD	0.18	SD	0.03
	n	2	2	n	3	n	3
	Gsd11ae/wt	0.77		Gsd11ae/wt	1.08	Gsd11ae/wt	0.96
	Gsd11as	5.52	0.59	Gsd11as	4.99	Gsd11as	0.28
	SD			SD	1.40	SD	0.01
	n	1	1	n	2	n	2
	Gsd11as/wt	1.09	0.99	Gsd11as/wt	0.98	Gsd11as/wt	1.09
	Gsd11ne	1.81	0.00	Gsd11ne	1.56	Gsd11ne	0.23
	SD			SD	0.41	SD	0.04
	n	1	1	n	2	n	2
	Gsd11ne/wt	1.02		Gsd11ne/wt	1.03	Gsd11ne/wt	0.99
	Gsd11ns	12.05	1.68	Gsd11ns	6.88	Gsd11ns	0.30
	SD			SD		SD	
	n	1	1	n	1	n	1
	Gsd11ns/wt	1.27	1.34	Gsd11ns/wt	1.08	Gsd11ns/wt	1.11
Tkt15	Tkt15ae	0.60	0.00	Tkt15ae	2.92	Tkt15ae	0.26
	SD	0.13	0.00	SD	0.55	SD	0.01
	n	2	2	n	3	n	4
	Tkt15ae/wt	0.51		Tkt15ae/wt	1.19	Tkt15ae/wt	1.08
	Tkt15as	7.18	0.79	Tkt15as	6.28	Tkt15as	0.35
	SD	1.37	0.50	SD	0.44	SD	0.06
	n	2	2	n	2	n	2
	Tkt15as/wt	1.42	1.31	Tkt15as/wt	1.23	Tkt15as/wt	1.34
	Tkt15ne	3.21	0.00	Tkt15ne	0.86	Tkt15ne	0.27
	SD			SD	0.32	SD	1.00
	n	1	1	n	2	n	
	Tkt15ne/wt	1.80		Tkt15ne/wt	0.57	Tkt15ne/wt	1.19
	Tkt15ns	20.71	3.08	Tkt15ns	5.13	Tkt15ns	0.29
	SD			SD		SD	1.00
	n	1	1	n	1	n	
	Tkt15ns/wt	2.18	2.46	Tkt15ns/wt	0.80	Tkt15ns/wt	1.07
Gnd20	Gnd20ae	0.78	0.00	Gnd20ae	2.47	Gnd20ae	0.25
	SD	0.13	0.00	SD	0.33	SD	0.04
	n	2	2	n	3	n	4
	Gnd20ae/wt	0.66		Gnd20ae/wt	1.01	Gnd20ae/wt	1.04
	Gnd20as	3.73	0.27	Gnd20as	6.56	Gnd20as	0.28
	SD	1.03	0.11	SD	0.55	SD	0.04
	n	2	2	n	2	n	2
	Gnd20as/wt	0.74	0.45	Gnd20as/wt	1.28	Gnd20as/wt	1.09
	Gnd20ne	1.98	0.00	Gnd20ne	1.24	Gnd20ne	nd
	SD			SD	0.44	SD	
	n	1	1	n	2	n	
	Gnd20ne/wt	1.11		Gnd20ne/wt	0.82	Gnd20ne/wt	
	Gnd20ns	6.04	0.57	Gnd20ns	5.74	Gnd20ns	nd
	SD			SD		SD	
	n	1	1	n	1	n	
	Gnd20ns/wt	0.64	0.45	Gnd20ns/wt	0.90	Gnd20ns/wt	

Figure S1. Residual variance of calibrated X and of validated Y (NADPH) in PLS regression shown in Fig. 4, where two PCs were used.
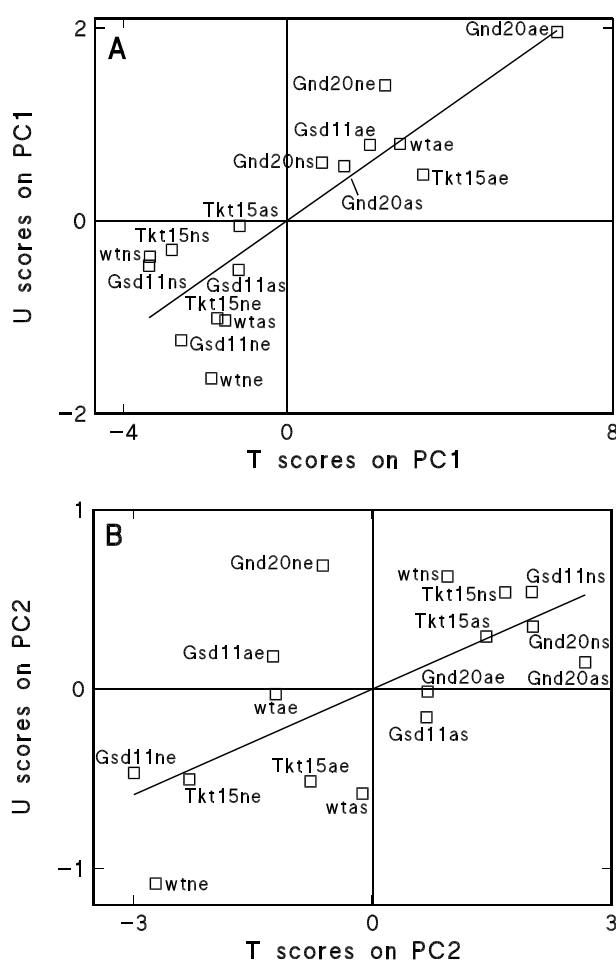

Figure S2. U versus T scores on PC1 (A) and on PC2 (B) in PLS regression shown in Fig. 4. Legends as in Figure 4.
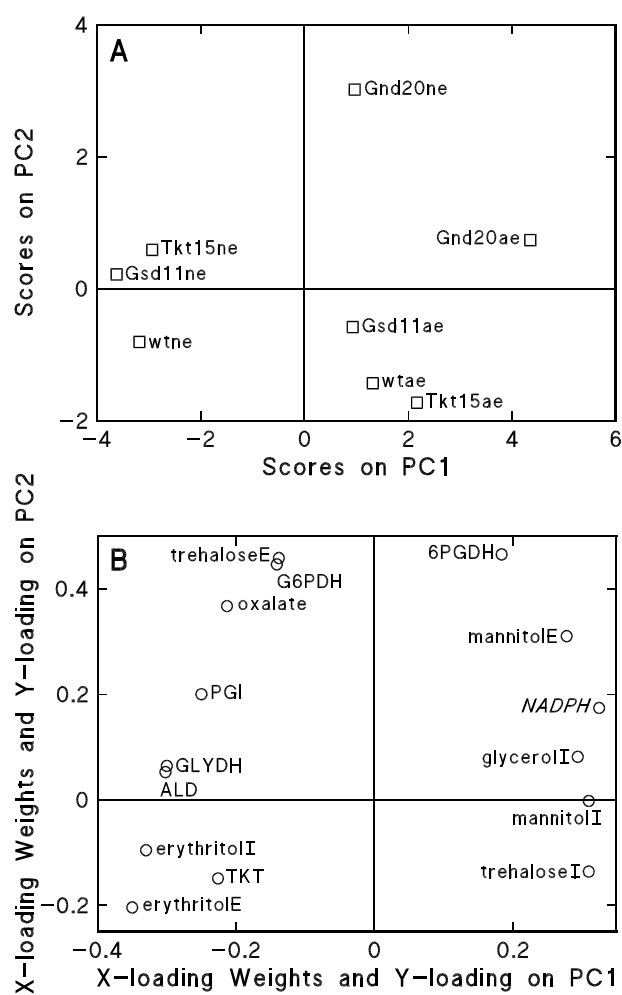
Figure S3. Scores (A) and X-loading Weights and Y-loadings (B) in PLS regression shown in Figure 5. Legends as in Figure 4.
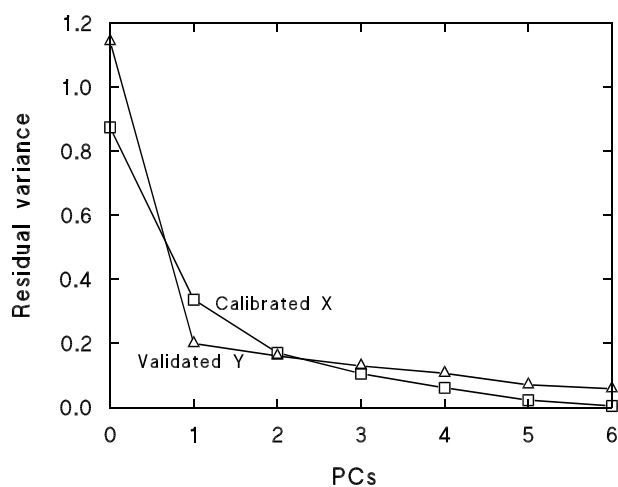

Figure S4. Residual variance of calibrated X and of validated Y (NADPH) in PLS regression shown in Figure 5, where two PCs were used.
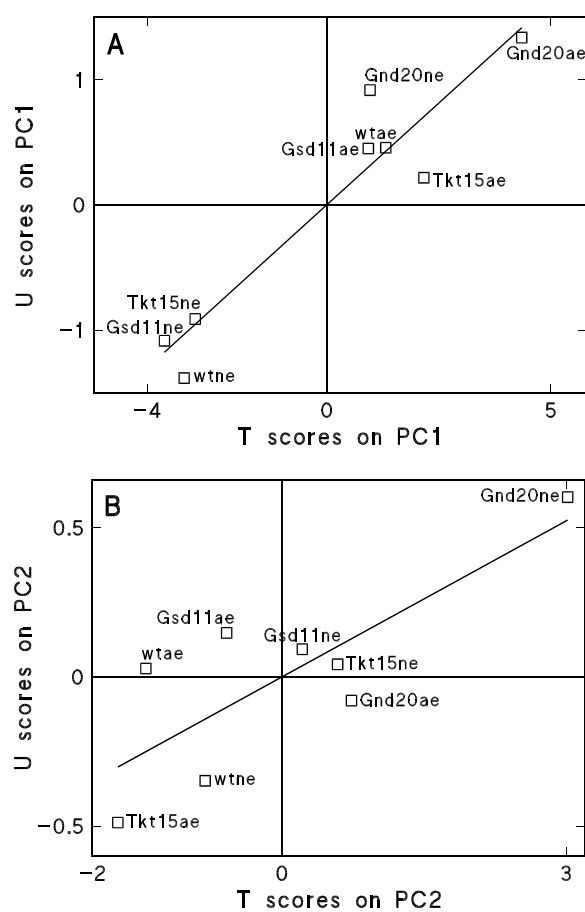
Figure S5. U versus T scores on PC1 (A) and on PC2 (B) in PLS regression shown in Figure 5. Legends as in Figure 4.

Can submerged cultures of filamentous fungi be made reproducible?
A prerequisite for the omics technologies

ABSTRACT

The omics technologies enable extensive and accurate analysis of samples from cell cultures. However, without reproducible cell cultures the many resources used for analysis of each sample are wasted. The results and the value thereof are just as dependent on the origin of the sample as on the analysis. In our opinion this is insufficiently appreciated at the moment. Cultures of filamentous fungi are particularly difficult to reproduce, because of complicated fungal morphology and tendency to adhere to surfaces. We emphasise the importance of profiling the morphology and, if possible to control it. Methods to prevent wall growth are presented in addition to how to obtain detailed information about the culture at the time of sampling. Using these techniques, it is possible to obtain reproducible samples from batch cultures of filamentous fungi.

INTRODUCTION

In recent years improvement of strains for industrial applications has shifted from classical to modern molecular techniques (e.g. Conesa *et al.* [2001]) since these are expected to deliver further improvements through a better understanding of metabolic control. The understanding requires precise measurement of the effects of the genetic engineering. The omics technologies may provide such information, but they must be done on samples from reproducible cultures to exclude effects from variations in culture conditions. Cultures of filamentous fungi are especially challenging because of their variation in morphology. In this paper we describe the challenges in obtaining reproducible cultures with filamentous fungi and knowledge about the culture at the time of sampling. Some tools to meet those challenges are given.

Continuous cultures remain the supplier of the most well-defined culture samples and have indeed been obtained with filamentous fungi [Carlsen *et al.* 1996a; Christensen *et al.* 1995; Mainwaring *et al.* 1999; Metwally *et al.* 1991; Pedersen *et al.* 2000; Poulsen *et al.* 2004c; Van der Vondervoort *et al.* 2004]. However, mostly low dilution rates (growth rates) have been obtained - considerably lower than maximum specific growth rates measured in batch cultures. This was recently explained by Poulsen *et al.* [2004c] by pellet formation at high dilution rates, creating biomass limited by diffusion of substrate into pellets causing washout.

Constant culture conditions and the possibility of changing only one parameter over an extended period of time can only be obtained in continuous cultures, but these are very elaborate. We argue in this paper that reproducible samples can also be obtained from batch cultures if sufficient knowledge about the culture at the time of sampling is available.

MACRO-MORPHOLOGY

Few will disagree that morphology is very important in submerged culturing of filamentous fungi just as well as most will agree that morphology is influenced by and on its turn influencing a large number of parameters and that this interplay is very complicated. The most important consequence of the macro-morphology for the physiology of filamentous fungi is formation of large pellets with a diffusion-limited centre causing inactive biomass (diameter >200-300 μm, dependent on conditions [Poulsen *et al.* 2004c]). This biomass is in a different physiological state than the mycelium at the boundary of the pellets and interpretation of any data from such inhomogeneous cultures is very difficult or impossible [Trinci 1970]. Carlsen *et al.* [1996b] were able to correlate ethanol production to the theoretical diffusion-limited biomass inside large pellets. Diffusion limitation of part of the biomass in a culture also results in a mixed transcriptome. Since transcription levels can differ with several orders of magnitude, very small amounts of mycelium in a different physiological state than the rest of the culture can impair the effort to obtain a reproducible transcriptome.
Most published methods of image analysis of pellets are based on projected area or numbers [Pazouki and Panda 2000], which cannot be used to find the amount of diffusion-limited biomass

in the core of large pellets. Exceptions might be the methods described by Treskatis *et al.* [1997] who used grey values and by Cui *et al.* [1998] who used separation of a large number of pellets for subsequent dry weight measurement. Poulsen *et al.* [2004c] have presented a method to measure the amount of diffusion-limited biomass in the centre of large pellets (Box 1). The authors also developed a macro-morphology profiling system that in addition gives the amounts of biomass in free hyphae, small pellets (< 200-300 μm) and large pellets. This profiling system can e.g. give a warning if small pellets are growing and are about to become large pellets with a diffusion-limited centre. The method can therefore be used to lay out the course of sampling to enable samples to be taken before such a limitation occurs.

BOX 1. HOW TO DETERMINE AMOUNT OF DIFFUSION LIMITED BIOMASS IN CORE OF PELLETS

The amount of biomass limited by diffusion of substrate into a pellet can be estimated by using image analysis and the critical core diameter.

We define the pellet core, d (m), as the part of the pellet-image without visible void volume (Fig. a), where substrate transport presumably is only by diffusion [Cox and Thomas 1992; Wittler *et al.* 1986]. The critical core diameter, d_{crit} (m), is defined as the largest core diameter without diffusion limitation of substrate in the centre.
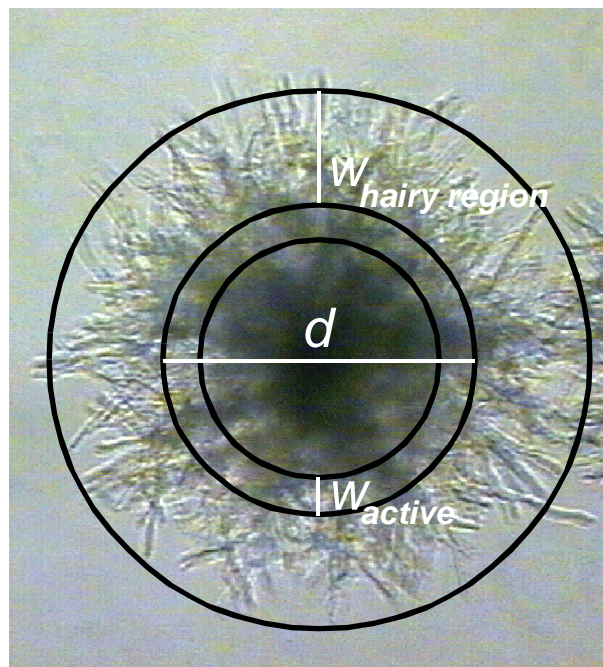

Figure a. Representative pellet from pH 6-batch culture of *A. niger* 29 h after inoculation, culture conditions: 30°C, 750 rpm, 0.40 vvm. d (here 0.36 mm) is diameter of core defined as the part of the pellet-image without visible void volume, where substrate transport presumably is only by diffusion [Cox and Thomas 1992; Wittler *et al.* 1986]. d is in this example larger than d_{crit} (0.19 mm, critical core diameter defined as the largest core diameter without diffusion limitation of substrate in the centre). w_{active} (here 0.04 mm) is width of active layer without diffusion limitation of substrate. $w_{hairy\ region}$ (0.13 mm) is width of hairy region. Figure from Poulsen *et al.* [2004c].

Determination of amount of diffusion-limited biomass in culture sample

- measure the core diameter of all pellets larger than the critical core diameter by image analysis
- estimate the total amount of diffusion-limited biomass ($DW_{limited}$). For pellets larger than the critical diameter the active width (w_{active}, m), which is not limited by diffusion of substrate into the pellet, decreases with diameter because of the effect of curvature. To take this effect into account, we assume uniform core biomass density and that the effect of external diffusion can be neglected, which is reasonable from the measurement of Wittler *et al.* [1986]. When $d = d_{crit}$, the total volume of the pellet is sufficiently supplied with substrate by diffusion. Since the volume of a sphere is $\pi/6 \cdot d^3$ and the area of a sphere is $\pi \cdot d^2$, the flux (amount per area per time) of substrate into the pellet (J, kg s^{-1} m^{-2}) can be calculated as:

$$J = \frac{\frac{\pi}{6} \cdot d_{crit}^3 \cdot r_v}{\pi \cdot d_{crit}^2} = \frac{1}{6} \cdot d_{crit} \cdot r_v$$

where r_v (kg m^{-3} s^{-1}) is the volumetric substrate consumption rate. When $d > d_{crit}$ the active volume (V_{active}, m^3) without diffusion can be calculated as the amount of substrate diffusing into the pellet per time divided with the volumetric substrate consumption rate:

$$V_{active} = \frac{J \cdot \pi d^2}{r_v} = \frac{\frac{1}{6} d_{crit} \cdot r_v \cdot \pi d^2}{r_v} = \frac{\pi}{6} d_{crit} \cdot d^2 \qquad \text{for } d > d_{crit}$$

The volume of limited biomass ($V_{limited}$, m^3) is:

$$V_{limited} = V - V_{active} = \frac{\pi}{6} d^3 - \frac{\pi}{6} d_{crit} \cdot d^2 = \frac{\pi}{6} d^2 (d - d_{crit}) \qquad \text{for } d > d_{crit}$$

Therefore calculating the total limited biomass as the core biomass density times the volume of limited biomass becomes:

$$DW_{limited} = \rho \frac{\pi}{6} \sum_{i=1}^{n_L} d_i^2 (d_i - d_{crit}) \qquad \text{for } d > d_{crit}$$

where n_L is number of pellets larger than the critical core diameter, ρ (kg dry weight·m^{-3}) is pellet core biomass density defined as biomass concentration in core, d_i is the core diameter of the i'th large pellets.

The diameter of the diffusion-limited pellet core ($d_{limited}$, m) is:

$$d_{limited} = \left(\frac{6 \cdot V_{limited}}{\pi}\right)^{\frac{1}{3}} = \left[d^2\left(d - d_{crit}\right)\right]^{\frac{1}{3}} \qquad \text{for } d > d_{crit}$$

Therefore, the width of the active layer without diffusion limitation of substrate can be calculated from:

$$w_{active} = \frac{d - d_{limited}}{2} = \frac{d - \left[d^2\left(d - d_{crit}\right)\right]^{\frac{1}{3}}}{2}$$

Determination of the critical core diameter

The critical core diameter is dependent on conditions. Poulsen *et al.* [2004] measured d_{crit} at one set of conditions. By using the core biomass density and assuming spherical symmetry, uniform core biomass density, molecular diffusion and zero order substrate consumption the following equation [Metz and Kossen 1977] can be applied:

$$d_{crit} = 2\sqrt{\frac{6 D_{eff} c_s Y}{\rho \mu}}$$

where D_{eff} ($m^2 \cdot h^{-1}$) is effective diffusion coefficient, c_s ($mol \cdot L^{-1}$) is concentration of diffusion-limiting substrate at surface, Y (kg dry weight·mol^{-1}) is yield coefficient of biomass of diffusion-limiting substrate, μ (kg dry weight·kg dry weight$^{-1} \cdot h^{-1}$) is specific growth rate, to find the new critical core diameter at any (new) conditions by dividing the new critical diameter ($d_{crit,new}$, m) with the critical diameter at the old conditions to obtain the following equation:

$$d_{crit,new} = d_{crit,old} \sqrt{\frac{D_{eff,new} c_{s,new} Y_{new}}{D_{eff,old} c_{s,old} Y_{old}} \cdot \frac{\rho_{old} \mu_{old}}{\rho_{new} \mu_{new}}}$$

where subscript ″new″ refers to present conditions and subscript ″old″ refers to conditions in *Aspergillus niger* cultures of pellets grown at pH 6 [Poulsen *et al.* 2004]: $d_{crit,old} = 0.19$ mm, $\rho_{old} = 25$ kg·m^{-3}, $\mu_{old} = 0.25$ h^{-1}, $D_{eff,old}$ $(O_2) = 9.0$ 10^{-6} $m^2 h^{-1}$, $c_{O2,old} = 0.16$ mM, $Y_{O2,old} = 43$ g DW mol^{-1}.

Determination of biomass density

If the core biomass density is unknown it can be determined in the following way:

- grow or isolate pellets of approximately equal size
- measure core diameters of pellets (volume determination)
- sonicate pellets till mycelium is dispersed into free hyphae
- measure optical density

- calculate dry weight from optical density - dry weight correlation (mass determination)
- calculate apparent core biomass density (ρ_{app}, kg·m^{-3}) by dividing mass with volume
- find core biomass density from apparent core biomass density by fitting the relationship found by Poulsen *et al.* [2004]:

$$\rho_{app} = \rho + \rho_{hairy\ region}(6w_{hairy\ region}d^{-1} + 12w_{hairy\ region}{}^2 d^{-2} + 8w_{hairy\ region}{}^3 d^{-3})$$

References

Cox PW and Thomas CR (1992) Classification and measurement of fungal pellets by automated image analysis. Biotechnol Bioeng 39: 945-952.

Metz B and Kossen NWF (1977) The growth of molds in the form of pellets - a literature review. Biotechnol Bioeng 19: 781-799.

Poulsen BR, Sørensen AB, Schuleit T, Ruijter GJG, Visser J, Iversen JJL (2004) Quantitative description of biomass distribution in free hyphae, pellets and diffusion-limited pellet cores in submerged cultures of filamentous fungi. Appl Environ Microbiol, submitted.

Wittler RH, Baumgartl DW, Lübbers, Schügerl K (1986) Investigations of oxygen transfer into *Penicillium chrysogenum* pellets by microprobe measurements. Biotechnol Bioeng 28: 1024-1036.

BIOREACTOR DESIGN

A bioreactor for submerged cultures can be as simple as a static flask containing medium and inoculum and having air supply through a cotton plug. The most widespread bioreactor is only slightly more sophisticated than that: shake flask cultures are widely used to characterize strains and obtain samples for any analysis done on submerged cultures.

Shake flask cultures have a low agitation/shear stress compared to stirred tank bioreactors. This often results in formation of large pellets and low transfer of oxygen to the medium causing an overall oxygen limitation if the cultures reach a certain density. The overall oxygen limitation then causes filamentous growth with long scarcely branched filaments and high viscosity culture broth. Therefore, most shake flask cultures are partly (inside large pellets) or fully oxygen limited (when dense cultures are used). One solution to this problem would be to produce a relatively large inoculum of free hyphae in a stirred tank bioreactor and transfer an amount sufficiently small to be sustained with oxygen to the shake flask. An oxygen concentration as low as 20% (of air saturation) is usually considered to have no effects on metabolism when growing free hyphae. When growing pellets the critical oxygen concentration in the medium increases with the size and density of the pellets. If precautions to these problems of morphology and oxygen limitation are not taken, plate cultures might be just as reproducible as shake flasks if a known amount of inoculum (usually number of spores) is used [vanKuyk *et al.* 2004]. However, it should be noted

that also in plate/solid state cultures oxygen limitation often occurs [Oostra *et al.* 2001].

Stirred tank bioreactors offer more possibilities to control conditions. However, also these bioreactors have their limitations. Filamentous fungi are obligate aerobic and the density of cultures should still be kept sufficiently low to prevent that oxygen demand does not exceed the oxygen transfer capacity of the bioreactor. This is most efficiently obtained by a certain amount of a final cell density limiting substrate e.g. nitrogen or carbon source. For example, 21 mM of ammonium as final cell density limiting substrate and glucose as carbon source in a minimal medium result in approximately 4 g dry weight$\cdot$L^{-1} when growing *A. niger*. The same amount of biomass is obtained if 42 mM of glucose is made the final cell density limiting substrate with ammonium as nitrogen source. Most conventional stirred tank bioreactors at a stirring rate of 1000 rpm can supply 4 g dry weight$\cdot$L^{-1} of filamentous fungal biomass with sufficient oxygen. However, this again depends on the morphology of the fungi. If most of the mycelium consists of long scarcely branched filaments resulting in a high viscosity, the mixing intensity is probably too low to keep the suspension homogeneous and zones of low oxygen or even depletion will form. However, the response time of most oxygen electrodes is too slow to detect these (small) volume units with low oxygen when passing the electrode. A unit volume with 4 g dry weight$\cdot$L^{-1} is likely to be oxygen depleted when oxygen supply is lacking for 10 to 20 seconds. Furthermore, the oxygen electrode is usually placed close to the stirrer, where mixing intensity and mass transfer is high, to avoid clogging of the electrode membrane. Therefore, problems with zones of low or no oxygen are often undetected.

In most bioreactors significant wall growth occurs when culturing filamentous fungi. Wall growth is initiated by adhesion of spores or mycelium to surfaces and develops by further adhesion and/or growth. It can be argued that stationary wall growth, especially in the head space, might only have little influence on mycelium samples withdrawn from the bioreactor. However, the biomass concentration will be lower than expected and concentrations of substrates and products will probably be different compared to a culture without wall growth. The effect of these differences is difficult to determine and since wall growth is almost impossible to reproduce and often not stationary, it should be avoided. Even small amounts of wall growth can impair determination of kinetic and stoichiometric parameters [Prosser 1994; Topiwala and Hamer 1971]. Several methods have been applied to overcome this obstacle (Box 2). Larsen *et al.* [2004] were successful by designing a novel principle for aeration and mixing - the so-called Variomixing.

BOX 2. METHODS FOR PREVENTION OF WALL GROWTH

- Thorough cleaning of bioreactor immediately before use with very hot water and a soap that leaves no film on surfaces, e.g. Rosal Liquid (Rogier Bosman Chemie B.V., Heijningen, NL).
- Coating of surface with repellent compound, e.g. Teflon or silanization.
- Manual removal with sterile metal rods after removal of top plate [Withers *et al.* 1994] or with an inside magnet moved by an outside horse-shoe magnet [Metwally *et al.* 1991; Schrickx *et al.* 1993].
- Use of different stirring modes, e.g. temporarily increasing stirring rate [Withers *et al.* 1994; Swift *et al.* 1998] or Variomixing (Fig. b, [Larsen *et al.* 2004]).
- Low head-space volume [Linton *et al.* 1984; Wiebe and Trinci 1991].
- Cooling of head-space [Larsen *et al.* 2004].
- Minimization of head-space area and air-liquid interface by inserting probes, sensors, cooling fingers and ports below the liquid surface [Larsen *et al.* 2004].
- Prevention of static regions with low liquid velocities e.g. by aligning probes, sensors, cooling fingers and ports with the bioreactor wall [Larsen *et al.* 2004].
- Minimization of air flow at the beginning of culture to prevent blowing out of hydrophobic non-germinated spores [Poulsen *et al.* 2003].
- Use of certain growth conditions (e.g. low or high pH) [van der Aa *et al.* 2002; Dynesen and Nielsen 2003; Jones 1994] at which ″sticky″ compounds (e.g. hydrophobins) are either non-active or not induced.
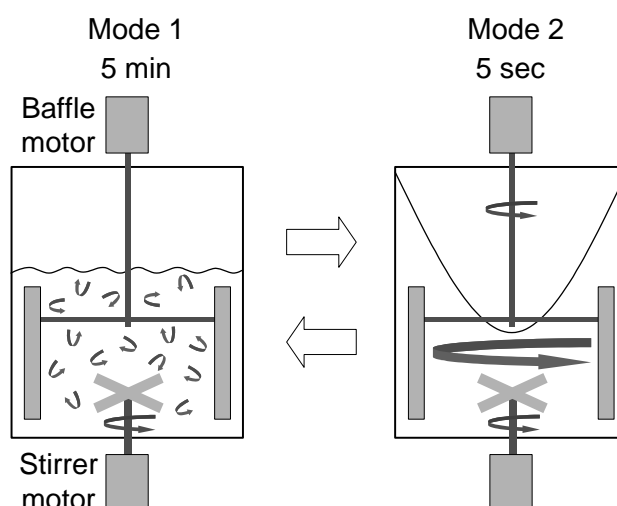- Engineering of strains to alter surface composition [Dynesen and Nielsen 2003]

Figure b. Stirring modes in Variomixing bioreactor. Mode 1 is traditionally used in conventionally stirred bioreactors, where effective mass transfer and mixing is obtained by static or very slow turning baffles as a resistance to the flow created by the stirrer, and the liquid flow is characterised by many small eddies in a turbulent flow regime. In Mode 2 baffles are turned shortly (5 sec) in the same direction as the stirrer, whereby the effect of the baffles is cancelled, a vortex is created with high circular flow rates at the reactor wall and deposits in head-space are flushed off. 5 min of Mode 1 and 5 sec of Mode 2 is automatically and continuously repeated.

References

Aa BC van der, Asther M, Dufrêne YF (2002) Surface properties of *Aspergillus oryzae* spores investigated by atomic force microscopy. Colloid Surface B: 24: 277-284.

Dynesen J, Nielsen J (2003) Surface hydrophobicity of *Aspergillus nidulans* conidiospores and its role in pellet formation. Biotechnol Prog 19: 1049-1052.

Jones EBG (1994) Fungal adhesion. Mycol Res 98: 961-981.

Larsen B, Eriksen NT, Poulsen BR, Iversen JJL (2004) Homogeneous batch cultures of *Aspergillus oryzae* by elimination of wall growth in the Variomixing bioreactor. Appl Microbiol Biotechnol 64: 192-198.

Linton JD, Austin RM, Haugh DE (1984) The kinetics and physiology of stipitatic acid and gluconate production by carbon sufficient cultures of *Penicillium stipitatum* growing in continuous culture. Biotechnol Bioeng 26: 1455-1464.

Metwally M, el Sayed M, Osman M, Hanegraaf PPF, Stouthamer AH, van Verseveld HW (1991) Bioenergetic consequences of glucoamylase production in carbon-limited chemostat cultures of *Aspergillus niger*. Antonie van Leeuwenhoek 59: 35-43.

Poulsen BR, Ruijter GJG, Visser J, Iversen JJL (2003) Determination of first order rate constants by natural logarithm of the slope plot exemplified by analysis of *Aspergillus niger* in batch culture. Biotechnol Lett 25: 565-571.

Schrickx JM, Krave AS, Verdoes JC, van den Hondel CAMJJ, Stouthamer AH, van Verseveld HW (1993) Growth and product formation in chemostat and recycling cultures by *Aspergillus niger* N402 and a glycoamylase overproducing transformant, provided with multiple copies of the glaA gene. J Gen Microbiol 139: 2801-2810.

Swift RJ, Wiebe MG, Robson GD, Trinci APJ (1998) Recombinant glucoamylase production by *Aspergillus niger* B1 in chemostat and pH auxostat cultures. Fungal Genet Biol 25: 100-109.

Wiebe MG, Trinci APJ (1991) Dilution rate as a determinant of mycelial morphology in continuous culture. Biotechnol Bioeng 38: 75-81.

Withers JM, Wiebe MG, Robson GD, Trinci APJ (1994) Development of morphological heterogeneity in glucose-limited chemostat cultures of *Aspergillus oryzae*. Mycol Res 98: 95-100.
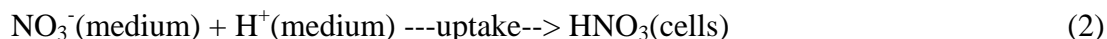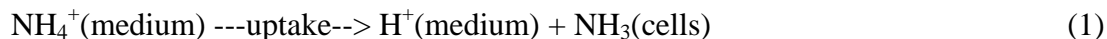
MEDIUM

As already mentioned it is necessary to limit the amount of biomass in the bioreactor by the final cell density limiting substrate to prevent overall oxygen limiting conditions. This is difficult with a complex medium because the final cell density limiting substrate is unknown and this is just one example of difficulties with using a complex medium in which the composition is not fully known. The most prominent problem is that the composition of different lots are never

completely the same and therefore cultures are not reproducible unless the same lot is used, which prevents others from repeating the experiments. Variations in medium components such as growth factors present in very low concentrations might have a large influence on the cultures. Therefore, a defined medium is required for reproducible cultures. Often a minimal medium is chosen because of simplicity in making and in interpretation of results.

However, for synchronous germination of spores of *A. niger* a low concentration of e.g. yeast extract is required. Of course, the concentration should be as low as possible. We found that 0.003% (mass/vol) yeast extract was the lowest concentration sufficient to support a synchronous germination of more than 95% of spores within 5-7 hours. Higher concentrations of yeast extract did not result in a faster or more synchronous germination, but in an alkanization of the medium, which in quantity and duration was correlated to the concentration of yeast extract. The alkalinization is probably caused by uptake of acids from the yeast extract. When using only 0.003% yeast extract a weak alkalinization was observed, restricted to the germination period. We did repeated batch experiments, in which the first batch culture was inoculated with spores and contained 0.003% yeast extract and the second batch culture was inoculated with 1/50 of vegetative cells from the first batch and was without yeast extract. Detailed characterization, including measurements of several intracellular and extracellular metabolites [Poulsen *et al.* 2004b] of the first and second batch culture showed no significant difference between the two. This is not surprising because as described above the consumption of the yeast extract was restricted to the germination period and therefore comparable in amount to endogenous substrates contained in the spores and because 4-5 generations of vegetative cells were grown before sampling. However, obviously we cannot exclude that the expression of certain genes was influenced by (trace amounts of) certain compounds in the yeast extract.

The performance of cultures of filamentous fungi is strongly influenced by pH. This influence includes induction (e.g. acidic proteases and acid production are induced at low and high pH, respectively) and morphology (e.g. pellet formation increases with pH). Especially in a culture without pH regulation, such as a shake flask, it is therefore important to know how pH changes upon metabolism of nutrients in the medium. This depends on the medium composition. As described above, pH increases upon metabolism of yeast extract, which is often used in concentrations as high as 0.5% (mass/vol). For such a high concentration we measured a pH increase lasting approximately 10 hours, where pH increased from 4 to 6 in a buffered (usually 1.5 g KH_2PO_4 per litre) minimal medium. After the consumption of yeast extract, further pH changes depend mainly on the nitrogen and carbon source and of course on production of acidic or alkaline compounds. The most frequently used nitrogen sources are ammonium and nitrate. It is important to note that the uptake of these has strong and opposite effects on pH. As shown in Equation 1, for every mole of ammonium taken up, one mole of protons is released and as shown in Equation 2, for every mole of nitrate taken up, one mole of protons is removed from the medium [Poulsen *et al.* 2004b]. These exchanges of protons with the medium have been used to follow growth very accurately [Christensen and Eriksen 2002; Eriksen *et al.* 2001; Hrdlicka *et al.* 2004; Iversen *et al.* 1994; Larsen *et al.* 2004; Poulsen *et al.* 2003 and 2004; Vicente *et al.* 1998] by measurement of added titrant to maintain constant pH. Carbon sources also have a strong influence on pH. E.g. when an *A. niger* wild type is grown on glucose, glucose oxidase is excreted into the medium and converts the glucose to gluconate resulting in a strong and fast

acidification of the medium. Generally, good carbon sources like glucose and fructose give a high acid production. The acid production is dependent on pH and the presence of the nitrogen source; high pH [Ruijter *et al.* 1999] and the absence of nitrogen source [Poulsen *et al.* 2003; 2004b and 2004c] induce acid production.

$$NH_4^+(medium) ---uptake--> H^+(medium) + NH_3(cells) \qquad\qquad (1)$$

$$NO_3^-(medium) + H^+(medium) ---uptake--> HNO_3(cells) \qquad\qquad (2)$$

INOCULUM

With most strains of filamentous fungi it is possible to use either spores or vegetative cells as an inoculum. Spores are preferred because a large number of growth units are easily obtained, they are easily stored and some genetic techniques are dependent on spore formation. It is possible to obtain spores of an aconidial (non-sporulating) strain using a (forced) heterokaryon, which is mycelium containing both the nucleus of the aconidial strain and another nucleus in which all its genes necessary for sporulation are functional. In addition both nuclei contain at least one gene essential for growth on minimal medium, that is not functional in the other [Van der Vondervoort *et al.* 2004]. When spores are formed from a heterokaryon they contain only one of the nuclei. Therefore, theoretically half of the spores from such a forced heterokaryon contain the nucleus of the aconidial strain.

However, spores have a tendency to agglomerate upon germination [Rohde *et al.* 2002; van der Aa *et al.* 2002] and in cultures with low stirring/shear stress such as shake flask cultures, pellets are formed and therefore an undesirable low number of growth units is obtained. The tendency of both spores and vegetative cells to agglomerate increases with pH up to around neutral pH and decreases again at alkaline conditions. This can be explained by the largely negatively charged surface of both spores and vegetative cells [Jones 1994]. At around neutral pH protons and cations form bridges between the cells, at low pH the negative charges on the cells are fully protonised preventing the bridging, and at high pH the concentration of free protons and cations are too low to allow for bridges. Therefore, to prevent pellet formation either a high or a low pH might be necessary dependent on the shear stress. Since most filamentous fungi grow poorly at high pH a low pH is preferred. Dynesen and Nielsen [2003] showed that pellet diameter increases linearly with pH above pH 4 in a shake flask, which is in line with the findings of free hyphae at pH below 3.5 and pellets at pH higher than 5 in a stirred bioreactor at 300-800 rpm [Carlsen *et al.* 1996b]. Our experience is that pellets become too large and diffusion-limited with oxygen in the centre at pH above 4.5 and a stirrer rate of 1200 rpm [Poulsen *et al.* 2004b]. At pH 3 and by direct spore inoculation in a stirred bioreactor with sufficient stirring/shear stress (down to 500 rpm) we were able to obtain non-agglomerated germinated spores and thereby mainly free hyphae [Poulsen *et al.* 2003; 2004b and 2004c]. Pellet formation is typically irreversible, but pellets can break up with high stirring rates and this tendency increases if pellets are loose, e.g. at low pH. At high pH pellets have a tendency to become very dense [Poulsen *et al.* 2004c]

especially when combined with a high stirring rate [Gomez *et al.* 1988]. Therefore using pellets as inoculum usually results in large pellets and an inoculum of vegetative cells must consist of free hyphae if pellets are to be prevented in the culture.

CULTURES

Most cultures are executed as batch cultures. They are characterised by always changing conditions. However, to monitor and control these changing conditions, we developed an exact method (Box 3 [Poulsen *et al.* 2003]) to determine the physiological state of the culture, e.g. exponential or stationary phase, which has a strong influence on the cells in almost every aspect. By analysing the amount of titrant added to maintain a constant pH with the Log of Slope (LOS) plot (Box 3 [Poulsen *et al.* 2003]) we were able to follow batch cultures accurately [Hrdlicka *et al.* 2004; Larsen *et al.* 2004; Poulsen *et al.* 2003; 2004b and 2004c] and thereby obtain samples reproducibly [Poulsen *et al.* 2004b]. One has to bear in mind that in a batch culture conditions are never constant. However, a pseudo-steady state may occur, in which growth is exponential and balanced, which means that all specific rates and intracellular concentrations are constant. At such a pseudo-steady state it is possible to obtain mycelial samples reproducibly for any purpose. However, concentrations of substrates decrease and concentrations of products increase during the batch culture. Therefore, mycelium samples are easier to reproduce than extracellular samples. One way to explain this, is that inside the cell metabolism results in growth – a new cell – and therefore the conditions in each cell, on average, stay constant; whereas outside the cell metabolism results in changing conditions. By making a LOS plot of on-line data it is easy to assess whether the fungi grow exponentially and presumably are in balanced growth (balanced growth in a batch culture of *A. niger* was confirmed by Poulsen *et al.* [2004c]). The exponential growth phase with sufficient biomass concentration for mycelium samples, obtained in a batch culture growing until 4 g dry weight per litre is usually 3-4 generations and therefore approximately 12 hours. This is a relatively long period to obtain mycelium samples from exponential growth phase and these samples are most likely independent of the lag phase. In contrast, extracellular concentrations change exponentially and they are dependent on the metabolism in the lag phase, which is usually the most difficult to reproduce. Therefore, several samples of the medium at different time points are necessary to evaluate the exchange or rate of exchange of metabolites with the medium. Of course it should be noted that the changing extracellular conditions may have an influence on the fungi e.g. on transcription levels, but it is possible to assess this by analysing mycelium samples from different time points.

In continuous cultures it is possible to obtain well-defined mycelium from steady states in which everything is constant except for culture age. It is therefore possible to measure the effect of changing only one single parameter and this is the major advantage of continuous cultures. Culture age is above all important because of genetic instability. Mutations may occur within a few hundred hours of continuous culturing [Mainwaring *et al.* 1999; Van der Vondervoort *et al.* 2004].

Pellet formation increases with dilution rate in a chemostat [Poulsen *et al.* 2004c;

Righelato *et al.* 1968]. At high dilution rates there is a tendency to form large pellets with a diffusion-limited centre, which does not grow exponentially and therefore wash-out occurs at a dilution rate much lower than predicted from the maximum specific growth rate obtained in batch cultures with only free hyphae [Poulsen *et al.* 2004c]. This is probably the reason why most results reported from continuous cultures with filamentous fungi are from dilution rates considerably lower than the theoretical critical dilution rate [Carlsen *et al.* 1996a; Christensen *et al.* 1995; Mainwaring *et al.* 1999; Metwally *et al.* 1991; Pedersen *et al.* 2000; Poulsen *et al.* 2004c; Van der Vondervoort *et al.* 2004]. It would only be possible to obtain high dilution rates if methods to prevent pellet formation are developed. Such methods could be 1) growth conditions, e.g. low pH or low oxygen, 2) addition of an anionic polymer (e.g. carbopol [Elmayergi and Scharer 1973]), 3) genetic modification of strains.

BOX 3. LOG OF SLOPE PLOT – EXPONENTIAL ANALYSIS TO FIND THE PHYSIOLOGICAL STATE

A log of slope plot or LOS plot is simply the natural logarithm of the slope plotted as a function of time. To find out why it is a good idea to do so we look at a general exponential function with an offset:

$$A(t) = A_0 \cdot \exp(\mu \cdot t) + \mathit{offset}$$

Where A could be a measure of growth, e.g. optical density, t is the time, μ is the rate constant, e.g. the specific growth rate, and *offset* is a background value. We differentiate to remove the offset and obtain the slope:

$$\mathrm{d}A/\mathrm{d}t = A_0 \cdot \mu \cdot \exp(\mu \cdot t)$$

We take the natural logarithm of the absolute value ($\log_e$[neg] is not possible) of the slope:

$$\log_e(\mathrm{abs}[\mathrm{d}A/\mathrm{d}t]) = \log_e(A_0 \cdot \mu) + \mu \cdot t$$

Whereby we can see that a plot of $\log_e(\mathrm{abs}[\mathrm{d}A/\mathrm{d}t])$ against time is a straight line if and only if growth is exponential and the slope of this plot is the rate constant, e.g. the specific growth rate. Most important feature of the LOS plot is identification of exponential intervals, which is very difficult with other analysis techniques - a fit of an exponential function to non-exponential interval data can easily give an apparent good fit, but erroneous rate constants [Poulsen *et al.* 2003]. The LOS plot has found widespread use in a variety of different applications [Hrdlicka *et al.* 2004; Larsen *et al.* 2004; Poulsen *et al.* 2004a and 2004b]. From data with much scatter the LOS plot becomes even more scattered because the slope of a curve is very sensitive to scatter and averaging data can be beneficial, However, even if the LOS plot is very scattered the final

result of the rate constant is usually accurate because the scatter evens-out when a linear regression is made. An example of LOS plot is shown in Figure c.
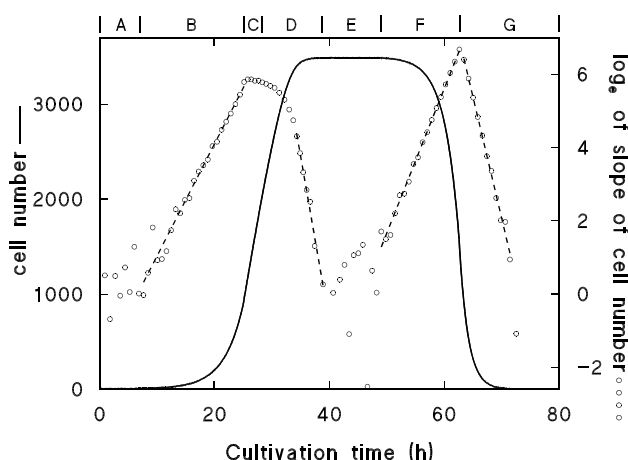

Figure c. Log_e of slope (LOS) plot of calculated cell number in culture with noise added to the data (± 5 cell number added randomly). A: Lag phase. B: Non-limited, exponential growth phase. C: Linear growth phase, e.g. as a result of limitation in oxygen transfer into medium. D: Decline phase following Monod kinetics because concentration of final cell density limiting substrate is in range of the Monod constant - becomes exponential when concentration of final cell density limiting substrate is much smaller than the Monod constant as expected from the Monod expression; LOS plot has a negative slope because slope of cell number decreases. E: Stationary phase. F: Death phase, LOS plot has a positive slope because the plot is the natural logarithm of the absolute value of the slope of cell number. G: Survival phase - metabolism on substrate from lysed cells prolongs the death phase. Dashed lines show linear regressions to rectilinear intervals of LOS plot i.e. exponential intervals of cell number.

References

Hrdlicka PJ, Poulsen BR, Sørensen AB, Ruijter GJG, Visser J, Iversen JJL (2004) Characterization of nerolidol biotransformation based on indirect on-line estimation of biomass concentration and physiological state in batch cultures of *Aspergillus niger*. Biotechnol Prog 20: 368-376.

Larsen B, Eriksen NT, Poulsen BR, Iversen JJL (2004) Homogeneous batch cultures of *Aspergillus oryzae* by elimination of wall growth in the Variomixing bioreactor. Appl Microbiol Biotechnol 64: 192-198.

Poulsen BR, Nøhr J, Douthwaite S, Hansen LV, Iversen JJL, Visser J, Ruijter GJG (2004a) Increased NADPH concentration obtained by metabolic engineering of the pentose phosphate pathway in *Aspergillus niger*. Eur J Biochem, submitted.

Poulsen BR, Ruijter GJG, Visser J, Iversen JJL (2003) Determination of first order rate constants by natural logarithm of the slope plot exemplified by analysis of *Aspergillus niger* in batch culture. Biotechnol Lett 25: 565-571.

Poulsen BR, Sørensen AB, Schuleit T, Ruijter GJG, Visser J, Iversen JJL (2004b) Quantitative description of biomass distribution in free hyphae, pellets and diffusion-limited pellet cores in submerged cultures of filamentous fungi. Appl Environ Microbiol, submitted.

SAMPLING

Accurate as well as frequent sampling can be crucial to obtain high quality and sufficient knowledge of submerged cultures. Again, the morphology of filamentous fungi makes it a challenge to obtain reproducible samples from these cultures. Filters, tubing and sampling ports are easily clogged by the mycelium, and these require special attention to their design. Often, commercially available equipment, such as sampling systems, developed for bacterial or yeast cultures are unsuited for cultures of filamentous fungi. Our experience is that tubings for transportation of mycelial suspensions must have an inner diameter of at least 5 mm. In one of our laboratories a rapid sampling port was developed [Iversen 1981], in which the culture is quenched within msec after leaving the conditions in the bioreactor. When modified with sharp edges and exchanging the rubber O-ring with a silicon gasket at the interface between culture suspension and ambient air the sampling port can be used for sampling from a continuous culture of filamentous fungi for several hundreds of hours [Van der Vondervoort *et al.* 2004]. Combined with a method for harvesting of mycelium and extraction of intermediary metabolites at -40°C [Ruijter and Visser 1996] developed in another of our laboratories, we have been able to obtain very reliable results for concentrations inside the cells [results to be published elsewhere]. In addition, a fast response filter module (Fig. 1 [Poulsen *et al.* 2004a]) was developed for sampling of culture filtrate, which was used in an automatic online sampling system. Thus detailed information could be obtained about extracellular nutrient and secreted metabolite concentrations in cultures with filamentous fungi.

STRAIN IMPROVEMENT

In fact, many of the problems mentioned above can probably be solved by or in combination with genetic modifications and we will probably see many such solutions in the future as the molecular mechanisms become elucidated. Classical genetics has been applied for many years in industry and has been successful in many cases (so far) without our precise understanding. However, more knowledge of the genetics involved will lead to better and more direct solutions. One example is strains lacking the kexin-like maturase. These strains have a compact, highly branched morphology [Jalving *et al.* 2000]. It is believed that such a strain will be beneficial in enzyme production because of the many hyphal tips, where protein production takes place, and because of a low viscosity suspension resulting from small compact pellets.
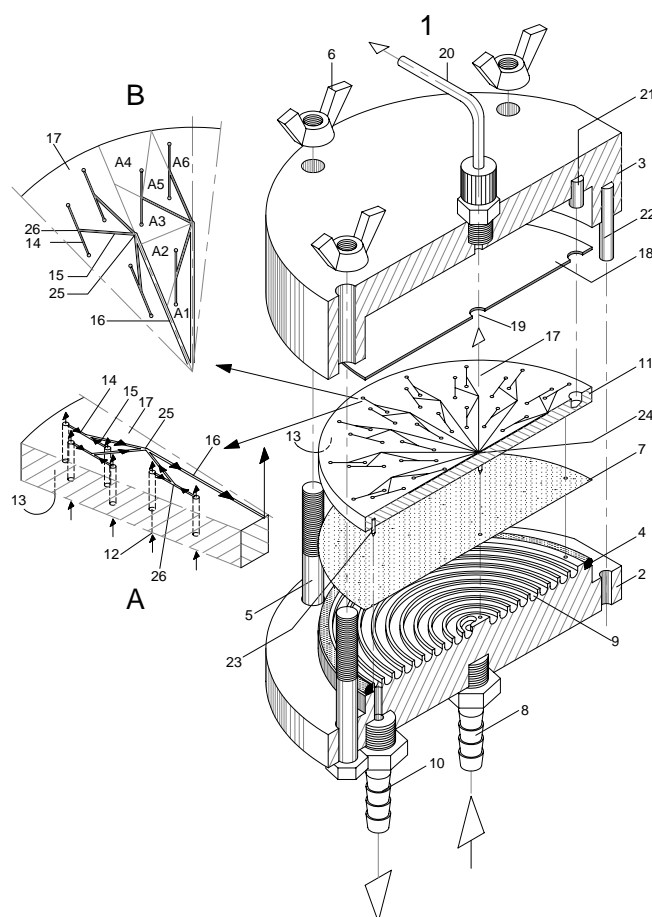
Figure 1. Cutted view of disassembled autoclavable fast response filter module (outer diameter 120 mm) with fluid collector, which ensures equal flow time from every location on the filter membrane to the outlet. Detail A shows cutted view with hidden lines of enlargement of part of the channel disc 11. Detail B shows top view of enlargement of part of the channel disc 11. Ultrafiltration membrane 7 (YM30 Diaflo, Amicon) form the interface between suspension and filtrate. Suspension flows into filter module 1 at suspension inlet 8, through semicircular spiral groove 9 (3 mm diameter) and out at suspension outlet 10. The lower surface of channel disc 11 is fluid inlet surface 13. In Detail A of channel disc 11 (PSU, 90.3×6 mm) it is shown how filtrate coming from the membrane 7 flows through inlets 12 in the fluid inlet surface 13. In the assembled filter module the filtrate further flows through channels formed by grooves 14, 15 and 16 (all channels at each branching level have the same length and cross sectional area) in the fluid outlet surface 17 (upper surface of channel disc 11) and rubber seal 18 (Viton, 90×0.5 mm) serving as covering means. At hole 19 in the rubber seal 18 the grooves 16 are uncovered, therefore the filtrate flows through the hole 19 and further to filter module outlet 20 in stainless steel part 3. Detail B of channel disc 11 is a top view to show that filtrate is collected via the inlets 12 from approximately the centre of mass of approximately equal areas (A1-A6). Assuming equal flux through the filter membrane areas, the channels ensure substantially equal flow time from each inlet 12 to outlet 20.

AKNOWLEDGEMENTS

REFERENCES

Aa BC van der, Asther M, Dufrêne YF (2002) Surface properties of *Aspergillus oryzae* spores investigated by atomic force microscopy. Colloid Surface B 24: 277-284.

Carlsen M, Nielsen J, Villadsen J (1996a) Growth and α-amylase production by *Aspergillus oryzae* during continuous cultivations. J Biotechol 45: 81-93.

Carlsen M, Spohr AB, Nielsen J, Villadsen J (1996b) Morphology and physiology of an α-amylase producing strain of *Aspergillus oryzae* during batch cultivations. Biotechnol Bioeng 49: 266-276.

Christensen LH, Henriksen CM, Nielsen J, Villadsen J, Egel-Mitani M (1995) Continuous cultivation of *Penicillium chrysogenum*. Growth on glucose and penicillin production. J Biotechnol 42: 95-107.

Christensen ML, Eriksen NT (2002) Growth and proton exchange in recombinant *Escherichia coli* BL21. Enzyme Microb Technol 31: 566-574.

Conesa A, Punt PJ, van Luijk N, van den Hondel CAMJJ (2001) The secretion pathway in filamentous fungi: A biotechnological view. Fung Gen Biol 33: 155-171.

Cui YQ, van der Lans RGJM, Luyben KCAM (1998) Effects of dissolved oxygen tension and mechanical forces on fungal morphology in submerged fermentation. Biotechnol Bioeng 57: 409-419.

Dynesen J, Nielsen J (2003) Surface hydrophobicity of *Aspergillus nidulans* conidiospores and its role in pellet formation. Biotechnol Prog 19: 1049-1052.

Elmayergi H, Scharer JM (1973) Physiological studies on *Aspergillus niger* fermentation with polymer additive. J Gen Appl Microbiol 19: 385-392.

Eriksen NT, Kratchmarova I, Neve S, Kristiansen K, Iversen JJL (2001) Automatic inducer addition and harvesting of recombinant *Escherichia coli* cultures based on indirect on-line estimation of biomass concentration and specific growth rate. Biotechnol Bioeng 75: 355-361.

Gomez R, Schnabel I, Garrido J (1988) Pellet growth and citric acid yield of *Aspergillus niger* 110. Enzyme Microb Technol 10: 188-191.

Hrdlicka PJ, Poulsen BR, Sørensen AB, Ruijter GJG, Visser J, Iversen JJL (2004) Characterization of nerolidol biotransformation based on indirect on-line estimation of biomass concentration and physiological state in batch cultures of *Aspergillus niger*. Biotechnol Prog 20: 368-376.

Iversen JJL (1981) A rapid sampling valve with minimal dead space for laboratory scale fermenters. Biotechnol Bioeng 23: 437-440.

Iversen JJL, Thomsen JK, Cox RP (1994) On-line growth measurements in bioreactors by titrating metabolic proton exchange. Appl Microbiol Biotechnol 42: 256-262.

Jalving R, van de Vondervoort PJ, Visser J, Schaap PJ. (2000) Characterization of the kexin-like maturase of Aspergillus niger. Appl Environ Microbiol 66: 363-368.

Jones EBG (1994) Fungal adhesion. Mycol Res 98: 961-981.

Larsen B, Eriksen NT, Poulsen BR, Iversen JJL (2004) Homogeneous batch cultures of *Aspergillus oryzae* by elimination of wall growth in the Variomixing bioreactor. Appl Microbiol Biotechnol 64: 192-198.

Mainwaring DO, Wiebe MG, Robson GD, Goldrick M, Jeenes DJ, Archer DB, Trinci APJ (1999) Effect of pH on hen egg white lysozyme production and evolution of a recombinant strain of *Aspergillus niger*. J Biotechnol 75: 1-10.

Metwally M, el Sayed M, Osman M, Hanegraaf PPF, Stouthamer AH, van Verseveld HW (1991) Bioenergetic consequences of glucoamylase production in carbon-limited chemostat cultures of *Aspergillus niger*. Antonie van Leeuwenhoek 59: 35-43.

Oostra J, le Comte EP, van den Heuvel JC, Tramper J, Rinzema A (2001) Intra-particle oxygen diffusion limitation in solid-state fermentation. Biotechnol Bioeng 74: 13-24.

Pazouki M, Panda T (2000) Understanding the morphology of fungi. Bioproc Eng 22: 127-143.

Poulsen BR, Iversen JJL, Ruijter GJG, Visser J (2004a) Fast response filter module with plug flow of filtrate for on-line sampling from submerged cultures of filamentous fungi. Anal Chim Acta 510: 203-212.

Poulsen BR, Nøhr J, Douthwaite S, Hansen LV, Iversen JJL, Visser J, Ruijter GJG (2004b) Increased NADPH concentration obtained by metabolic engineering of the pentose phosphate pathway in *Aspergillus niger*. Eur J Biochem, submitted.

Poulsen BR, Ruijter GJG, Visser J, Iversen JJL (2003) Determination of first order rate constants by natural logarithm of the slope plot exemplified by analysis of *Aspergillus niger* in batch culture. Biotechnol Lett 25: 565-571.

Poulsen BR, Sørensen AB, Schuleit T, Ruijter GJG, Visser J, Iversen JJL (2004c) Quantitative description of biomass distribution in free hyphae, pellets and diffusion-limited pellet cores in submerged cultures of filamentous fungi. Appl Environ Microbiol, submitted.

Prosser JI (1994) Kinetics of filamentous growth and branching. In: Gow AR, Gadd GM (eds) The growing fungus. Chapman and Hall, pp 301-335.

Righelato RC, Trinci APJ, Pirt SJ (1968) The influence of maintenance energy and growth rate on the metabolic activity, morphology and conidiation of *Penicillium chrysogenum*. J Gen Microbiol 50: 399-412.

Rohde M, Schwienbacher M, Nikolaus T, Heeseman J, Ebel F (2002) Detection of early phase specific surface appendages during germination of *Aspergillus fumigatus* conidia. FEMS Microbiol Lett 206: 99-105.

Ruijter GJG, van de Vondervoort PJI, Visser J (1999) Oxalic acid accumulation by *Aspergillus niger*. An oxalate non-producing mutant accumulates citric acid at pH 5 and in the presence of manganese. Microbiology 145: 2569-2576.

Ruijter GJG, Visser J (1996) Determination of intermediary metabolites in *Aspergillus niger*. J Microbiol Meth 25: 295-302.

Topiwala HH, Hamer G (1971) Effect of wall growth in steady-state continuous culture. Biotechnol Bioeng 13: 919-922.

Treskatis SK, Orgeldinger V, Wolf H, Gilles ED (1997) Morphological Characterisation of filamentous microorganisms in submerged cultures by on-line digital image analysis and pattern recognition. Biotechnol Bioeng 53: 191-201.

Trinci APJ (1970) Kinetics of the growth of mycelial pellets of *Aspergillus niger*. Arch Mikrobiol 73:353-367.

vanKuyk, PA, Diderich J, MacCabe AP, Hererro O,. Ruiter GJG, Visser J (2004) *Aspergillus niger mst*A encodes a sugar: H+ symporter which is regulated in response to extracellular

pH. Biochem J 379:375-383.

Vicente A, Castrillo JI, Teixeira JA, Ugalde U (1998) On-line estimation of biomass through pH control analysis in aerobic yeast fermentation systems. Biotechnol Bioeng 58: 445-450.

Vondervoort van de PJI, Poulsen BR, Ruijter GJG, Schuleit T, Visser J, Iversen JJL (2004) Isolation of a fluffy mutant of *Aspergillus niger* from a chemostat culture and its potential as a morphological stable host for protein production. Biotechnol Bioeng 86: 301-307.

Summary

Filamentous fungi are used by the industry for making a variety of products, e.g. penicillin, high-protein food, washing powder and soft drinks. Synthesis of many of these products requires reducing equivalents in the form of NADPH, which is a potential limiting factor. The pentose phosphate pathway (PPP) is believed to be the major source of NADPH. Our main goal has been to make strains of *Aspergillus niger* with increased NADPH availability and/or increased flux through the PPP by overexpression of enzymes in this pathway. Cloning of genes encoding for these enzymes enabled transformation to obtain multicopy transformants. To measure the effect(s) of overexpression, comparison with wild type in well-defined cultures is necessary. A bioreactor was designed especially for cultures of filamentous fungi and techniques were developed for automatic sampling of culture filtrate, rate analysis of culture data, morphology profiling and continuous culturing. NADPH availability was increased in multicopy transformants of the gene encoding for 6-phosphogluconate dehydrogenase.

For comparison of data or samples from different cultures it is important to monitor the status of the culture. We have been successful in recording and analyzing titrant addition on-line; this gives very detailed information with a high resolution and almost every biological or even chemical process requires titration units to maintain conditions (Chapters 2, 3, 4, 6 and 8).

In Chapter 2 we describe a method, which is useful in analysis of among others, titrant data and we applied this method in Chapters 3, 4, 6 and 8. The natural logarithm of the slope (LOS) plot enables identification of (1) data intervals that develop exponentially, (2) the rate constant (e.g. the growth rate) and (3) small and/or sudden changes in the rate constant. The identification requires no assumption about or pretreatment of the data and is furthermore independent of data intervals before and after the exponential intervals. Often erroneous rate constants are derived from experimental data, because the offset or non-exponential intervals contained in experimental data is not found by a plot on semi-log paper or a plot of the natural logarithm. These traditional plots give apparently good results, but the offset has a large influence on the (erroneous) rate constant or doubling time derived from them (e.g. see Figure 1 of Chapter 2). The error arises because it is impossible to know in advance which part of the data is a real exponential interval. The LOS plot solves this problem adequately by showing an exponential interval as a straight line and the rate constant as the slope.

Wall growth (the adhesion of cells to and growth on surfaces) is particularly a problem in cultures of filamentous fungi. The adhesion and the metabolism of attached cells can obstruct the interpretation of the culture (e.g. yields, kinetics, induction) and cause in-homogeneity. In the bioreactor described in Chapter 3 wall growth was kept to a minimum (2%) compared to the wall growth obtained when the same culturing was done in a conventional laboratory-scale bioreactor (30%). This was achieved by computer-controlled rotation of the baffles at a similar speed and direction as the impeller for 5 sec every 5 min, which resulted in a temporary cancellation of the effect of the baffles and a deep vortex and high peripheral liquid flow rates at the reactor wall then developed. The vortex ensures that the headspace of the reactor wall is flushed and any

deposits are removed. During the rest of the time baffles were rotating slowly (5-10 rpm for 5 min) and the highly turbulent flow regime characteristic of conventional bioreactors with high mixing and mass transfer capacities was developed. We named this principle "Variomixing".

It is well known that the morphology of filamentous fungi has a strong influence on culture performance. In case of pellets, we found that the amount of mycelium in the pellet core limited by diffusion of substrate from the medium into the core is the main factor determining growth and production rate (Chapter 4). This was investigated with the method described in Chapter 2 in combination with another novel finding, i.e. that the biomass content of a pelletous culture could be measured by optical density when sonicated. Furthermore, image analysis was used and we determined the pellet core biomass concentration (25 kg dry weight biomass per m^{-3} pellet in pH 6-batch culture) and the critical core diameter (0.19 mm in pH 6-batch culture) defined as the largest pellet core diameter without diffusion limitation of substrate. We made a segregated model of the pellet, comprising a hairy region and a core. By fitting this model to the apparent core biomass density as a function of core diameter, we found the core biomass density independent of the diameter. These findings enabled us to develop a "Macro-morphology Profiling System" (MPS), which describes the amount of biomass in different morphological classes: free hyphae, pellets with core diameters smaller or larger than the critical core diameter, and in diffusion-limited biomass inside pellet cores larger than the critical core diameter. MPS has the advantage that it can be used with manual image analysis and therefore no sophisticated equipment is required. To obtain well-defined biomass we did chemostat cultures in the Variomixing bioreactor described in Chapter 3. MPS was used in batch, washout and chemostat cultures. Pellet formation resulted in significant amounts of diffusion-limited biomass, which explained why the apparent critical dilution rate causing washout (0.23 h^{-1}) was lower than the maximum specific growth rate (0.29 h^{-1}) observed in batch cultures with free hyphae only.

Most of the extracellular processes in a submerged microbial culture have a characteristic time of 30 min or more. However, upon exhaustion of substrates or addition of compounds influencing physiology, changes in extracellular concentrations might have a characteristic time in the order of minutes. Automatic and accurate sampling is both convenient and sometimes necessary to obtain detailed information about cell cultures, but conventional filter units were found to have a response time around 15 min. Therefore a new principle for collection of a filtrate from a suspension with a fast response time was invented (Chapter 5). A response time of around 1 min for sampling of 1 $mL \cdot min^{-1}$ was obtained, which we found sufficient to monitor even glucose pulse experiments. The low response time was obtained by avoiding backmixing of the filtrate – the fitrate was flowing with equal flow time from every location on the filter to the collecting point. The equal flow time was obtained by using a construction of channels. Constant pressure difference across the membrane filter and prevention of leakage was obtained by squeezing the tubing with culture broth between two flexible spring steel plates fixed at one corner. With this automatic on-line sampling system, we were able to obtain detailed monitoring of fast transients of substrates and products in cultures of filamentous fungi for more than 5 days.

Many biotransformations are hydroxylations catalyzed by monooxygenases, which require reducing equivalents in the form of NADPH. A strain with increased availability of NADPH potentially has an increased biotransformation rate. For later comparison of biotransformation by wild type with strains having increased availability of NADPH we

characterized the wild type biotransformation of nerolidol to hydroxy-nerolidol (Chapter 6). 12-hydroxy-*trans*-nerolidol is a precursor in the synthesis of the industrially interesting flavor α-sinensal. We used the method described in Chapter 2 to monitor the physiological state of the fungus at addition of biotransformation substrate. The physiological state was shown to be of major importance for the product yield. The maximal molar yield of 12-hydroxy-*trans*-nerolidol (9%) was obtained by addition of a (±)-*cis*/*trans*-nerolidol mixture to the culture in the post-exponential phase at high dissolved oxygen tension in minimal and rich medium, but for the latter the rate of biotransformation was doubled.

In the chemostat cultures described in Chapter 4 the duration was often limited by the appearance of spontaneous morphological mutants (Chapter 7), which is a common problem in chemostat cultures of filamentous fungi. After the appearance of mutants cultures are usually stopped, because effects of these mutations are unknown. We attempted to optimize the morphological stability using different conditions. Longer culture times before appearance of the first morphological mutant were obtained in glucose-limited cultures (240 h) than in ammonium-limited cultures (110 h). Most of the mutants were aconidial (fluffy), dominant and appeared stable in the chemostat culture for up to 600 hours, which gave us the idea to use this mutant as inoculum for the chemostat. However, this was difficult because this strain only produces very little spores. Therefore, a reproducible inoculum was obtained by producing spores in a forced heterokaryon - a cell with both the nucleus of the aconidial strain and a nucleus of a sporulating strain. Furthermore, it was shown that the fluffy mutant could be transformed with usual techniques.

Since many biosyntheses and bioconversions are limited by low availability of intracellular NADPH we aimed to increase it. The PPP is believed to be the major source of NADPH in most cells. Therefore, our strategy was to increase the flux through this pathway. We overexpressed three enzymes in the pathway, i.e., glucose 6-phosphate dehydrogenase, 6-phosphogluconate dehydrogenase and transketolase (Chapter 8). To make a strain in which all glycolytic flux from glucose 6-phosphate is forced through the PPP we attempted to disrupt the gene encoding for phosphoglucose isomerase, which was not successful. Overexpressions of all three genes resulted in significant changes in concentrations of intracellular metabolites. Overexpression of 6-phosphogluconate dehydrogenase and transketolase also resulted in changes in concentrations of extracellular metabolites. None of the modified strains had an altered growth rate, which indicates that *A. niger* has a relatively robust primary metabolism. Only overexpression of 6-phosphogluconate dehydrogenase increased the intracellular concentration of NADPH (2-9 fold, depending on conditions). Partial least square regressions showed the correlations between NADPH and up to 40 other variables and that it is possible to predict the intracellular NADPH concentration from relatively easy obtainable data.

Concluding remarks

We succeeded to reach our main goal: to increase the availability of NADPH in *A. niger*. This was obtained by overexpression of 6-phosphogluconate dehydrogenase, but also overexpression of glucose 6-phosphate dehydrogenase and transketolase showed interesting effects and a combination of these overexpressions might result in even higher availability of NADPH and/or flux through the PPP. It has been confirmed by NMR studies that the flux through the PPP is increased in the 6-phosphogluconate dehydrogenase overexpressing strain [Hesse SJA, Dijkema C, de Graaf AA, Ruijter GJG, Visser J, unpublished results].

Many tools for characterization of strains of filamentous fungi were developed in this study. We believe that the tools supplement each other well and different combinations can be very beneficial in characterization of strains as well as in production.

Samenvatting

Filamenteuze schimmels worden door de industrie gebruikt voor het produceren van een grote verscheidenheid aan producten, zoals bijvoorbeeld penicilline, eiwitrijk voedsel, waspoeder en frisdrank. Voor de synthese van veel van deze producten zijn reductie equivalenten in de vorm van NADPH nodig, wat mogelijk een limiterende factor kan zijn. Ons hoofddoel was om *Aspergillus niger* stammen te maken met een verhoogde NADPH productie en/of een verhoogde flux door de pentose fosfaat route (PPP) door de overexpressie van de enzymen in deze route. Het kloneren van de genen die coderen voor deze enzymen maakte het mogelijk om door transformaties multicopy transformanten te construeren. Om de effecten van de overexpressie te meten was vergelijking nodig met het wild type in goed gedefinieerde kweken. Hiertoe werd een bioreactor ontworpen speciaal voor het kweken van filamenteuze schimmels en werden technieken ontwikkeld voor automatische bemonstering van het kweekfiltraat, analyse van de kinetiek van kweekgegevens, macroscopische beschrijving van schimmelmorfologie en continue kweken. NADPH concentratie was verhoogd in 6-fosfogluconaat dehydrogenase multicopy transformanten .

Voor de vergelijking van gegevens of monsters van verschillende kweken is het belangrijk om de status van de kweek te volgen. Wij hebben dit goed kunnen doen d.m.v. on line registratie en analyse van titrant toevoeging. Dit geeft zeer gedetailleerde informatie met een hoge resolutie en in bijna elk biologisch of zelfs chemisch proces is titratie nodig om de condities te handhaven. (Hoofdstukken 2, 3, 4, 6 en 8).

In Hoofdstuk 2 beschrijven we een methode die nuttig is voor de analyse van o.a. titratie gegevens en we hebben deze methode toegepast in de Hoofdstukken 3, 4, 6 en 8. De plot van de natuurlijke logaritme van de helling ("Log Of Slope"; LOS) maakt het mogelijk om 1) data intervallen die exponentieel verlopen, 2) de snelheidsconstante daarvan (b.v. groeisnelheid) en 3) kleine of plotselinge veranderingen in deze snelheidsconstante te identificeren. Het identificeren van snelheidsconstanten m.b.v. de LOS plot behoeft geen aannames over of voorbehandeling van de meetgegevens en is verder onafhankelijk van de gegevens voor en na de exponentiële intervallen. Vaak worden onjuiste snelheidsconstanten verkregen uit experimentele data, omdat het begin (de offset) of niet-exponentiële intervallen in meetgegevens niet worden gevonden bij het plotten op semi-log papier of door een plot van de natuurlijke logaritme. Deze conventionele plots lijken vaak goede resultaten te geven, maar de offset heeft een grote invloed op de (onjuiste) snelheidsconstante of verdubbelingtijd (b.v. zie Figuur 1 van Hoofdstuk 2). De fout ontstaat doordat het onmogelijk is om bij voorbaat te weten welk gedeelte van de data werkelijk een exponentieel interval is. De LOS plot lost dit probleem adequaat op door het exponentiële interval als een rechte lijn te laten zien en de snelheidsconstante als de helling.

Wandgroei (de hechting van cellen aan en de groei op oppervlaktes) is vooral een probleem in kweken met filamenteuze schimmels. De adhesie en het metabolisme van de aangehechte cellen kan heterogeniteit veroorzaken en de interpretatie van de kweek (b.v. groeiopbrengst, kinetiek en fysiologie) bemoeilijken. In de bioreactor die beschreven wordt in

Hoofdstuk 3 was de wandgroei tot een minimum beperkt (2%) in vergelijking met wandgroei verkregen in eenzelfde kweek die was uitgevoerd in een conventionele laboratorium-schaal bioreactor (30%). Dit werd gerealiseerd door computergecontroleerde rotatie van de baffles met gelijke snelheid en richting als de impeller gedurende 5 sec éénmaal per 5 minuten, wat resulteerde in tijdelijke opheffing van het effect van de baffles waarbij een sterke vortex en een hoge vloeistofstroomsnelheid bij de wand van de reactor werd verkregen. De vortex zorgt ervoor dat eventuele afzettingen op de wand in de kopruimte van de reactor worden weggespoeld. Gedurende de rest van de tijd roteerden de baffles langzaam (5-10 rpm gedurende 5 min) en werd het hoog-turbulente mengregime, karakteristiek voor conventionele bioreactoren, met hoge roersnelheid en massa-overdrachtscapaciteit ontwikkeld. We hebben dit principe "Variomixing" genoemd.

Het is bekend dat de morfologie van filamenteuze schimmels een sterke invloed heeft op het resultaat van een kweek. Voor pellets vonden we dat de hoeveelheid mycelium in de kern van de pellet, dat gelimiteerd wordt door diffusie van substraat vanuit het medium naar de kern de belangrijkste factor hiervoor is (Hoofdstuk 4). Dit is onderzocht met de methode die beschreven staat in Hoofdstuk 2, in combinatie met een andere nieuwe vinding, n.l. dat de biomassa inhoud van een kweek van pellets kon worden gemeten met behulp van optische dichtheid na sonicatie. Verder werd beeld analyse gebruikt en hebben we de biomassa concentratie in de pelletkern (25 kg per m^3 pellet in pH 6 batch kweek) bepaald en de "kritische kern diameter" (0.19 mm in pH 6 batch kweek), gedefinieerd als de grootste pelletkern diameter zonder diffusie limitatie gemeten. We construeerden een model van de pellet waarin een perifere "harige" regio en een kern werden beschreven. Door dit model te fitten met de gemeten kern biomassa dichtheid als een functie van de kern diameter vonden we dat de biomassa dichtheid onafhankelijk was van de diameter. Deze bevindingen maakten het mogelijk om een "Macro-morfologie Profilering Systeem" (MPS) te ontwikkelen, welke de hoeveelheid biomassa beschrijft in verschillende morfologische klassen: losse hyfen, pellets met kern diameter kleiner of groter dan de kritische kern diameter, en diffusie-gelimiteerde biomassa in pellets waarvan de kern groter is dan de kritische kern diameter. MPS heeft het voordeel dat het kan worden gebruikt met handmatige beeldanalyse, zodat er geen verfijnde apparatuur nodig is. Om goed gedefinieerde biomassa te krijgen voerden we chemostaat kweken uit in de Variomixing bioreactor, beschreven in Hoofdstuk 3. MPS werd gebruikt in zowel batch, washout en chemostaat kweken. Pelletvorming resulteerde in significante hoeveelheden diffusie-gelimiteerde biomassa, hetgeen verklaarde waarom de schrijnbare kritische verdunningssnelheid die washout veroorzaakte, lager was dan de maximale specifieke groeisnelheid (0.29 h^{-1}) waargenomen in batch kweken met alleen vrije hyfen.

De meeste van de extracellulaire processen in een microbiële kweek in vloeistof hebben een karakteristieke tijd van een half uur of langer. Echter, bij uitputting van substraten of toevoeging van componenten die de fysiologie beïnvloeden kunnen veranderingen in extracellulaire concentraties een karakteristieke tijd hebben in de orde van minuten. Automatische en accurate monstername is zowel makkelijk als soms noodzakelijk om gedetailleerde informatie over celkweken te verkrijgen. Conventionele filtereenheden bleken echter een respons tijd van ongeveer 15 minuten te hebben. Daarom werd een nieuw principe voor het verkrijgen van filtraat uit een suspensie met een snelle respons tijd ontwikkeld (Hoofdstuk 5). Een respons tijd van

ongeveer 1 minuut voor monstername van 1 mL·min^{-1} werd gehaald, welke voldoende werd bevonden om zelfs glucose puls experimenten te volgen. De lage respons tijd werd gehaald door menging van het filtraat te vermijden – het filtraat stroomde even snel vanaf elke locatie van het filter naar het verzamelpunt. De gelijkmatige uitstroomtijd werd verkregen door de constructie van een groot aantal kanaaltjes. Een constant drukverschill over het membraanfilter en het voorkomen van lekkage werd gerealiseerd door het platknijpen van de slang met kweekvloeistof tussen twee veerkrachtige stalen plaatjes die aan één hoek verbonden waren. Met dit automatische monstername systeem was het mogelijk om in kweken van filamenteuze schimmels, gedurende minstens 5 dagen, gedetailleerde informatieover snelle veranderingen in de concentraties van substraten en producten te verkrijgen.

Veel biotransformaties zijn hydroxylatie reacties gekatalyseerd door monooxygenases die reductie equivalenten nodig hebben in de vorm van NADPH. Een stam met verhoogde beschikbaarheid van NADPH heeft mogelijk een verhoogde biotransformatie capaciteit. Om later biotransformatie door het wild type enerzijds en stammen met verhoogde beschikbaarheid van NADPH anderzijds te kunnen vergelijken, karakteriseerden we biotransformatie van nerolidol tot hydroxy-nerolidol door wild type *A. niger* (Hoofdstuk 6). 12-hydroxy-*trans*-nerolidol is een uitgangsverbinding in de synthese van de, voor de industrie interessante, smaakstof α-sinensal. We gebruikten de methode beschreven in Hoofdstuk 2 om de fysiologische toestand van de schimmel tijdens toevoeging van het biotransformatie substraat te bepalen. Er werd aangetoond dat de fysiologische toestand van groot belang was voor de product opbrengst. De maximale molaire opbrengst van 12-hydroxy-*trans*-nerolidol (9%) werd verkregen door toevoeging van een (±)-*cis/trans*-nerolidol mengsel aan de kweek in de post-exponentiële fase bij hoge zuurstofspanning in minimaal en rijk medium, maar voor de laatstgenoemde was de biotransformatiesnelheid verdubbeld t.o.v. minimaal medium.

In de chemostaat kweken, beschreven in Hoofdstuk 4, was de duur van de kweek vaak gelimiteerd door het ontstaan van spontane morfologische mutanten (Hoofdstuk 7), hetgeen een algemeen probleem is in chemostaat kweken van filamenteuze schimmels. Na het ontstaan van mutanten worden kweken normaliter gestopt, omdat de eigenschappen van deze mutanten niet bekend zijn. We hebben geprobeerd om de morfologische stabiliteit van de uitgangsstam te optimaliseren door verschillende kweekcondities te gebruiken. Langere kweektijden voordat de eerste morfologische mutant verscheen waren mogelijk in glucose gelimiteerde kweken (240 u) t.o.v. ammonium- gelimiteerde kweken (110 u). De meeste van de mutanten waren aconidiaal (pluizig) en dominant, en bleken stabiel in de chemostaat kweek tot 600 uur, wat ons het idee gaf dat om deze mutant te gebruiken als entmateriaal voor de chemostaat. Echter, dit was lastig omdat deze stam slechts erg kleine hoeveelheden sporen produceerde. Daarom werd reproduceerbaar entmateriaal gemaakt door sporen te produceren met een stam die in elke cel zowel de kern van de aconidiale stam als de kern van een sporenvormende stam heeft: een geforceerd heterokaryon. Bovendien werd aangetoond dat de pluizige mutant kon worden getransformeerd met normale technieken.

Aangezien vele biosyntheses en biotransformaties zijn gelimiteerd door de lage beschikbaarheid van intracellulair NADPH hebben wij geprobeerd deze te verhogen. Van de PPP wordt gedacht dat dit de belangrijkste bron is van NADPH in de meeste cellen. Daarom was onze

strategie het verhogen van de flux door deze route. We brachten een aantal enzymen van deze route tot overexpressie, namelijk de enzymen glucose 6-fosfaat dehydrogenase, 6-fosfogluconaat dehydrogenase en transketolase (Hoofdstuk 8). Door te proberen het gen dat codeert voor fosfogluconase isomerase te inactiveren wilden we een stam maken in welke al het glucose 6-fosfaat wordt gedwongen de PPP te nemen, maar waren hierin niet succesvol. Overexpressie van glucose 6-fosfaat dehydrogenase, 6-fosfogluconaat dehydrogenase en transketolase resulteerden allemaal in significante veranderingen in de concentraties van intracellulaire metabolieten. Overexpressie van 6-fosfogluconaat dehydrogenase en transketolase resulteerde ook in veranderingen in concentraties van extracellulaire metabolieten. Geen van de gemodificeerde stammen had een veranderde groeisnelheid, wat erop duidde dat *A. niger* een relatief robuust primair metabolisme heeft. Alleen de overexpressie van 6-fosfogluconaat dehydrogenase verhoogde de intracellulaire concentratie van NADPH (2- tot 9-voudig, afhankelijk van de condities). 'Partial least square' regressies toonden de correlaties tussen NADPH en tot 40 andere variabelen en toonden aan dat het mogelijk is om de intracellulaire NADPH concentratie te voorspellen uit relatief eenvoudige gegevens.

Concluderende opmerkingen

We zijn succesvol geweest in het bereiken van ons hoofddoel, namelijk het verhogen van de beschikbaarheid van NADPH in *A. niger*. Dit werd bereikt door de overexpressie van 6-fosfogluconaat dehydrogenase, maar ook overexpressie van glucose 6-fosfaat dehydrogenase en transketolase gaven interessante resultaten en gecombineerde overexpressie van deze enzymen zou kunnen resulteren in nog hogere beschikbaarheid van NADPH en/of verhoogde flux door de PPP. Door NMR studies is vastgesteld dat de flux door de PPP is verhoogd in de stam met overexpressie van 6-fosfogluconaat dehydrogenase [Hesse SJA, Dijkema C, de Graaf AA, Ruijter GJG, Visser J, ongepubliceerde resultaten]

Vele methoden voor de karakterisering van stammen van filamenteuze schimmels zijn ontwikkeld tijdens deze studie. We zijn van mening dat deze methoden elkaar goed aanvullen en dat verschillende combinaties van de ontwikkelde technieken erg nuttig kunnen zijn in zowel de karakterisering van stammen als in productieprocessen.

List of publications and patents

Iversen JJL, Poulsen BR (1993) Airlift bioreactor. Declared ready for Patent pending, DTI-Innovation reference no.: S-53005, The Danish Patent Agency reference no. S-3227-93.

Poulsen BR, Iversen JJL (1997) Mixing determinations in reactor vessels using linear buffers. Chem Eng Sci 52: 979-984.

Poulsen BR, Iversen JJL (1998) Characterization of gas transfer and mixing in a bubble column equipped with a rubber membrane diffuser. Biotechnol Bioeng 58: 633-641.

Eriksen NT, Poulsen BR, Iversen JJL (1998) Dual sparging laboratory-scale photobioreactor for continuous production of microalgae. J Appl Phycol 10: 377-382.

Poulsen BR, Iversen JJL (1999) Membrane sparger in bubble column, airlift and combined membrane - ring sparger bioreactors. Biotechnol Bioeng 64: 452-458.

Poulsen BR, Ruijter GJG, Visser J, Iversen JJL (2003) Determination of first order rate constants by natural logarithm of the slope plot exemplified by analysis of *Aspergillus niger* in batch culture. Biotechnol Lett 25: 565-571.

Larsen B, Eriksen NT, Poulsen BR, Iversen JJL (2004) Homogeneous batch cultures of *Aspergillus oryzae* by elimination of wall growth in the Variomixing bioreactor. Appl Microbiol Biotechnol 64: 192-198.

Hrdlicka PJ, Poulsen BR, Sørensen AB, Ruijter GJG, Visser J, Iversen JJL (2004) Characterization of nerolidol biotransformation based on indirect on-line estimation of biomass concentration and physiological state in batch cultures of *Aspergillus niger*. Biotechnol Prog 20: 368-376.

Vondervoort PJI van de, Poulsen BR, Ruijter GJG, Schuleit T, Visser J, Iversen JJL (2004) Isolation of a fluffy mutant of *Aspergillus niger* from a chemostat culture and its potential as a morphological stable host for protein production. Biotechnol Bioeng 86: 301-307.

Poulsen BR, Sørensen AB, Schuleit T, Ruijter GJG, Visser J, Iversen JJL (2005) Quantitative description of biomass distribution in free hyphae, pellets and diffusion-limited pellet cores in submerged cultures of filamentous fungi. Biotechnol Prog, in prep.

Poulsen BR, Iversen JJL, Ruijter GJG, Visser J (2004) Fast response filter module with plug flow of filtrate for on-line sampling from submerged cultures of filamentous fungi. Anal Chim Acta 510: 203-212.

Poulsen BR (2004) Fluid collector (used for fast response filter module). Patent PA200400087.

Poulsen BR (2004) Flexible clamp (used for filtrate sampling system). Patent PA200400161.

Poulsen BR, Nøhr J, Douthwaite S, Hansen LL, Iversen JJL, Visser J, Ruijter GJG (2005) Increased NADPH concentration obtained by metabolic engineering of the pentose phosphate pathway in *Aspergillus niger*.FEBS J, in press.

Poulsen BR, Ruijter GJG, Iversen JJL, Visser J, Tramper J. (2004) Can submerged cultures of filamentous fungi be made reproducible? A need for the omics technologies. Trends in Biotechnology, in prep.

Curriculum vitae

Bjarne Rask Poulsen was born on 8 of March 1968 in Lønne (Denmark). Combining biology and technology has always been common to him since he grew up on his parents farm. After completing high school in 1987 at Varde Gymnasium he did the two-year study to become laboratory technician including practical experience at Brøns Experimental Fish Farm. In 1989 he started the MSc study of natural sciences at Odense University. He made his own individual study in biotechnology including experimental courses at the physics department, courses at the Technical University of Denmark and a five-month study abroad, which was his first experience at Molecular Genetics of Industrial Microorganisms (MGIM), Wageningen Agricultural University. Here he worked on characterization of *Aspergillus niger* strains as part of his MSc project. The part done in Odense was on the design of an airlift bioreactor. After finishing the MSc project in 1997 with the highest mark possible he returned to MGIM with a grant for a PhD study abroad from The Danish Research Academy. He joined the work on metabolic engineering of *Aspergillus niger*, more specifically, to increase the flux through the pentose phosphate pathway. Also his PhD project benefited from the expertise both in Odense and Wageningen. He has been the connective tissue in this joint project with both Danish and Dutch students attached and exchanged.

Thanks

I have seeked the knowledge, advice and/or help of others when my own limitations have been met and I am very happy to say that everyone I have turned to during this study has surprised me with positivism and enthusiasm - I feel that my thesis has been made around an axes of good ☺

Therefore there is a lot of people I am thankful to:

Thank you people at MGIM and Fungal Genomics, Wageningen University and at Department of Biochemistry and Molecular Biology, University of Southern Denmark. George, I admire your efficiency and you tried to teach me as well although I sometimes wanted to do it my way. Thanks for your patience and good supervision. Jaap, thanks for hosting me in a competitive environment at MGIM, for many good discussions on manuscripts (and other things) in your home and for nice hunting trips. Løns, thanks for a stay in a unique innovative environment at Technical Microbiology SDU, many intensive discussions, catalpa parties and other get-togethers. Hans, thank you for being willing to become my promoter at such a late stage, for good cooperation and help and for the advice to keep running. Johan, thanks for giving me a chance to finish my work at Fungal Genomics. Henk, thanks for many fruitful discussions and giving supervision in molecular biology to someone not familiar with these techniques. Raymond, thanks for many late discussions and for drawing my attention to the Guggenheim plot.

Thanks for good cooperation to fellow PhD-students; Marco, Ruud, Steph, Danielle, Lieke, Niels, Mads, Morten, Nawaf, Line, Patrick and Thomas – also for your friendship and times outside the lab. Ruud also for your late company in the lab. I am grateful to the beneficial and inspiring cooperation with several Danish and Dutch students; including Tina, Line, Bo, Baoleri, Antonio, Sumi, Jasper and Allard.

Harry, Peter and Erling thank you for your patience with my many questions and requests. Peter also for private discussions and welcoming people in your home - that meant a lot to us international people. Thanks to the people in lab 1023 and 1067 for good cooperation and for making daily working hours easier. Thank you people at the university workshops for making things urgently, enthusiasm and expertise – a special thanks to Hans de Rooy and Svend Aage. Thanks to Dorinde for help on the layout of the thesis.

Thanks to friends in the international environment of Wageningen and neighbours for a lot of nice company and to running friends for keeping me fit. Thanks to Miew-Woen, Jos and Lucie for being there for me ever since my first stay in Wageningen.

Kayak people, thank you for your support and great company in all my time here, I still remember from who I learned different steps of the eskimo roll. I don't expect to find such a club anywhere again and if I start my own club in Kalundborg I will try to do it in your spirit.

Vivian and Hans thank you for always receiving me with open arms and house – for your support, many good hours and deep discussions – I don't know what I would have done without you.

I want to thank my family for keeping believing in me and support. Mum and Dad, thank you for your faith in me and your unconditional love.

Photo(s) on the cover: *Aspergillus niger* mycelium grown in submerged bioreactor cultures in minimal medium at pH 3. Sample from the second exponential phase of repeated batch culture described in Chapter 2. Magnification 1000 times.